A Psychophysically-based Model for the Perceived Directionality of Textured Surfaces

Pratik Shah

Thesis submitted
for the
Degree of Doctor of Philosophy

Heriot-Watt University
School of Mathematical and Computer Sciences
April 2010

Abstract

Directionality is known to be an important dimension in human perception and classification of visual textures. Through a series of psychophysical experiments, this thesis investigates further the perception of directionality in textured surfaces, and uses the results to propose a measurement model for the perceived directionality of random-phase surfaces.

Height maps of textured surfaces were rendered and animated in real-time with controlled illumination. Observers' judgements of the directionality of surfaces were obtained by *direct-ratio estimation*, and either the *method of pair-wise comparisons* or the *method of constant stimuli*. The responses were used to derive a perceptual scale of directionality (*perceived directionality*) that could be related to physical properties of the surfaces.

The thesis first investigates the relationships between each of two existing computational measures of directionality (*Tamura's variance* and *Davis' variance*) and human perception of directionality. This was done by using height maps captured from real surfaces, which were then manipulated to vary the computational measures of their directionality. From the psychophysical experiment, it was found that these two measures do not fully account for human perception of directionality, which must therefore be influenced by other properties of the textures.

In order to investigate more fully the factors determining perceived directionality, synthetic random-phase surfaces defined by a mathematical model were used in the subsequent experiments. It was found that three properties of the magnitude spectrum of such surfaces significantly affect human perception of their directionality: angular variance (σ^2), RMS roughness (δ) and central radial frequency (f_c). After determining these effects, the thesis proposes a measurement model of perceived directionality, which predicts human perception of directionality of a random-phase surface.

Dedicated To

MY FAMILY

Acknowledgements

I would like to express my gratitude to my supervisors, Professor Mike Chantler and Professor Patrick Green, for their help in the accomplishment of this thesis. Thanks Mike for giving me an opportunity to conduct this research and for your constant support, innovative ideas, valuable suggestions and discussions. Thanks Patrick for your help and comments in the designing of psychophysical experiments and for explaining me the crucial statistics used in the thesis.

Specially, I would like to thank Dr. Stefano Padilla for providing me a tool to present surfaces in 3D. Thanks to Dr. Khemraj Emrith for the valuable technical and non-technical discussions at many points during my tenure in the Texture Lab. Also, thanks to the other members of the Texture Lab and the members of the department for their help whenever needed. I would also like to thank all observers who took part in the psychophysical experiments.

I am also grateful to my wife, Kajal, for providing me a continuous inspiration. Finally, I would also like to thank all my family members and friends for their constant support and enthusiasm.

ACADEMIC REGISTRY
Research Thesis Submission

Name*:*	Pratik Jitendrakumar Shah		
School/PGI:	Mathematical and Computer Sciences		
Version: *(i.e. First, Resubmission, Final)*	Final	Degree Sought (Award **and** Subject area)	Doctor of Philosophy

Declaration

In accordance with the appropriate regulations I hereby submit my thesis and I declare that:

1) the thesis embodies the results of my own work and has been composed by myself
2) where appropriate, I have made acknowledgement of the work of others and have made reference to work carried out in collaboration with other persons
3) the thesis is the correct version of the thesis for submission and is the same version as any electronic versions submitted*.
4) my thesis for the award referred to, deposited in the Heriot-Watt University Library, should be made available for loan or photocopying and be available via the Institutional Repository, subject to such conditions as the Librarian may require
5) I understand that as a student of the University I am required to abide by the Regulations of the University and to conform to its discipline.

* *Please note that it is the responsibility of the candidate to ensure that the correct version of the thesis is submitted.*

Signature of Candidate*:*	PJSHAH	Date:	05/07/2010

Submission

Submitted By *(name in capitals):*	
Signature of Individual Submitting:	
Date Submitted:	

For Completion in Academic Registry

Received in the Academic Registry by *(name in capitals):*			
Method of Submission *(Handed in to Academic Registry; posted through internal/external mail):*			
*E-thesis Submitted (**mandatory for final theses from January 2009**)*			
Signature:		Date:	

Table of Contents

List of Figures

List of Tables

List of Symbols, Terms and Abbreviations

Symbols	Description
u	Horizontal frequency
v	Vertical frequency
f	Radial frequency
θ	Angular frequency
W_{ij}	Energy features for the wedge shaped region between θ_i and θ_j
θ_i	Lower limit of a wedge shaped region of a magnitude spectrum
θ_j	Upper limit of a wedge shaped region of a magnitude spectrum
$M(f,\theta)$	Polar representation of a magnitude spectrum
s	Surface height map
Δ_h	Horizontal gradient (Tamura's Method)
Δ_v	Vertical gradient (Tamura's Method)
h_{df}	Horizontal partial derivative estimator (Tamura's Method)
v_{df}	Vertical partial derivative estimator (Tamura's Method)
$\lvert\Delta\rvert$	Magnitude of a gradient (Tamura's Method)
$\emptyset$	Angle of a gradient (Tamura's Method)
d_h	Directional histogram (Tamura's method)
t_h	Threshold (Tamura's Method)
$N_\emptyset(k)$	the number of points where $(2k-1)\pi/2n_b < \emptyset < (2k+1)\pi/2n_b$ and $\lvert\Delta\rvert$ is greater than t (Tamura's Method)
n_b	Number of quantizing levels for $\emptyset$ (Tamura's Method)
$\emptyset_d$	Dominant direction of a surface (Tamura's Method)
σ_T^2	Tamura's variance
$\Gamma(\theta)$	Polarogram-directional histogram obtained using Davis' method
f_{max}	Upper limit of radial frequency to calculate the polarogram
σ_D^2	Davis' variance

ρ	Perceived directionality of a surface
ρ_o	Observers' perceived directionality of surface
ρ_{fit}	Best fit values to ρ
p	Significant value of the statistical test
m_D	Slope of the linear regression associated with log (σ_P^2)
m_T	Slope of the linear regression associated with log (σ_T^2)
C_D	Constant of the linear regression associated with log (σ_P^2)
C_T	Constant of the linear regression associated with log (σ_T^2)
R_U	Un-normalized response of the given observer
$R_{U,max}$	Maximum value of R_U
$R_{U,min}$	Minimum value of R_U
R_N	Normalized responses of the given observer
$R_{N,max}$	Maximum value of the normalized responses
$R_{N,min}$	Minimum value of the normalized responses
N_o	Number of observers
$s(x,y)$	2D time domain representation of a surface
$S(u,v)$	2D frequency domain representation of a surface
k_1	Factor controlling the expansion and shrinking of a surface in *x-direction*
k_2	Factor controlling the expansion and shrinking of a surface in *y-direction*
$s_i(x,y)$	An input surface being shrunk or expanded
$S_i(u,v)$	DFT of an input surface being shrunk or expanded
$s_o(x,y)$	An output surface (shrunk or expanded)
$S_o(u,v)$	DFT of an output surface (shrunk or expanded)
$s_{ir}(x)$	Row of an input surface being shrunk or expanded
$S_{ir}(u)$	DFT of a row of an input surface being shrunk or expanded
$s_{or}(y)$	Row of an output surface (shrunk or expanded)
$S_{or}(u)$	DFT of a row of an output surface (shrunk or expanded)
N_s	Length of output row of a surface after shrinking

N	Length of input row of a surface before shrinking or expansion
N_e	Length of output row of a surface after expansion
s_f	Shrinking factor
e_f	Expansion factor
μ_s	Mean height of surface
δ	RMS roughness of surface
p_s	Perceptual scale of a stimulus
$s_r(i,j)$	Sense-ratio of stimuli i and j
n_s	Surface normal vector
k_d	Percentage of reflected diffuse light
l_s	Light vector
p_x	Surface partial derivative in x-direction
q_y	Surface partial derivative in x-direction
σ^2	Angular variance
δ_n	RMS Roughness normalization factor
$D(f)$	Distribution of radial frequency components
$D(\theta)$	Distribution of angular frequency components
β	Roll-off factor
θ_0	Dominant angular frequency
a	Number of rows of a surface
b	Number of columns of a surface
δ_{est}	Estimated RMS roughness
$D_{est}(\theta)$	Estimated distribution of angular frequency components
$D_{est}(f)$	Estimated distribution of radial frequency components
f_c	Central radial frequency
B_w	Bandwidth
f_h	Upper cut-off frequency of the Butterworth band-pass filter
f_l	Lower cut-off frequency of the Butterworth band-pass filter
n	Order of the Butterworth band-pass filter
F	*F-statistics* (ANOVA)

Terms	**Description**
Albedo	Colour information of a surface
Assumption of sphericity	Equality of variances of the differences between parameters (condition) levels
binocular stereo	A tool to obtain surface height map
Brodatz	Photographic album used for the study of textures
Bump map	Surface gradient components
Contrast (gray level)	Visual characteristic of surface
Contrast (ANOVA)	Test for statistical significance of differences in specific parts of repeated measures design
Degrees of freedom	Number of parameter levels - 1
Degrees squared	Unit of angular variance
Direct ratio estimation	Psychophysical scaling method
directionality	visual characteristic of the surfaces
Expansion	A method to stretch a surface
Fractals	Different types of surfaces
Greenhouse-Geisser	An estimation method to correct *degrees of freedom* when sphericity assumption is violated
Height map	Surface topology
Linear regression	Mathematical fitting to data
MATLAB	A software tool for technical computing
Mauchly's test	A test to assess the sphericity
Method of constant stimuli	Psychophysical experiment method
Method of pair-wise comparisons	Psychophysical experiment method
Naturalistic Surface	Surface that look like natural surfaces
Nyquist frequency	Highest frequency of a digital signal
Partial-eta squared	Effect size of the parameter
Perceived directionality	Perceived magnitude of directionality of surfaces
photometric stereo	A tool to obtain surface height map

polarogram	Directional histogram obtained from the polar spectrum
Polynomial contrast	Type of contrast analysis
Random phase	Random numbers with complex conjugate symmetry
Repeated contrast	Type of contrast analysis
RMS roughness	RMS height of the surface
shape from shading	A tool to obtain surface height map
Shrinking	A method to squeeze a surface
Simple (first) contrast	Type of contrast analysis
Simple (last) contrast	Type of contrast analysis
Synthetic Surface	Surface generated using mathematical model

Abbreviations	**Description**
cm	Centimetre
cpd	Cycles per degree
cpi	Cycles per image width
DFT	Discrete Fourier transform
LCD	Liquid crystal display
RMS	Root mean square
SPSS	Statistical Package for the Social Sciences
TFT	Thin film transistor
MDS	Multi-dimensional scaling
ANOVA	Analysis of variance

Chapter 1

Introduction

This thesis develops a measurement model of perceived directionality of textured surfaces. Section 1.1 describes importance of perceptual studies of textured surfaces. The motivation and goals of this thesis are explained in section 1.2. The scope and limitation of the work are described in section 1.3. The main contributions and the organisation of the thesis are mentioned in section 1.4 and section 1.5 respectively.

1.1 Background

Texture is an important visual cue that human uses to analyse surfaces. The performance of surface evaluation applications in context of a specific task depends on how well texture algorithms match human visual system. Human often uses terms like *roughness*, *directionality*, *coarseness* etc. to describe and differentiate textured surfaces. For applications such as automated perception based classification and retrieval of surfaces, many researchers have proposed computational approaches either to measure visual characteristics directly or to obtain set of features in order to classify surfaces the way human would classify it.

Tamura *et al.* (1978) were the first who highlighted importance of human perception in texture evaluation applications. They proposed computational measurements of visual characteristics based on spatial variation of surfaces and conducted psychophysical experiments to correlate those measurements with human perception. Amadasun and King (1989) used Neighbourhood Gray-Tone Difference Matrix (NGTDM) to measure the visual characteristics computationally and evaluated those measurements against human perception. Abbadeni (Abbadeni, 2000; Abbadeni *et al.*, 2000) proposed auto-covariance based perceptual texture features corresponding to human perception.

Psychophysical research has shown that human analyse images according to spatial frequencies and orientations of surfaces (Campbell and Robson, 1968). Therefore,

Fourier domain based approaches are also widely in use for the classification and segmentation of surfaces.

Many of such Fourier based approaches used *FRF* (filter-rectify-filter) models which are inspired by frequency channel models in human visual cortex. *FRF* models are also known as *back pocket model* in vision science as they have been routinely used in classification and segmentation task (Landy and Oruç, 2002). Usually, Gabor filter tuned in both orientation and frequency has been used as the first filter in the FRF models for the classification and segmentation of images (Landy and Bergen, 1991; Randen and Husoy, 1999; Bovik *et al.* 1987; Palm and Lehman, 2002). The rectification is used to transform negative amplitudes into corresponding positive amplitudes and smoothing responses from the first filter. Either lower frequency band pass filter (Landy and Oruç, 2002; Dakin *et al.*, 1999) or averaging filter (Randen and Husoy, 1999; Bovik *et al.*, 1990) is often used as the second filter. Texture segmentation using Gabor filters has also shown a strong correlation with actual human segmentation (Reed and Wechsler, 1990).

Another approach for the classification of surfaces using Fourier domain is to divide Fourier spectrum into rings (frequency information) and wedges (orientation information) and to use the total energy into regions created by rings and wedges as texture features (Weszka *et al.*, 1976). In general, there are numbers of studies showing the importance of spatial frequency and orientation of surfaces in human visual system.

In summary, surfaces textures have been studied psychophysically and mathematically to improve the performance of automated perception based applications of surface textures.

1.2 Motivation and Goal

The studies described above have shown importance of different factors that could be possibly affecting human perception of visual characteristics but they were carried out by selecting surfaces from databases like *Broadtz* (1966) and hence it is not clear how these measurement or textural features would perform evaluation task if different datasets is used. To the author's knowledge, none of the studies proposed specifically measurement models of visual characteristics (apart from measurement model of

roughness proposed by Padilla (2008)) describing perceptual estimation of visual characteristics.

Furthermore, researchers have found it difficult to show a reliable match between such computational measures and human perception of surface characteristics. Hence, the strategy of this thesis is to study how humans perceive one particular visual characteristic of textured surfaces. There are many visual characteristics of surfaces, including *directionality*, which numbers of studies (Tamura *et al.*, 1978; Rao and Lohse, 1993b; Liu and Picard, 1996; Abbadeni *et al.*, 2000; Abbadeni, 2000) have shown to be important in human perception of textured surfaces. Therefore, in this thesis human perception of directionality will be investigated. Human perception of directionality of directional surfaces will be described by the term *perceived directionality* in this thesis. The main goal of this thesis is to develop a measurement model of perceived directionality of uni-directional surfaces which will predict human perception of directionality of a given surface.

1.3 Scope of the Work

Synthetic uni-directional surfaces defined in frequency domain will be used to investigate human perception of directionality. To generate surfaces of varying directionality, distributions of frequency components in the magnitude spectrum will be varied and frequency components will have random phase spectrum. The final results will represent those surfaces only. Phase-rich surfaces will also be used in a small study *chapter 3*. However, no investigation will be carried out to find out how the information within phase spectra is related to human perception of directionality. Thus we will focus purely on the effects of 1^{st} and 2^{nd} order statistics.

1.4 Original Contributions

The contributions of this thesis are as follows:

1. It identifies the relevance of existing computational measures to human perception of directionality in *chapter 3*.

2. It reveals the effects of parameters that define distribution of the frequency components, on observers' perception of directionality in *chapter 4* and *chapter 5*.
3. The main contribution of this thesis is to propose a measurement model of perceived directionality. This model, given a height map of a random-phase surface, will predict how directional an average human observer would consider that surface to be.

1.5 Organisation of this Thesis

The organisation of this thesis is as follows. In *chapter 2*, first, reader is introduced to directional surfaces to make them familiar with the kind of directional surfaces used in this thesis. Then, different methods of investigating human perception of visual characteristics are reviewed to determine a suitable approach for the perceptual investigation of directionality. It also reviews existing methods used to measure directionality mathematically, and suggests two for further investigation.

In *chapter 3*, relevance of these two computational measurements to human perception is tested using sets of directional surfaces. *Photometric stereo* is used to obtain surface height maps of real samples of textured surfaces. A *shrinking* technique (Watson, 1988) is used to create sets of directional surfaces having different directionality. It also explains how stimuli will be presented throughout this thesis and describes tools used for the psychophysical experiments.

In *chapters 4* and 5, the effects of different magnitude spectrum parameters are investigated. Synthetic directional surfaces are used to control each parameter independently.

In *chapter 6*, the measurement model of perceived directionality is proposed based on the observed effects of parameters on perceived directionality. *Chapter 7* summarizes the conclusions of this thesis and suggests future work to extend the model.

Chapter 2

A Methodology for Investigating Human Perception of Directionality

Previously, with the exception of a few studies on human perception of roughness (Ho *et al.*, 2006, 2007; Padilla *et al.*, 2008) perceptual investigations of different visual characteristics of textures, including directionality, have been carried out using images from *de facto* data sets such as the Brodatz album (1966). However, the illumination conditions used to capture these images are unknown and Chantler (1995) has shown that common computational features are significantly affected when the illumination direction changes (Chantler, 1994b, 1995)

Therefore the objective of this chapter is to determine a suitable approach for the investigation of human perception of directionality without any illumination bias. It also introduces directional surfaces and, later, reviews existing methods of measuring directionality.

The organisation of this chapter is as follows. Section 2.1 gives an introduction to directional surfaces and describes directional surfaces which will be considered in this thesis. Section 2.2 reviews perceptual investigations of surfaces' visual characteristics and suggests an appropriate methodology. Section 2.3 explains how surface height data can be obtained using photometric stereo. Section 2.4 reviews existing methods of measuring the directionality of surfaces. We then describe the two, widely used, computational measures which will be tested in *chapter 3* to see if they match human perception.

2.1 Types of Directional Surfaces

In this thesis, directional surfaces are categorised based on the number of *dominant directions* of surface. The scope of this thesis is limited to uni-directional surfaces (see *Figure 2-1*). Examples of surfaces with no directionality or with more than one

dominant direction are shown in *Figure 2-2*, and such surfaces will not be discussed further in this thesis.

From *Figure 2-1*, it can be noticed that these two uni-directional surfaces have different *amount of directionality*. This thesis will investigate how humans judge the *amount of directionality*.

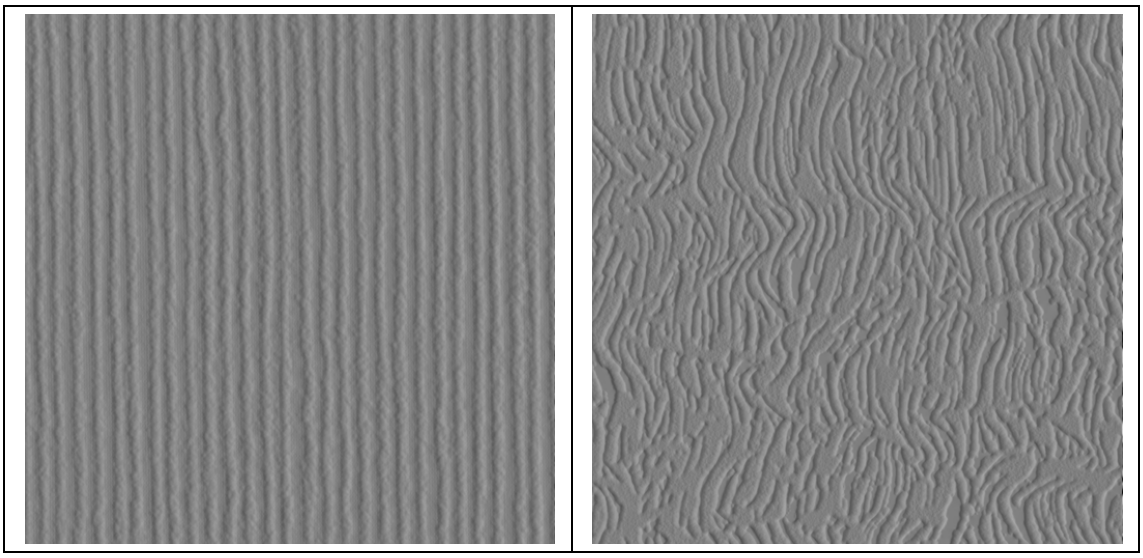

Figure 2-1: Example of uni-directional surfaces with varying directionality

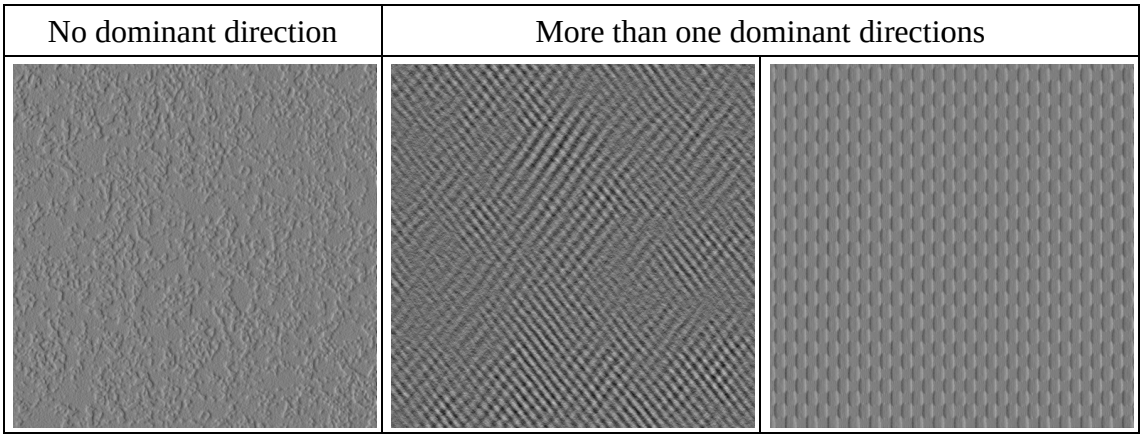

Figure 2-2: Example of surfaces having no or more than one dominant directions

2.2 Review of Perceptual Investigations of Visual Characteristics

The objective of this section is to determine an appropriate methodology for the investigation of human perception of directionality. Therefore it reviews how perceptual investigations of different visual characteristics carried out in the past.

Early methods for image classification and retrieval used features measured either from spatial or structural information (Haralick *et al.*, 1973) or from the Fourier domain (Weszka *et al.*, 1976; Bajcsy, 1972). In these methods, two textured surfaces were compared by matching the complete set of features. These studies did not investigate the human perception of visual characteristics of textured surfaces but some of the features were later used to obtain computational measurements of perceived characteristics (Battiato, 2002).

In man-aided approach, human decides criteria for the comparison of textured surfaces. Therefore, it is necessary to define set of features that are appropriate to human perception. Tamura *et al.* (1978) investigated the match between human perception of six basic visual characteristics and corresponding computational measures. These visual characteristics were named as *coarseness*, *contrast*, *directionality*, *line-likeness*, *regularity* and *roughness*. To identify how well the computational measurements describe corresponding visual characteristics, they conducted psychophysical experiments in which 48 human observers made pair-wise comparison of 16 images from the *Brodatz* album (1966). The observers selected a texture from each pair according to six visual characteristics i.e. coarser, more directional, high in contrast, more line-like, more regular and rougher. Perceptual scale for each stimulus was obtained and ranking of textures were compared with the computational ranking to judge the discrepancy between human judgements and computational measurements. The main conclusion was that there was a high correlation between human judgements and computational measurements of *coarseness, directionality* and *contrast*, while the correlation for the other three characteristic was not very good. The computational method to measure directionality using Tamura's method is discussed later in this chapter.

Similarly, Amadasun and King (1989) gave conceptual definitions and computational measures of five visual characteristics: *coarseness*, *contrast*, *busyness*, *complexity* and *texture strength*. They evaluated human ranking and computation ranking of images from *Brodatz* album (1966) and found very high correspondence between them.

Many others (Liu and Picard, 1996; Wu *et al.*, 1999; Payne *et al.*, 1999; Payne, 2000; Abbadeni, 2000; Abbadeni *et al.*, 2000; Payne and Stonham, 2001; Battiato *et al.*, 2003; Fujii *et al.*, 2003) followed similar procedures and compared human judgements of predefined visual characteristics, including directionality, with the corresponding

computational measures to show the relevance of suggested computational measures to human perception. In these studies, human perception of directionality was studied by comparing the perceptual ranking of textured surfaces with computational ranking of directionality and no relationship between the computational measures of directionality and human perception of directionality was obtained.

Another approach used in the perceptual investigation of textured surfaces was to identify the perceptual space of textured surfaces which includes visual characteristics important to human perception, instead of selecting visual characteristics without knowing their significance to human perception as done by the researchers reviewed above.

Rao and Lohse (1993a, 1993b) indentified the perceptual dimensions of textured surfaces that are relevant to human perception. They used free-sorting tasks and multi-dimensional scaling (MDS) and found that the most significant orthogonal dimensions of textured surfaces were, *repetitive* vs. *non-repetitive*; *high contrast* and *non-directional* vs. *low contrast* and *directional*; *granular*, *coarse* and *low complexity* vs. *non-granular*, *fine* and *high complexity*.

Heaps and Handle (1999) conducted a similar experiment and concluded that textured surfaces cannot be arranged into perceptual space because human perception of visual characteristics is context dependent. Long and Leow (2001) found four dimensions of textured surfaces using similar procedure. However, they didn't name the dimensions. Instead, they compared the perceptual space with the computational space. Harvey and Gervais (1981) and Gurnsey and Fleet (2001) also used the MDS to correlate computational and perceptual texture spaces. As this thesis is concerned with one dimension of perceptual texture space, the techniques of free-sorting tasks and MDS will not be used in this thesis.

The methodology, used by researchers who investigated human perception of predefined visual characteristics by comparing human judgements of visual characteristics with the corresponding computational measures, can be used to develop the measurement model.

This methodology involves four steps: selection of textured surfaces, defining a computational measure of a visual characteristic, conducting psychophysical

experiments with human observers and mapping of psychophysical data on to computational measurements.

The perceptual investigations of directionality, and other visual characteristics, reviewed so far have a common limitation. They used single still images of two-dimensional textured surfaces from databases like the *Brodatz* album (1966) for the psychophysical experiments and computational measurements. The illumination and viewpoint conditions of these images are unknown. There are various studies which show how illumination and viewpoint conditions affect human perception of visual characteristics.

The appearance of textured surfaces changes with the change in illumination position (Chantler, 1994b, 1995) (see *Figure 2-3*) and hence performance of classification is adversely affected (Chantler, 1994b; McGunnigle, 1998). Koenderink *et al.* (2003) used a set of images that Dana *et al.* (1999) obtained under 200 different illumination and viewing directions and demonstrated that humans can judge the illumination azimuth direction from a two-dimensional image of a textured surface.

Illuminated from left	Illuminated from top
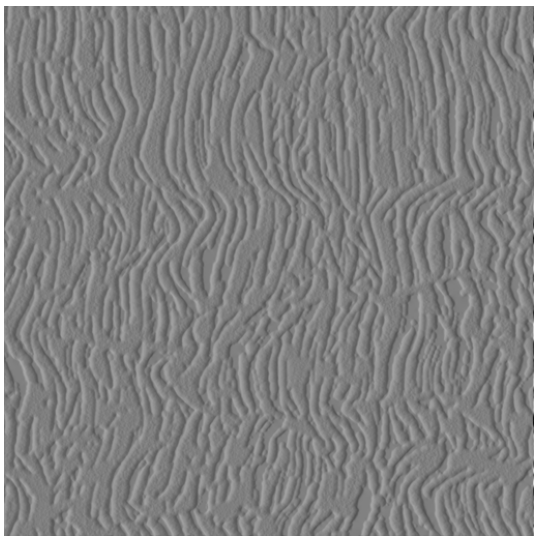	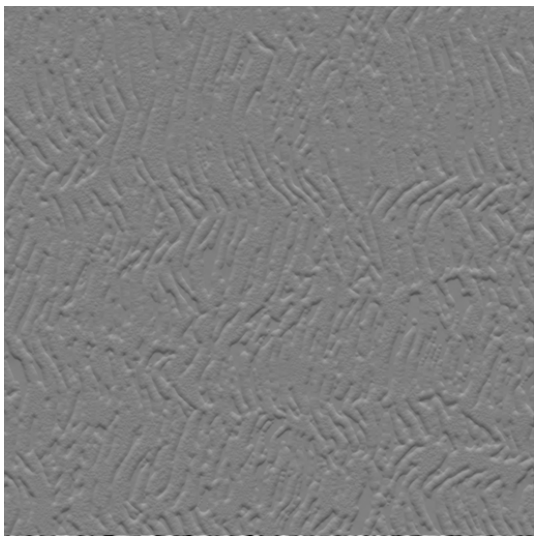

Figure 2-3: Effect of illumination direction on appearance of surface

Belhumeur *et al.* (1999) showed that the images of 3D objects have an inherent ambiguity about the depth information, known as *bas-relief ambiguity*. This effect is shown in *Figure 2-4* where the same cylinder is illuminated from different positions and viewed from a fixed position. It can be noted that the cylinder on right appears taller

than the cylinder on left. Using synthetic surfaces, Ho *et al.* (2006, 2007) showed that both illumination and viewpoint significantly affect perception of roughness. These results confirm the necessity for controlled illumination and view point conditions for the set of textured surfaces undergoing psychophysical investigation.

Furthermore, computational features of textured surfaces vary significantly with the change in illumination azimuth angle (Chantler *et al.*, 1994a). Therefore, the computational measures obtained from the images of textured surfaces are influenced by illumination direction and may not represent the surfaces' intrinsic physical characteristics.

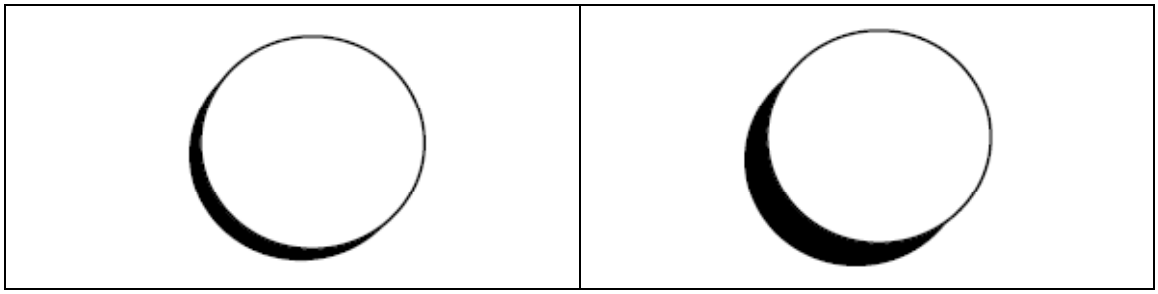

Figure 2-4: Example of bas-relief ambiguity

These effects of illumination and viewpoint on human perception and computational measurement suggest the following:

- Perceptual investigation needs to be carried out using textured surfaces illuminated under controlled lighting conditions
- The investigation should use computational measures that are independent of illumination.

This is possible by obtaining surface *height maps* (relief information) of real sample of textured surfaces. A surface *height map* provides information about surface topology and does not have any illumination information. Thus computational measures obtained from surface height map do not have any illumination bias. Furthermore, these surface height maps can be rendered under specified illumination conditions to provide controlled and consistent illumination condition during psychophysical experiments.

Surface relief information can be obtained by using *binocular stereo* (Barnard and Fischler, 1982; Dhond and Aggarwal, 1989), *shape from shading* (Horn, 1975, 1986;

Horn and Brooks, 1989) or *photometric stereo* (Woodham, 1980). It is beyond the scope of this thesis to discuss all of these methods. Photometric stereo will be used in this thesis and will be explained later as it is cheap, easy to implement and has been used extensively in the Texture lab (McGunnigle, 1998; Dong and Chantler, 2005; Emrith, 2008).

Surface height map can be illuminated under specified conditions to solve the problems associated with previous studies. Padilla (2008) developed a novel methodology to investigate perceived characteristics of textured surfaces. He rendered and animated surface height maps in real time to simulate wobbling the surface under a fixed illumination source. This eliminates the problems associated with illumination and view point ambiguity and depth perception when perceiving visual characteristics of textured surfaces.

Thus **s**urface height maps obtained using photometric stereo and Padilla's method of presenting surfaces to human observers can be utilized for the perceptual investigation of directionality under controlled and consistent illumination conditions. The detailed study of photometric stereo and Padilla's method of presenting stimuli in 3D is beyond the scope of this thesis. However, photometric stereo and Padilla's method are explained, briefly, in section 2.3 and section 3.3.1 respectively.

In summary, the investigation of perceived directionality will be carried out using surface height maps which will be rendered and animated under controlled and consistent illumination conditions. The computational directionality will be obtained directly from the surface height maps and finally the measurements of human perception of directionality obtained from the psychophysical experiments will be mapped on to the computational measurement to identify the relevance of these measurements to human perception. The next section gives a brief introduction to photometric stereo which will be used to obtain the surface height maps.

2.3 Photometric Stereo: A Tool to Obtain Surface Height Map

This section gives a brief summary of photometric stereo and the process of obtaining a surface height map. Photometric stereo uses the reflectance models (such as Lambertian model, named after its founder J. H. Lambert in 1760, Phong's model (Phong, 1975),

Blinn's model (Blinn, 1977), Cook's model (Cook and Torrance, 1982)) and images of surfaces illuminated from different directions with constant viewing direction for estimating surface derivatives and *albedo*. Reflectance models describe the intensity and spatial distribution of light reflected from the object for a given light source and view point. It is assumed that the light sources are point sources and the surfaces are Lambertian. The geometry of the set up is shown in *Figure 2-5***.** In this thesis, surface height maps will be obtained by capturing four images as shown in *Figure 2-5***.** The surface plane is xy-plane which is perpendicular to the camera axis (*z-axis*).

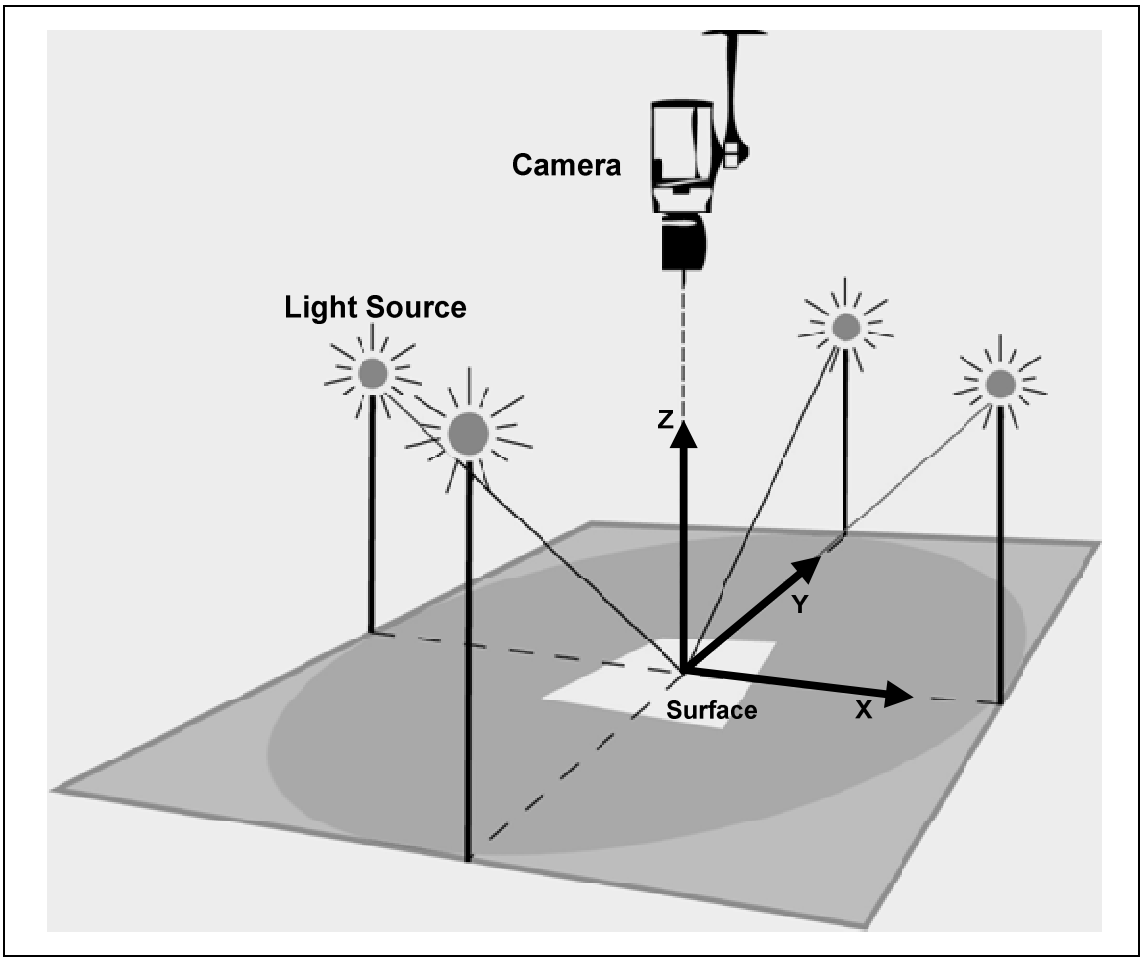

Figure 2-5: Geometry of photometric stereo

To obtain surface characteristics at a given point on the surface, the surface unit normal vector is calculated from the captured images. The magnitude of surface normal at a given point gives the *albedo* image i.e. colour information and the direction of surface normal gives the *bump map* i.e. surface derivatives along *x-axis* and *y-axis*. The height map of surface such as shown in *Figure 2-6* can be obtained by integration of the surface derivatives in the Fourier domain.

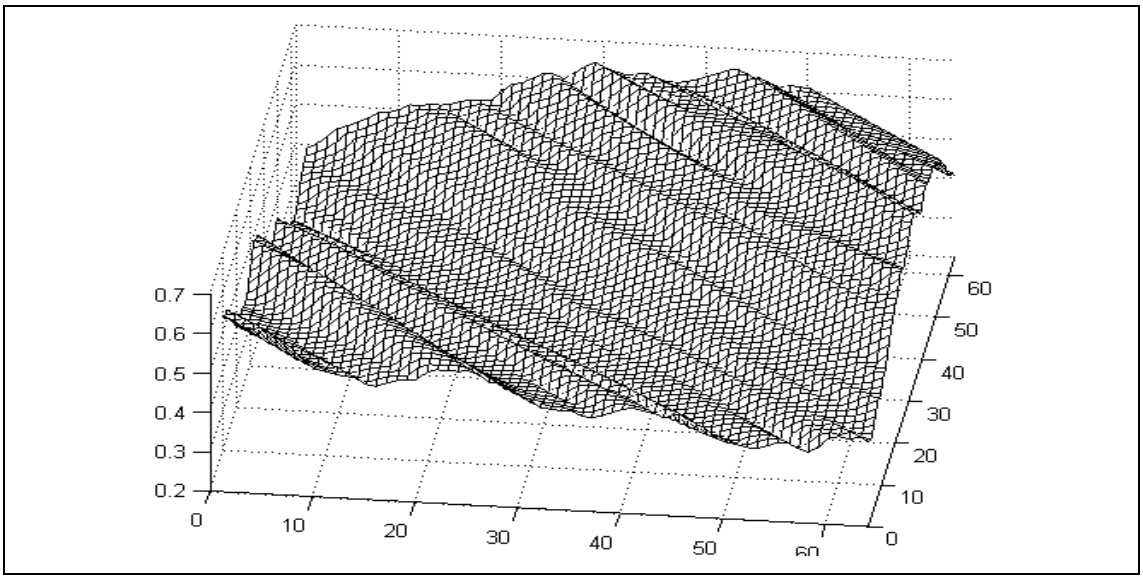

Figure 2-6: Surface height map

2.4 Computational Measurements of Directionality

Various computational measures have been proposed to represent human perception of directionality. However, it is not clear whether these computational measures actually represent human perception. Therefore, investigation is required to identify the relevance of these computational measures to human perception. However, it is not possible to investigate the relevance of all measures to human perception. Therefore, this section reviews different measures of directionality and selects two for further investigation.

Liu and Picard (1996, 1999) used 2D Wold decompositions which decompose an image pattern into three mutually orthogonal components named as *periodicity*, *directionality* and *randomness*. Wold decomposition theorem (named after its founder Herman Wold (1938, 1954)) allows to forecast any stationary process by using weighted average of past forecast errors. (Liu and Picard, 1996, 1999) decomposed image patterns by extracting Fourier spectral peaks supported by point-like and line-like regions to obtain features (named as Wold features) related to *periodicity*, *directionality* and *randomness*. However, no direct method for the measurement of directionality was suggested. Instead, an algorithm based on the grey-level Hough transform was suggested for identification of directional surfaces. A multi-resolution simultaneous auto-regressive

(MRSAR) process was used to obtain the set of features that was then used for similarity based retrieval. Even though the Wold model offered perceptually satisfying results when used in image retrieval systems, the set of features were not studied further to derive the measures of directionality as they were intended to detect evanescent components such as straight lines within an image.

Lee and Chen (2005) proposed MPEG 7 texture descriptors to characterise textures' regularity, directionality and coarseness. The Hough transform was used to extract two dominant directions of surfaces. Earlier, Wu (Wu *et al.*, 1999) suggested perceptual browsing components for perceptual characterisation of texture in terms of texture directionality and coarseness. However, these descriptors measure the direction rather than directionality and so they are not investigated in this thesis.

Abbadeni (2000) and Abbadeni *et al.* (2000) proposed a new method of measuring directionality using the auto-covariance function. They estimated two parameters: dominant orientation (i.e. dominant direction) and degree of directionality (i.e. amount of directionality). The second was based on a number of pixels having dominant orientation. However the variance about dominant orientation has not been considered and so this work will not be considered further here.

Lepistö *et al.* (2002, 2003) used another method for the retrieval of rock texture images and non-homogenous textures based on directionality. They used directional histogram to identify the directionality. The directional histogram was obtained using two different methods - directional filtering and the Hough Transform (Duda and Hart, 1972). For the first method they used a set of eight different line masks for eight directions and their projections on the image, to estimate directionality. In the second method, the Hough Transform was used to detect directions occurring in image. Again they used eight direction bins to detect edges in eight directions. These approaches will not be used to estimate dominant direction and directionality for two reasons: the significance of these approaches was tested only for a specific class of textured surface and distributions of only eight directions were obtained which may be insufficient for the other class of textured surfaces.

Kourosh and Hamid (2005) have used the radon transform to estimate texture direction. The radon transform has a very large variation along the direction of texture. Therefore, variance of the radon transform gives an estimate of texture direction. However, this

approach was intended for rotation invariant feature calculation and it has never been studied in context with human perception and therefore it will not be investigated further in this thesis.

Tamura *et al.* (1978) defined directionality as "*the measure of directions of the grey values within the image*." He used the histogram of local edge probabilities against their directional angle to estimate the overall directionality. A histogram was obtained by counting number of pixels (points) in surface having the same directional angle. The directional feature of Tamura has been used for image retrieval in the QBIC system (Flickner *et al.*, 1995; Niblack *et al.*, 1993). The Photobook system (Pentland *et al.*, 1996), a set of interactive tools for browsing and searching images, also implements Tamura's feature to provide perceptually significant results. Therefore, it is possible that this measurement may represent human perception of directionality. So it was decided to investigate the directionality measure given by Tamura. The measurement method is described later in this section.

Apart from spatial domain methods, Fourier techniques are also widely used to extract information about directionality of textured surfaces. The directionality of textured surfaces is preserved in the magnitude spectrum (Bajcsy, 1972; Weszka *et al.*, 1976) as shown in *Figure 2-7*.

In order to extract features, the magnitude or power spectrum is converted from *Cartesian co-ordinate* system (u, v) to *Polar co-ordinate* system (f, θ) and divided into rings and wedges (Bajcsy, 1972; Weszka *et al.*, 1976) as shown in *Figure 2-8*. The parameters u and v are horizontal and vertical frequency respectively. In this thesis, f and θ are called *radial frequency* and *angular frequency* respectively as they are *polar co-ordinates* of 2D *Fourier transform*, elsewhere in the literature they are called radius and angle respectively.

The directional features are computed from different wedges as shown in *Equation (2-1)*, where W_{ij} is the energy feature for wedge shaped region between θ_i and θ_j and $M(f, \theta)$ is the magnitude of the *Discrete Fourier transform* of the input height function.

$$W_{ij} = \sum_{\theta_i}^{\theta_j} M(f, \theta) \tag{2-1}$$

Surface	Magnitude Spectrum
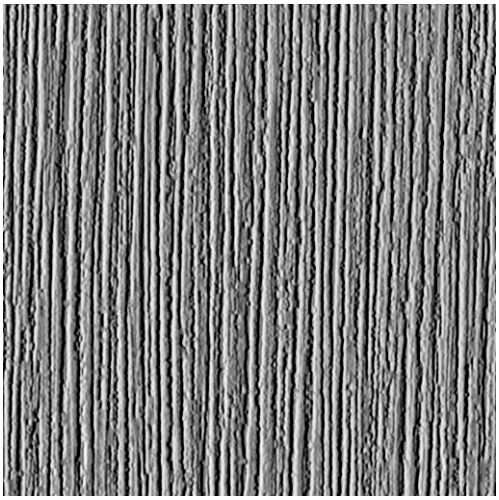	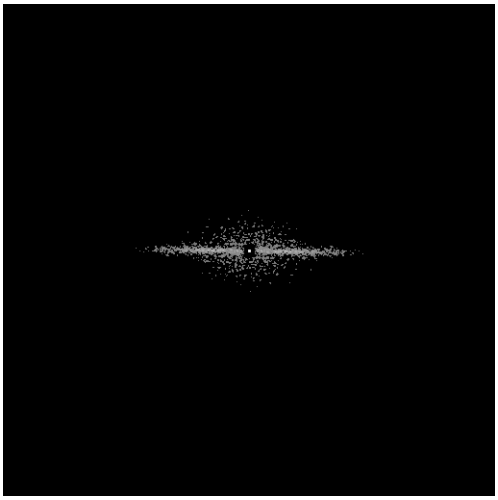
	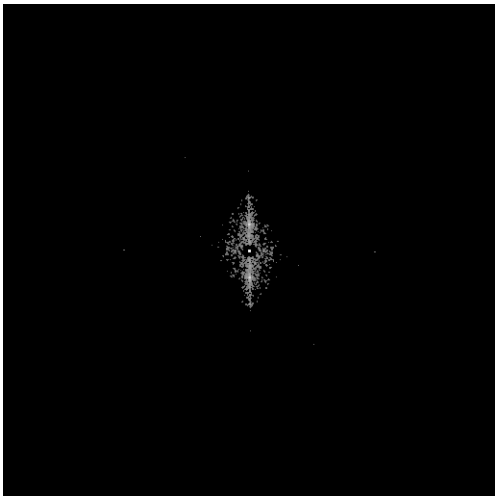

Figure 2-7: Directional information within magnitude spectrum

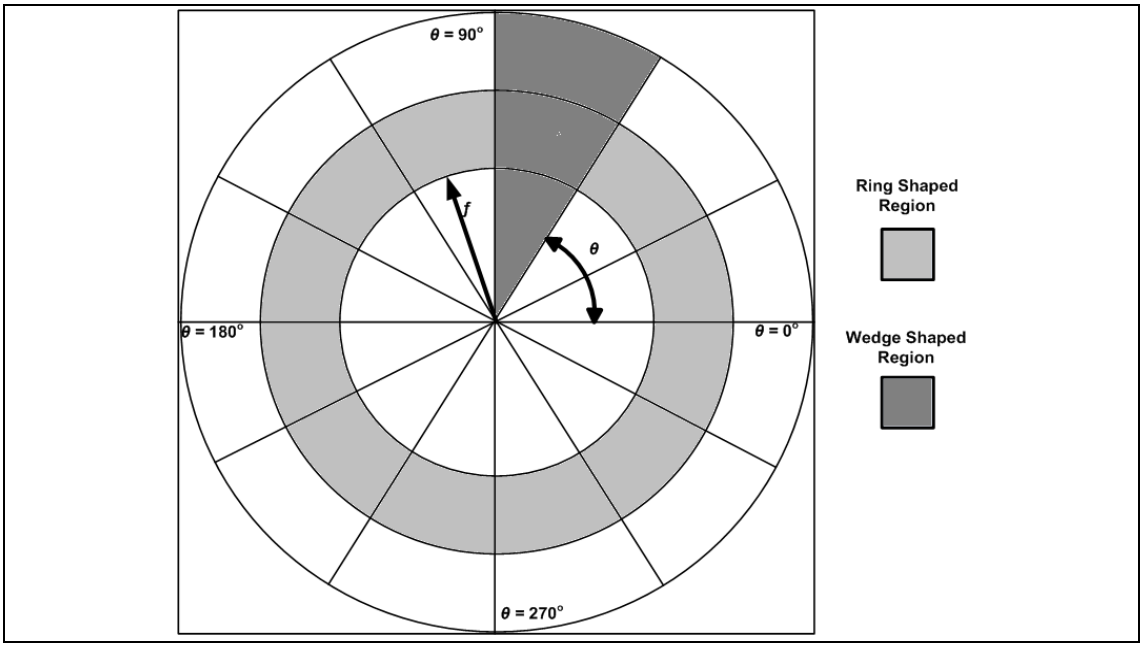

Figure 2-8: Ring and wedge shaped regions of 2D Fourier domain

Davis (1981) suggested a new method based on the *polarogram*, which can be used to estimate directionality. The polarogram is obtained from the polar representation of magnitude spectrum by summing along each value of θ as given by *Equation (2-2)*.

$$\Gamma(\theta) = \sum_{f=1}^{f=f_{max}} M(f,\theta) \tag{2-2}$$

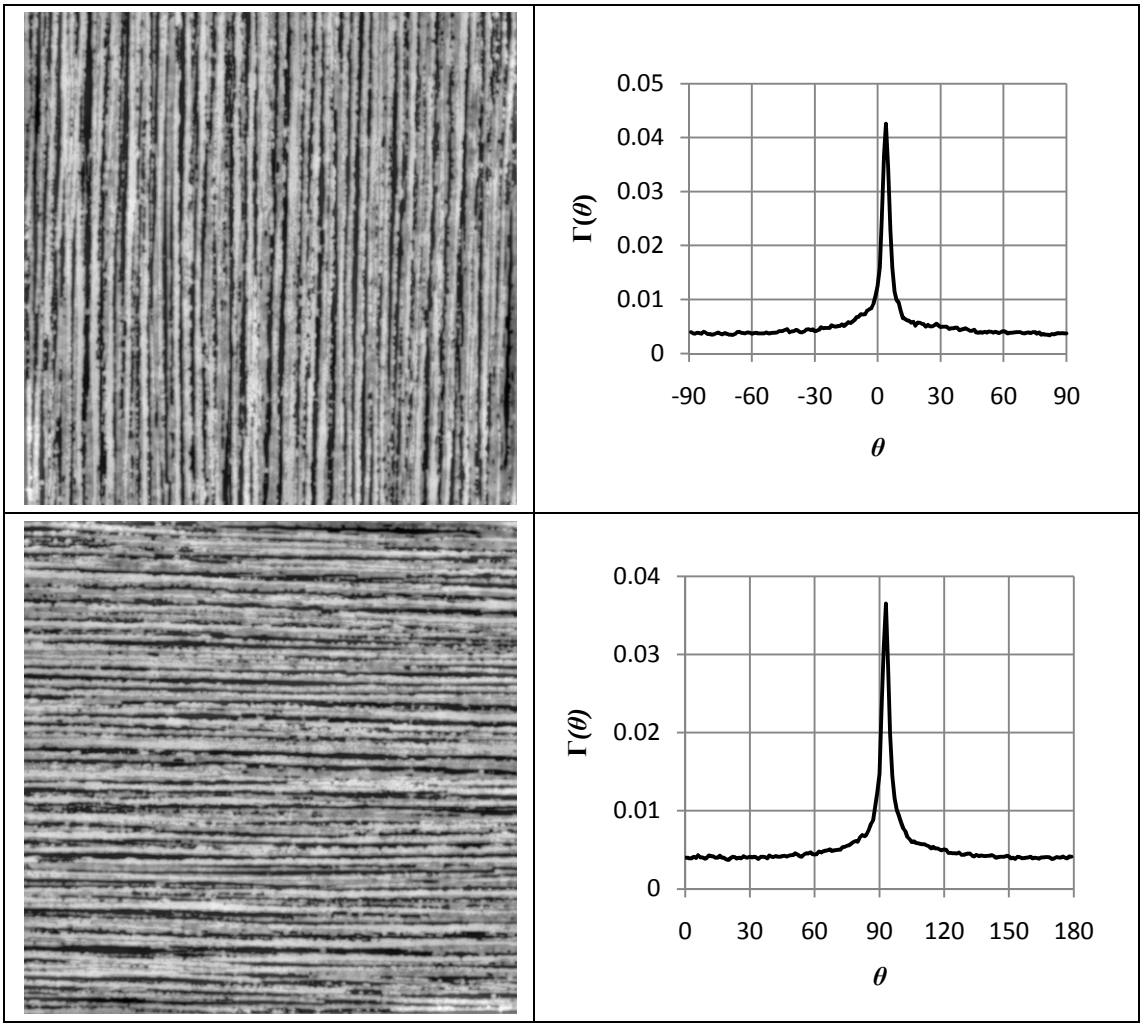

Figure 2-9: Effect of rotation of surface height map on polarogram

As seen previously, directional information in magnitude spectrum is sensitive to surface rotation i.e. magnitude spectrum rotates if surface is rotated. Therefore the wedge features, obtained using *Equation (2-1)*, do not remain constant. However, the polarogram obtained using *Equation (2-2)* is shifted with the surface rotation as shown in *Figure 2-9*, statistics such as second moment remain unaffected. Apart from this

shift, the small differences in the two polarograms, shown in *Figure 2-9* are due to *interpolation*, used to estimate the polarogram from discrete magnitude spectrum.

As Fourier based techniques are extensively used for surface related applications, it is interesting to test relevance of the measures of directionality obtained from the Fourier domain using Davis' method against human perception.

Thus, the two computational directionalities obtained using Tamura's and Davis' methods will be tested in the next chapter to identify if they match human perception. As both methods produce directional histograms, computational directionality is obtained by calculating their *variance*. The measures obtained using Tamura's method and Davis' method will be called *Tamura's variance* (σ_T^2) and *Davis' variance* (σ_D^2) respectively. For estimation of these variances, mean value i.e. *dominant direction* will be estimated with reference to the *positive x-direction*. The detailed descriptions of the computation of directionality using both methods are given below.

2.4.1 Measuring Tamura's Variance

a. The horizontal (Δ_h) and vertical (Δ_v) gradient at each pixel is estimated by convolving an input surface height map (s) with the following horizontal (h_{df}) and vertical (v_{df}) partial derivative estimators respectively.

$$h_{df} = \begin{vmatrix} -1 & 0 & 1 \\ -1 & 0 & 1 \\ -1 & 0 & 1 \end{vmatrix} \tag{2-3}$$

$$v_{df} = \begin{vmatrix} 1 & 1 & 1 \\ 0 & 0 & 0 \\ -1 & -1 & -1 \end{vmatrix} \tag{2-4}$$

$$\Delta_h = convolution\ (s, h_{df}) \tag{2-5}$$

$$\Delta_v = convolution\ (s, v_{df}) \tag{2-6}$$

b. The magnitude ($|\Delta|$) and angle ($\emptyset$) of the gradient are calculated using *Equations (2-7)* and *(2-8)* respectively. The angle ($0^o < \emptyset < 180^o$) is measured counter clockwise so horizontal direction becomes zero.

$$|\Delta| = \frac{|\Delta_h| + |\Delta_v|}{2} \tag{2-7}$$

$$\emptyset = \tan^{-1}\left(\frac{\Delta_v}{\Delta_h}\right) + 90^o \tag{2-8}$$

c. The directional histogram (d_h) is obtained by quantizing $\emptyset$ and counting number of points with $|\Delta|$ greater than threshold t_h as shown in *Equation (2-9)*. $N_\emptyset(k)$ is number of points where $(2k-1)\pi/2n_b < \emptyset < (2k+1)\pi/2n_b$ and $|\Delta|$ is greater than t_h. n_b is number of quantizing levels for $\emptyset$ and k varies from 0 to n_b - 1. The purpose of threshold is to prevent use of unreliable edge points. However, as it is difficult to define threshold for different surfaces, threshold is kept at zero in this thesis. Also n_b is kept equal to 180. *Figure 2-10* shows the surface and corresponding directional histogram obtained using this method.

$$d_h(k) = \frac{N_\emptyset(k)}{\sum_{i=0}^{n_b} N_\emptyset(i)} \tag{2-9}$$

d. The location of sharp peak in the directional histogram gives dominant direction ($\emptyset_d$) and sharpness of peak gives measure of directionality. The dominant direction (i.e. mean value) is measured as shown in *Equation (2-10)*. The measure of directionality, *Tamura's variance*, is calculated using *Equation (2-11)*.

$$\emptyset_d = \sum_{\emptyset=0}^{\emptyset=179} (\emptyset)\, d_h(\emptyset) \tag{2-10}$$

$$\sigma_T^2 = \sum_{\emptyset=0}^{\emptyset=179} (\emptyset - \emptyset_d)^2\ d_h(\emptyset) \tag{2-11}$$

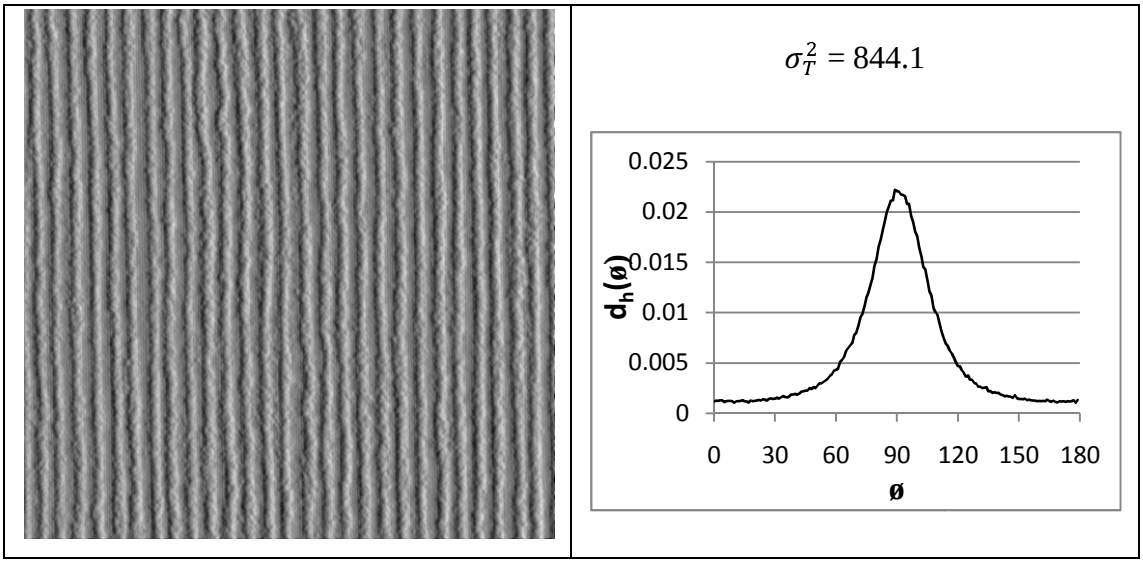

Figure 2-10: Surface and Tamura's variance

2.4.2 Measuring Davis' Variance

a. An input surface (s) is multiplied with a 2D Hanning window to remove artefacts related to discontinuities at boundaries. The Fourier transform of resultant surface is obtained.

b. The magnitude spectrum is used to extract the polarogram. As this spectrum is discrete, bi-cubic interpolation is used to estimate magnitude of frequency components at intermediate values of radial and angular frequencies.

c. The polarogram is obtained from interpolated values and is given once again in equation (2-12) for convenience. f_{max} is the maximum radial frequency present in magnitude spectrum. θ varies from 0 to 179. In *Figure 2-11*, the surface and corresponding polarogram are shown.

$$\Gamma(\theta) = \frac{\sum_{f=1}^{f=f_{max}} M(f,\theta)}{\sum M(f,\theta)} \tag{2-12}$$

d. Similar to Tamura's method, the dominant direction ($\emptyset_d$) and the measure of directionality (*Davis' variance,* σ_D^2) are calculated using *Equations (2-13)* and *(2-14)* respectively. As magnitude spectrum tends to lie in direction perpendicular to direction of surface, dominant direction and directionality is obtained by shifting the polarogram by 90^o.

$$\emptyset_d = \sum_{\theta=0}^{\theta=179} (\theta + 90)\, \Gamma(\theta + 90) \tag{2-13}$$

$$\sigma_D^2 = \sum_{\theta=0}^{\theta=179} (\theta + 90 - \emptyset_d)^2\ \Gamma(\theta + 90) \tag{2-14}$$

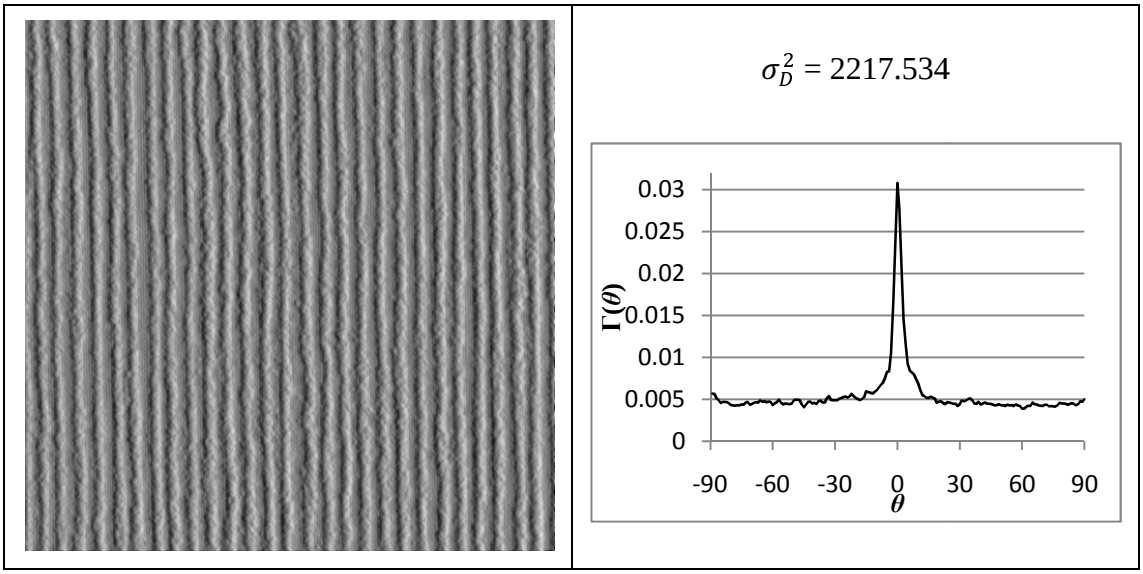

Figure 2-11: Surface and Davis' variance

2.5 Summary

The beginning of this chapter introduced different types of directional surfaces specified by number of dominant directions. Surfaces having only one dominant direction, named *uni-directional surfaces*, will be considered and multi-directional surfaces will not be.

This chapter then reviewed methodologies previously used to investigate human perception of visual characteristics of surfaces. It found that human perception of directionality had been investigated using still images of surfaces whose illumination conditions and viewpoints were unknown. At the same time, many results show that illumination conditions and view point affect appearance of surfaces and hence human perception.

Therefore it was decided to investigate human perception of directionality using the following method. The surface height maps will be obtained using photometric stereo.

As surface height maps do not have any illumination information, computational directionality will be obtained from surface height map. During psychophysical experiment, observers will be presented with surface height map, rendered and animated under controlled and consistent illumination conditions as described in Padilla's methodology. This eliminates problems related to illumination and viewpoint conditions. Finally, the psychophysical measurements obtained will be mapped on to computational directionality to determine the relation between human perception and computational directionality.

To take the first step towards investigation, this chapter briefly describes how photometric stereo can be used to obtain surface height maps and then reviews different measures of computational directionality. It was found that among many different methods of measuring directionality, Tamura's and Davis' methods are widely used and therefore, these two methods were described fully. The next chapter will investigate relevance of these measures to human perception under controlled and consistent illumination and viewpoint conditions.

Chapter 3

Human Perception and Computational Directionality of Surfaces

As discussed in *chapter 2*, the relationship between the two computational directionalities (*Davis' variance* (σ_D^2) and *Tamura's variance* (σ_T^2)) and human perception has not been investigated independently of illumination conditions. Therefore the goal of this chapter is to investigate if there is any correspondence between human perception of directionality and these two computational directionalities under controlled illumination.

To achieve the goal of this chapter, consistency of computational directionality and human perception will be tested across six different sets of surfaces. Each set will be comprised of five surfaces which will be obtained by *shrinking* (Watson, 1988) a surface height map in one direction. It is assumed that this will generate surfaces those are both visually different and have different values of computational directionality, making it possible to establish relationship between computational directionality and human perception of directionality. The *shrinking* method is chosen because it is simple and it is not possible to obtain sets of surfaces by controlling computational directionality directly. Two computational directionalities, σ_D^2 and σ_T^2, will be measured from the *shrunken* height maps. The surface height maps will be rendered and animated under the same illumination conditions during psychophysical experiment to obtain the perceptual measurements. The perceptual measurement of directionality will be a numeric value assigned to each surface using a psychophysical scaling method. A numeric value will be called *perceived directionality* and denoted as ρ. Statistical significance tests will be carried out to find out if either of the two computational directionalities is consistent with *perceived directionality*.

The chapter is organized as follows: Section 3.1 describes how sets of surface height maps were generated. In section 3.2, the two computational directionalities are calculated and reported. Section 3.3 describes the way psychophysical experiments were conducted to obtain the perceived directionality of surfaces, and reports how perceived directionality varies with the two computational directionalities. In section 3.4, results

of the statistical significance test are reported and discussed. The chapter concludes with a summary in section 3.5.

3.1 Producing Stimuli of Varying Directionality

To find out if either of the two computational directionalities represents human perception of directionality, consistency of mathematical relationship between the two computational directionalities and perceived directionality across different sets of surfaces will be tested. To establish this relationship, each set of surfaces is required to have visually different surfaces with different values of computational directionalities. The method of obtaining a set of surface height maps is discussed in the next sub-section.

3.1.1 Method of Manipulation of Directional Surfaces

As discussed in *chapter 2*, the surface height map can be obtained from real samples of textured surfaces using *photometric stereo*. To obtain the six sets of surfaces mentioned earlier, six surface height maps were obtained using photometric stereo and each of these six height maps were manipulated to generate visually different and realistic looking directional surfaces.

It was observed that when frequency components were distributed in many directions, the values of *Davis's variance* and *Tamura's variance* were high compared to when frequency components were dominant in one direction. This can be observed from the directional histograms shown in *Figure 3-1*.

Therefore if the distribution of frequency components is changed e.g. to make it wider in one direction or conversely concentrated in one direction, then its physical appearance and values of the two computational directionalities can be changed. This can easily be achieved by either *expansion* or *shrinking* of a surface in one (either horizontal or vertical) direction as shown in *Figure 3-2*.

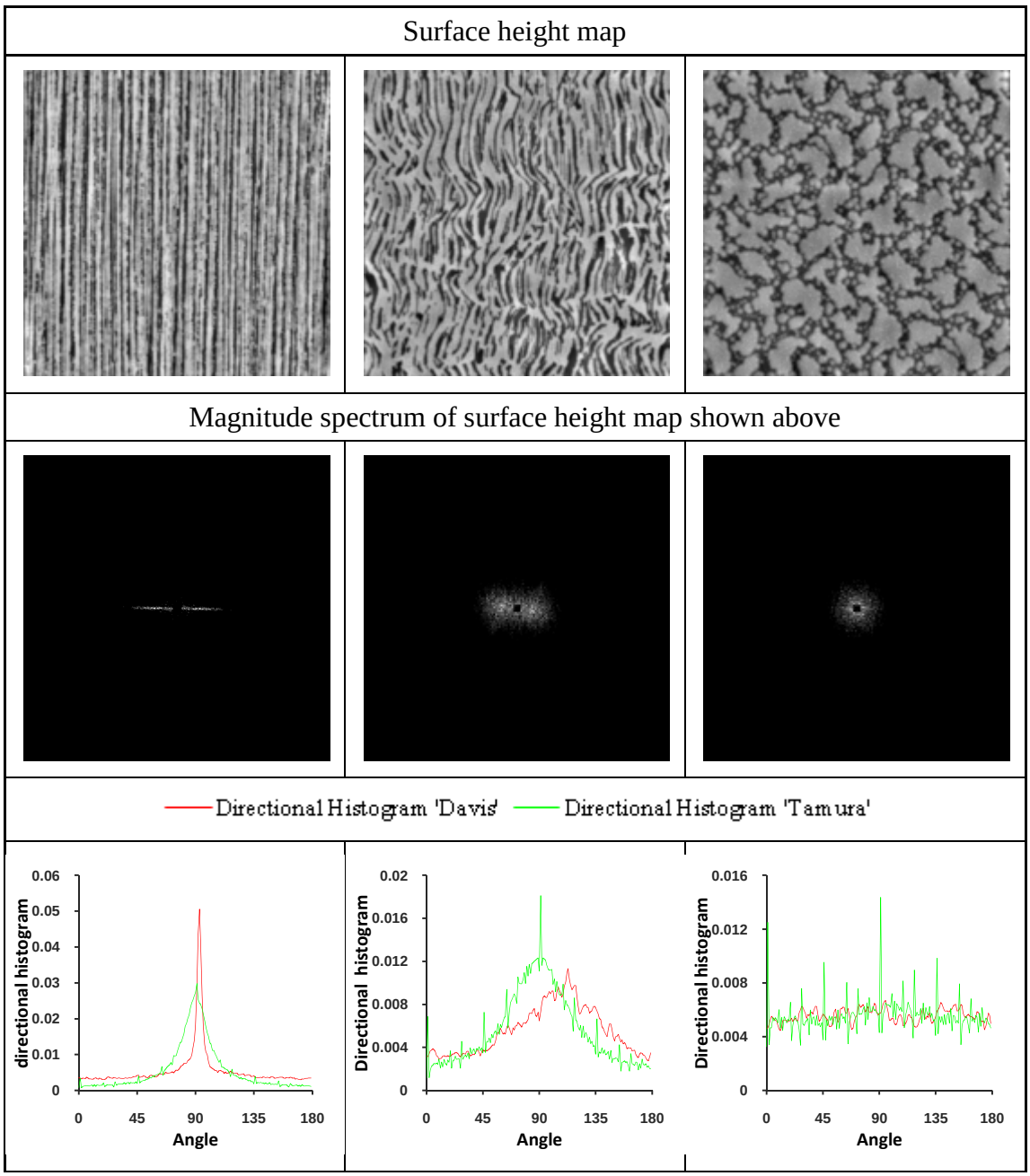

Figure 3-1: Effect of distribution of frequency components on the computational *directionality.*

Expansion and *shrinking* of a surface are performed in the frequency domain using a simple sub-ideal algorithm suggested by Watson (1988). *Expansion* is simply achieved by padding a number of zeros above the Nyquist frequency of an input surface and *shrinking* is achieved by discarding the high frequencies of an input surface that cannot be represented in the shrunk surface. These processes are briefly explained here for convenience.

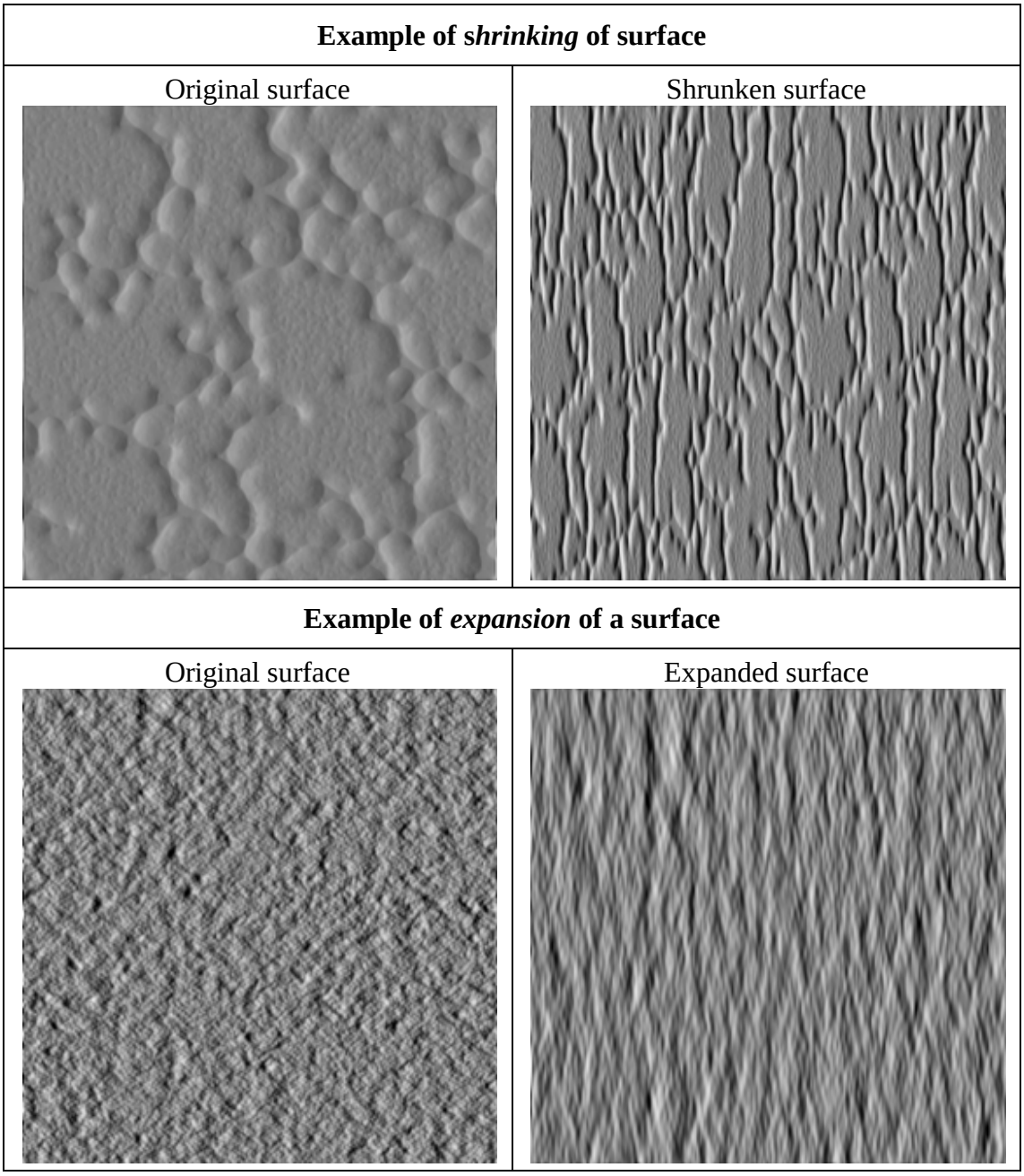

Figure 3-2: Examples of expansion and shrinking of surface height map.

The surface which is to be expanded or shrunk is called an input surface and denoted as $s_i(x, y)$. The corresponding discrete Fourier transform (DFT) is denoted as $S_i(u, v)$. Similarly, the expanded or shrunk surface is called an output surface and denoted as $s_o(x, y)$. The corresponding DFT is denoted as $S_o(u, v)$. For simplicity, the methods are explained in one-dimension (with one row of a surface) that can easily be applied to two-dimensions as the DFT of a 2D surface can be obtained by taking a 1D DFT of each row (or column) followed by a 1D DFT of each column (or row).

A row of an input surface $s_i(x, y)$ is treated as a 1D sequence of discrete data and denoted as $s_{ir}(x)$. A 1D DFT in the *x-direction* is performed with horizontal frequency (u), a 1D DFT of an input row $s_{ir}(x)$ is denoted as $S_{ir}(u)$. Similarly, an output row and its DFT is denoted as $s_{or}(y)$ and $S_{or}(u)$ respectively.

A row of an input surface with length N (even) is shrunk to a row of output surface with length N_s (even, $N_s < N$) by taking inverse DFT of $S_{or}(u)$ given by *Equation (3-1)*.

$$\left.\begin{aligned} S_{or}(u) &= (N/N_s)S_{ir}(u), \quad u = -(N_s/2)+1, .., (N_s/2)-1 \\ S_{or}(u) &= 0, \qquad\qquad\qquad u = -(N_s/2) \end{aligned}\right\} \tag{3-1}$$

A row of an input surface with length N (even) is expanded to a row of output surface with length N_e (even, $N_e > N$) by taking inverse DFT of $S_{or}(u)$ given by *Equation (3-2)*.

$$\left.\begin{aligned} S_{or}(u) &= (N/N_e)S_{ir}(u), \; u = -(N/2)+1, .., (N/2)-1 \\ S_{or}(u) &= 0, \qquad\qquad\qquad u = -(N_e/2), .., -(N/2) \;\&\; (N/2), .., (N_e/2)-1 \end{aligned}\right\} \tag{3-2}$$

The factors (N/N_s) and (N/N_e) are termed as shrinking factor (s_f) and expansion factor (e_f) respectively. The *Nyquist frequencies* are discarded during expansion and shrinking as suggested by Watson (1988) in his simpler sub-ideal algorithm for shrinking and expansion. The two dimensional version of these techniques, used to generate directional surfaces, is shown graphically in *Figure 3-3*. This is achieved by applying *Equations (3-1) and (3-2)* to each row (or column) of a 2D representation of frequency spectra. MATLAB codes of *expansion* and *shrinking* methods are given in *Appendix 3-A*. These techniques are used in the next subsection to obtain different sets of directional stimuli.

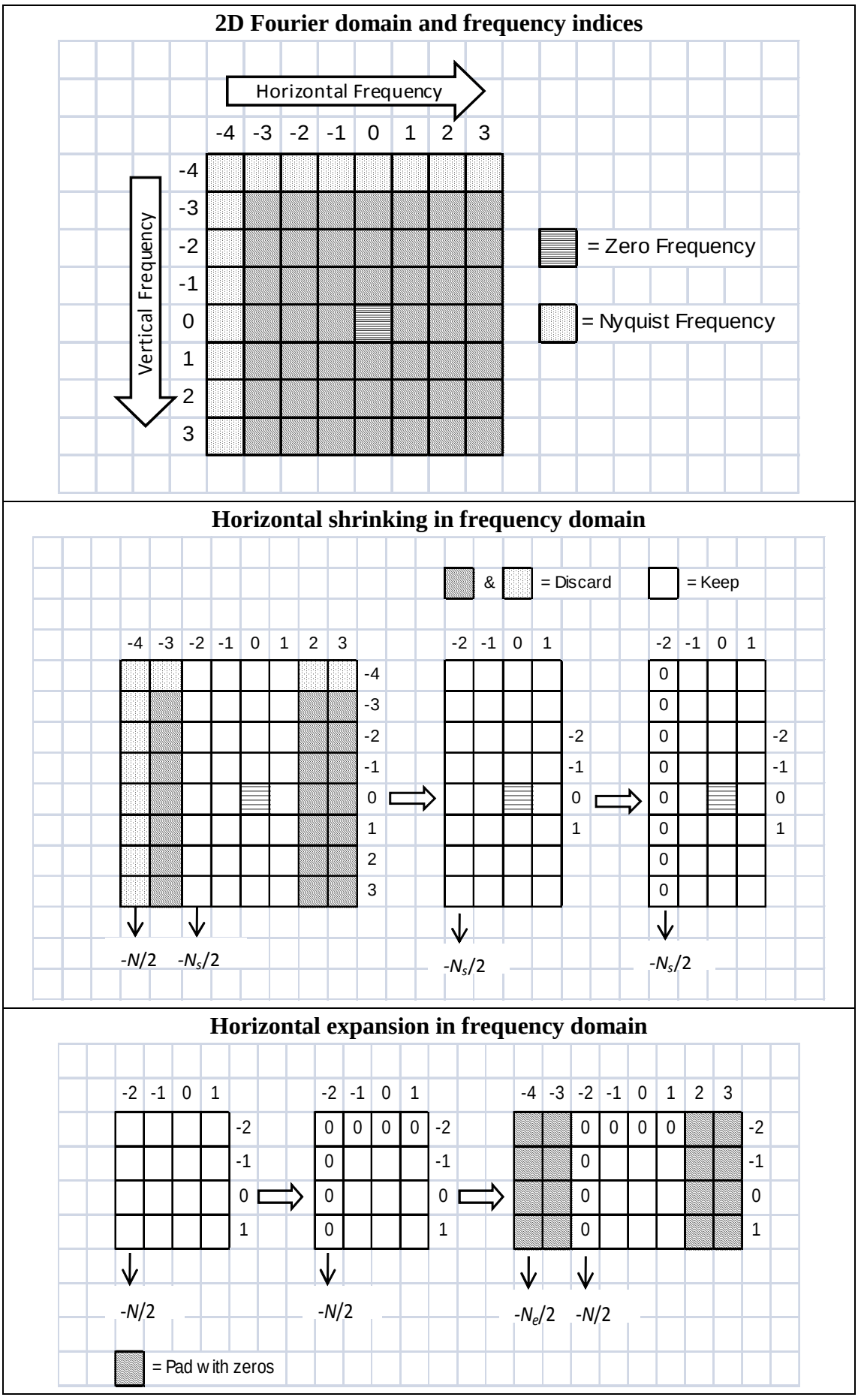

Figure 3-3: shrinking and expansion of surface in the frequency domain

3.1.2 Sets of Directional Stimuli

Six surface height maps, having a wide distribution of frequency components, were obtained using photometric stereo. Each of these height maps was then manipulated as shown in *Figure 3-4* to obtain five surfaces for each of six sets making a total of 30 test surfaces.

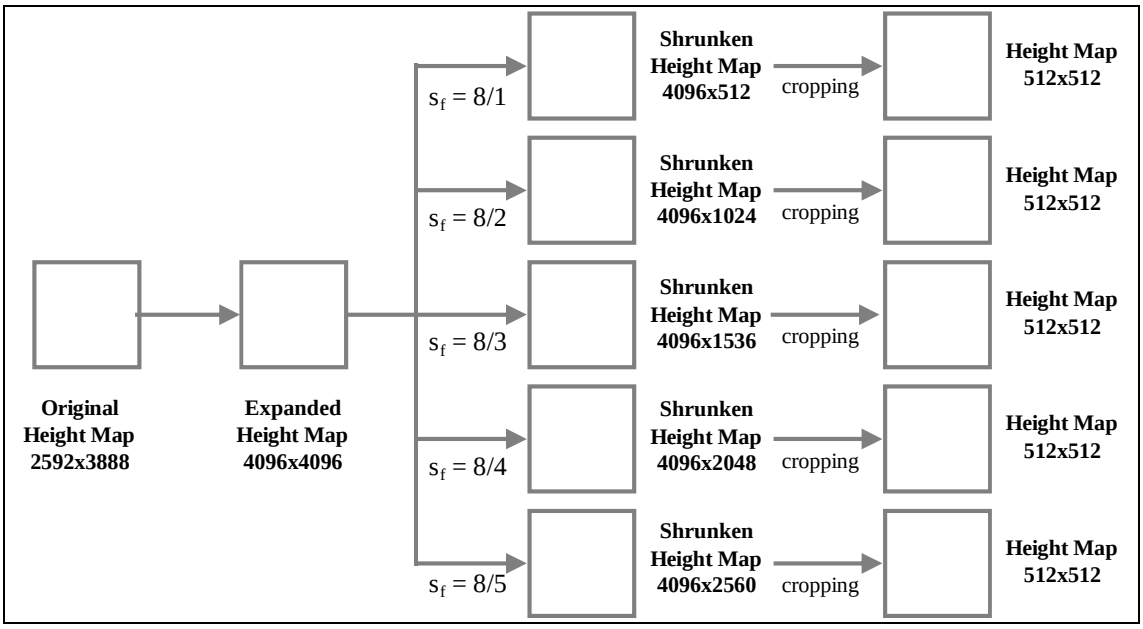

Figure 3-4: Illustration of steps to obtain surface height maps

The complete process of obtaining five surfaces from a height map is as follows: The size of an original height map was 2592x3888. To obtain five visually different surfaces, an original height map was first expanded to the size of 4096x4096. This height map was then shrunken in a horizontal direction by a factor of 8/5, 8/4, 8/3, 8/2 and 8/1 to create five new surfaces (see *Figure 3-5*). After shrinking, a 512x512 sized surface was cropped randomly from each shrunk surface height map. These 512x512 sized height maps were then low pass filtered to attenuate high frequencies to remove aliasing effects due to shrinking. The surfaces' average height (the arithmetic mean of a surface height map) was made equal to zero which was then adjusted to 2.5 cm (height of the stimuli stand) during rendering process (See section 3.3.1) to display all surfaces at the same height. Also, standard deviation of surface height maps was made equal to 0.02 cm. The surfaces from one set with final rendering in 3D (See section 3.3.1) are shown in *Figure 3-5*. The other surfaces are shown in *Appendix 3-B*.

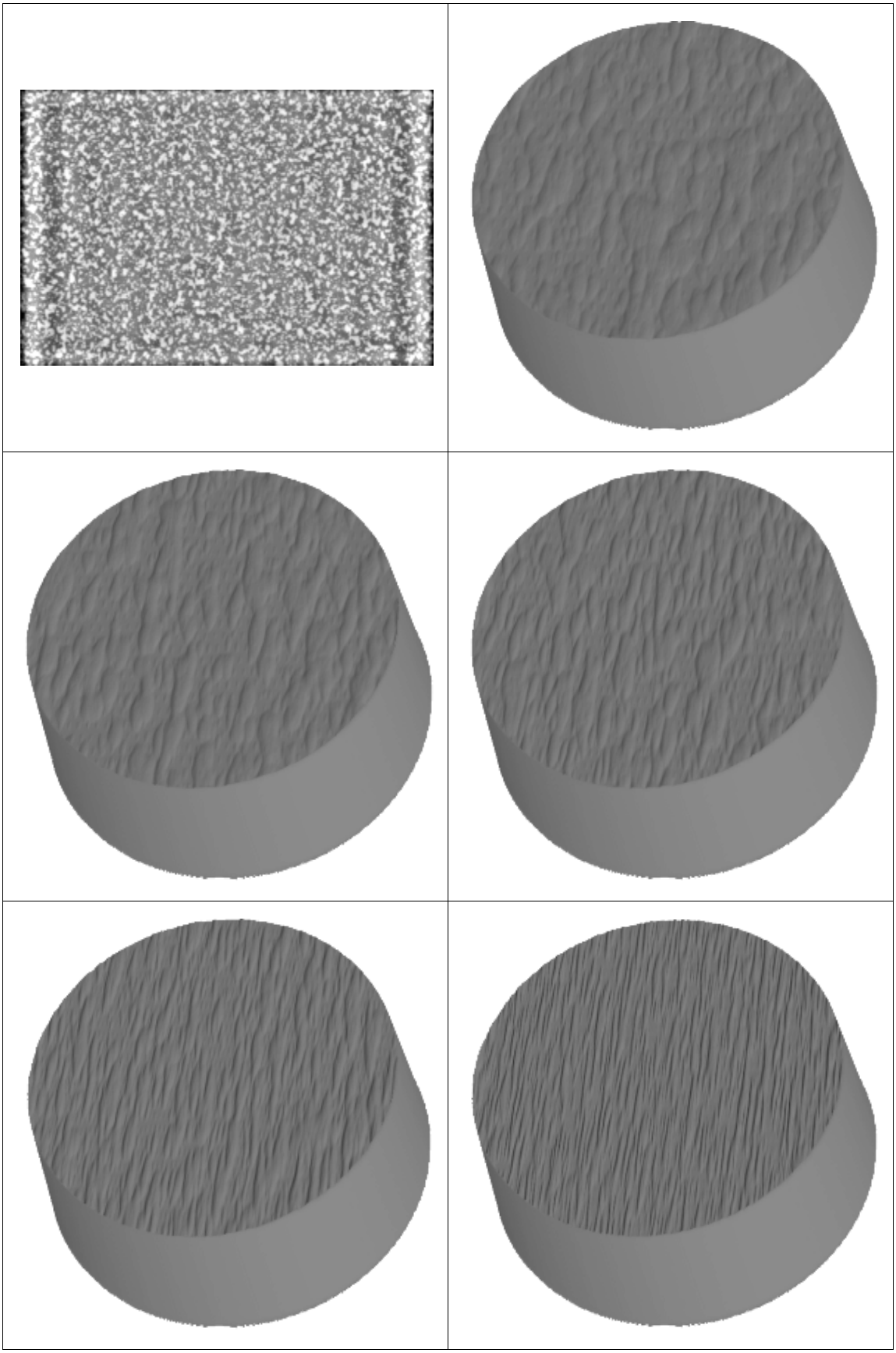

Figure 3-5: Animated surfaces from set 1. Surface height map used to generate five surfaces in the top left.

3.2 Obtaining Computational Directionality

The directional histograms and corresponding computational directionalities were obtained using Davis and Tamura's methods. The directional histograms for one set of surfaces are shown in *Figure 3-6*. The *Davis' variance* and *Tamura's variance* of all surfaces in all sets are plotted in *Figure 3-7*. Computational directionalities of surfaces with the same shrinking factor are plotted together and it can be seen that each set has different computational directionalities. It can be also noted that the surfaces with the same shrinking factor do not have same values of computational directionality. This is due to the fact that original surfaces of different sets had different distributions of frequency components.

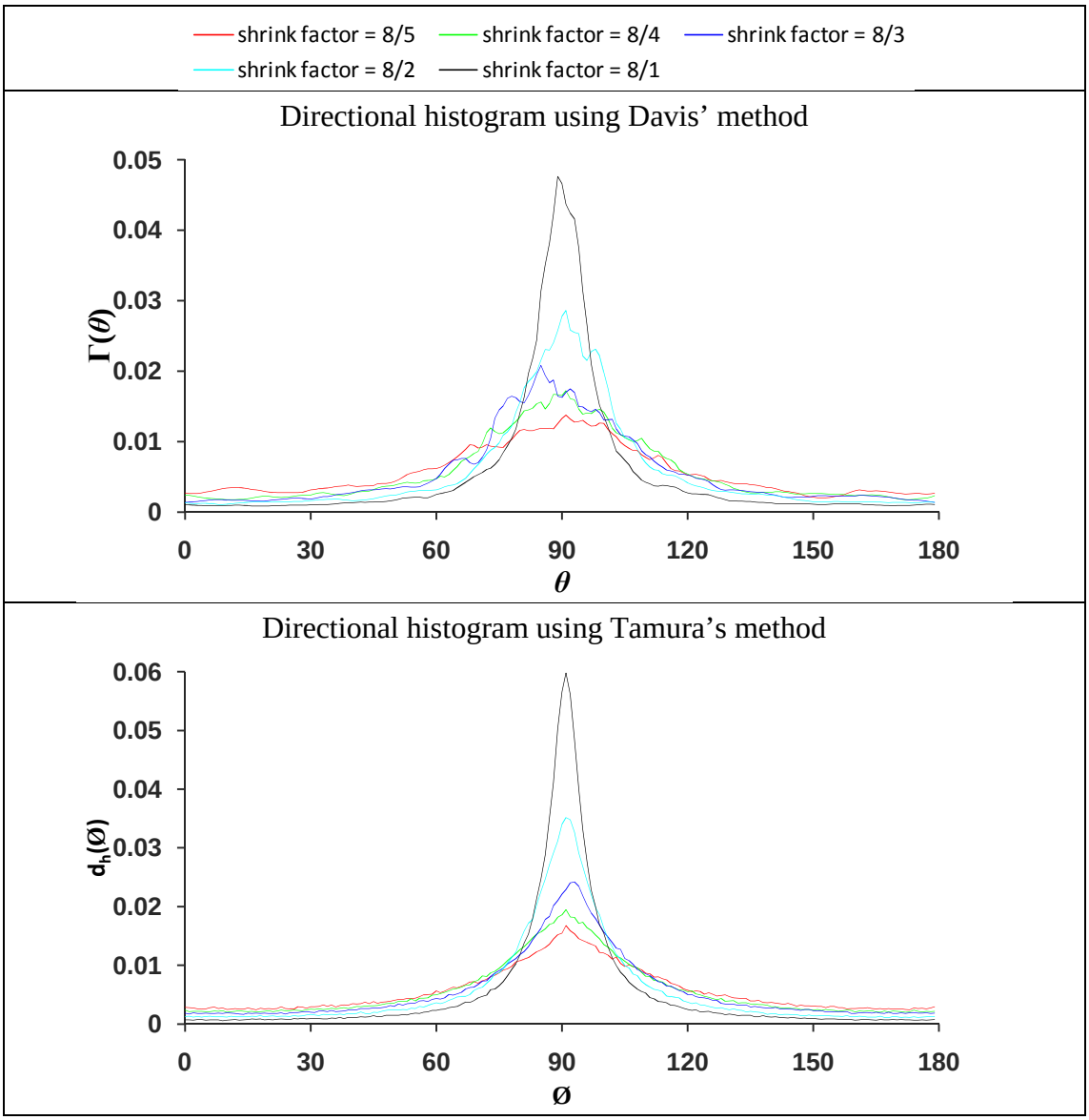

Figure 3-6: Directional histograms of the surfaces from set 1

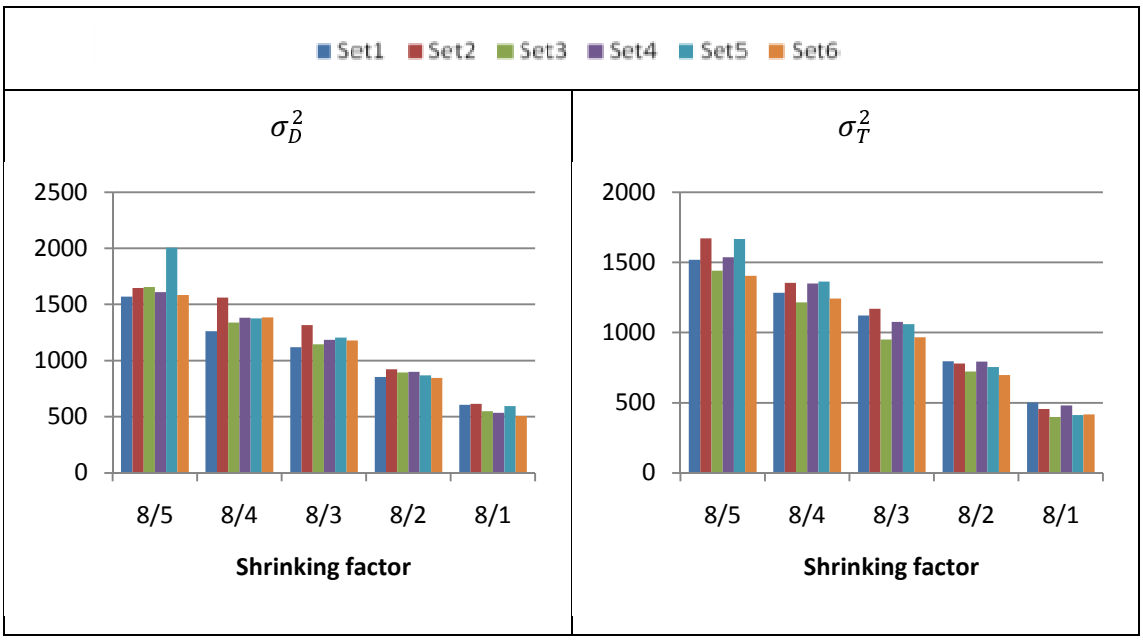

Figure 3-7: Computational directionality of surfaces from different sets

3.3 Psychophysical Experiment

In this section, the perceptual measurement of surfaces, produced in section 3.1, will be obtained by conducting a psychophysical experiment under controlled and consistent illumination conditions to avoid illumination biases in human responses as discussed in *chapter 2*. To achieve this, section 3.3.1 explains Padilla's (2008) method, section 3.3.2 describes the psychophysical method and scaling method used to assign a numeric values, *perceived directionality*, to surfaces, section 3.3.3 describes tools and arrangements for psychophysical experiment and finally section 3.3.4 reports how perceived directionalities of surfaces were obtained using the methodology described in this section.

3.3.1 Padilla's Surface Presentation Method

As stated in *chapter 2*, to overcome limitations due to illumination and viewpoint ambiguities during the perceptual investigation of directionality, surfaces will be rendered and animated in 3D as proposed by Padilla (Padilla, 2008). This is briefly described in this section and for complete explanation, the reader is requested to refer PhD thesis of Padilla (2008).

To cover all radial frequencies necessary for human visual acuity (0.1 to 30 *cycles per degree*) as specified by Campbell and Robson (1968), the sizes of surfaces are kept to 512x512 (13.056 *cm* on the display screen) and presented on a small display screen with high resolution (1200x1600 with a pixel size of 0.255 *mm*) at a fixed viewing distance of 88 *cm* as it was employed by Padilla (2008) in the investigation of perceived roughness. The radial frequencies in this thesis will be described in *cycles per degree (cpd)* instead of *cycles per image width (cpi)* as the experiments will have a fixed viewing distance (see section 3.3.3). The conversion from *cpi* to *cpd* is explained in section 3.3.3.

To render the surfaces in 3D, the following definition of the Lambertian model with a constant illumination comprising of a single point source was used.

$$I_{lambert} = k_d \cdot \max(0, l_s \cdot n_s) \tag{3-3}$$

In *Equation (3-3)*, k_d is the percentage of reflected diffuse light, l_s is the light vector and n_s is the normalised surface normal vector. The surface unit normal vector is given by *Equation (3-4)*, where p_x and q_y are the partial derivatives of surface in the *x-direction* and *y-direction* respectively.

$$n_s = \left(\frac{p_x}{\sqrt{1 + (p_x)^2 + \left(q_y\right)^2}}, \frac{q_y}{\sqrt{1 + (p_x)^2 + \left(q_y\right)^2}}, \frac{1}{\sqrt{1 + (p_x)^2 + \left(q_y\right)^2}} \right) \tag{3-4}$$

The partial derivatives of surfaces are calculated in frequency domain and transformed into spatial domain in order to preserve the high frequency data. MATLAB code to calculate the partial derivatives is given *Appendix 3-C*. Cast shadows are calculated using shadow mapping technique given in PhD thesis of Padilla (2008). The surfaces are rendered on the circular stimuli stand of height 2.5 cm as shown in *Figure 3-8* to avoid any biasing effect at the edges of surfaces. The surfaces are animated to enhance depth perception and to perform a pre-defined *wobble* (motion of a surface as described in PhD thesis of Padilla (2008)). Padilla captured this motion from observers evaluating perceptual characteristics of surfaces displayed using the real-time graphics in a *free-play* mode.

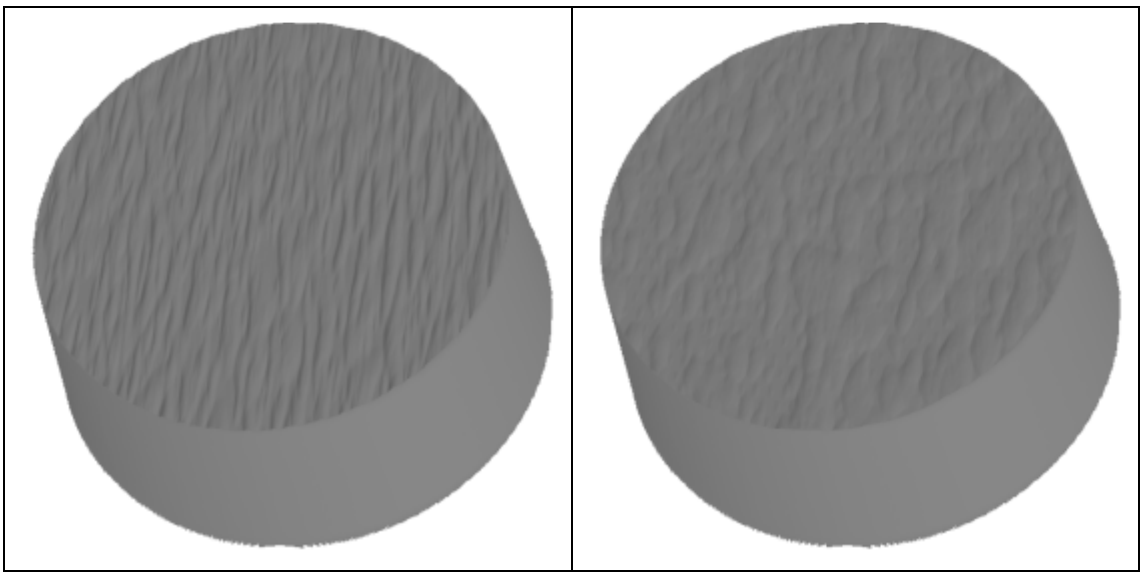

Figure 3-8: The surfaces rendered in 3D on 2.5 cm stimuli stand using Padilla's surface presentation method

3.3.2 Psychophysical experiment and scaling method

Psychophysical experiment and scaling methods are used to measure sensory attributes of physical stimulus such as perceived directionality of surfaces. Among many different psychophysical methods (Pelli and Farell, 1995; Gescheider, 1997; Ehrenstein et al., 1999) and scaling methods ((Torgerson, 1958; Maloney and Yang, 2003; Irtel, 2005), the *method of pair-wise comparisons* and *direct ratio estimation* (Torgerson, 1958) were used to measure perceived directionality of surfaces from six sets. These methods produce interval scales that provide relative difference between perceptual magnitudes of a sensory attribute.

The *method of adjustment* and *magnitude/ratio production methods* are not candidate method because of the difficulty of varying directionality in real-time. The *method of limits* is time consuming and a large number of surfaces would be required for each set of surfaces. Probability based methods such as *maximum likelihood difference scaling* (Maloney and Yang, 2003) are also time consuming and demand a large number of surfaces. The disadvantage of the *pair-wise comparisons* method is that number of pairs increases considerably as number of stimuli increases. However, number of pairs of surfaces for experiment in this chapter is low.

An alternative to the *method of pair-wise comparisons* is the *method of constant stimuli*. In the latter, one stimulus, known as *standard* stimulus, is kept fixed and the other stimuli, known as *comparison* stimuli, are compared to *standard* stimulus, while in the *method of pair-wise comparisons*, each stimulus is compared to all other stimuli. Therefore, the *method of pair-wise comparison* can produce more reliable results compared to the *method of constant stimuli*, while the *method of constant stimuli* is suitable when number of stimuli is large.

Next, the method of deriving a perceptual scale of a sensory attribute using *pair-wise comparisons* of stimuli and the *direct ratio estimation* method is described. Observers provide a ratio of sensory magnitudes of stimuli i and j, (called the *sense-ratio* $s_r(i,j)$) for each stimuli pair (i,j) presented. The perceptual scale of stimuls i is obtained by taking a geometric mean of sense-ratios of stimulus i with all other stimuli j (see *Equation (3-5)*).

$$p_s(i) = \left(\prod_{j=1}^{j=t} s_r(i,j) \right)^{1/t} \tag{3-5}$$

To reduce number of pairs to be presented, it is assumed that the *sense-ratio* of stimulus with itself is equal to one ($s_r(i,i) = 1$) and the *sense-ratio* of stimulus i and stimulus j is equal to one divided by the *sense-ratio* of stimulus j and stimulus i ($s_r(i,j) = 1/s_r(j,i)$). Hence no stimulus is paired with itself and two stimuli are paired only once to obtain either $s_r(i,j)$ or $s_r(j,i)$. Thus for t stimuli, $C(t,2) = t!/((2!)(t-2)!)$ pairs are presented. $C(t,2)$ is number of combinations of any 2 stimuli from t stimuli without repetitions and $t!$ is the factorial of t.

3.3.3 Tools Used for the Experiment

This section explains how experiments were conducted using calibrated tools under an environment free of all possible distractions.

The surfaces were presented with a black background and experiments were conducted in a dark room to avoid distractions. Two TFT screens (NEC MultiSync LCD2090UXi)

with a resolution of 1200x1600 and 0.255*mm* square pixels were used at a display distance of 88 cm from the observer to provide an angular resolution of approximately 30 cycles per degree at the retina. The screens were calibrated to a linear gamma and had a maximum luminance of 120cd/m^2. The Gretag-Macbeth Eye-One Pro spectrometer was used to calibrate screens. For this viewing distance, the conversion formulae between radial frequency in *cpd* and radial frequency in *cpi* is given by *Equation (3-6).* The geometry from which *Equation (3-6)* is derived is shown in *Figure 3-9* along with the mathematical steps.

$$f(cpd) = (60/512)\, f(cpi) \tag{3-6}$$

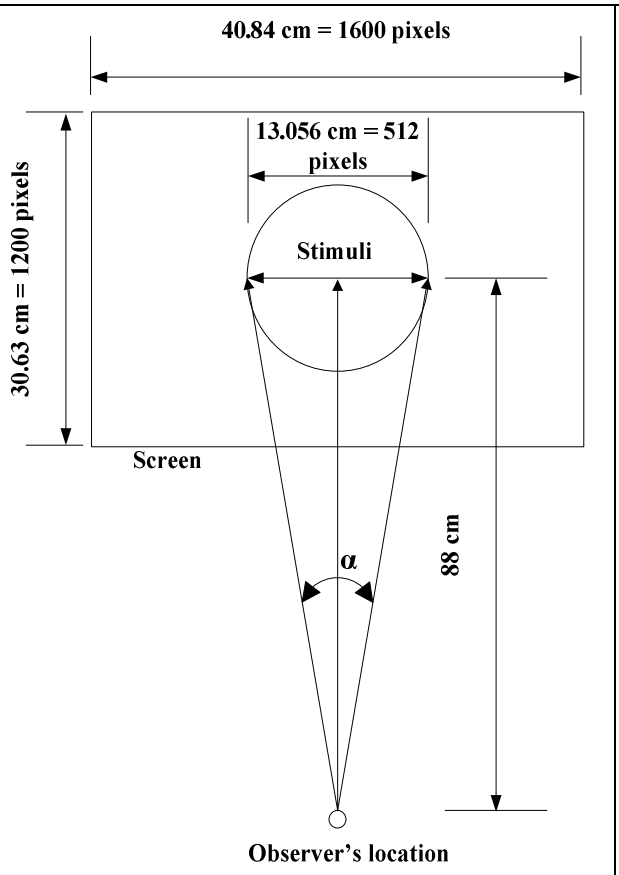

Mathematical steps for conversion formulae given in *Equation (3-6)*

1. $\tan\left(\frac{\alpha}{2}\right) = \frac{13.056/2}{88}$
2. $\alpha = 8.5101\ degree = 512\ pixels$
3. $1\ degree \cong 60\ pixels$
4. $1\ image\ width = 512\ pixels$
5. $1\ degree \cong 60/512\ image\ width$

Figure 3-9: The geometry of the experimental set up and derivation of conversion formulae between cpi and cpd

To render the surfaces, OpenGL 2.0 was used and the interface was programmed by Padilla (Padilla, 2008) in C++. This interface was modified to record responses from an

observer. The observers were provided with a normal keyboard and used arrow and numeric keys to answer the questions asked.

MATLAB was used to obtain surface height maps and surface normal vectors. MATLAB was also used to process responses from the observers. The DEVIL image library was used to incorporate surface height map generated using MATLAB into the rendering program. Two NVIDIA cards (GeForce 8800 GT) and Intel processor (Core 2 Quad CPU Q6600 @ 2.4 GHz) with 3GB RAM were used.

3.3.4. Perceived Directionality

In this section, changes in perceived directionality are compared with changes in the two computational directionalities.

The perceived directionality of each manipulated surface was obtained using the direct ratio estimation method described previously. Four naïve observers with normal or corrected to normal vision were asked to compare the two surfaces displayed side by side, and to answer the following two questions:

1. Which of these two surfaces is more directional?
2. How many times (>1) is that surface more directional than the other?

The surfaces were animated as explained earlier. The observers did not know how the surfaces had been produced. They were instructed to use their own scale of ratios, without any minimum and maximum being specified except that the minimum had to be greater than 1. To make a task easier and to make observers familiar with surfaces, trial pairs were shown to observers before starting an experiment. During an experiment, each surface from a given set was compared with all the other surfaces from the same set. As we wish to compare the relationship between computational directionality and perceptual measurement of directionality across different sets of stimuli, the pairs from all six sets were presented in one single experiment, to ensure that perceptual ratio scales of subjects remained same across different sets.

As each set contained 5 surfaces, a total of 10 surface pairs were possible without repetitions of surfaces. Since there were six sets, there were a total of 60 (10 times 6)

pairs of surfaces. Each pair was presented twice to the observers. To reduce any bias in the sequence of pairs, their order was randomised. The position (left or right) of each surface in a pair was also randomised. Observers were instructed to key in the response for a given pair within 20 seconds, but they were not prevented from taking more time if they found it difficult to choose a suitable response. After 20 seconds the animation was stopped to give a notice to an observer that 20 seconds was over and that they should provide a response and proceed.

The order of surfaces and corresponding responses given by observers are given in *Appendix 3-D*. The process of obtaining perceived directionality of these surfaces is given below.

As observers were allowed to use different ranges of values for their responses, the responses of all observers were normalised between common minimum and maximum values (denoted as $R_{N,min}$ and $R_{N,max}$ respectively). These values can be chosen arbitrarily ($R_{N,min} > 1$) as the purpose is only to derive observers' responses within the same range of values. Here $R_{N,min}$ and $R_{N,max}$ were obtained from minimum and maximum responses of all observers respectively as shown by *Equation (3-7) and (3-8)* respectively.

$$R_{N,min} = \left(\prod_{i=1}^{N_o} (R_{U,min})_i \right)^{1/N_o} \tag{3-7}$$

$$R_{N,max} = \left(\prod_{i=1}^{N_o} (R_{U,max})_i \right)^{1/N_o} \tag{3-8}$$

In *Equations (3-7) and (3-8)*, N_o is number of observers, $R_{U,min}$ and $R_{U,max}$ are the minimum and maximum values of non-normalised responses of each observer. The observers' responses were then normalised using *Equation (3-9)* where R_U and R_N are non-normalised and normalised responses of the given observer respectively.

$$R_N = \frac{R_U - R_{U,min}}{R_{U,max} - R_{U,min}} \left(R_{N,max} - R_{N,\min}\right) + R_{N,min} \qquad (3\text{-}9)$$

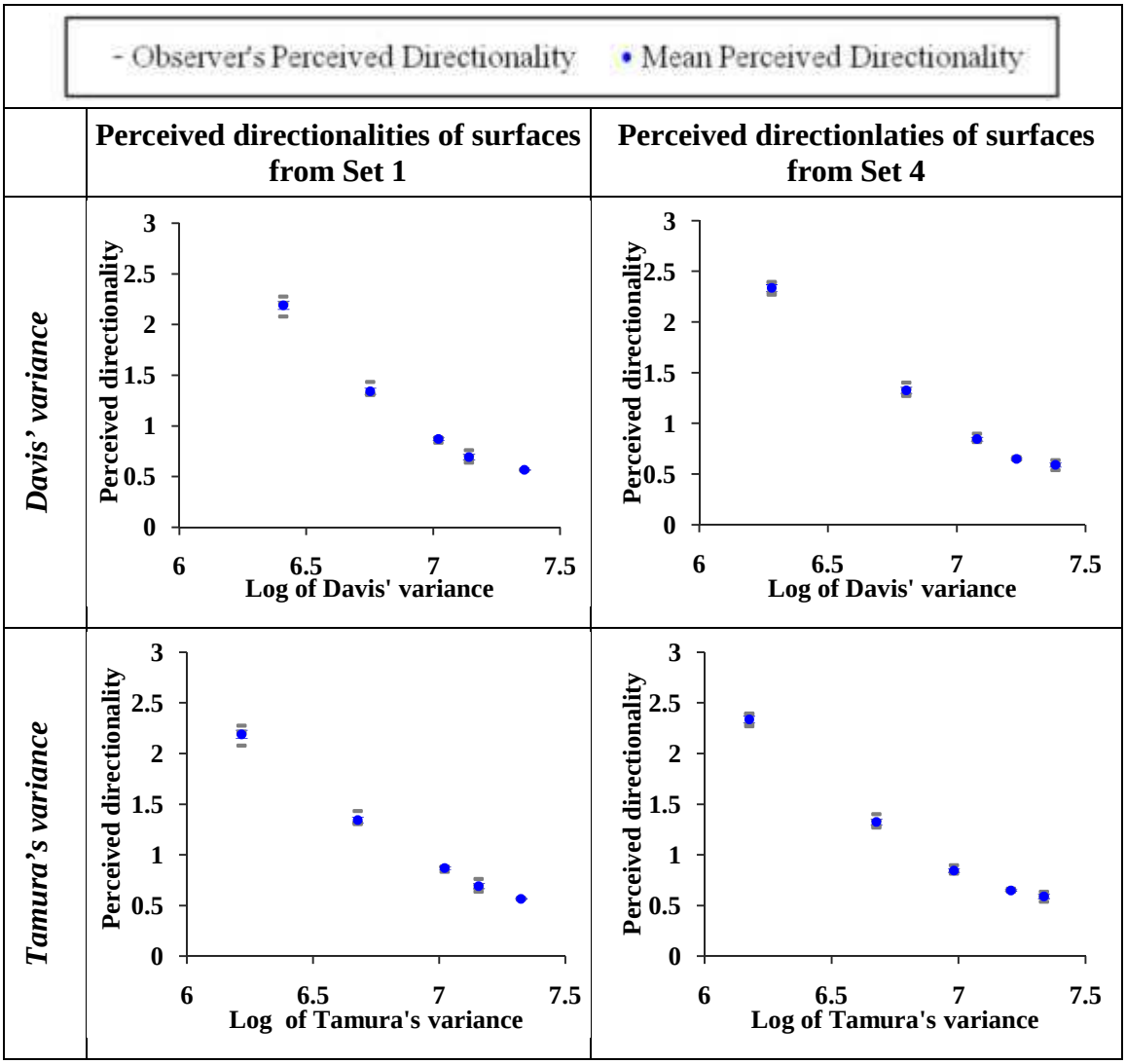

Figure 3-10: The relationship between perceived directionality (ρ) and logarithm of computational directionality. The error bars represent the standard errors of mean.

After normalisation, the response ratios for different sets were separated. As each pair from set was repeated twice, the ratio of perceived directionality of the two surfaces was obtained by taking geometric mean of the two. From these ratios, the *observers' perceived directionality* (ρ_o) was obtained as explained in section 3.3.2. As the perceptual scale of directionality (see *Figure 3-10*) is an interval scale, the *perceived directionality* of a surface, called a *mean perceived directionality* (ρ), was obtained by taking arithmetic mean of *observers' perceived directionality* values. These values are given in *Appendix 3-E*. *Figure 3-10* shows change in perceived directionality with

change in the logarithm of *Davis's variance* (log (σ_D^2)) and the logarithm of *Tamura's variance* (log (σ_T^2)) for two of the six sets. *Appendix 3-F* shows the plots for remaining sets.

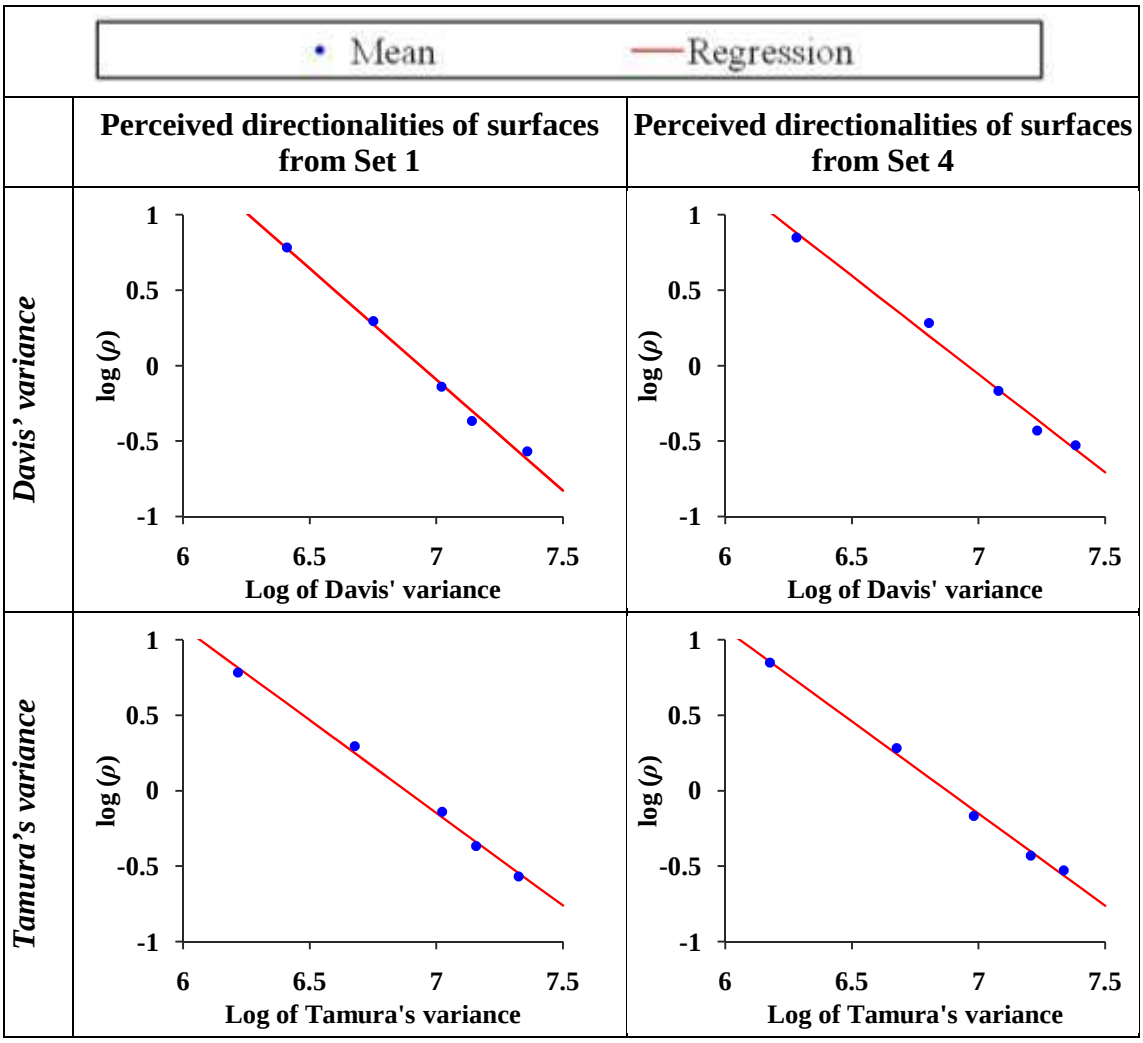

Figure 3-11: Linear regression on $log(\rho)$ when plotted against the logarithm of computational directionality

Several functions were used to establish the relationship between ρ and computational directionalities (σ_D^2 and σ_T^2). A decaying exponential relationship was found between ρ and the logarithm of the two computational directionality, σ_D^2 and σ_T^2. Therefore a linear regression was applied to log (ρ) and the logarithm of the best fit values ρ_{fit} was obtained. The slopes (m_D and m_T) and constants (C_D and C_T) of the linear regression associated with the variances σ_D^2 and σ_T^2 are given in *Table 3-1* and *Table 3-2* respectively. A linear fit to log (ρ) for the two computational directionalities is

shown in *Figure 3-11* for set 1 and set 4. *Appendix 3-G* shows the plots for the remaining sets.

	Set 1	Set 2	Set 3	Set 4	Set 5	Set 6
C_D	10.21	10.53	9.80	9.06	5.70	8.43
m_D	-1.473	-1.496	-1.410	-1.302	-0.813	-1.218
R^2-*Stat*	0.993	0.995	0.980	0.989	0.954	0.985

Table 3-1: Regression results when observing the relationship with σ_D^2

	Set 1	Set 2	Set 3	Set 4	Set 5	Set 6
C_T	8.457	8.293	8.045	8.398	4.698	7.753
m_T	-1.229	-1.202	-1.189	-1.221	-0.686	-1.145
R^2-*Stat*	0.995	0.998	0.986	0.996	0.959	0.996

Table 3-2: Regression results when observing the relationship with σ_T^2

It can be seen from regression results given in *Table 3-1* and *Table 3-2*, that relationship between perceived directionality and two computational directionalities are not identical for each set. In order to determine whether the differences are significant, a two-way repeated measure analysis of variance (ANOVA) is performed in the next section. If the differences are not significant then the relationship can be used as a measurement model of perceived directionality otherwise it cannot. The information about the repeated measure ANOVA and its terminology used in this thesis can be found in a book written by Field (2005).

3.4 Statistical Significance test

3.4.1 Analysis

For repeated measure analysis, perceived directionality was considered as the dependent variable. As the objective is to find whether the differences in relationship between perceived directionality and computational directionality across sets are significant,

computational directionality (σ_D^2 and σ_T^2) and *set of surfaces* were considered as the independent variables.

The repeated measure analysis requires independent variables to have the same quantitative or categorical value across the observers and the other independent variable. The measure of directionality is a quantitative value and its value must be same across different sets. However, because the *shrinking* process, used to generate stimuli within each set, does not control these measures directly, they are not the same within each set. As a result, *observers' perceived directionality* (ρ_o) could not be obtained at the same levels of *Davis's variance* and *Tamura's variance* across different sets.

This problem was addressed by sampling from the functions fitted to each observer's perceived directionality. A linear regression was performed on $\log(\rho_o)$ and the results for all observers and for all sets are given in *Appendix 3-H*. The perceived directionality was then obtained at six levels of measure of directionality ($\log(\sigma_D^2)$ and $\log(\sigma_T^2)$ = 6, 6.3, 6.6, 6.9, 7.2, 7.5) using regression results.

The results of ANOVA are given in *Table 3-3*, which shows effects of $\log(\sigma_D^2)$ and stimulus set on perceived directionality. As *Mauchly's test* indicates that the assumption of sphericity is violated, the significance values were corrected using *Greenhouse – Geisser* and shown in *Table 3-3*. It can be seen that both independent variables have significant effects ($p < 0.05$) on perceived directionality. There is also a significant effect ($p < 0.05$) of the interaction between independent variables.

A similar analysis was performed to test effects of $\log(\sigma_T^2)$ and set of surfaces, and the results are shown in *Table 3-4.* Again it can be seen that both variables have a significant effect ($p < 0.05$) on perception of directionality, and that an interaction term has also a significant effect ($p < 0.05$).

Assumption of sphericity		*F - Statistics*	*Sig. Value* (p)
$\log(\sigma_D^2)$	Greenhouse-Geisser	951.253	**<0.001**
Set	Greenhouse-Geisser	49.315	**<0.001**
($\log(\sigma_D^2)$) (*Set*)	Greenhouse-Geisser	39.485	**0.001**

Table 3-3: Tests of within-subjects effects: $\log(\sigma_D^2)$ and set of surfaces

Assumption of sphericity		*F - Statistics*	*Sig. Value* (p)
log (σ_T^2)	Greenhouse-Geisser	1016.691	**<0.001**
Set	Greenhouse-Geisser	92.591	**<0.001**
(log (σ_T^2)) (Set)	Greenhouse-Geisser	39.482	**0.001**

Table 3-4: Tests of within-subjects effects $log(\sigma_T^2)$ and set of surfaces

The results of ANOVA show that both computational directionalities have significant effects on observers' perception of directionality. However, in both cases, stimulus set has also a significant effect on perceived directionality, and so the relationship between perceived directionality and two computational directionalities is not consistent across the different sets of surfaces.

3.4.2 Discussion

The results of an experiment imply that other variables, differing between the types of surfaces, must also be affecting human perception of directionality. There are many physical parameters that can affect appearance of a surface and hence affect perception of surfaces, and it is difficult to say which parameters are affecting the perception of directionality of surfaces. However, in this chapter, it was observed that a surface with a concentrated distribution of frequency components in one direction is perceived as a more directional than a surface with a wider distribution of frequency components.

Hence it can be said that physical parameters representing the distribution of frequency components in magnitude spectrum are very important when perceiving the directionality of a surface. The surfaces for a psychophysical experiment were obtained by *shrinking* a surface in horizontal direction, which changes both angular and radial location of frequency components in the magnitude spectrum. As the distribution of angular and radial frequency components were changed together, it is not clear how this information was used by observers when perceiving the directionality of surfaces. Therefore controlled changes in the distribution of frequency components need to be investigated to find out what matters when perceiving the directionality of surface texture.

Surface in the frequency domain is described by both magnitude spectrum and phase spectrum, where magnitude spectrum specifies amplitude of sinusoids and phase spectrum specifies position of those sinusoids. These sinusoids are superimposed to give a surface in the spatial domain. As phase spectrum specifies relative positions of sinusoids, the appearance of surface is significantly affected by phase spectrum particularly when surfaces are structured (Clarke, 1992; Kovesi, 1999)**.** Therefore it is possible that phase spectrum is also affecting the perception of directionality.

The surfaces used in a psychophysical experiment had equal standard deviation of height which is a mathematical measure of the RMS roughness, δ, (Padilla et al., 2008; Padilla, 2008). The RMS roughness is given by *Equation (3-11)* , where $s(x,y)$ is surface height at point (x,y) and μ_s is mean height of a surface given by *Equation (3-10).* As zero RMS roughness produces a planar surface, associated surface characteristics disappear and therefore this term also could be playing an important role in the perception of directionality.

$$\mu_s = \frac{1}{ab}\sum_{x=1}^{x=a}\sum_{y=1}^{x=b} s(x,y) \tag{3-10}$$

$$\delta = \sqrt{\frac{1}{ab}\sum_{x=1}^{x=a}\sum_{y=1}^{x=b}(s(x,y)-\mu_s)^2} \tag{3-11}$$

The separate and combined effects of the frequency distributions in magnitude spectrum, the phase spectrum and the RMS roughness need to be investigated to find out which of them are related to perception of directionality and in which combination they affect perception of directionality. The surfaces used for a psychophysical experiment in this chapter are not suitable for an independent investigation, as phase spectrum, distributions of angular and radial frequency components were not changed independently.

The parameters can be regulated independently if synthetic surfaces defined by a mathematical model are used. The next chapter discusses how independent effects of parameters possibly affecting perception of directionality will be investigated using

synthetic surfaces. The effect of distribution of angular frequency components and RMS roughness on the perception of directionality is also investigated in the next chapter.

3.5 Summary

In this chapter, a psychophysical investigation was carried out to determine if there is any relationship between perceived directionality and two computational directionalities (σ_D^2 and σ_T^2). For this, six sets of five directional height maps were created from height maps obtained from real surfaces. These height maps were rendered and animated in 3D under the same illumination conditions to give observers an impression of real surfaces and to avoid any bias due to different illumination conditions.

The following conclusions were obtained from the psychophysical investigation.

1. *Davis' variance* (σ_D^2) and *Tamura's variance* (σ_T^2) both have significant correlation with the perception of directionality.
2. The relationship between perceived directionality and two computational directionalities is not consistent across different sets of stimuli.

Therefore the chapter concludes that further investigation using synthetic stimuli is required to observe the independent and combined effects of the following variables, which possibly affect perception of directionality.

1. The parameters describing distribution of angular frequency components.
2. The parameters describing distribution of radial frequency components.
3. The phase spectrum.
4. The RMS roughness.

Chapter 4

Psychophysical Investigation using Synthetic Surfaces: Effects of Angular Distribution of Frequency Components and RMS roughness

As discussed in *chapter 3*, manipulation of height maps obtained from real surfaces does not allow good control of either magnitude spectrum or phase spectrum, and so the effects of these properties on the perception of a surface directionality cannot be established. An alternative approach is to create synthetic surfaces defined by mathematical models with parameters that can be varied independently in order to investigate their perceptual effects.

Therefore, this chapter proposes how the investigation using synthetic surfaces will be carried out and reports the effects on perceived directionality due to variation in distribution of angular frequency components and RMS roughness of synthetic surfaces.

The chapter is organised as follows: In section 4.1, the criteria for a mathematical model of synthetic directional surfaces suitable for testing the effects of physical parameters, discussed in *chapter 3*, on perception are proposed. This section also describes how the investigation will be carried out in this and subsequent chapters. Section 4.2 discusses synthesis of directional random-phase surfaces and section 4.3 investigates the effects of random phase, angular variance (σ^2) and RMS roughness (δ) individually on the perception of directionality. The effect of varying both angular variance and RMS roughness is then investigated.

4.1 Criteria for Psychophysical Investigation using Synthetic Directional Surfaces

Surfaces generated using a parametric model allow us to observe change in the appearance of a surface due to change in the values of its parameters. To carry out such investigations, the following criteria will be considered for a surface model.

1. As discussed in *chapter 3*, the distributions of angular and radial frequency components in magnitude spectrum, phase spectrum and RMS roughness may affect perception of directionality. Therefore, the separate and combined effects of these terms on perception of directionality need to be observed. In the first case, each parameter is varied while holding the other constant and in the second case, all are varied together in one experiment. To achieve this, a mathematical model of the surfaces must be defined in such way that each of the terms mentioned above can be regulated independently of the other terms.
2. The main goal of this thesis is to develop a psychophysically based measurement model of perceived directionality. To use this model in an application such as automated retrieval of surfaces, it must be possible to estimate the parameters of a surface model from an unknown surface.
3. Different kinds of surfaces are seen in the real world. They can be *natural* (e.g. rock surfaces, sand waves, wooden surfaces etc.) or *man-made* (e.g. wall papers, carpets etc.). In this thesis, *natural* surfaces means they are not made by human as described in MONAT (Measurement of Naturalness) project at National Physical Laboratory (Goodman *et al.*, 2008). The mathematical model can be defined to generate surfaces which look like either *natural* or *man-made* surfaces. In this thesis, synthetic surfaces will have random phase spectrum which produces *natural* looking surfaces. In practice, a limit must be placed on the range of possible magnitude spectra in order to ensure that the appearance of surfaces look like natural surfaces i.e. *naturalistic*.

The mathematical model of surfaces can be specified either using spatial domain descriptions (Mandelbrot, 1982; Saupe, 1988) or frequency domain descriptions (Kube and Pentland, 1988; Mulvaney *et al.*, 1989; Ogilvy, 1991; McGunnigle, 1998; Wu, 2003). However:

1. Spatial domain descriptions of surfaces are often based on texton placement rules. The structural information in these kinds of surfaces contains phase information (Clarke, 1992; McGunnigle, 1998; Kovesi, 1999). Hence these surfaces are good candidates for investigating phase spectra effects. However these kinds of surfaces are not suitable for investigating the effects of angular and radial frequency distributions because the placement rules do not give

control over distributions of angular and radial frequency components independently.

2. In frequency domain methods, magnitude and phase spectra must be described and combined to generate frequency spectra. These frequency spectra are inverse Fourier transformed to generate surfaces. However phase spectrum is a very complex term and is difficult to describe and control directly. Hence phase spectra are often simply randomised. As random phase spectra generate unstructured surfaces (such as rock surfaces) and such surfaces have little or no information in their phase spectra (Clarke, 1992), these surfaces are not suitable for investigating the effect of phase spectra.

It is beyond the scope of this thesis to identify and investigate how information in phase spectrum of a surface is related to the perception of directionality. Therefore frequency domain methods with random phase spectra will be considered throughout this thesis.

Surfaces based on the following kind of frequency domain description are suitable for the investigation of separate and combined effects of distributions of angular and radial frequency components and RMS roughness:

$$M(f,\theta) = D(f)\,D(\theta)\left(\frac{\delta}{\delta_n}\right) \tag{4-1}$$

$$P_R(f,\theta) = \text{Random Numbers} \tag{4-2}$$

Where f and θ are the polar co-ordinates of 2D frequency and specify radial and angular frequency respectively. They are given below in terms of Cartesian co-ordinates of 2D frequency space, u and v.

$$f = \sqrt{u^2 + v^2} \text{ and } \theta = \tan^{-1}(v/u) \tag{4-3}$$

A random phase spectrum $P_R(f,\theta)$ will be generated using MATLAB random number generator as shown in *Appendix 4-A*. The different instances of random phase spectrum can be generated using the MATLAB internal state (seed) of uniform pseudorandom number generator. This description in Polar co-ordinates is converted to Cartesian co-

ordinates and the complex conjugate symmetry is added to obtain the Fourier Transform of a surface height map.

$D(f)$ and $D(\theta)$ specify magnitude of radial and angular frequency components, respectively. The term (δ/δ_n) controls RMS roughness of surfaces where δ is desired RMS roughness of a surface generated and δ_n is a normalisation factor (RMS roughness of a surface height map associated with the magnitude spectrum as $D(f)D(\theta)$). The value of δ_n can be calculated either using *Equation (4-4)* or by measuring standard deviation of a surface height map obtained from $D(f)D(\theta)$.

$$\delta_n = \sqrt{\frac{\sum_{f,\theta}\left(\frac{|D(f)D(\theta)|^2}{ab}\right)}{ab}} \tag{4-4}$$

Where, a and b are number of rows and columns of a surface height map respectively. The magnitude spectrum specified by *Equation (4-1)* also satisfies the second criterion for parameter estimation of unknown surfaces. If it is assumed that an unknown surface has distribution of frequency components in form of magnitude spectrum described by *Equation (4-1)*, then RMS roughness, distributions of angular and radial frequency components can be estimated as described below.

1. **RMS roughness:** If RMS roughness measured from surfaces is specified as estimated RMS roughness (δ_{est}), then δ_{est} can be obtained by calculating standard deviation of a surface height map.
2. **Distribution of angular frequency components:** An estimated distribution of angular frequency components $D_{est}(\theta)$ can be calculated by summing magnitude spectrum along radial frequency as described below. f_{max} and f_{min} are the maximum and minimum radial frequency. θ_{max} and θ_{min} are the minimum and maximum angular frequency.

$$D_{est}(\theta) = \frac{\sum_{f_{min}}^{f_{max}} M(f,\theta)}{\sum_{f_{min}}^{f_{max}} \sum_{\theta_{min}}^{\theta_{max}} M(f,\theta)} \tag{4-5}$$

$$\Rightarrow \qquad D_{est}(\theta) = \frac{\sum_{f_{min}}^{f_{max}} D(f)\, D(\theta) \left(\frac{\delta}{\delta_n}\right)}{\sum_{f_{min}}^{f_{max}} \sum_{\theta_{min}}^{\theta_{max}} D(f)\, D(\theta) \left(\frac{\delta}{\delta_n}\right)} \tag{4-6}$$

$$\Rightarrow \qquad D_{est}(\theta) = \frac{D(\theta) \left(\frac{\delta}{\delta_n}\right) \left(\sum_{f_{min}}^{f_{max}} D(f)\right)}{\left(\frac{\delta}{\delta_n}\right) \left(\sum_{f_{min}}^{f_{max}} D(f)\right) \left(\sum_{\theta_{min}}^{\theta_{max}} D(\theta)\right)} \tag{4-7}$$

$$\Rightarrow \qquad D_{est}(\theta) = \frac{D(\theta)}{\sum_{\theta_{min}}^{\theta_{max}} D(\theta)} \tag{4-8}$$

Thus, $D_{est}(\theta)$ is simply a normalised $D(\theta)$ from which the parameters defining $D(\theta)$ can be estimated.

3. **Distribution of radial frequency component:** An estimated distribution of radial frequency components $D_{est}(f)$ can be calculated by following above procedure with f and θ interchanged.

Thus magnitude spectrum described by *Equation (4-1)* satisfies the first two criteria of investigation. The investigation of perception of directionality is divided into three parts.

1. The separate and combined effects of physical parameters defining distribution of angular frequencies and RMS roughness (These are determined in experiments described in this chapter).
2. The separate and combined effects of physical parameters defining distributions of radial frequencies (These effects are investigated in *chapter 5*).
3. The combined effects of physical parameters defining both distributions and RMS roughness and the development of a mathematical model of perceived directionality based on observed effects of parameters (The effects will be discussed and a measurement model will be proposed in *chapter 6*).

During the first and second parts, the mathematical relations between physical parameters and perceived directionality will not be obtained as they do not provide

useful information. This is because observers will not see the effects of all parameters together during the experiments in those parts. Therefore, responses provided by observers and perceived directionality obtained from those responses will reflect only change in parameters varied in a given experiment.

4.2 Surfaces for the Investigation of the Effects of Angular Frequency Distribution and RMS roughness

In this section, a definition of magnitude spectrum will be proposed that will be used to produce *naturalistic* surfaces and that will allow us to investigate independent effects of varying distribution of angular frequency components and RMS roughness.

Fractal surfaces resemble certain surfaces seen in nature e.g. rock or sand ripples (Mandelbrot, 1982; Kube and Pentland, 1988; Linnett, 1991; Russ, 1994). Hence these surfaces will be considered for use in psychophysical investigations. The definitions of magnitude spectrum given by Ogilvy (1991) and Wu (2002) are not suitable for use here as the distribution patterns of angular and radial components are changed together and hence separate investigation of parameters associated with these distributions is not possible.

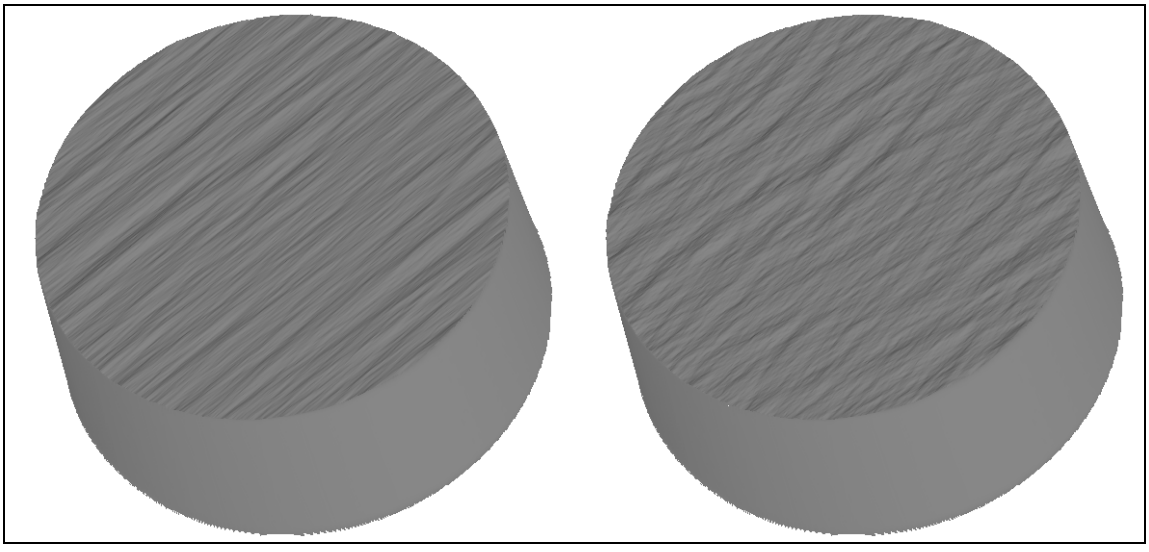

Figure 4-1: Example of naturalistic synthetic surfaces

Thus, terms $D(f)$ and $D(\theta)$ have been defined separately for independent investigation of directionality. There are several possible definitions which can be used for $D(f)$

and $D(\theta)$. The definitions of terms $D(f)$ and $D(\theta)$, which together generate *naturalistic* surfaces (see *Figure 4-1*), are explained below.

Padilla (Padilla *et al.*, 2008) used $1/f^{\beta}$ noise surfaces for the investigations of perceived roughness because this term generates *naturalistic* surfaces. It is therefore reasonable to assume that combining term $1/f^{\beta}$ with $D(\theta)$ will generate *naturalistic* directional surfaces. Therefore $D(f)$ is defined by *Equation* (4-9).

$$D(f) = 1/f^{\beta} \tag{4-9}$$

Where β is frequency roll-off factor. The MATLAB code for generating $1/f^{\beta}$ noise spectrum is provided in *Appendix 4-B*. 1D and 2D graphical demonstrations of $D(f)$ term are given in *Figure 4-2*.

The term $D(\theta)$ will define dominant direction of a surface and variation about dominant direction to add the directionality in a surface. One such definition is given in *Equation (4-10)*.

$$D(\theta) = e^{-(\theta-\theta_0)^2/2\sigma^2} \tag{4-10}$$

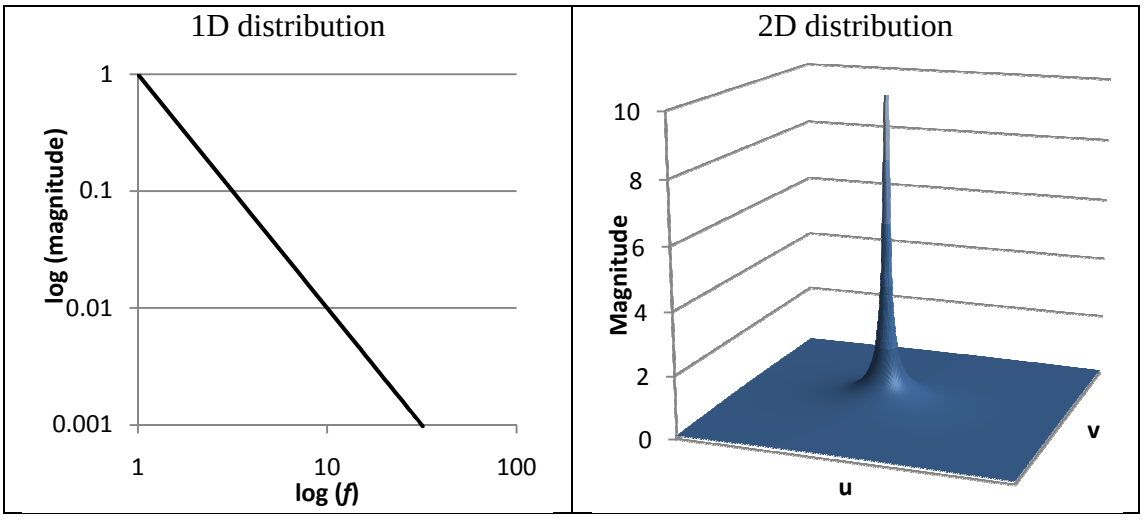

Figure 4-2: Frequency domain representation of $D(f)$

In *Equation (4-10)*, θ_0 is dominant angular frequency component which controls dominant direction of a surface and σ^2 is angular variance which controls rate of fall of

magnitude of angular frequency components away from θ_0. For low values of σ^2, amplitude of angular frequency components decreases very rapidly away from dominant direction and so a highly directional surface is generated. Similarly, as the values of σ^2 increases, a surface becomes less directional. The 1D and 2D graphical demonstration of $D(\theta)$ is shown in *Figure 4-3*. The MATLAB code of $D(\theta)$ can be found in *Appendix 4-C*.

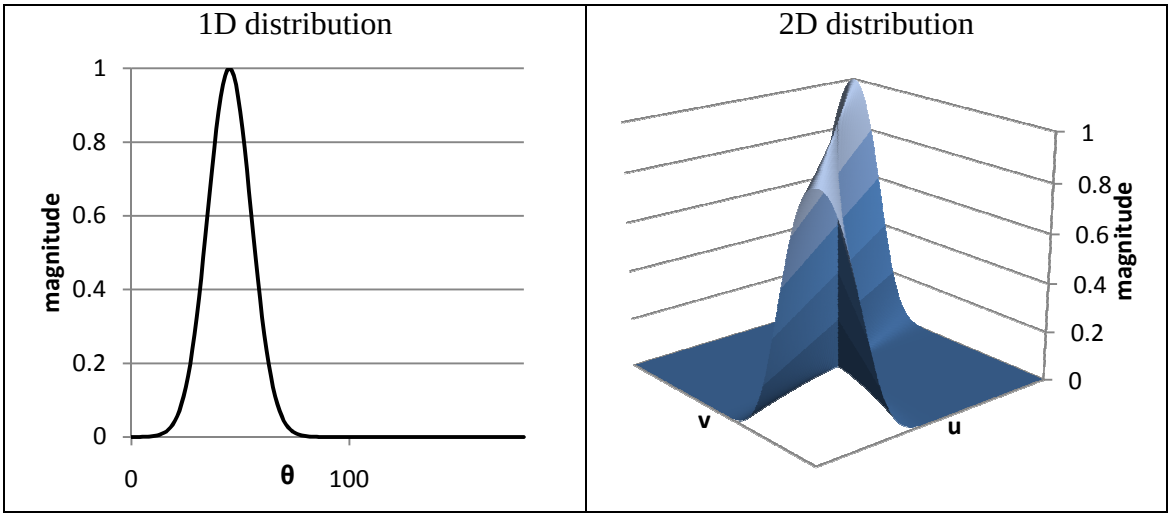

Figure 4-3: Frequency domain representation of $D(\theta)$

The definition of magnitude spectrum is given by *Equation (4-11)*.

$$M(f,\theta) = (1/f^{\beta})\,(e^{-(\theta-\theta_0)^2/2\sigma^2})\,\left(\frac{\delta}{\delta_n}\right) \qquad (4\text{-}11)$$

The normalisation factor δ_n will be calculated using the definitions of $D(f)$ and $D(\theta)$ given by *Equations (4-9)* and *(4-10)* respectively. A graphical representation of $M(f,\theta)$ is shown in *Figure 4-4*.

The unit of f is *cpd* as discussed in *chapter 3*. RMS roughness (δ) is measured in *centimetres* (*cm*) as unit height on the screen is adjusted to one *centimetre* ((Padilla, 2008)). θ and θ_0 are specified in *degrees* and so angular variance (σ^2) is specified by *degrees squared*.

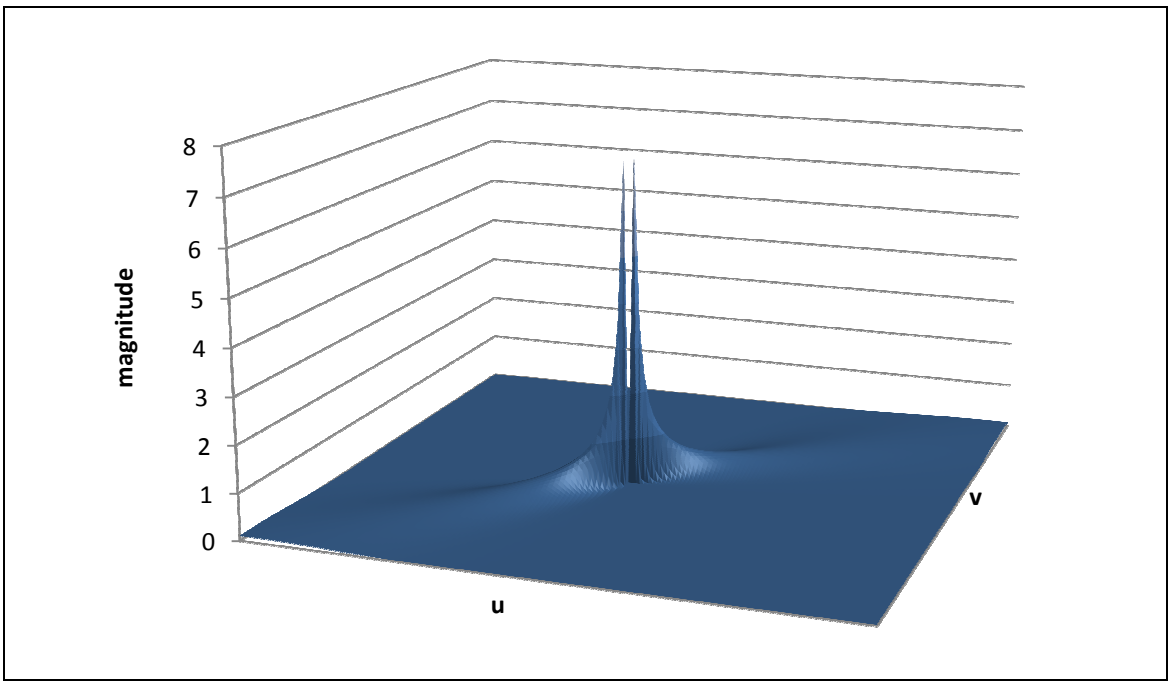

Figure 4-4: Frequency domain representation of $M(f,\theta)$

The process of obtaining a surface height map using *Equation (4-11)* is as follows: a magnitude spectrum $M(f,\theta)$ given by *Equation (4-11)* and a random phase spectrum with complex conjugate symmetry are used to produce the Fourier Transform of a surface. This Fourier Transform is inverse Fourier Transformed to obtain a surface height map. The complete MATLAB code for generating surfaces is given in *Appendix 4-D*. The surface height map is then rendered and animated for use in the psychophysical investigations as described in *Chapter 3*.

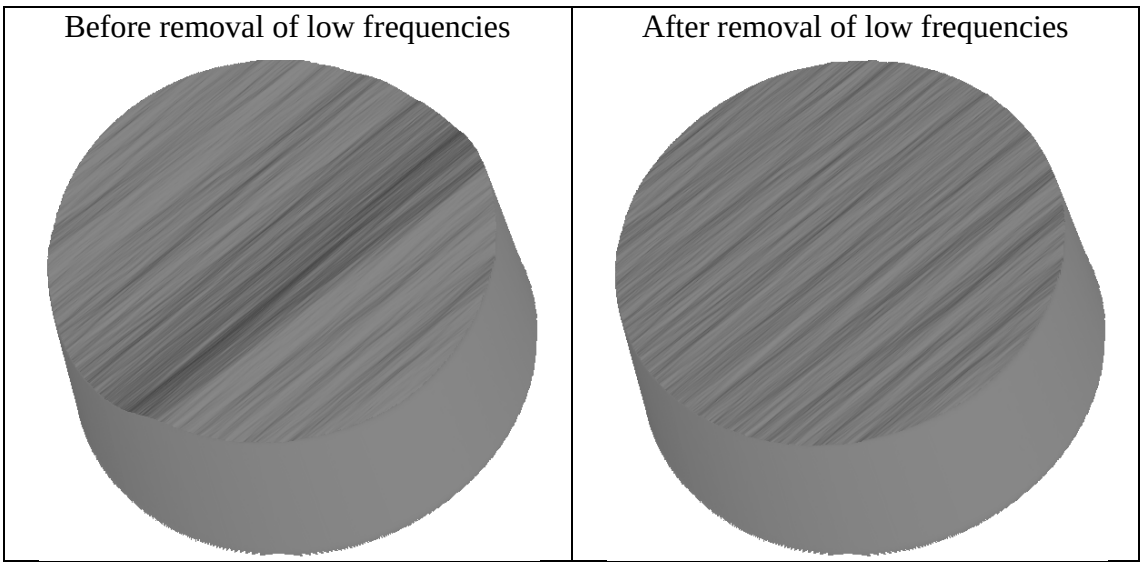

Figure 4-5: Effect of low frequencies on appearance of surface

The size of surface height maps will be kept 512x512 as in *chapter 3*. Synthetic directional surfaces with all frequencies (0.1 *cpd* to 30 *cpd*) were generated. However, they did not appear *naturalistic* when the value of σ^2 was low because of the presence of low frequencies. Hence, the magnitude of frequencies less than 0.937 *cpd* was made equal to zero in order to provide *naturalistic* surfaces. *Figure 4-5* shows the surfaces before and after removing frequencies below this cut-off.

4.3 Psychophysical Investigation

To the author's knowledge, independent effects of the parameters proposed here have not previously been investigated in a controlled manner. In the following subsections, the separate and combined effects of physical parameters (random phase spectrum, σ^2 and δ) will be investigated. β is kept constant for all experiments presented in this chapter. The parameter θ_0 describes the orientation of surfaces and will be also kept constant. Unless specified, β and θ_0 will be kept equal to 2 and 45^o throughout this chapter.

4.3.1 Effect of Different Random Phase Spectra on Perceived Directionality

As discussed earlier, unstructured surfaces have little or no information in their phase spectra. However, it cannot be assumed that the random phase spectrum do not affect human perception of directionality. Therefore this section tests the effect of using random phase spectra (see *Figure 4-6*) on perceived directionality.

It can be seen from *Figure 4-6* that it is difficult to judge differences in directionality of surfaces with the same magnitude spectrum and different random phase spectrum. But it is easy to judge differences in directionality of surfaces with different magnitude spectra (see *Figure 4-1*). Therefore, the *direct ratio estimation method* and the *method of constant stimuli* were used to observe the effects of using different random phase spectra.

Surfaces, with different random phase spectra and the same magnitude spectrum, were considered as *comparison* surfaces and compared with a *standard* surface having a magnitude spectrum different from *comparison* surfaces. Observers were asked to

compare the directionality of *comparison* and *standard* surfaces and to give the ratio between the directionalities of the two surfaces. Perceived directionality of *comparison* surfaces were then obtained from the ratios by assigning a value 1 arbitrarily to a *standard* surface. The change in perceived directionality of *comparison* surfaces for a given *standard* surface was then observed to determine if changing a random phase spectra have significant effects on the perception of directionality. An experiment is described below.

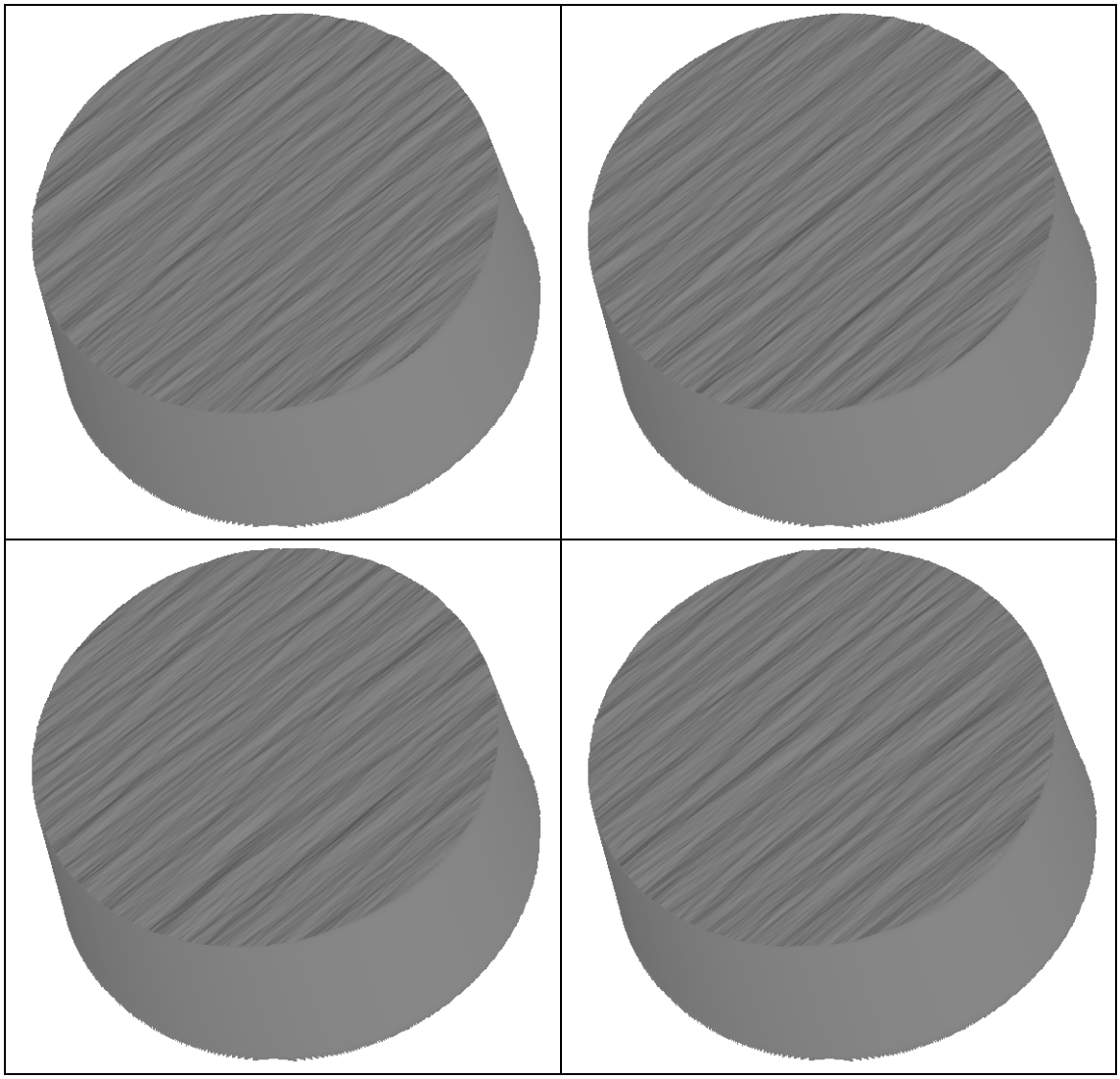

Figure 4-6: Effect of the random phase spectrum (surfaces with the same magnitude spectrum and different random phase spectra)

An effect of a random phase spectra was investigated using the two sets of five *comparison* surfaces and three standard surfaces as shown in *Figure 4-7*. Each *standard* surface is compared with five *comparison* surfaces to obtain perceived directionality of each *comparison* surface. The magnitude spectra of *comparison* and *standard* surfaces

had different angular variances. The values of angular variance of the two sets of *comparison* surfaces and corresponding three *standard* surfaces are shown in *Figure 4-7*.

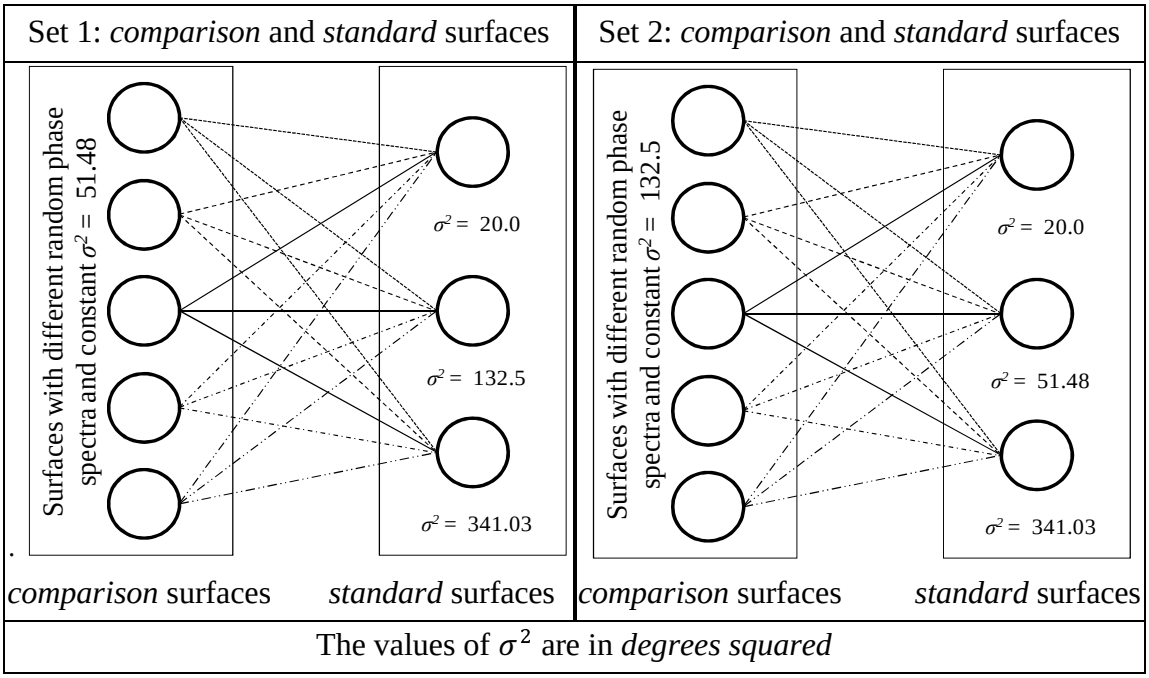

Figure 4-7: Graphical representation of pairs of comparison and standard surfaces to evaluate the effect of random phase spectrum

As each *comparison* surface is compared with each *standard* surface, 30 pairing are possible with three *standard* surfaces and two sets of five *comparison* surfaces. Each *comparison* surface was presented three times with a *standard* surface (i.e. each pair was repeated 3 times), and so in total each observer made 90 comparisons. As before, the order of presentation of pairs was randomised as was the positions of surfaces in pairs. The order of surfaces and corresponding responses given by five naïve observers are given in *Appendix 4-E*. Surface presentation, experimental set up and observers' instructions were the same as those used for the experiment described in section 3.3.

As observers were allowed to use different ranges of values from each other, the responses were normalised using *Equation (3-8)*. As each pair was repeated three times, the ratios of perceived directionalities of *comparison* and *standard* surfaces were obtained by taking geometric mean of the three normalised ratios. Perceived directionalities of *comparison* surfaces for each combination of *comparison* and *standard* surfaces were obtained by assigning a value of 1 to *standard* surfaces as

described earlier. Mean perceived directionalities of *comparison* surfaces for each combination was obtained in a similar manner to that described in *Chapter 3*. Perceived directionalities of *comparison* surfaces for each combination are plotted in *Figure 4-8*.

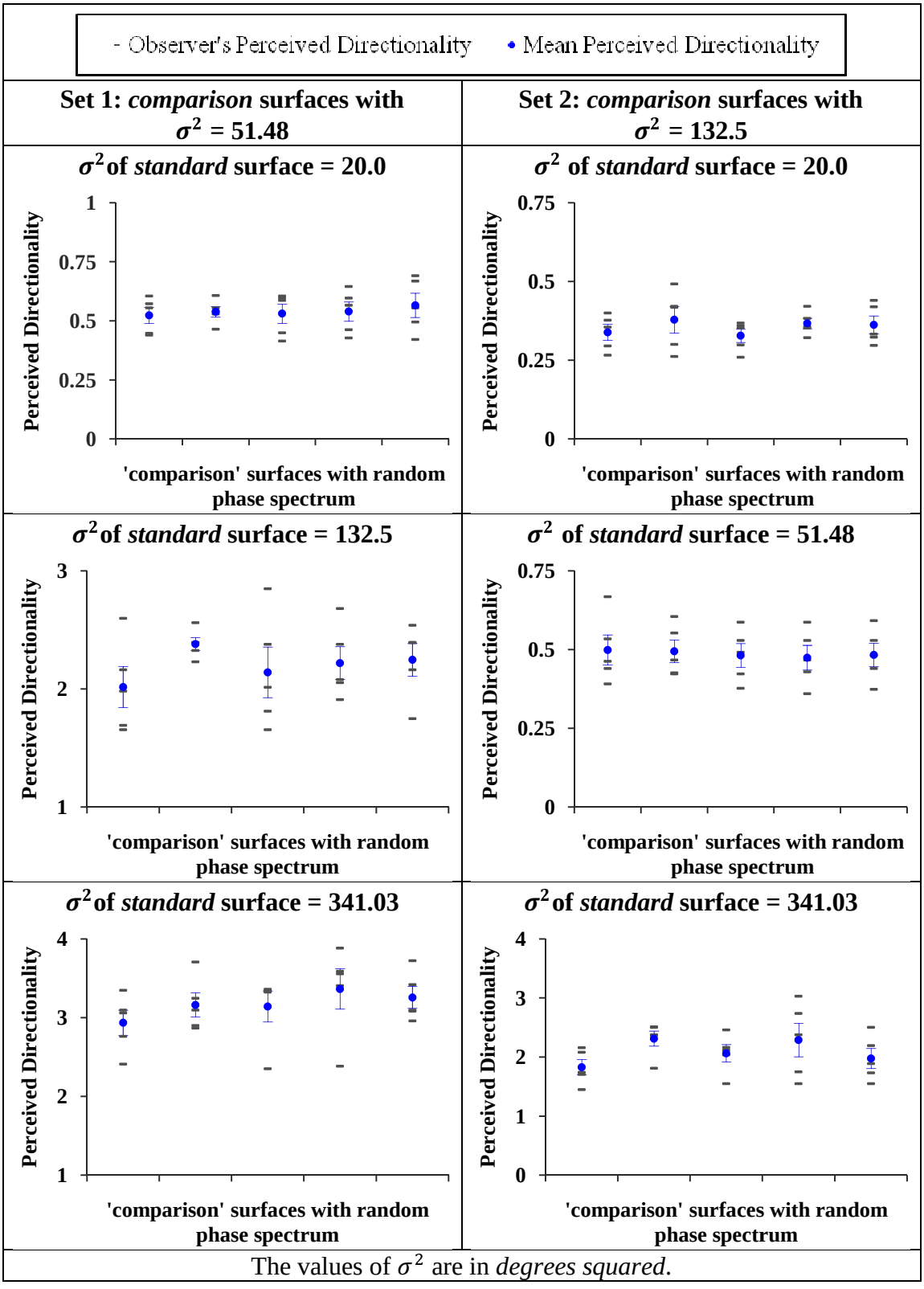

Figure 4-8: Perceived Directionality vs. surfaces with random phase spectra. The error bars show the standard error of mean

From *Figure 4-8*, it can be seen that there is little difference in mean perceived directionalities of surfaces with different random phase spectra for a given *standard* surface. A one-way repeated measures ANOVA was carried out to determine whether this effect is significant.

The null hypothesis of the repeated measures ANOVA is that random phase spectrum has no effect on perceived directionality. The results of the analysis for all six combinations are listed in *Table 4-1*. The results are shown with an assumption of sphericity because *Mauchly's test* indicated that an assumption of sphericity is not violated ($p > 0.05$) for all six combinations. It can be seen that significance value obtained for all combinations is greater than 0.05 and hence the null hypothesis is accepted.

Assumption of sphericity	Surfaces		*F-Statistics*	*Sig. Value* (p)
	standard surfaces-σ^2 (*degrees squared*)	*comparison* surfaces-σ^2 (*degrees squared*)		
Sphericity Assumed	20.0	51.48	0.449	**0.772**
Sphericity Assumed	132.5	51.48	1.886	**0.162**
Sphericity Assumed	341.03	51.48	1.620	**0.218**
Sphericity Assumed	20.0	132.5	0.902	**0.486**
Sphericity Assumed	51.48	132.5	0.277	**0.889**
Sphericity Assumed	341.03	132.5	2.405	**0.093**

Table 4-1: Tests of within-subjects effects: random phase spectrum

Thus it can be concluded that different random phase spectra do not affect the perception of directionality. In the following sub-sections, the effects of angular variance and RMS roughness on perception of directionality will be investigated independently and together.

4.3.2 Effect of Varying Angular Variance on Perceived Directionality

In this section, effect of variation of angular variance is investigated using surfaces generated by changing only σ^2 in *Equation (4-11)*. The effect of varying σ^2 is shown in *Figure 4-9*. High values of σ^2 make distribution of frequency components wider and so

generate less directional surfaces. Therefore the hypothesis is that perceived directionality of surfaces decreases as value of σ^2 increases.

To test the above hypothesis, the *direct ratio estimation* method, with *pair-wise comparison*, described in *Chapter 3* was used. The surfaces had five different values of σ^2 (20.0, 51.48, 132.5, 341.03, 877.8 *degrees squared*), chosen at equal distances on the scale of $\log(\sigma^2)$ to provide visually distinct appearances. The effect of change in angular variance was observed at four levels of RMS roughness (δ = 0.012, 0.016, 0.02 and 0.024 *cm*). During experiments, the pairs of surfaces having different σ^2 and the same RMS roughness were presented to observers. No comparison was made between surfaces having different RMS roughness.

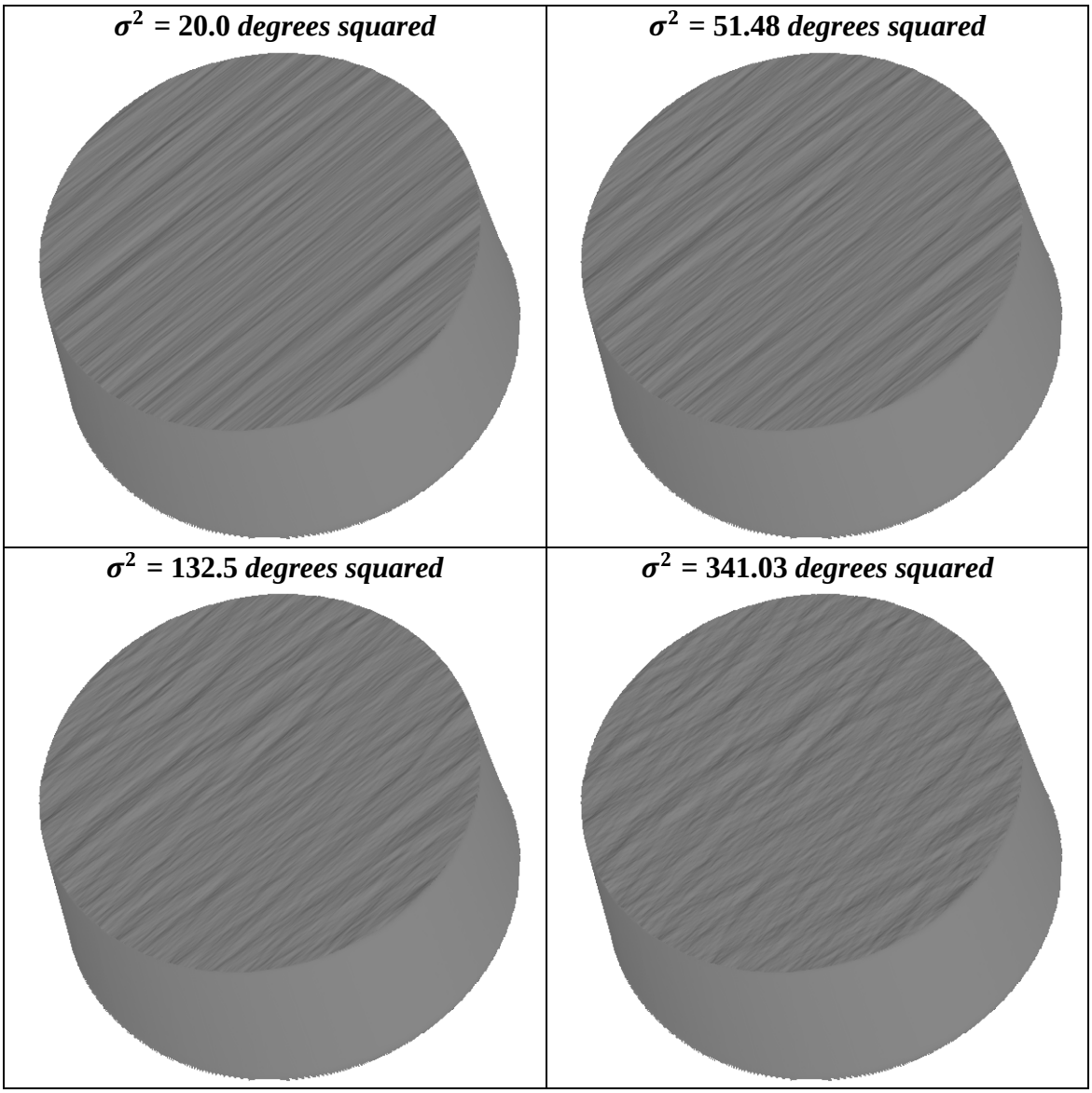

Figure 4-9 Effect of varying σ^2 with a constant level of RMS roughness (δ = 0.016 cm)

All ten possible combinations of five surfaces with different σ^2 and constant δ were presented twice during experiment. As the same set up was used at four levels of RMS roughness, a total of eighty (10 x 2 x 4) pairs were presented to observers in random order. Observers again provided the ratios of perceived directionalities of surfaces in each pair.

Five naïve observers, with normal or corrected to normal vision, took part in experiment and the corresponding order of surface pairs and responses are given in *Appendix 4-F*. These responses were normalised using *Equation (3.8)* and the geometric mean of normalised responses of repeated pairs was taken to obtain ratios of surface pairs with different σ^2 and same δ. These ratios were processed to obtain perceived directionalities of surfaces as described in section 3.3.2 of *chapter 3*.

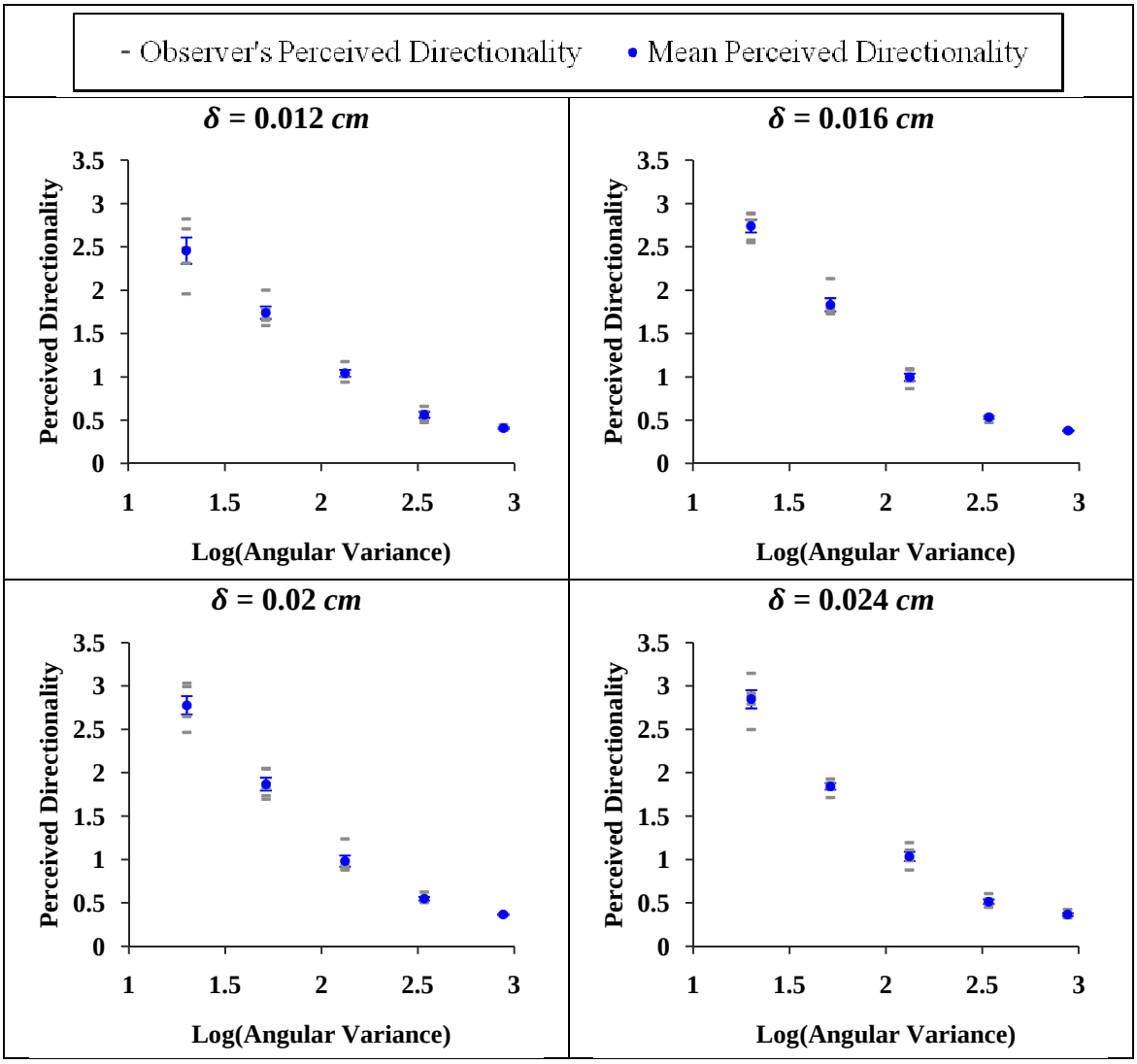

Figure 4-10: Perceived directionality vs. $log(\sigma^2)$ at constant level of RMS roughness. σ^2 is given in degrees squared. The error bars shows the standard errors of mean.

The observers' perceived directionalities (ρ_o) and mean perceived directionality for each value of δ are plotted against log (σ^2) in *Figure 4-10*. It can be seen that observers perceived surfaces with low values of σ^2 as more directional.

A one way repeated measures ANOVA was performed to find out whether the change in perceived directionality, due to change in σ^2, is significant. The results of ANOVA tests for each value of δ are shown in *Table 4-2*, which shows that σ^2 significantly ($p < 0.05$) affects the perception of directionality at all four levels of δ. The results are reported with sphericity assumed as *Mauchly's test* indicated that the assumption of sphericity is not violated.

Assumption of sphericity	Constant level of RMS Roughness (*cm*)	*F-Statistics*	*Sig. Value* (p)
Sphericity Assumed	0.012	106.915	**<0.001**
Sphericity Assumed	0.016	317.598	**<0.001**
Sphericity Assumed	0.02	202.512	**<0.000**
Sphericity Assumed	0.024	294.058	**<0.001**

Table 4-2: Tests of within-subjects effects of σ^2

4.3.3 Effect of Varying RMS Roughness on Perceived Directionality

The effect of varying δ on surfaces generated using *Equation (4-11)* is shown in *Figure 4-11*. It is clear that as δ increases, directional features become more clear and discernible. Therefore the hypothesis was made that human observers will perceive the surfaces with larger values of δ as being perceptually more directional, given the other parameters are constant.

To test this hypothesis, an approach similar to that was used for the investigation of σ^2 was used and the surfaces were sampled at five values of δ (0.0012, 0.0016, 0.02, 0.024, and 0.028 *cm*). It was observed that surfaces with δ higher than 0.028 did not look *naturalistic* and so higher values were not used. The surfaces with these values of δ were obtained at four values of σ^2 (20.0, 51.48, 132.5 and 341.03 *degrees squared*).

The surfaces having different δ and constant σ^2 were compared. No comparison was made between the surfaces having different σ^2. Ten possible pairs of surfaces having

five different values of δ were presented to observers twice. As the same set up was used to investigate the effect of δ at four levels of σ^2, a total of eighty pairs were presented to observers in random order.

Five naïve observers took part in this experiment. The instructions and the method of calculating observers' perceived directionalities were the same as those used in the previous experiment. Presentation order of surface pairs and observers' responses are given in *Appendix 4-G*. Observers' perceived directionalities (ρ_o) and their arithmetic means (ρ) are plotted against δ in *Figure 4-12* for each value of σ^2. It can be seen that as δ increases, ρ increases, supporting the hypothesis that observers perceive surfaces with higher δ as more directional when other parameters are constant.

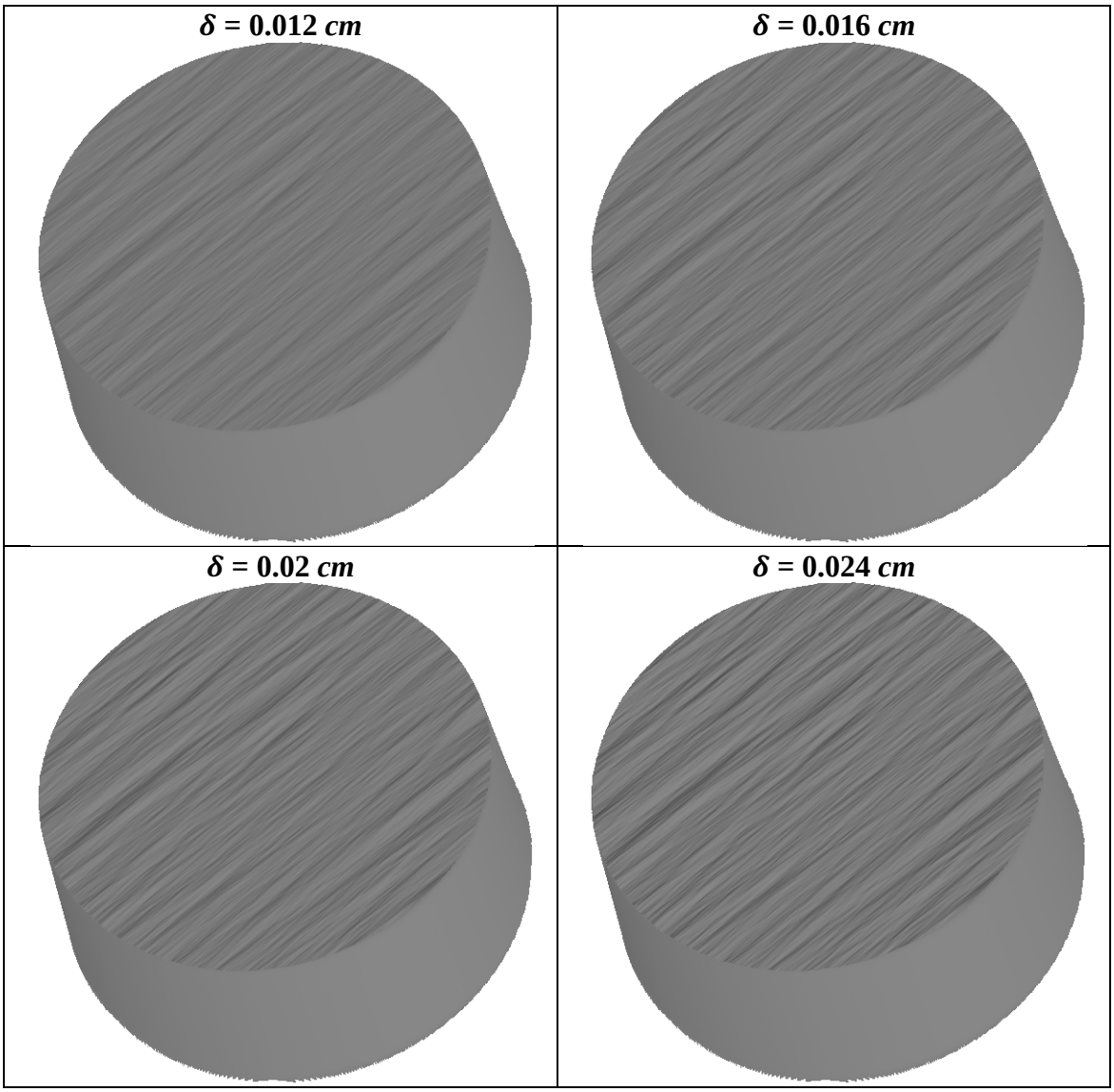

Figure 4-11: Effect of varying RMS roughness (δ) at constant level of angular variance (σ^2 = 51.48 degrees squared)

Again, a one way repeated measures ANOVA was conducted to test an effect of δ. When *Mauchly's test* is not violated, the results are considered with sphericity assumed and when the assumption of sphericity is violated, the *degrees of freedom* were corrected using *Greenhouse-Geisser* estimates to obtain significance values. The results of ANOVA tests for each value of σ^2 are shown in *Table 4-3*, which show that δ significantly ($p < 0.05$) affects the perception of directionality at all four levels of σ^2.

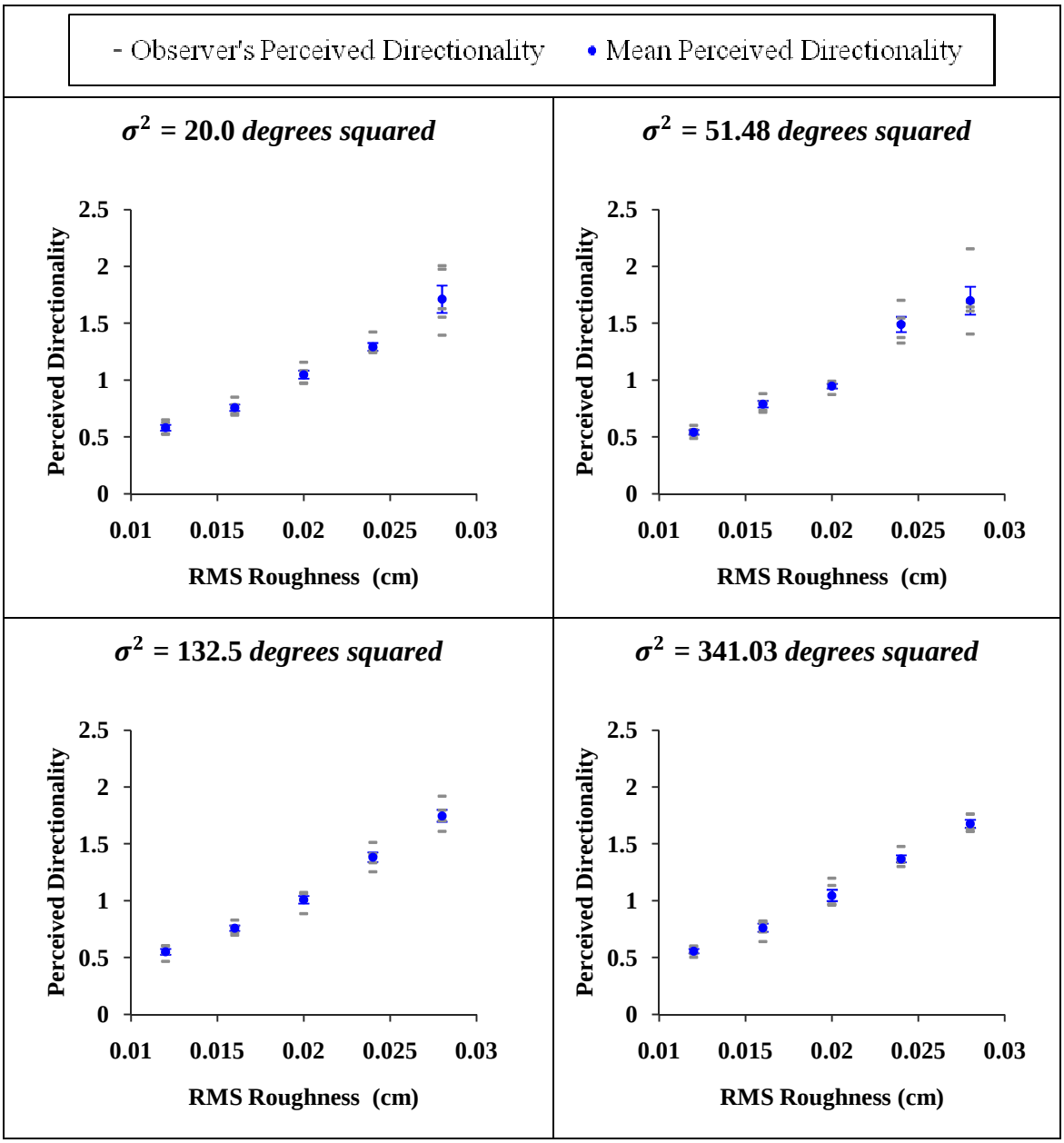

Figure 4-12: Perceived directionality vs. RMS roughness (δ) at constant levels of angular variance (σ^2). The error bars show the standard errors of mean.

Assumption of sphericity	Constant level of Angular Variance (*degrees squared*)	*F-Statistics*	*Sig. Value* (p)
Sphericity assumed	20.0	46.929	<**0.001**
Greenhouse-Geisser	51.48	45.688	**0.001**
Sphericity assumed	132.5	147.793	<**0.001**
Greenhouse-Geisser	341.0	138.198	<**0.001**

Table 4-3: Tests of within-subjects effects: RMS roughness

4.3.4 Effects of Varying Both Angular Variance and RMS Roughness on Perceived Directionality

In section 4.3.2 and 4.3.3, the effects of angular variance and RMS roughness were investigated in two separate experiments. While these experiments demonstrated that both physical parameters affect perceived directionality, they cannot measure combined effects of the two parameters, and they cannot test for interactions between the two parameters. This is because the range of ratios used by each individual observer depends upon the range of differences that they see between pairs, and the data from separate experiments presenting pairs differing in angular variance and in RMS roughness have different scales and cannot be combined. To obtain information about the effect sizes and a possible interaction, it was necessary to conduct another experiment, in which observers compared all possible paired combinations of surfaces with different values of $\sigma^2$and δ.

For the experiment a total of twenty surfaces were generated using *Equation (4-11)* with five different values of angular variance (σ^2 = 20.0, 51.48, 132.5, 341.0 and 877.8 *degrees squared*) and four different values of RMS roughness (δ = 0.012, 0.016, 0.02 and 0.024 *cm*). The use of five levels of δ was not considered as number of surfaces and hence number of pairs becomes prohibitively high. Observers compared 190 possible pairs of these twenty surfaces, presented in a random order. As number of pairs was high, each pair was presented only once to avoid effects of fatigue and loss of attention. To provide further replication, more observers were used in experiment.

Eight observers took part in the experiment and provided ratio judgements for each pair. The order of pairs of surfaces for the given observer and corresponding responses are

given in *Appendix 4-H*. These responses were normalised using *Equation (3-8)* and perceived directionalities as described in section 3.3.2 of *chapter 3*. *Figure 4-13* and *Figure 4-14* shows the change in perceived directionality against angular variance (σ^2) and RMS roughness (δ) respectively.

From *Figure 4-13*, it can be seen that perceived directionality increases as σ^2 decreases at all levels of δ. From *Figure 4-14*, it can be observed that perceived directionality increases with δ when σ^2 is low but remains almost constant with varying δ when σ^2 is high.

A two-way repeated measures ANOVA was conducted to test the significance of these differences in perceived directionality due to changes in the two parameters and an interaction effect of the two parameters. The effect sizes (*partial eta squared*, η) of an individual parameter and the interaction terms of the two parameters were measured to indicate which parameter has greater effect than the other. A value of η near to 1 indicates a high effect of parameter.

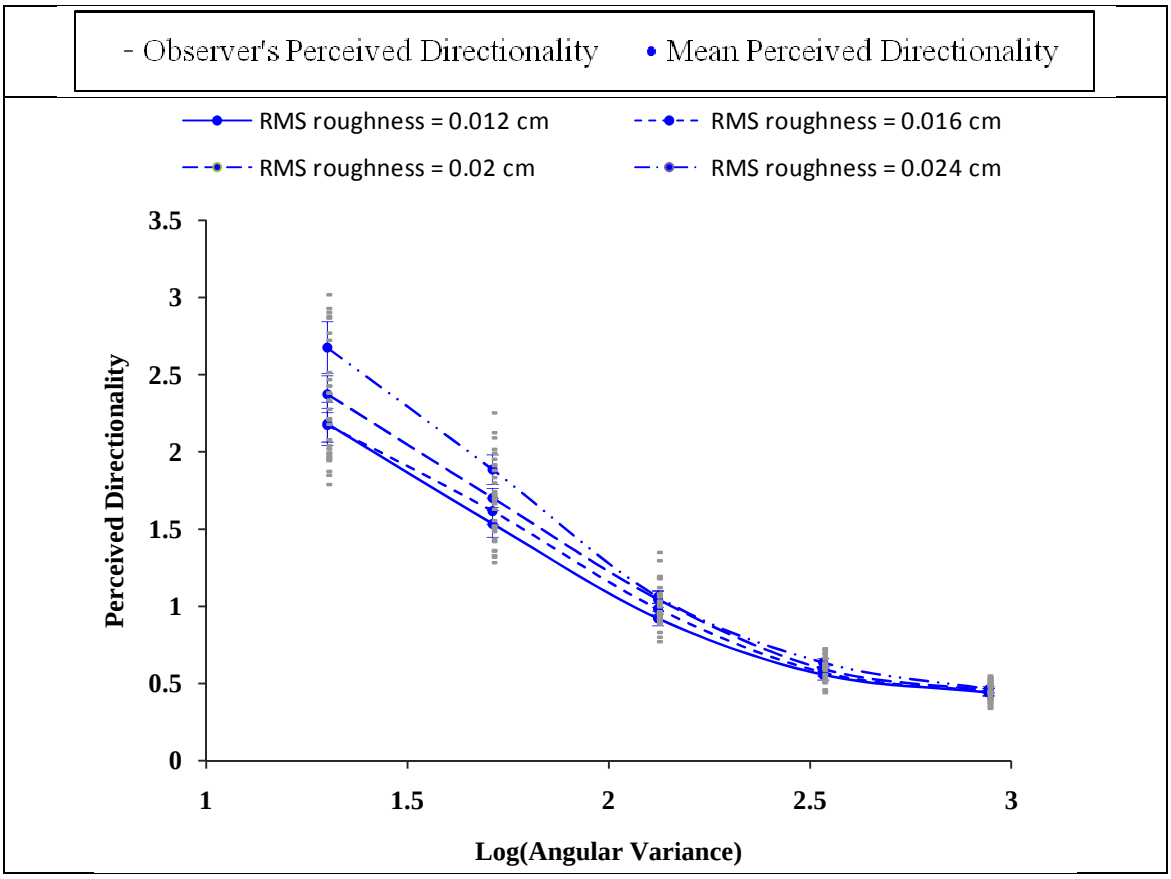

Figure 4-13: Perceived directionality vs. logarithm of angular variance at different level of RMS roughness. The error bars show the standard error of mean.

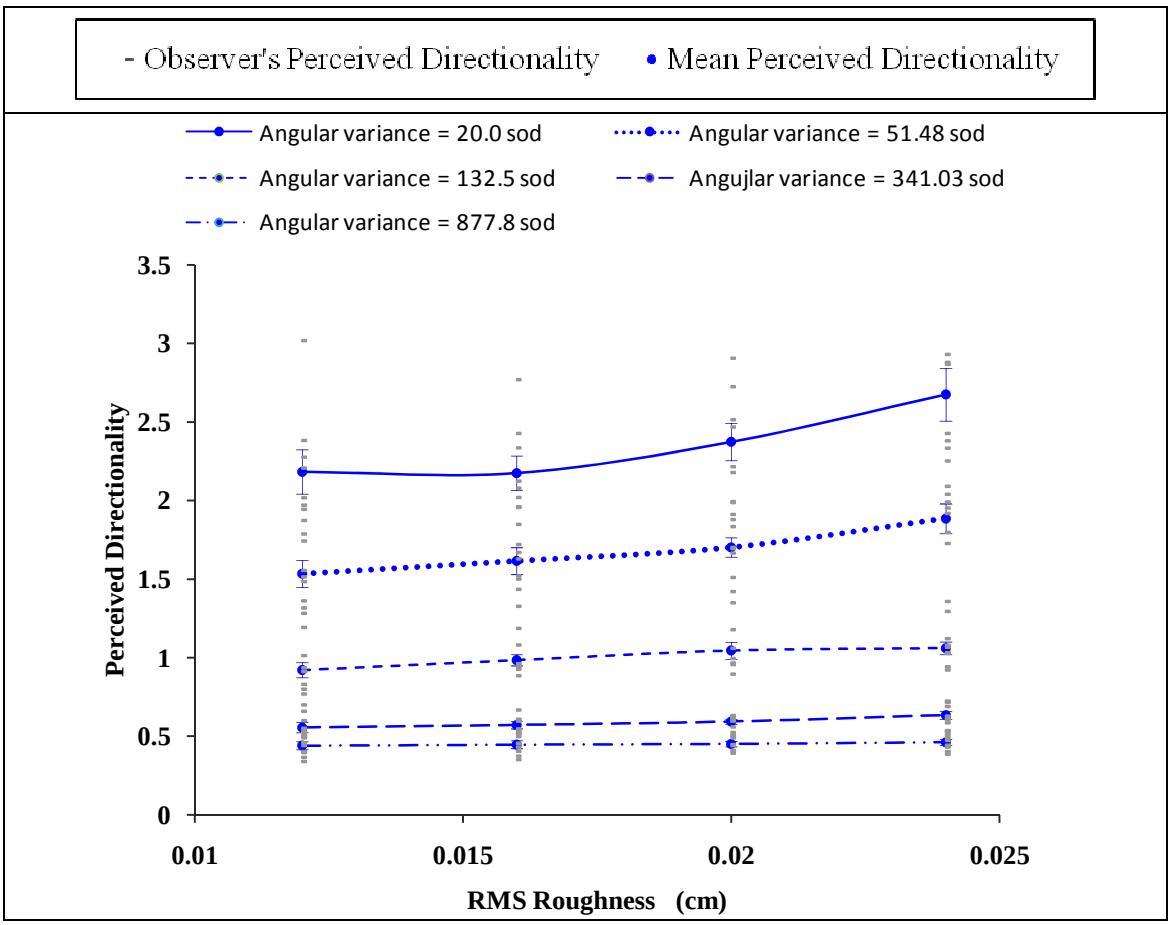

Figure 4-14: Perceived directionality vs. RMS roughness at different level of angular variance. The error bars shows standard errors of mean.

The results of the main significant effects (with *degrees of freedom* corrected using *Greenhouse-Geisser* estimates of sphericity) are given in *Table 4-4*, which shows that σ^2 and δ both have significant effects ($p < 0.05$) on the perception of directionality and their interaction also has a significant effect ($p < 0.05$). Furthermore, the values of η show that the effect sizes of δ and an interaction term are less than that of σ^2.

Source	Assumption of sphericity	*F-Statistics*	*Sig. Value* (p)	*Partial eta squared* (η)
σ^2	*Greenhouse-Geisser*	154.422	**<0.001**	**0.957**
δ	*Greenhouse-Geisser*	7.385	**0.026**	**0.513**
(σ^2) (δ)	*Greenhouse-Geisser*	6.002	**0.018**	**0.462**

Table 4-4: Tests of within-subjects effects: σ^2 and δ

4.4 Summary

In the beginning of this chapter, the following three criteria were proposed for the model of a surface.

1. A mathematical model of the surfaces must allow us to vary parameters independent of each other to investigate the separate and combined effects of parameters.
2. It must be possible to estimate parameters of a surface model from unknown surfaces.
3. Surfaces must be *naturalistic*.

Following specific class of frequency domain descriptions were found suitable for the criteria proposed.

$$M(f,\theta) = D(f)\,D(\theta)\left(\frac{\delta}{\delta_n}\right) \tag{4-12}$$

$$P_R(f,\theta) = \text{Random Numbers} \tag{4-13}$$

After proposing the criteria and class of surfaces, the following mathematical definition of the surfaces was used for psychophysical investigation of distribution of angular frequency components and RMS roughness.

$$M(f,\theta) = (1/f^{\beta})\,(e^{-(\theta-\theta_0)^2/2\sigma^2})\,\left(\frac{\delta}{\delta_n}\right) \tag{4-14}$$

The separate effects of changing random phase, σ^2 and δ on the perception of directionality were investigated and the following were found:

1. Variation of random phase does not have a significant effect on perception of directionality.

2. Angular variance (σ^2) has a significant effect on perception of directionality; increasing σ^2 decreases perceived directionality.
3. RMS roughness (δ) has a significant effect on perception of directionality; increasing δ increases perceived directionality.

Finally, the effect of changing σ^2 and δ together was investigated and the following were observed:

1. Angular variance (σ^2) and RMS roughness (δ) have significant effects on perceived directionality when both were varied in the same experiment. The effect of σ^2 was larger than that of δ.
2. There is an interactive effect of σ^2 and δ on the perception of directionality.

The investigations presented in this chapter do not consider the effect that variation in the distribution of radial frequency components has on perceived directionality. Hence the next chapter investigates the effects of parameters controlling the distributions of radial frequency components.

Chapter 5

Effect of Radial Frequency on Perceived Directionality

In the previous chapter, the effects of varying angular variance and RMS roughness on the perception of directionality were presented. This chapter investigates the effect of varying radial frequency distribution on the perception of directionality.

As described earlier in *chapter 3*, it is possible that radial frequency components may affect the perception of directionality. These radial frequency components may be spread over small to large radial frequency regions positioned at different locations. Therefore, perception of directionality may be affected by a width of radial frequency region (bandwidth, B_w) or location of radial frequency region (central radial frequency, f_c) or both.

This chapter is organised as follows: Section 5.1 describes generation of new surfaces to evaluate the effects of varying distribution of radial frequency components according to criteria described in *chapter 4*. The psychophysical experiments described in section 5.2 investigate the effect of change in the distribution of radial frequency components. In section 5.2.1, 5.2.2 and 5.2.3 the effects of change in random phase spectra, central radial frequency and bandwidth respectively are separately investigated, while in section 5.2.4 the combined effect of f_c and B_w is investigated by varying both f_c and B_w together. Section 5.3 gives a short summary of this chapter.

5.1 Directional surfaces to investigate the effect of radial frequency distributions

Aim of this section is to generate *naturalistic* directional stimuli needed to observe the effects of varying radial distribution on the perception of directionality. The criteria for synthetic surfaces as described in section 4.1 will be considered here and magnitude spectrum will have the same form to that is given by *Equation (4-1)*. For convenience, the description of magnitude spectrum is given below.

$$M(f,\theta) = D(f)\,D(\theta)\left(\frac{\delta}{\delta_n}\right) \quad (5\text{-}1)$$

In *Equation (5-1)*, δ_n will be calculated using new definitions of $D(f)$ and $D(\theta)$ in the same way to that described in *chapter 4*, in order to normalise RMS roughness of a surface and to allow it to be specified by δ. As the effect of RMS roughness (δ) has been investigated in *chapter 4*, δ will be kept constant at 0.01 *cm* unless specified. $D(\theta)$ will be kept constant as the aim of this chapter is to investigate the effect of varying distribution of radial frequencies. $D(\theta)$ is defined in the same way as it was defined in *chapter 4* and given again in *Equation (5-2)*. If σ^2 and θ_0 are not specified, they will be kept equal to 51.48 *degrees squared* and 45° respectively, throughout this chapter.

$$D(\theta) = e^{-(\theta-\theta_0)^2/2\sigma^2} \quad (5\text{-}2)$$

The term $D(f)$ will be used to define a specific distribution of radial frequency components and the effects of varying parameters that control the distributions will be investigated. In *chapter 4*, the term $1/f^{\beta}$ was used to define distribution of radial frequency components, where β controls rate of fall of amplitude of frequency components and thus changes distribution of radial frequencies. It was found in *chapter 4* that product of $1/f^{\beta}$ and $e^{-(\theta-\theta_0)^2/2\sigma^2}$ produces *naturalistic* surfaces for a specific range of (β, σ^2) space . However, varying β is not a promising way to investigate the effect of varying distribution of radial frequencies on the perception of directionality, for the following reasons.

1. As β increases, amplitude of low radial frequencies increases and that of high radial frequencies decreases, and vice versa (sees *Figure 5-1*). These surfaces are generated using magnitude spectrum defined by *Equation (5-1)* with $D(f)$ equal to $1/f^{\beta}$ and $D(\theta)$ equal to $e^{-(\theta-\theta_0)^2/2\sigma^2}$. According to the author's observations, the surfaces with different values of β do not have significantly different perceived directionality.
2. In nature, certain directional surfaces, e.g. sand waves, have their spectral contents concentrated at different positions in their magnitude spectra. Examples of such distributions of radial frequencies are shown in *Figure 5-2*. Human

perception of directionality may be affected by a central position and a width of such distributions. However, a $1/f^{\beta}$ term does not allow us to investigate these effects.

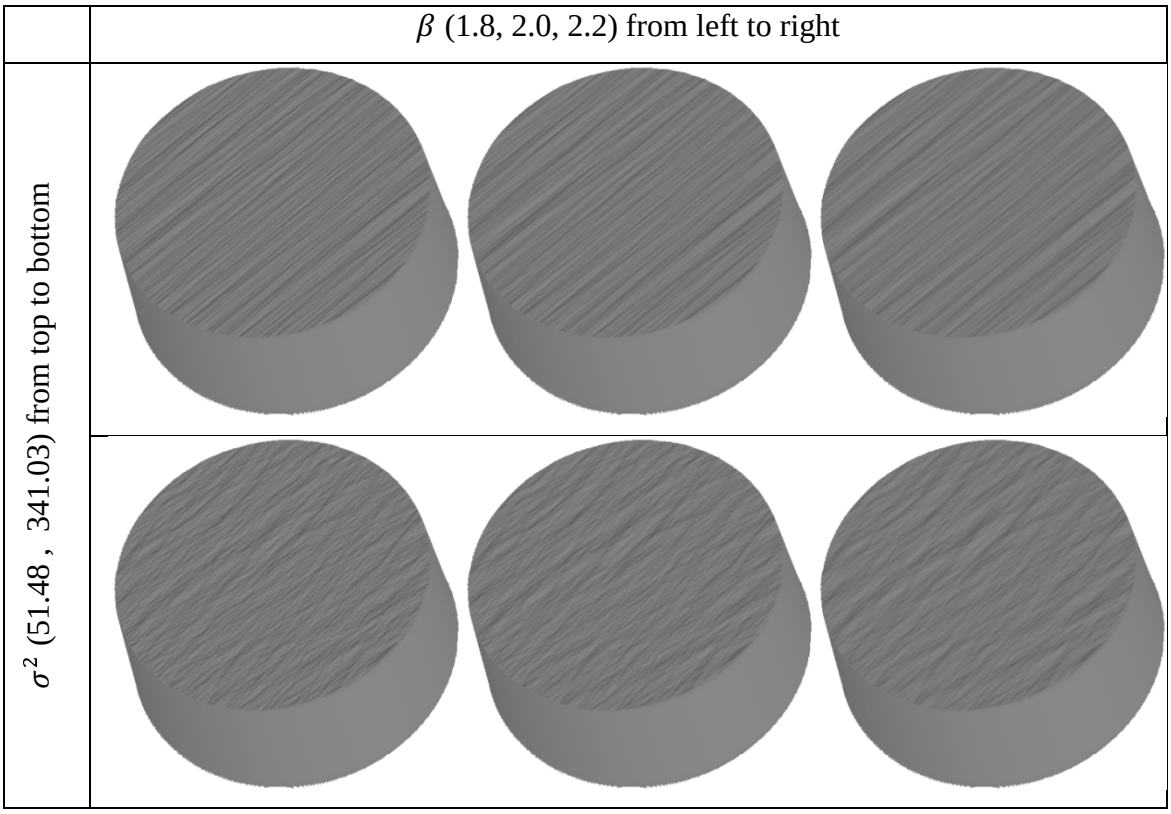

Figure 5-1: Effect of β with constant levels of σ^2

Therefore, the term $D(f)$ must allow us to control a central position and a width of the distribution of radial frequency components in order to investigate their effects on perceived directionality. There are several possibilities for such distribution patterns of radial frequency components. Two such definitions are shown in *Table 5-1*. Parameters affecting a central position and a width of radial frequency region are also shown in *Table 5-1*. The suitability of each definition was evaluated with respect to the criteria described in *chapter 4*. After visual inspection of these surfaces, it was found that these definitions do not generate *naturalistic* surfaces. The Gaussian band-pass filter produces sinusoidal surfaces when a width parameter is low while surfaces generated using the Butterworth band-pass filter do not look *naturalistic* because of the presence of high frequencies.

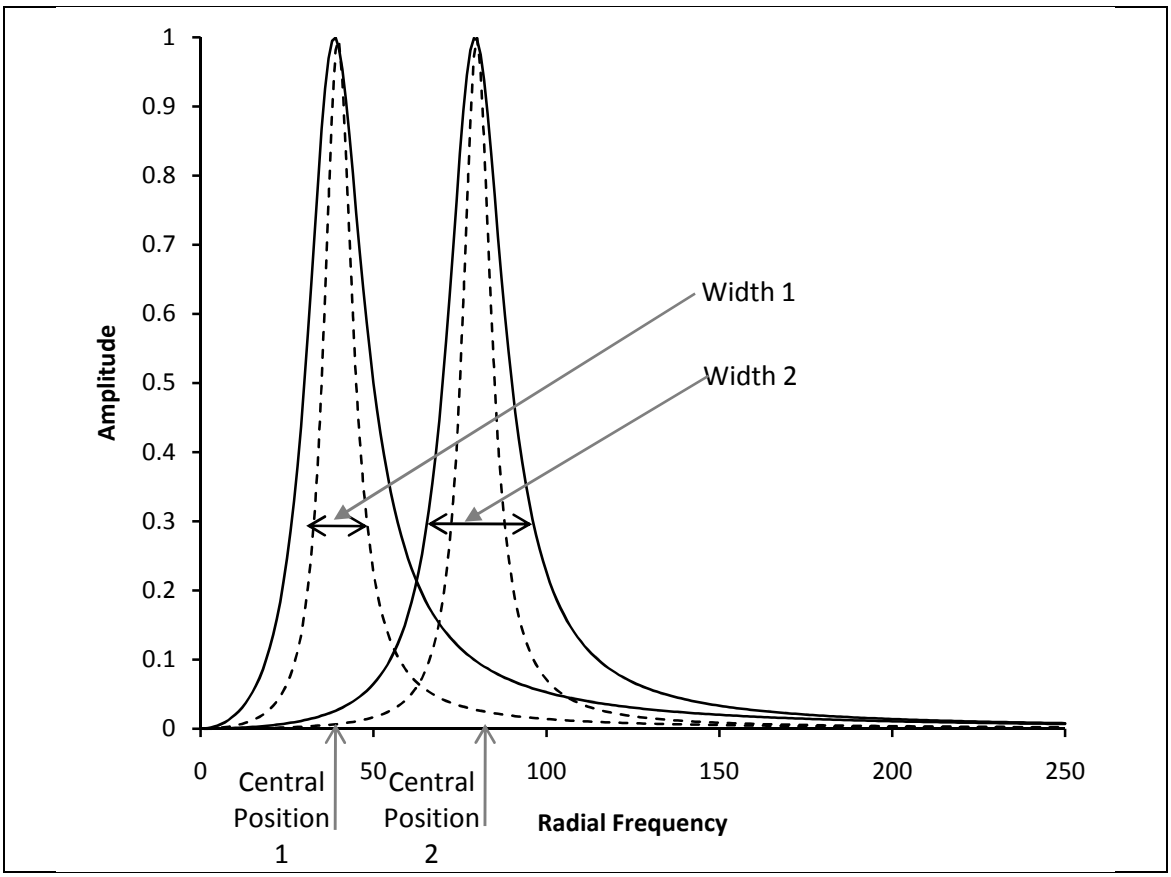

Figure 5-2: Examples of distribution patterns of radial frequency components and the parameters that may affect human perception of directionality.

Name of the Definition	Definition of the term $D(f)$ and Parameter Description	Central position	Width
Gaussian band-pass filter	$e^{-(f-\mu_f)^2/(2\sigma_f^2)}$ Parameter description: μ_f = mean radial frequency σ_f = standard deviation from μ_f	μ_f	σ_f
Butterworth band-pass filter	$\sqrt{\frac{1}{1+\left(\left(\frac{1}{f_h-f_l}\right)\left(\frac{(f_h f_l)-f^2}{f}\right)\right)^{2n}}}$ Parameter description: f_h= upper 3-dB cut-off frequency f_l = lower 3-dB cut-off frequency n = order of the Butterworth filter.	$\frac{(f_h+f_l)}{2}$	f_h-f_l

Table 5-1: The definitions and parameter descriptions of band-pass filters.

However, combination of the Butterworth band-pass filter and $1/f^{\beta}$ term given by *Equation (5-3)* produces *naturalistic* surfaces as shown in *Figure 5-3*. As change in β does not affect perceived directionality, according to the author's observations, *Equation (5-3)* will be used to investigate the effects of varying f_c and B_w (*Equations (5-4)* and *(5-5)* respectively) on the perception of directionality and β will be kept constant throughout this chapter. The parameters f_c (central radial frequency) and B_w (bandwidth) define a central position of distribution of radial frequency components and a width of radial frequency region respectively.

$$D(f) = (1/f^{\beta}) \sqrt{\frac{1}{1 + \left(\left(\frac{1}{f_h - f_l} \right) \left(\frac{(f_h\, f_l) - f^2}{f} \right) \right)^{2n}}} \tag{5-3}$$

$$f_c = (f_h + f_l)/2 \tag{5-4}$$

$$B_w = f_h - f_l \tag{5-5}$$

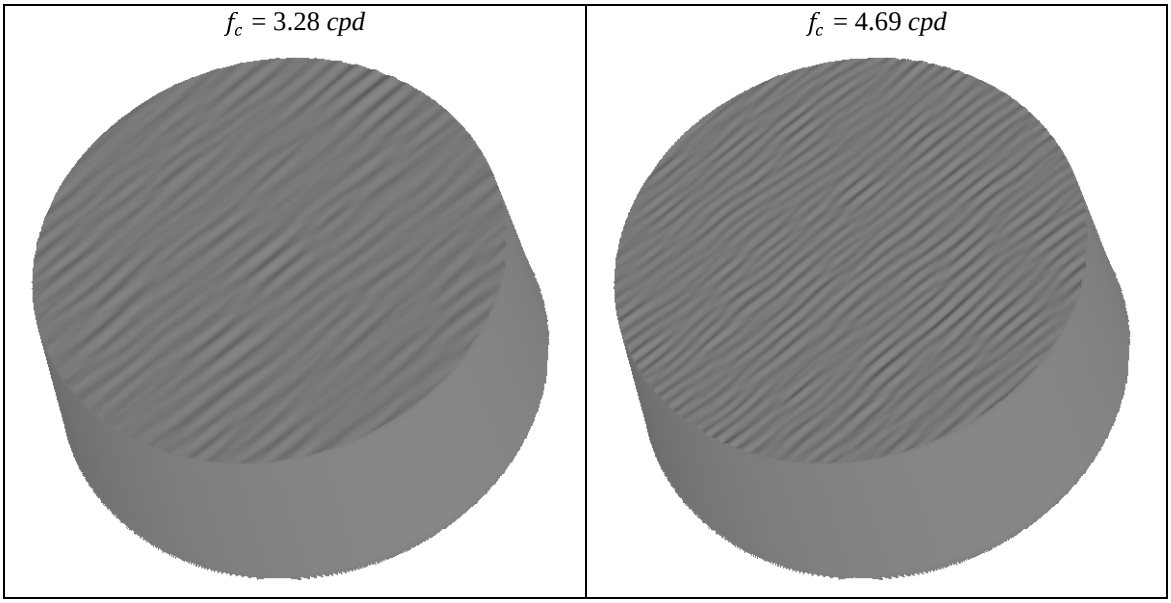

Figure 5-3: Naturalistic surfaces to investigate the effects of radial distribution of frequency components.

An order n of the Butterworth filter will be kept equal to 1 throughout this chapter. For n > 1, surfaces appear sinusoidal and do not look *naturalistic*. As an order of the

Butterworth filter increases, amplitudes of radial frequency components drop sharply as shown in *Figure 5-4* and hence, amplitudes of radial frequencies adjacent to f_c reduce to nearly zero, which makes the surfaces sinusoidal.

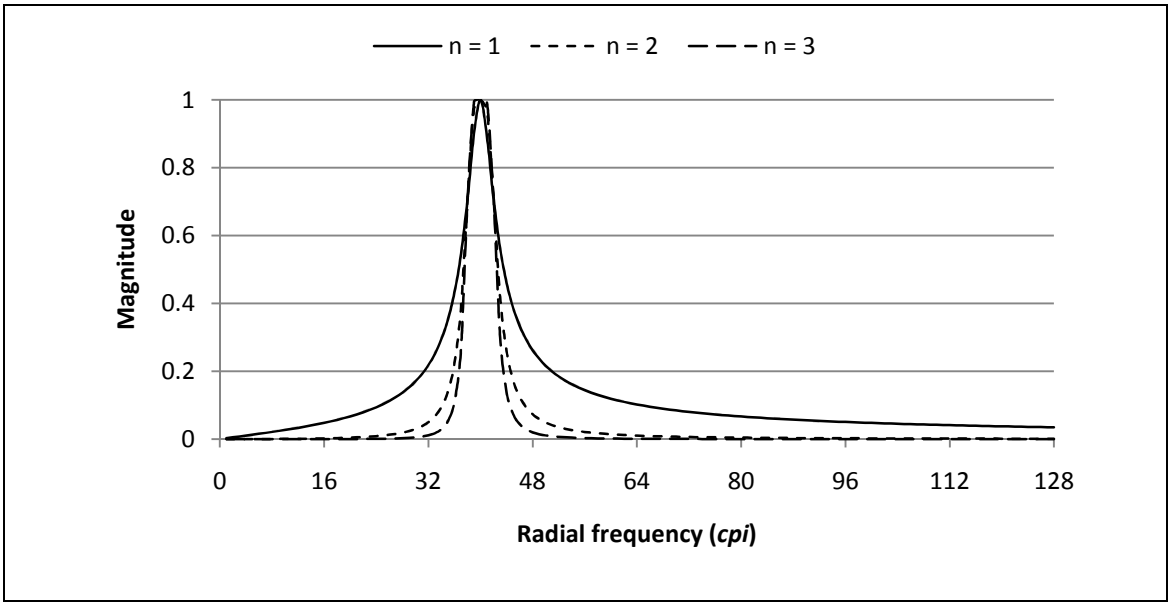

Figure 5-4: Effect of Butterworth order on distribution of radial frequency components

Thus, the magnitude spectrum is defined by *Equation (5-6)* and will be used to generate surfaces for psychophysical investigation. MATLAB program to generate these surfaces is given in *Appendix5-A*. As before, random phase spectra will be used to generate surfaces as described in *chapter 5*.

$$M(f,\theta) = \left(\frac{\delta}{\delta_n}\right)\left(1/f^{\beta}\right)\sqrt{\frac{1}{1+\left(\left(\frac{1}{f_h - f_l}\right)\left(\frac{(f_h\, f_l) - f^2}{f}\right)\right)^{2n}}}\;\left(e^{-(\theta-\theta_0)^2/2\sigma^2}\right) \quad (5\text{-}6)$$

5.2 Psychophysical Investigation

In this section, the separate and combined effects of change in random phase spectra, central radial frequency and bandwidth are investigated in the same way the effects of different random phase spectra, angular variance and RMS roughness were investigated in the previous chapter.

5.2.1 Effect of Different Random Phase Spectra on Perceived Directionality

In section 4.3.1, it was found that different random phase spectra do not affect the perception of directionality of surfaces generated using magnitude spectra described by *Equation (4.11).* However, it is not known whether perceived directionality of surfaces described by *Equation (5-6)* generated with low bandwidth (B_w), such as those shown in *Figure 5-5,* are affected by different random phase spectra. Surfaces in *Figure 5-5* have the same magnitude spectra described by *Equation (5-6)* with B_w and f_c set to 0.47 *cpd* and 3.28 *cpd* respectively, but with different random phase spectra.

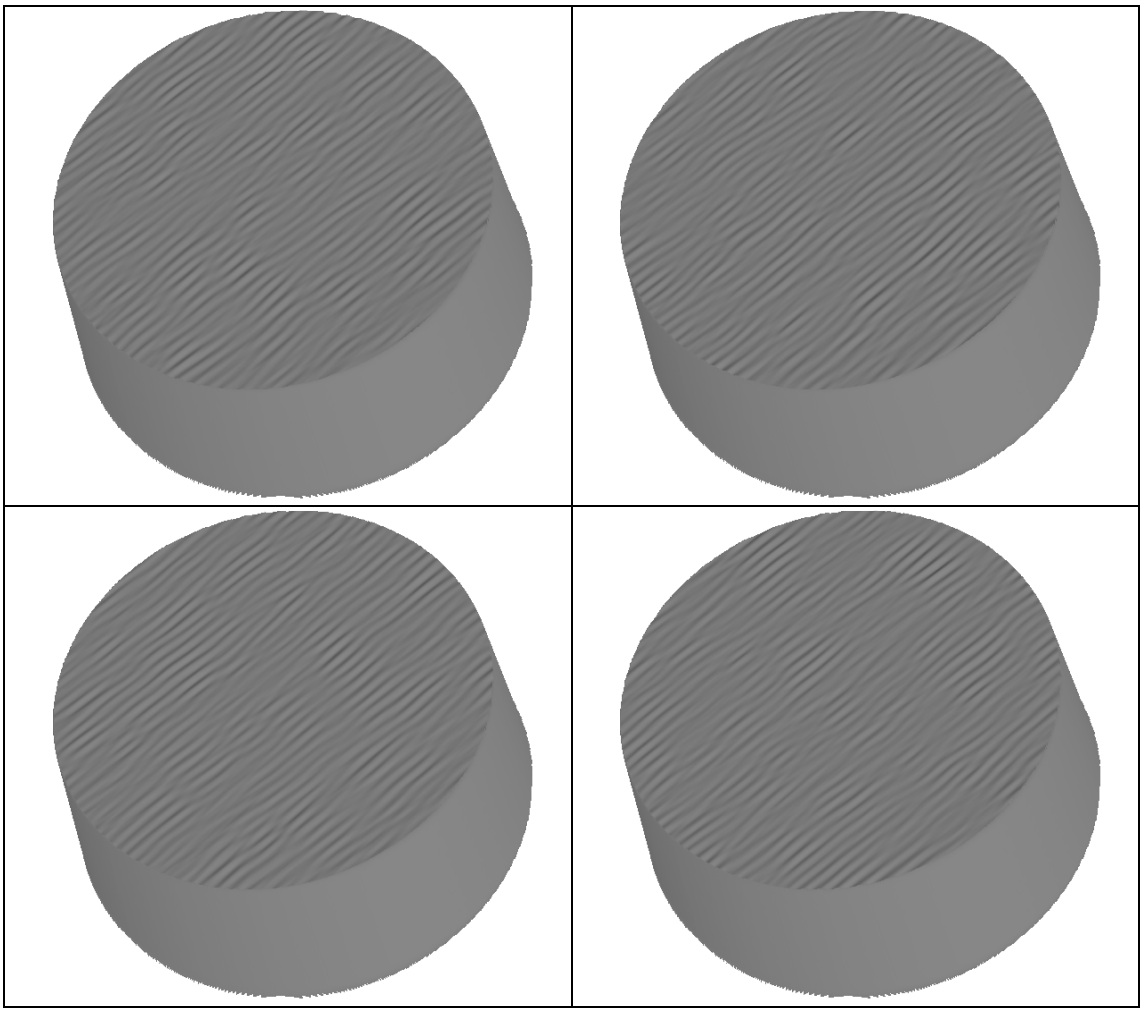

Figure 5-5: Effect of random phase spectra. Surfaces with the same magnitude spectrum and different random phase spectra

It can be observed from *Figure 5-5* that it is difficult to judge differences in directionality of surfaces. These surfaces have identical magnitude spectra but different random phase spectra. However, it is easy to compare and judge directionality of

surfaces with different magnitude spectra as was reported in *chapter 4*. Therefore to investigate the effects of different random phase spectra on perceived directionality of surfaces described by *Equation (5-6)*, the *method of constant stimuli* and *direct ratio estimation method*, described in section 4.3.1, was used.

During the experiment, *comparison* surfaces, with different random phase spectra and the same magnitude spectrum, were compared with a *standard* surface having a magnitude spectrum different from those of *comparison* surfaces. The magnitude spectra of *comparison* surfaces and a *standard* surface had different central radial frequencies as it is easy to judge differences in directionality between such surfaces (see *Figure 5-3*).

The effect of changing random phase spectra was tested for two values of central radial frequencies (f_c = 1.88 and 4.69 *cpd*). Five *comparison* surfaces were generated with different random phase spectra at both levels of f_c. Each set of five *comparison* surfaces were compared with three *standard* surfaces. *Figure 5-6* shows a graphical representation of the comparisons made by observers. The parameters B_w (0.47 *cpd*), σ^2(51.47 *degrees squared*) and δ (0.01 *cm*) were kept constant. No comparison was made between *comparison* surfaces and no comparison was made between *standard* surfaces.

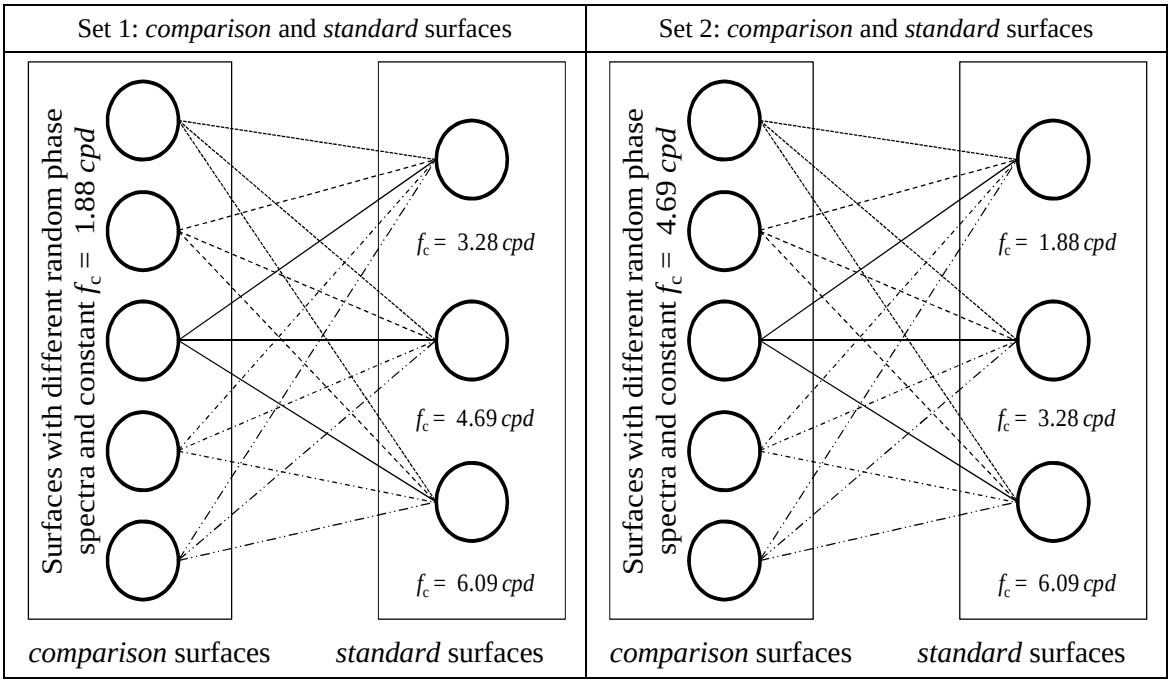

Figure 5-6: Graphical representation of pairs of comparison and standard surfaces to evaluate the effect of different random phase spectra

As each *comparison* surface needs to be compared with each *standard* surface, 30 pairings are possible with three *standard* surfaces and two sets of five *comparison* surfaces. Each *comparison* surface was presented three times with *standard* surfaces (each pair was repeated 3 times), and so in total each observer made 90 comparisons. As before, the order of pairs was randomised and the positions of surfaces in pairs were randomised.

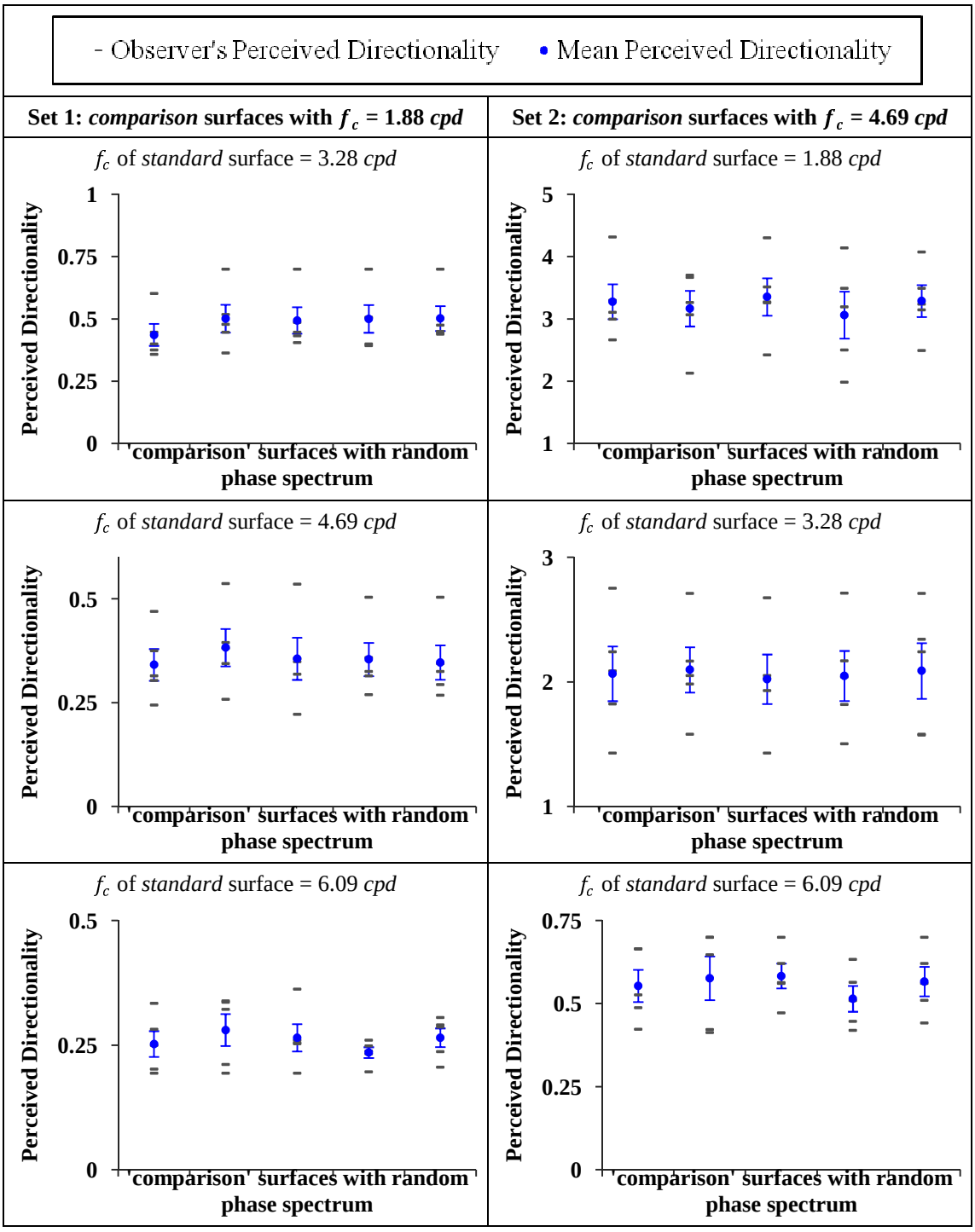

Figure 5-7: Perceived directionality of surfaces with random phase spectra. The error bars show the standard errors of mean.

Five naïve observers estimated the ratios of directionalities of *comparison* surfaces against *standard* surfaces. Surface presentation, experimental set up and observers' instructions were the same as those used for the experiment described in section 3.3. Observers' responses were processed as described in section 4.3.1. The order of surfaces and corresponding responses provided by observers are given in *Appendix5-B*. Perceived directionalities of *comparison* surfaces for each combination are plotted in *Figure 5-7*.

It can be observed that mean perceived directionality remains almost constant for all six combinations of *comparison* surfaces and *standard* surfaces. A one-way repeated measures ANOVA was carried out to determine whether there was any significant effect of random phase spectrum on the perception of directionality.

The results of an ANOVA tests for all six combinations are listed in *Table 5-2*. The results are shown with the assumption of sphericity as *Mauchly's test* indicated the assumption of sphericity is not violated ($p > 0.05$). It can be seen that the effect of phase spectra is significant when *comparison* surfaces' f_c is 1.88 *cpd* and *standard* surface's f_c is 3.28 *cpd*. However, for the other combinations of *standard* and *comparison* surfaces, significance values are greater than 0.05, and therefore it can be concluded that the change in random phase spectra has no general effect on the perception of directionality.

Assumption of Sphericity	Set of Surfaces		*F-Statistics*	*Sig. Value* (p)
	Standard Surface's f_c (*cpd*)	Comparison Surfaces' f_c (*cpd*)		
Sphericity Assumed	3.28	1.88	3.312	**0.037**
Sphericity Assumed	4.69	1.88	1.976	**0.147**
Sphericity Assumed	6.09	1.88	1.315	**0.306**
Sphericity Assumed	1.88	4.69	1.016	**0.428**
Sphericity Assumed	3.28	4.69	0.064	**0.992**
Sphericity Assumed	6.09	4.69	0.479	**0.751**

Table 5-2: Tests of within-subjects effects: random phase spectra

5.2.2 Effect of Varying Central Radial Frequency on Perceived Directionality

In this section, the effect of separately varying f_c with a constant B_w is investigated. Two experiments were conducted to test the effect of f_c on the perception of directionality. In the first experiment, bandwidth was kept low (B_w = 0.47 *cpd*) to determine how the perception of directionality changes over a wide range of f_c. In the second experiment, the effect over a smaller range of f_c, at high values of bandwidth is investigated.

5.2.2.1 Effect of varying f_c over a wider range at low value of bandwidth

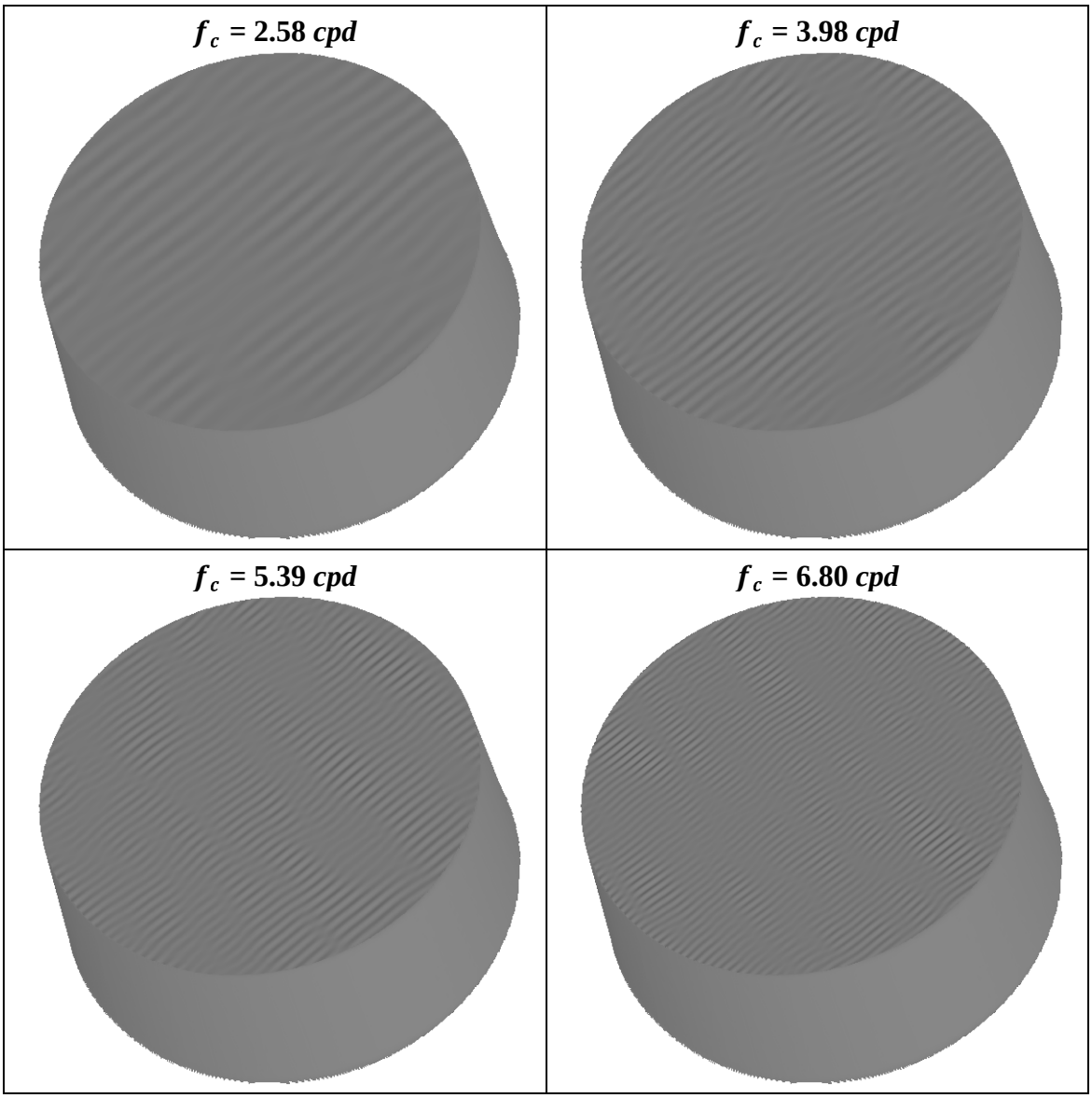

Figure 5-8: Effect of the change in f_c with a low B_w (0.47cpd)

High values of bandwidth do not provide sufficient freedom to allow us to examine the effects of low, medium and high central radial frequencies. However, surfaces with low bandwidth do allow us to investigate how observers perceive directionality at these central radial frequencies. Therefore, perceived directionalities of sixteen surfaces with different f_c and constant B_w (0.47 *cpd*) were obtained using the *direct ratio estimation* method. In *Figure 5-8*, the effect of changing central radial frequency is shown.

Sixteen surfaces were generated with the values of f_c at an interval of 0.70 *cpd* to have non-overlapping 3-dB bandwidth regions between surfaces. The lowest value of f_c was equal to 1.88 *cpd*. RMS roughness of surfaces was kept low (0.005 *cm*) to maintain a *naturalistic* appearance of surfaces with high values of f_c. A total of 120 pairs of sixteen surfaces were presented to six naïve observers in random order (*Appendix 5-C*). Surface presentation, experimental set up, instructions to observers and the method of obtaining perceived directionality were the same as those described in section 3.3. Observers' perceived directionality (ρ_o) and mean perceived directionality (ρ) are plotted in *Figure 5-9*.

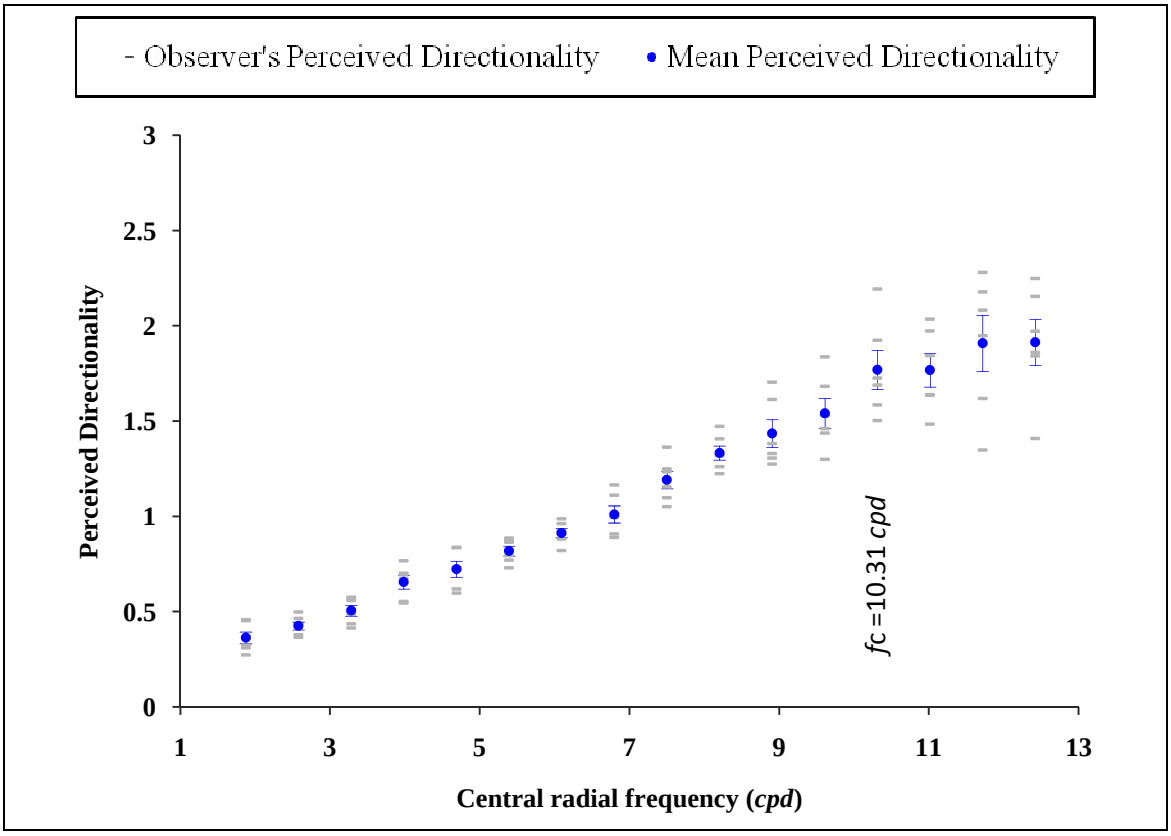

Figure 5-9: Perceived directionality vs. central radial frequency at low bandwidth. The error bars show the standard errors of mean.

An ANOVA results indicate that there is a significant effect of f_c (*F-statistic* = 63.358, $p < 0.05$) on the perception of directionality. The *degree of freedom* was corrected with *Greenhouse-Geisser* correction as *Mauchly's test* of sphericity did not specify if the assumption of sphericity is violated, because a number of levels of f_c is greater than a number of observers. However, from *Figure 5-9* it can be seen that there is large variation in observers' perceived directionality for f_c greater than 10.31 *cpd*. It is therefore interesting to verify if the change in perceived directionality is significant at high values of f_c. As it is not clear if the assumption of sphericity is violated, the *contrast*[1] results cannot be considered in order to evaluate if the differences at high frequencies are significant.

Therefore, another ANOVA test was conducted for the last six levels of f_c (from 8.91 to 12.42 *cpd*) with *repeated contrast*. The result shows that the assumption of sphericity is not violated ($p > 0.05$) and there is a significant main effect of f_c ($p < 0.05$). *Contrast* results (*Table 5-3*) reveal that there are significant differences in perceived directionality between values of f_c from 8.91 to 9.61 *cpd* and from 9.61 to 10.31 *cpd*, but there are no significant differences from 10.31 to 11.02, 11.02 to 11.72 and 11.72 to 12.42 *cpd*.

Levels of f_c (*cpd*)	*F – Statistics*	*Sig. Value* (*p*)
8.91 to 9.61	10.460	**0.023**
9.61 to 10.31	31.859	**0.002**
10.31 to 11.02	0.003	**0.960**
11.02 to 11.72	3.319	**0.128**
11.72 to 12.42	0.006	**0.941**

Table 5-3: Tests of within-subject contrasts at high frequencies

Thus, in general it can be concluded that perceived directionality of surfaces used in the experiment increases with the increase in f_c up to 10.31 *cpd* and thereafter does not change significantly.

[1] This is not a *contrast*, a visual characteristic of surface. *Contrast* is the test for statistical significance of differences in specific parts of repeated measures design.

5.2.2.2 Effect of varying f_c over a smaller range at high values of bandwidth

To observe the effect over a small range of f_c, an approach similar to that used for the investigation of the effects of varying only σ^2 at different constant levels of δ (section 4.3.2) in *chapter 4* was used. The surfaces were sampled at four values of f_c (2.81, 4.22, 5.63, and 7.03 *cpd*) and constant B_w.

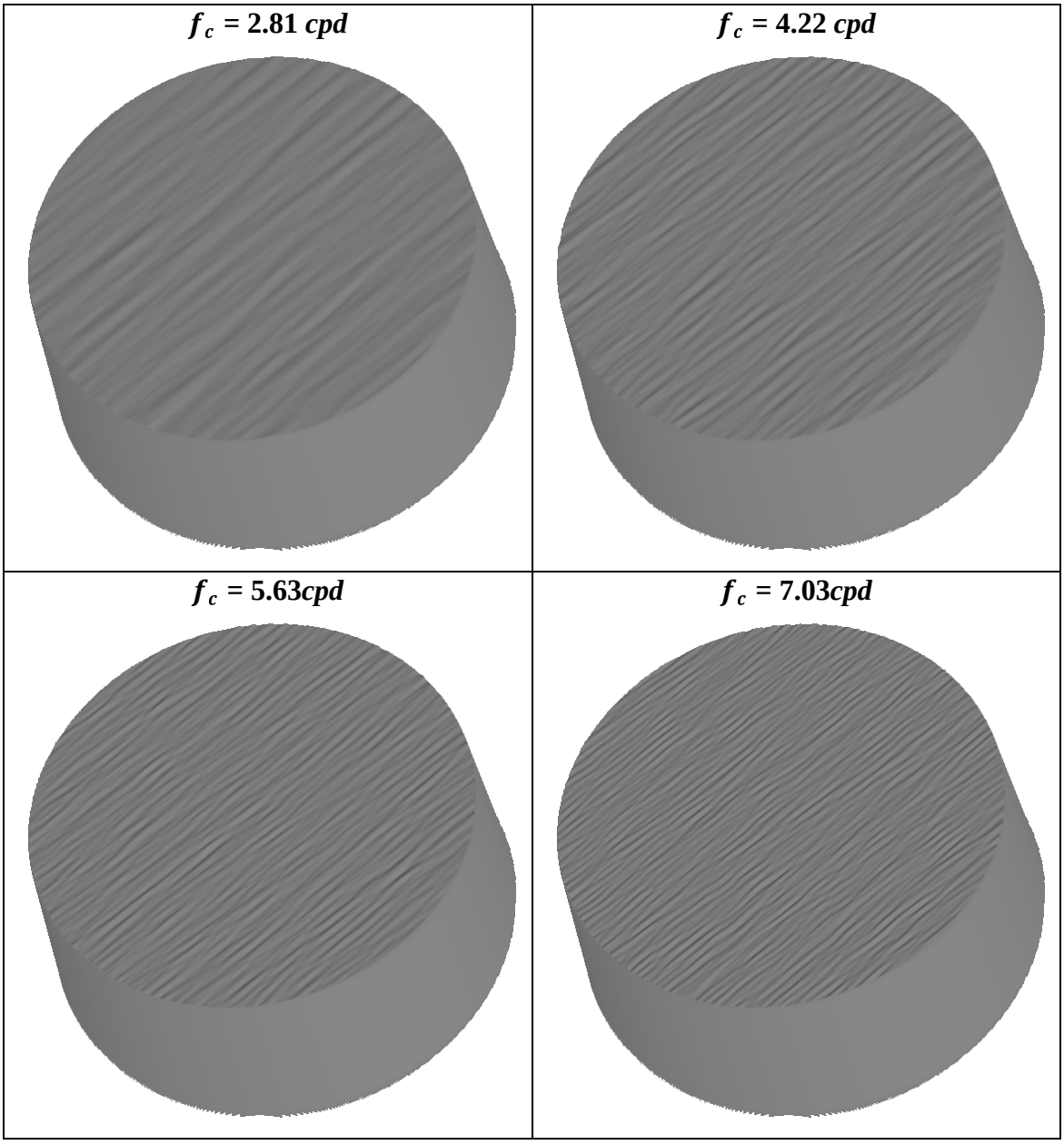

Figure 5-10: Effect of the change in f_c at higher bandwidth (B_w = 1.88 cpd)

Surfaces with different f_c (2.81, 4.22, 5.63, and 7.03 *cpd*) and constant B_w (1.88 *cpd*) are shown in *Figure 5-10*. The effect of varying f_c was observed at three constant levels

of bandwidths (B_w = 0.94, 1.88, and 2.81 *cpd*). No comparison was made between surfaces having different bandwidths.

Six possible pairs of surfaces having four different values of f_c with constant bandwidth were presented to observers thrice. As the same set up was investigated at three levels of B_w, a total of 54 pairs (6 pairs of varying f_c times 3 repetitions of pairs times 3 levels of B_w) were presented to observers in random order (see *Appendix5-D*)

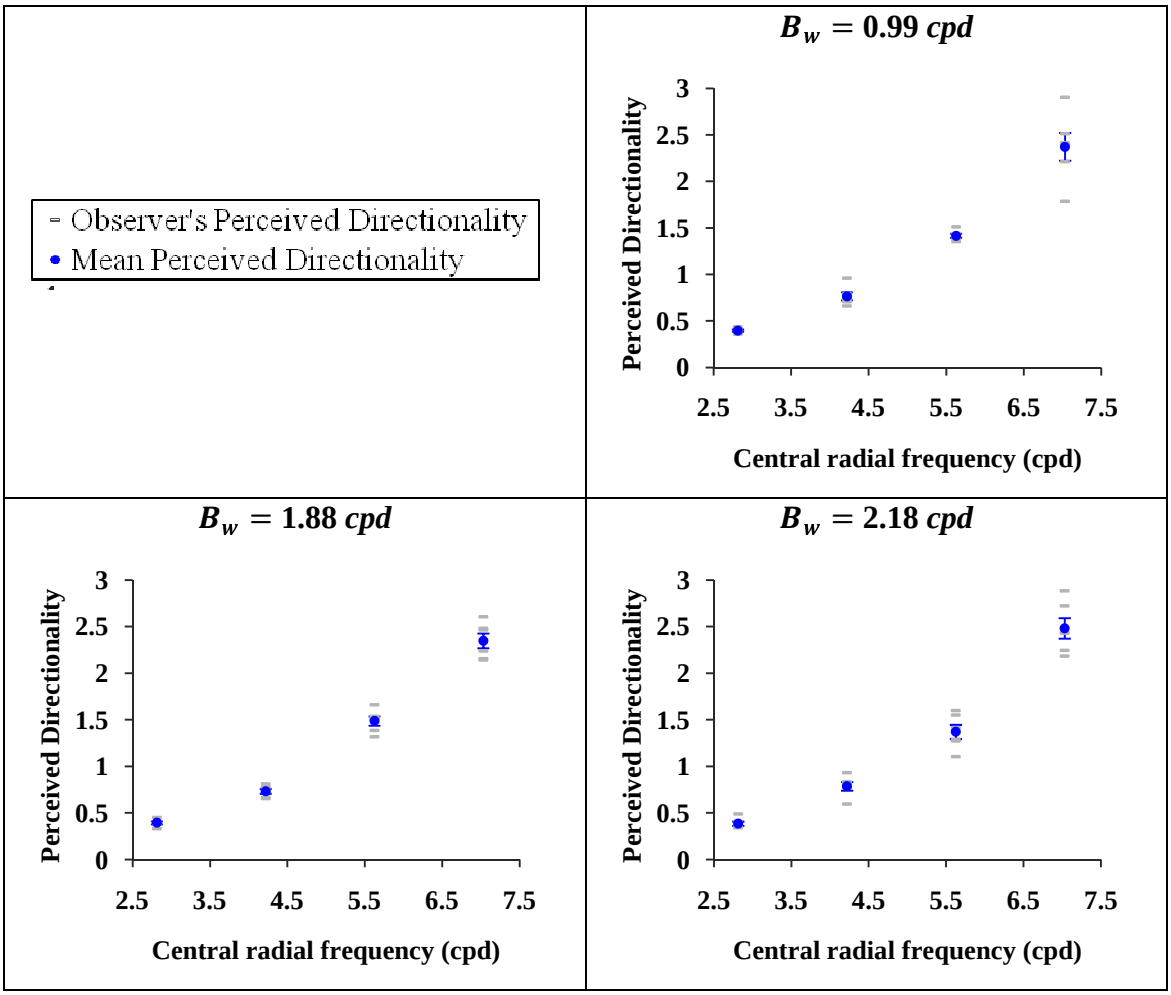

Figure 5-11: Perceived directionality vs. central frequency at constant levels of B_w

Six naïve observers took part in this experiment. Surface presentation, experimental set up, observers' instructions and method of obtaining perceived directionality were the same as those described in section 3.3. Observers' perceived directionalities (ρ_o) and their arithmetic means (ρ) are plotted against f_c in *Figure 5-11* for each value of B_w. It can be seen that as f_c increases, ρ also increases.

A one-way repeated measures ANOVA was conducted to test the significance of effect of f_c on the perception of directionality. The *degrees of freedom* were corrected using *Greenhouse-Geisser* estimates of sphericity for the main effect of f_c when the assumption of sphericity was violated. *Table 5-4* shows that there is significant main effect ($p < 0.05$) of f_c at all levels of B_w.

Assumption of sphericity	Constant level of B_w (*cpd*)	*F - Statistics*	*Sig. Value* (p)
Sphericity Assumed	0.94	100.901	<**0.001**
Greenhouse-Geisser	1.88	266.829	<**0.001**
Sphericity Assumed	2.81	124.939	<**0.001**

Table 5-4: Tests of within-subjects effects of f_c at different levels of B_w

5.2.3 Effect of Varying Bandwidth on Perceived Directionality

To investigate how perceived directionality changes with the change in bandwidth (B_w), perceived directionalities of surfaces with different B_w and constant f_c were obtained using the approach similar to that described in the previous section.

Four different values of B_w (0.47, 1.88, 3.28 and 4.69 *cpd*) were used. Three constant levels of f_c (2.81, 4.69 and 6.56 *cpd*) were chosen at which the effect of separately varying B_w was investigated by comparing the surfaces with different B_w and constant f_c. No comparison was made between the surfaces having different central radial frequencies (f_c).

Surfaces at different B_w (0.47, 1.88, 3.28 and 4.69 *cpd*) and constant f_c (4.69 *cpd*) are shown in *Figure 5-12*. Six pairs are possible with four different values of B_w, each pair was presented thrice, and the effect of B_w was observed at three different levels of f_c. A total of 54 pairs (6 pairs of varying B_w times 3 repetitions of pairs times 3 levels of f_c) were presented to six naïve observers in random order (see *Appendix5-E*). Surface presentation, experimental set up, observers' instructions and method of obtaining perceived directionality were the same as those described in section 3.3.

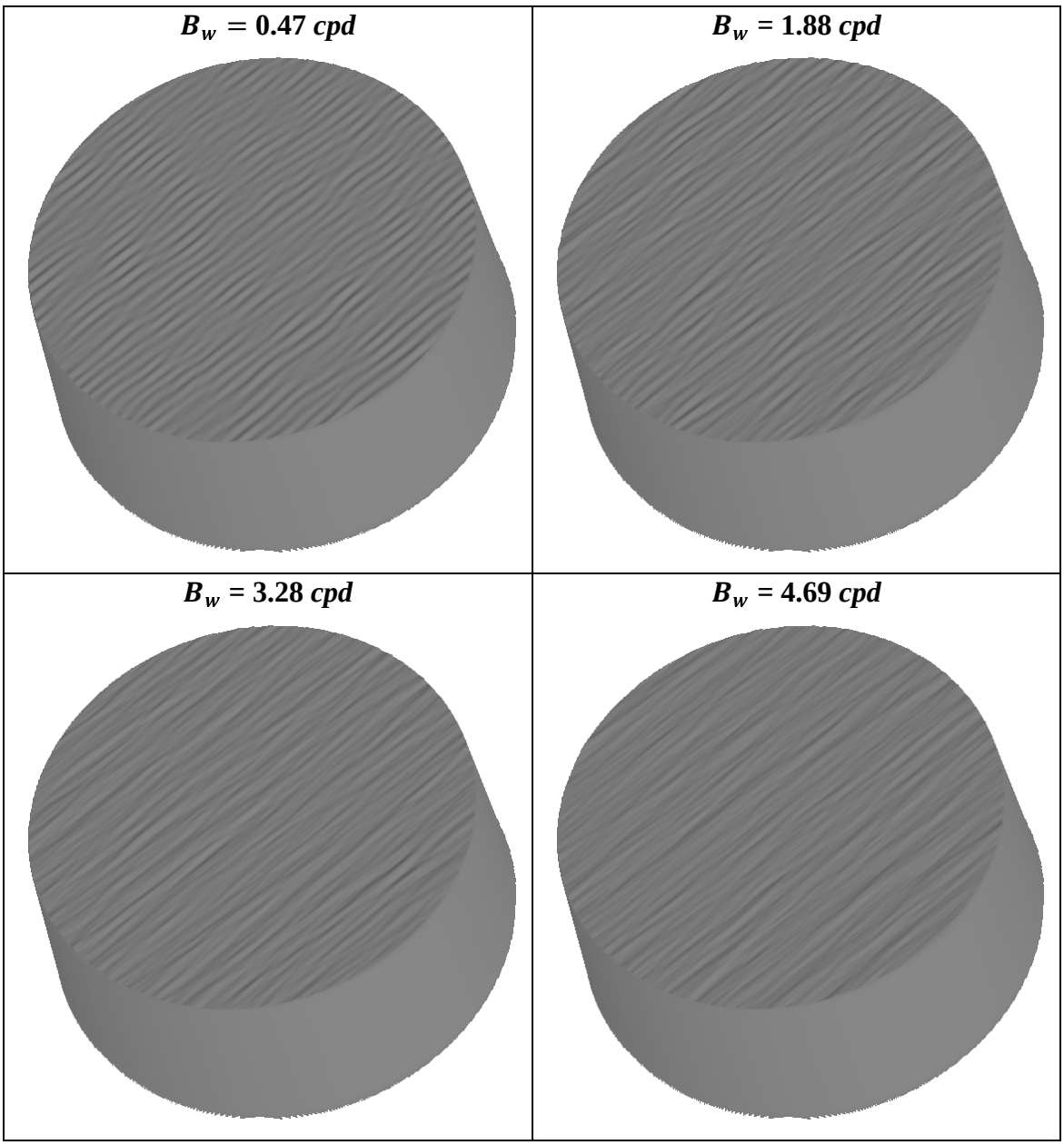

Figure 5-12: Effect of B_w with constant f_c (4.69 cpd)

Their perceived directionalities (ρ_o) and arithmetic means (ρ) are plotted against B_w in *Figure 5-13* for each value of f_c. It can be observed from *Figure 5-13* that the trend in the change in perceived directionality with the change in B_w is different at different levels of f_c. When f_c is equal to 2.18 *cpd*, perceived directionality increases up to B_w equal to 3.28 *cpd* then decreases but for higher values of f_c, ρ increases monotonically with B_w. Therefore, it would be interesting to verify if the change in perceived directionality between levels of bandwidth is significant.

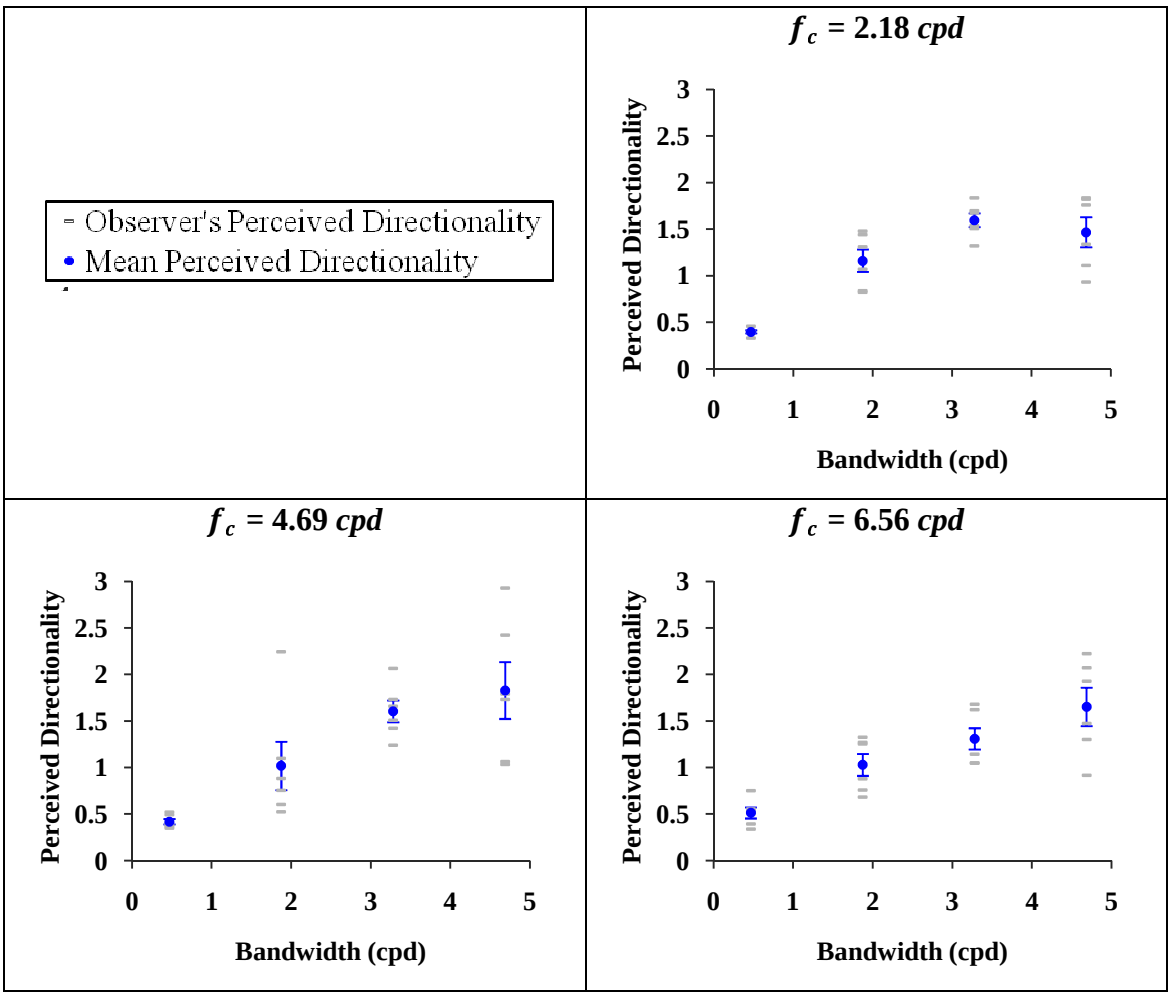

Figure 5-13: Perceived directionality vs. bandwidth at constant levels of f_c. The error bars show the standard errors of mean.

A one-way repeated measures ANOVA was conducted with different kinds of *contrast* tests (*Simple (first) contrast*, *Simple (last) contrast*, r*epeated contrast*) to reveal if the differences in ρ between levels of B_w are significant. The results of an ANOVA tests for each value of f_c are reported below. To aid the reader four levels of B_w are denoted as B_{w1} (= 0.47 *cpd*), B_{w2} (= 1.88 *cpd*), B_{w3} (= 3.28 *cpd*), B_{w4} (= 4.69 *cpd*) in this section only. The *degrees of freedom* were corrected using *Greenhouse-Geisser* estimates of sphericity when *Mauchly's test* indicated that the assumption of sphericity was violated ($p > 0.05$) and no correction to *degrees of freedom* were applied when the assumption of sphericity was not violated.

1. Effect of B_w when f_c = 2.81 *cpd*

The results show that the perception of directionality is significantly affected by bandwidth, $p < 0.05$, when f_c is equal to 2.81 *cpd*.

Contrast results revealed that perceived directionality at B_{w1} is significantly different from ρ at B_{w2}, B_{w3} and B_{w4} ($p < 0.05$). Furthermore, ρ at B_{w2} is significantly different from ρ at B_{w3} ($p < 0.05$) but ρ at B_{w2} and B_{w3} ($p > 0.05$) is not significantly different from ρ at B_{w4} of bandwidth.

2. Effect of B_w when f_c = 4.69 *cpd*

The results show that the perception of directionality is significantly affected by bandwidth, when f_c is equal to 4.69 *cpd*, $p < 0.05$.

Contrast results revealed that perceived directionality (ρ) at B_{w1} is significantly different from ρ at B_{w2}, B_{w3} and B_{w4} ($p < 0.05$). Perceived directionality (ρ) at B_{w2} is not significantly different from ρ at both, B_{w3} and B_{w4} ($p > 0.05$). Also no significant difference is found between B_{w3} and B_{w4} ($p > 0.05$).

3. Effect of B_w when f_c = 6.56 *cpd*

The results show that the perception of directionality is significantly affected by bandwidth, $p < 0.05$, when f_c is equal to 6.56 *cpd*.

As the assumption of sphericity is violated, the *degrees of freedom* in *contrast* results are not corrected and hence the results of *contrast* are ignored in this case and only result of main effect is taken into account.

Above analysis for the effects of B_w at all levels of f_c is summarised in *Table 5-5* (main effects) and *Table 5-6* (*contrast* results where applicable). From the results of the ANOVA tests, it can be concluded that there is a significant effect of bandwidth on the perception of directionality of surfaces used in the experiment. The effect is found significant, for the levels of B_w chosen in this experiment, up to value of B_w equal to 3.28 *cpd* and saturates above B_w equal to 3.28 *cpd*.

Source	Constant level of f_c (*cpd*)	*F - Statistics*	*Sig. Value* (p)
Sphericity Assumed	2.18	19.163	**<0.001**
Sphericity Assumed	4.68	7.047	**0.004**
Greenhouse-Geisser	6.56	10.345	**0.017**

Table 5-5: Tests of within-subjects effect of B_w

Levels of Bandwidth	Constant level of f_c (*cpd*)	*F – Statistics*	*Sig. Value* (p)
B_{w1} Vs B_{w2}	2.18	38.399	**0.002**
B_{w1} Vs B_{w3}	2.18	262.936	**<0.001**
B_{w1} Vs B_{w4}	2.18	41.629	**0.001**
B_{w2} Vs B_{w3}	2.18	9.605	**0.027**
B_{w2} Vs B_{w4}	2.18	1.278	**0.310**
B_{w3} Vs B_{w4}	2.18	0.417	**0.547**
B_{w1} Vs B_{w2}	4.68	4.801	**0.080**
B_{w1} Vs B_{w3}	4.68	99.303	**<0.001**
B_{w1} Vs B_{w4}	4.68	21.829	**0.005**
B_{w2} Vs B_{w3}	4.68	3.124	**0.137**
B_{w2} Vs B_{w4}	4.68	2.368	**0.184**
B_{w3} Vs B_{w4}	4.68	0.436	**0.538**

Table 5-6: Tests of within-subjects contrasts reveal if the differences in ρ between any two levels of bandwidth (used in the experiment) are significant

5.2.4 Effect of Varying Both Central Radial Frequency and Bandwidth on Perceived Directionality

In section 5.2.2 and 5.2.3, it has been observed that both f_c and B_w affect the perception of directionality when their effects are investigated separately. However, in these experiments, surfaces with different f_c and B_w have not been compared and so observers did not see the differences between surfaces differing in both f_c and B_w. Therefore, the combined effect of the two parameters or for any interaction between these two parameters cannot be inferred.

To obtain the effect sizes and a possible interactions, it was necessary to conduct another experiment in which observers compared all possible paired combinations of surfaces with different values of f_c and B_w. For the experiment, a total of sixteen surfaces were generated with four different values of f_c (2.58, 4.22, 5.86 and 7.5 *cpd*) and four different values of B_w (0.47, 1.88, 3.28 and 4.69 *cpd*). The value of B_w equal to 4.69 *cpd* was included, even though in section 5.2.3 it was found that there is no significant difference in perception between B_w equal to 3.28 and 4.69 *cpd*, in order to

observe how these two levels of bandwidth affect the perception of directionality between different levels of f_c.

Observers compared each of the 120 possible pairs of these sixteen surfaces two times. They were presented in random orders. Six naïve observers took part in the experiment and provided ratio judgements for each pair. The order of pairs of surfaces for each observer and corresponding responses are given in *Appendix5-F*. These responses were normalised using *Equation (3-8)* and then perceived directionalities of surfaces were obtained using the procedure described in section 3.3.2 of *chapter 3*.

Observers' perceived directionality (ρ_o) and mean perceived directionality (ρ) are plotted against f_c at different levels of B_w; and against B_w at different levels of f_c in *Figure 5-14* and *Figure 5-15* respectively. It can be seen that the effect of changes in f_c on perceived directionality is greater than the effect of changes in B_w. The result of a two-way repeated measures ANOVA test, shown in *Table 5-7*, reveals how these two parameters together affect the perception of directionality. *Table 5-7* also shows the effect sizes (*partial eta square*, η) of the main effects and the interactions indicating which parameter has greater effect than the other.

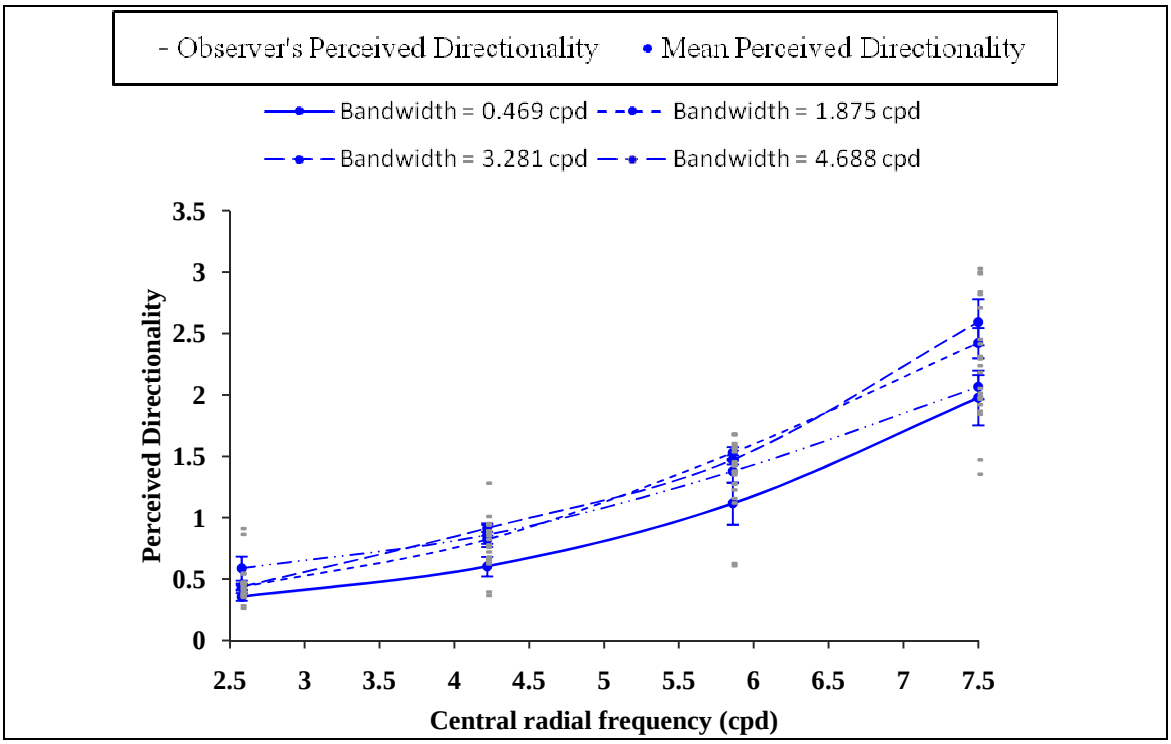

Figure 5-14: Perceived directionality vs. central radial frequency (f_c) at different levels of bandwidth (B_w).The error bars show the standard errors of mean.

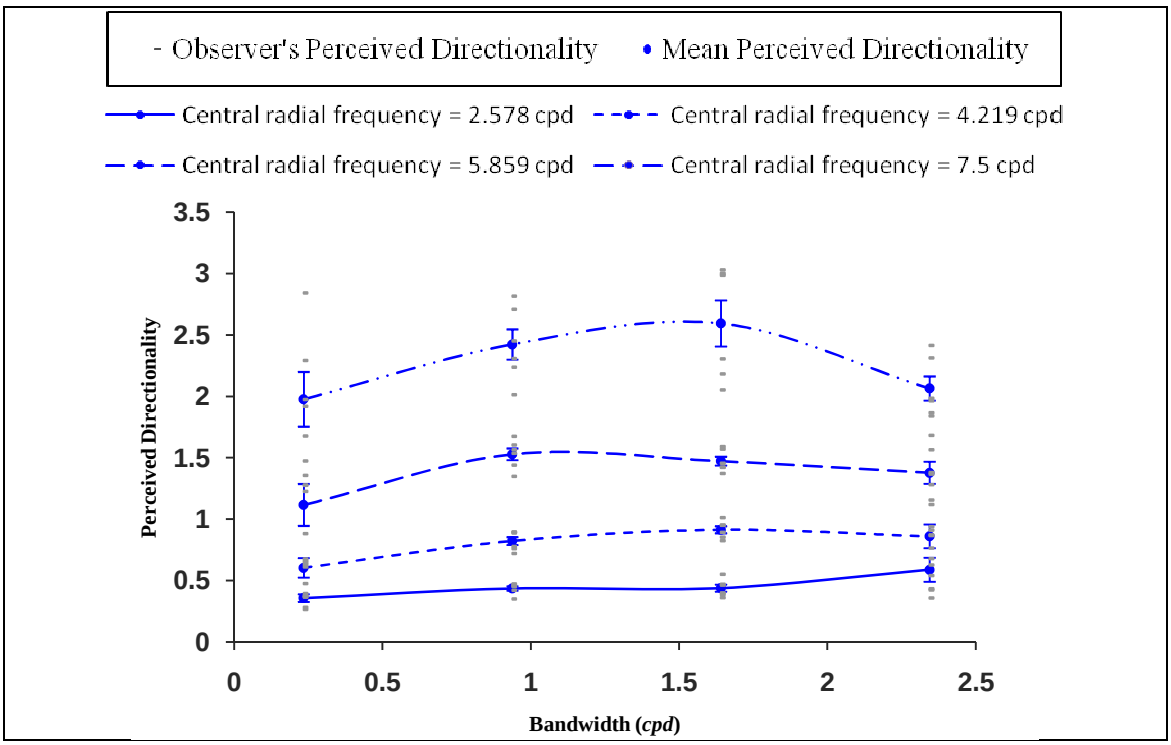

Figure 5-15: Perceived directionality vs. bandwidth (B_w) at different levels of central radial frequency (f_c). The error bars show the standard errors of mean.

From *Table 5-7*, it can be observed that there is a significant effect only for f_c ($p < 0.05$) on the perception of directionality. Neither bandwidth ($p > 0.05$) nor the interaction ($p > 0.05$) between f_c and B_w affects the perception of directionality significantly. The corrected results (*Greenhouse-Geisser* estimates of sphericity) were considered where the assumption of sphericity was violated. Thus, the effect of bandwidth is negligible when observers are presented with the surfaces differing in both f_c and B_w. The values of η suggest that only f_c has a high effect on the perception of directionality. As there is no significant main effect of B_w or of the interaction term, no further analysis was carried out.

Source		*F - Statistics*	*Sig. Value* (p)	*Partial eta squared* (η)
f_c	Sphericity Assumed	296.514	**<0.001**	**0.983**
B_w	*Greenhouse-Geisser*	2.913	**0.142**	**0.368**
(f_c) (B_w)	*Greenhouse-Geisser*	2.941	**0.99**	**0.370**

Table 5-7: Tests of within-subjects effects (combined effect of f_c and B_w)

5.3 Summary and discussion

To investigate the effects of varying distributions of radial frequency components, a new random phase surface model was defined. Through a series of psychophysical experiments investigating the effects of variation in the distributions of radial frequencies the following have been shown:

1. Changes in random phase spectra do not have a significant effect on perceived directionality of surfaces defined by *Equation (5-6)*.
2. Variation of central radial frequency (f_c) has a significant effect on perceived directionality when the effect of separately varying f_c was observed; increasing f_c increases perceived directionality.
3. Variation of bandwidth (B_w) has a significant effect on perceived directionality when the effect of separately varying B_w was observed; increasing B_w increases perceived directionality. However, no significant differences in perceived directionality were observed between values of B_w greater than or equal to 3.28 *cpd*.
4. When the combined effects of f_c and B_w were observed, the perception of directionality was significantly affected by only f_c. Neither B_w nor the interaction between f_c and B_w has a significant effect on perceived directionality of surfaces used in the experiment.

Thus, the observations in *chapter 4* and in this chapter indicate that the distributions of both angular and radial frequency components affect human perception of directionality. However, neither of these chapters investigated the effects of all possible interactions between the parameters.

Chapter 6

Measurement Model of Perceived Directionality

In this chapter a measurement model of perceived directionality of random-phase surfaces will be developed. Previously, it was found that the distributions of angular and radial frequency components, together with RMS roughness, affect human perception of directionality. However, in the psychophysical experiments reported in *chapter 4* and *chapter 5*, all parameters affecting perceived directionality were not varied simultaneously. Furthermore, it was found that when the two parameters were varied together, the effects of parameters on perceived directionality change. Therefore, ideally all four parameters would be needed to vary simultaneously in one experiment to investigate the effects of all possible interactions between parameters. However, due to practical limitations (discussed later) it is not possible to investigate the effects of three-way and four-way interactions between parameters. Therefore, this chapter assumes that there are no significant effects of three-way and four-way interactions between parameters and investigates the separate (one-way) and two-way interaction effects of parameters.

Previously, the effects of four parameters (angular variance (σ^2), RMS roughness (δ), central radial frequency (f_c) and bandwidth (B_w)) were tested. This chapter further investigates how two-way interactions between these parameters affect human perception of directionality. The surface model defined in *chapter 5* allows us to vary all of these parameters and therefore this surface model will also be used in this chapter.

As the parameter space is four-dimensional, several practical problems arise in conducting the psychophysical experiment. These problems will be discussed in section 6.1 and the method of conducting psychophysical experiment to analyse the main and interaction effects of parameters will be described. In section 6.2, the psychophysical results and their statistical significance will be investigated. In section 6.3, a model of perceived directionality will be developed based on the significance test results. The chapter ends with a small summary in section 6.4.

6.1 Method

As the goal of this chapter is to propose a measurement model of perceived directionality, ideally all four surface parameters need to be varied in one experiment to ensure the use of consistent perceptual scaling across these parameters and the following need to be investigated:

1. Separate effects of the four parameters on the perception of directionality.
2. Two-way interaction terms ($\{\sigma^2, \delta\}$, $\{\sigma^2, f_c\}$, $\{\sigma^2, B_w\}$, $\{\delta, f_c\}$, $\{\delta, B_w\}$ and $\{f_c, B_w\}$) where the effects of the two parameters are tested together.
3. Three-way interaction terms ($\{\sigma^2, \delta, f_c\}$, $\{\sigma^2, \delta, B_w\}$, $\{\sigma^2, f_c, B_w\}$ and $\{\delta, f_c, B_w\}$) where the effects of the three parameters are tested together.
4. Four-way interaction term ($\{\sigma^2, \delta, f_c, B_w\}$) where the effects of the four parameters are tested together.

At first sight it would seem that this goal can be achieved simply by conducting a psychophysical experiment using all surfaces generated with the complete set of combinations of parameter values. However, there are following practical limitations in sampling four-dimension parameter space for an investigation of the effects of three-way and four-way interactions between parameters:

1. If the sampling of parameter space that generates *naturalistic* surfaces was possible and if four values of each parameter were selected then a total of 256 different surfaces would be needed to investigate the effects of three-way ($4^3 + 4^3 + 4^3 + 4^3 = 256$) and four-way ($4^4 = 256$) interactions between parameters. With this many surfaces, numbers of pairs of surfaces are 8064 for the three-way interactions and 32640 for the four-way interactions and so a psychophysical experiment using the method of *pair-wise comparisons* is not practical, as it will produce erroneous responses due to effects of fatigue and loss of attention.
2. To achieve this sampling, the range of parameter values would have to be kept small to ensure *naturalistic* appearance of surfaces. For example, to investigate the perception of directionality at a high value of f_c and a low value of B_w, the maximum value of δ must be kept low, or the minimum value of σ^2 must be kept high. This is because surfaces do not look *naturalistic* when the values of f_c

and δ are high and the values of B_w and σ^2 are low. Therefore, an investigation of the three-way and four-way interactions of parameters is not practical even if the experiment is conducted using the *method of constant stimuli* with 256 pairs, as the design will result in unreliable measurements of effects of parameters and their combinations.

However, there are no such problems in the sampling of parameter space to investigate the effects of parameters separately and the two-way interactions between parameters. So these effects will be tested to achieve the goal of this chapter with an assumption that there are no significant effects of the three-way and four-way interactions between parameters.

In *chapter 4* and *chapter 5*, two-way interactions $\{\sigma^2, \delta\}$ and $\{f_c, B_w\}$ were investigated. To have consistent perceptual scaling across all two-way interaction terms, these interactions together with the remaining four two-way interactions will be investigated in this chapter.

Once again it is not practical to use the *method of pair-wise comparisons* because if four values of each parameter are selected, 16 surfaces and 120 surface pairs are required for each two-way interaction, making a total of 720 pairs. Therefore the *method of constant stimuli* will be used in which all surfaces will be paired with one constant surface. The drawback of this method is that there is a possibility of higher variability in the responses due to the large number of unique surface pairs. This will be minimized by repeating each pair and by conducting experiment with more observers.

In the next section, the parameter values for each two-way interaction term are specified, and associated perceived directionalities are provided. Furthermore, the statistical significance testing of the separate and two-way interaction effects will be carried out.

6.2 Results

To observe the effect of two-way interaction, *variable parameter 1* and *variable parameter 2* in *Table 6-1* were varied while the remaining two parameters were kept

constant. The parameter values were chosen to ensure *naturalistic* appearance of surfaces.

Two-way interaction term	*Constant parameter 1*	*Constant parameter 2*	*Variable parameter 1*	*Variable parameter 2*
$\{\sigma^2, \delta\}$	f_c (3.75)	B_w (2.34)	σ^2 (20.0, 51.48, 132.5, 341.04)	δ (0.005, 0.01, 0.015, 0.02)
$\{\sigma^2, f_c\}$	δ (0.01)	B_w (2.34)	σ^2 (20.0, 51.48, 132.5, 341.04)	f_c (1.88, 3.75, 5.63, 7.5)
$\{\sigma^2, B_w\}$	δ (0.01)	f_c (3.75)	σ^2 (20.0, 51.48, 132.5, 341.04)	B_w (0.94, 2.34, 3.75, 5.16)
$\{\delta, f_c\}$	σ^2 (132.5)	B_w (2.34)	δ (0.005, 0.01, 0.015, 0.02)	f_c (1.88, 3.75, 5.63, 7.5)
$\{\delta, B_w\}$	σ^2 (132.5)	f_c (3.75)	δ (0.005, 0.01, 0.015, 0.02)	B_w (0.94, 2.34, 3.75, 5.16)
$\{f_c, B_w\}$	σ^2 (82.58)	δ (0.01)	f_c (1.88, 3.75, 5.63, 7.5)	B_w (0.47, 1.41, 2.34, 3.28)

Table 6-1: Parameter values of surfaces for two-way interaction terms. f_c and B_w are in cpd. σ^2 is in degrees squared. δ is in cm.

As the *variable parameters* have four values, a total of 96 surfaces (16 times 6 two-way interaction terms) were generated using *Equation (5-6)* for the psychophysical experiment. However some of the combinations of parameter values are same for more than one two-way interaction terms. For example, the parameter combination f_c = 1.88 *cpd*, B_w = 2.34 *cpd*, σ^2 = 132.5 *degrees squared* and δ = 0.01 *cm* is used for the two-way interaction terms $\{\sigma^2, \delta\}$ and $\{\delta, f_c\}$. There is therefore no need to include this

surface twice in the experiment. After removing all such duplications, only 74 surfaces were left.

These 74 *comparison* surfaces were compared with a *standard* surface twice. Only one *standard* surface was used for all six two-way interaction terms in order to use a single reference point. A *standard* surface was chosen to be less directional than all *comparison* surfaces. In *chapter 4* and *chapter 5*, it was observed that perceived directionality of random-phase surfaces decreases when angular variance (σ^2) increases; when RMS roughness (δ) decreases; when central radial frequency (f_c) decreases, or when bandwidth (B_w) decreases. Therefore, a *standard* surface was generated with lower values of f_c (1.88 *cpd*), B_w (0.47 *cpd*) and δ (0.005 *cm*) and a higher value of σ^2 (341.04 *degrees squared*) compared to values of parameters of *comparison* surfaces to ensure that it appeared less directional than all 74 *comparison* surfaces.

Observers were told that a *standard* surface was always less directional than *comparison* surfaces and asked to give the ratio between *comparison* and *standard* surface. Surface presentation and experimental set up were the same as those described in section 3.3. Observers' responses were processed as described in section 4.3.1. Observers' responses were normalised using *Equation (3-8)* as they used different scales for the ratios. As each of *comparison* surfaces was presented twice, the geometric mean of the two ratios of perceived directionalities of *comparison* surface and *standard* surface was taken as the ratio between that *comparison* and *standard* surfaces. Observers perceived directionalities (ρ_o) of *comparison* surfaces were obtained by assigning a value of 1 to a *standard* surface. Mean perceived directionality was obtained by taking an arithmetic mean of observers' perceived directionalities. A total of nine naïve observers took part in the experiment. Observers' perceived directionalities and mean perceived directionalities of the surfaces used in this experiment are given in *Appendix 6-A.*

The two-way repeated measures ANOVA tests were carried out for each of the six two-way interactions. Perceived directionalities were plotted to show the change in perceived directionality against the changes in parameters. In these sub-sections, the ANOVA results are reported with sphericity assumption when *Mauchly's test* of sphericity is not violated ($p > 0.05$) and the results were reported using corrected *degrees of freedom* using *Greenhouse-Geisser* estimates of sphericity when the

assumption of sphericity is violated. As the final goal is to obtain a measurement model of perceived directionality, *polynomial contrasts* were used for the ANOVA tests in order to identify the type of trend of perceived directionality. The effect sizes were also calculated.

6.2.1 Separate and Interaction Effects of Angular Variance and RMS Roughness

Observers' perceived directionality and mean perceived directionality are plotted against σ^2 and δ in *Figure 6-1*. It can be clearly seen that perceived directionality decreases with an increase in σ^2 at all levels of δ and perceived directionality increases with an increase in δ at all levels of σ^2. A similar effect was observed in *chapter 4* when observers viewed surfaces having different σ^2 and δ.

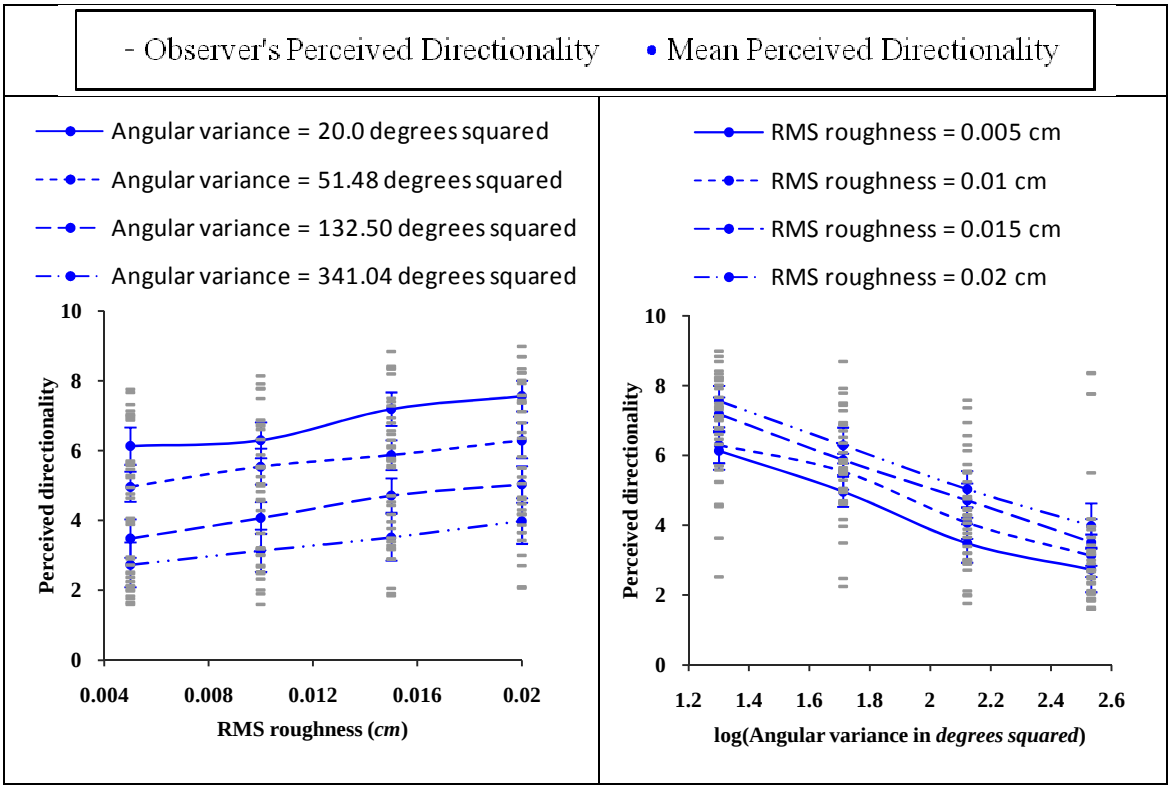

Figure 6-1: Effect of RMS roughness (left) at different levels of angular variance and effect of angular variance (right) at different levels of RMS roughness. The error bars show standard errors of mean.

The results of the ANOVA tests (*Table 6-2*) show that there are significant effects ($p <$ 0.05) of σ^2 and δ on perceived directionality but the interaction between these two

parameters is not significant (p > 0.05). *Contrast* results (*Table 6-3*) indicate that the parameters (log (σ^2) and δ) have linear (p < 0.05) trend with perceived directionality. The trend is linear with the logarithm of angular variance as surfaces with different angular variances were equally separated on the logarithm scale. The effect sizes (η) show that σ^2 has greater effect on the perception of directionality than δ.

Source	Assumption of sphericity	*F - Statistics*	*Sig. Value* (p)	Partial Eta Square (η)
σ^2	Greenhouse-Geisser	16.052	**0.002**	**0.667**
δ	Sphericity assumed	10.462	**<0.001**	**0.567**
(σ^2) (δ)	Greenhouse-Geisser	0.286	**0.877**	**0.035**

Table 6-2: Tests of Within-Subjects Effects: σ^2 and δ

Source	Trend	*F-Statistics*	*Sig. Value*	*Partial Eta Squared*
log (σ^2)	**Linear**	**18.449**	**.003**	**.698**
	Quadratic	.103	.757	.013
	Cubic	2.146	.181	.212
δ	**Linear**	**17.354**	**.003**	**.684**
	Quadratic	.014	.909	.002
	Cubic	.250	.630	.030

Table 6-3: Tests of within-subjects contrasts, log (σ^2) and δ

6.2.2 Separate and Interaction Effects of Angular Variance and Central Radial Frequency

Observers' perceived directionalities and mean perceived directionality are plotted against σ^2 and f_c in *Figure 6-2*. Again it can be seen that perceived directionality decreases with an increase in σ^2 at all levels of f_c. Also perceived directionality increases with an increase in central radial frequency (f_c) as was observed in *chapter 5*.

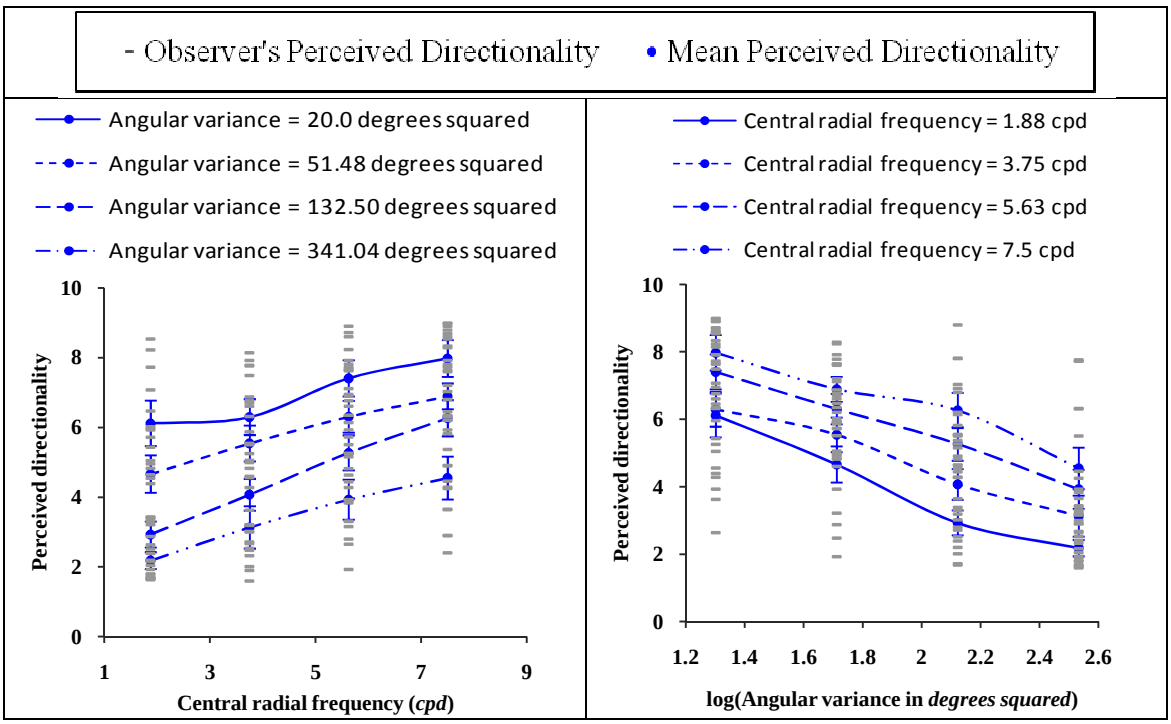

Figure 6-2: Effect of central radial frequency (left) at different levels of angular variance and effect of angular variance (right) at different levels of central radial frequency. The error bars show the standard errors of mean.

The results of the ANOVA tests (*Table 6-4*) show that both σ^2 and f_c affect perceived directionality significantly ($p < 0.05$), but that there is no significant interaction between these two parameters. *Contrast* results (*Table 6-5*) reveal that perceived directionality varies linearly ($p < 0.05$) with both parameters. The values of η indicate that the effect of f_c is greater than σ^2. However, the values of the effect sizes (η) of both parameters are high and close to each other, which suggests that both f_c and σ^2 have an important role in the perception of directionality.

Source	Assumption of sphericity	F – Statistics	*Sig. Value* (p)	*Partial Eta Squared* (η)
σ^2	Greenhouse-Geisser	18.316	**<0.001**	**0.696**
f_c	Sphericity assumed	38.298	**<0.001**	**0.827**
(σ^2) (f_c)	Greenhouse-Geisser	0.836	**0.515**	**0.095**

Table 6-4: Tests of Within-Subjects Effects: σ^2 and f_c

Source	Trend	*F-Statistics*	*Sig. Value*	*Partial Eta Squared*
log (σ^2)	**Linear**	**25.326**	**.001**	**.760**
	Quadratic	.024	.880	.003
	Cubic	.041	.844	.005
f_c	**Linear**	**93.225**	**<.001**	**.921**
	Quadratic	.070	.797	.009
	Cubic	.512	.494	.060

Table 6-5: Tests of within-subject contrasts, log (σ^2) and f_c

6.2.3 Separate and Interaction Effects of Angular Variance and Bandwidth

The effects of σ^2 and B_w on perceived directionalities are plotted in *Figure 6-3*, which shows that perceived directionality decreases with increase in σ^2 at all levels of B_w. However, there is no tendency for perceived directionality to change as B_w changes.

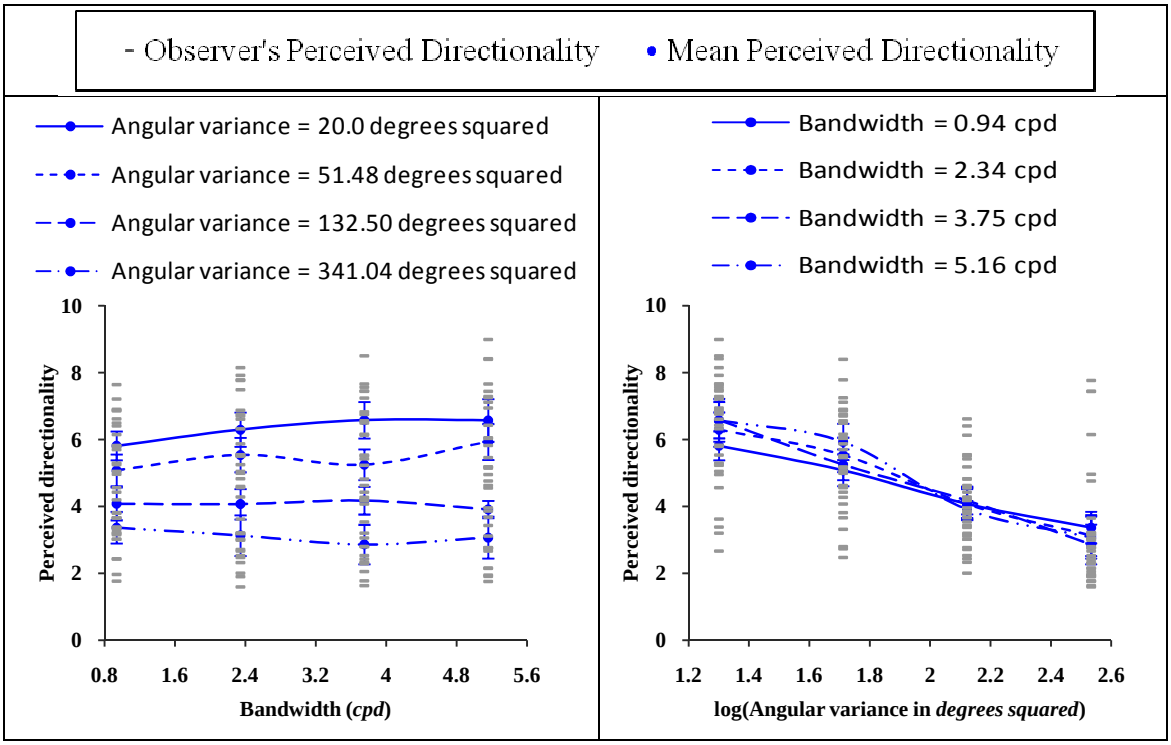

Figure 6-3: Effect of bandwidth (left) at different levels of angular variance and effect of angular variance (right) at different levels of bandwidth. The error bars show standard errors of mean.

The results of the ANOVA tests (*Table 6-6*) indicate that σ^2 significantly affect the perception of directionality, but that neither B_w nor the interaction between σ^2 and B_w have a significant effect. *Contrast* results (*Table 6-7*) reveal that perceived directionality changes linearly with the logarithm of σ^2.

Source	Assumption of sphericity	*F - Statistics*	*Sig. Value (p)*	*Partial Eta Squared* (η)
σ^2	Greenhouse-Geisser	16.311	**0.001**	**0.671**
B_w	Sphericity assumed	0.488	**0.721**	**0.053**
(σ^2) (B_w)	Greenhouse-Geisser	1.466	**0.230**	**0.155**

Table 6-6: Tests of within subject effects: σ^2 and B_w

Source	Trend	*F-Statistics*	*Sig. value*	*Partial Eta Squared*
log (σ^2)	**Linear**	**19.160**	**.002**	**.705**
	Quadratic	.047	.833	.006
	Cubic	2.244	.173	.219

Table 6-7: Tests of within-subjects contrasts, log (σ^2)

6.2.4 Separate and Interaction Effects of RMS Roughness and Central Radial Frequency

The effects of δ and f_c on perceived directionality are plotted in *Figure 6-4*, which shows that perceived directionality increases with increase in both f_c and δ.

The results of the ANOVA tests (*Table 6-8*) show that both f_c and δ significantly affect the perception of directionality but that the interaction between them does not. The values of η shown in *Table 6-8* indicates that both f_c and δ have a large effect on the perception of directionality. Furthermore, *contrast* results (*Table 6-9*) reveal that perceived directionality has a linear trend with both parameters (f_c and δ).

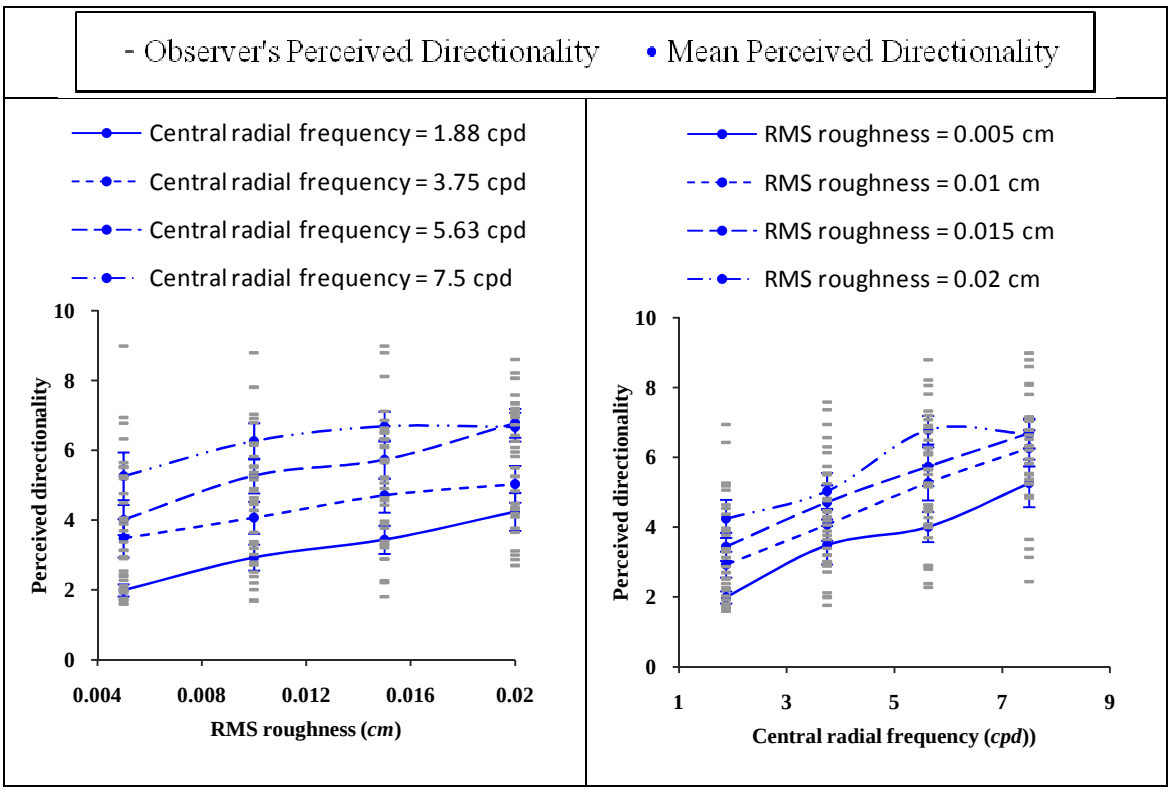

Figure 6-4: Effect of RMS roughness (left) at different levels of central radial frequency and effect of central radial frequency (right) at different levels of RMS roughness. The error bars show the standard errors of mean.

Source	Assumption of sphericity	*F - Statistics*	*Sig. Value* (p)	*Partial Eta Squared* (η)
f_c	Greenhouse-Geisser	32.110	**<0.001**	**0.801**
δ	Sphericity assumed	22.131	**<0.001**	**0.734**
(δ) (f_c)	Greenhouse-Geisser	0.965	**0.437**	**0.108**

Table 6-8: Tests of within subject effects: f_c and δ

Source	Trend	*F-Statistics*	*Sig. value*	*Partial Eta Squared*
f_c	**Linear**	**42.654**	**.000**	**.842**
	Quadratic	1.273	.292	.137
	Cubic	.432	.530	.051
δ	**Linear**	**35.258**	**.000**	**.815**
	Quadratic	2.728	.137	.254
	Cubic	.481	.508	.057

Table 6-9: Tests of within-subjects contrasts: f_c and δ

6.2.5 Separate and Interaction Effects of RMS Roughness and Bandwidth

Figure 6-5 shows that perceived directionality increases with the increase in δ at all levels of bandwidth but it remains almost constant with the change in B_w. The ANOVA tests (*Table 6-10*) revealed that δ significantly affects perceived directionality while B_w has no significant effect. The interaction between δ and B_w also has no effect on perceived directionality. *Contrast* results (*Table 6-11*) indicate that there is a linear trend between perceived directionality and δ.

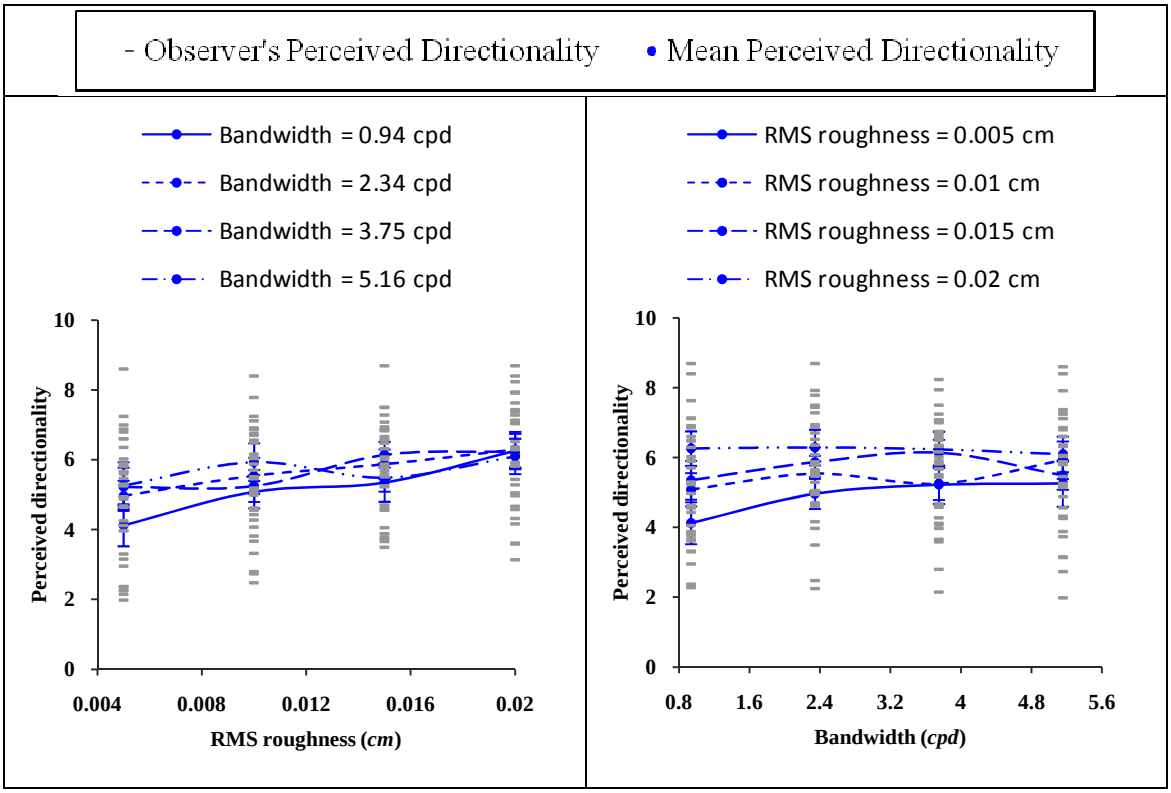

Figure 6-5: Effect of RMS roughness (left) at different levels of bandwidth and effect of bandwidth (right) at different levels of RMS roughness. The error bars show the standard errors of mean.

Source	Assumption of sphericity	*F - Statistics*	*Sig. Value* (p)	*Partial Eta Squared* (η)
B_w	Greenhouse-Geisser	1.172	**0.322**	**0.128**
δ	Greenhouse-Geisser	6.563	**0.023**	**0.451**
(δ) (B_w)	Greenhouse-Geisser	2.183	**0.089**	**0.214**

Table 6-10: Tests of within subject effects: B_w and δ

Source	Trend	*F-Statistics*	*Sig. value*	*Partial Eta Squared*
δ	**Linear**	**7.477**	**.026**	**.483**
	Quadratic	.048	.833	.006
	Cubic	2.721	.138	.254

Table 6-11: Tests of within-subjects contrasts, δ

6.2.6 Separate and Interaction Effects of Central Radial Frequency and Bandwidth

It can be seen from *Figure 6-6* that perceived directionality increases with f_c, while increasing B_w seems to increase perceived directionality only at low central radial frequency (f_c = 1.88 *cpd*). At other levels of f_c, perceived directionality remains almost constant with the change in B_w.

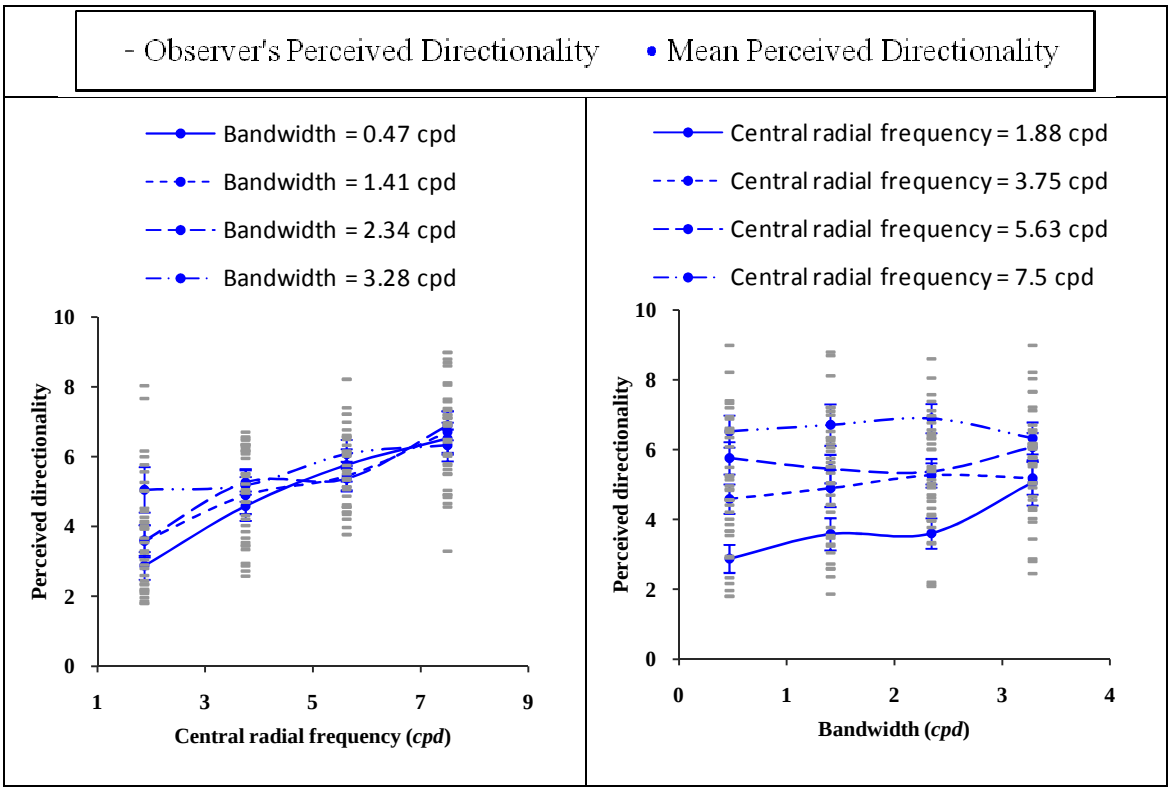

Figure 6-6: Effect of central radial frequency (left) at different levels of bandwidth and effect of bandwidth (right) at different levels of central radial frequency. The error bars show the standard errors of mean

Source	Assumption of sphericity	*F - Statistics*	*Sig. Value* (p)	*Partial Eta Squared* (η)
f_c	Greenhouse-Geisser	48.052	**<0.001**	**0.857**
B_w	Sphericity assumed	3.361	**0.035**	**0.296**
(f_c) (B_w)	Greenhouse-Geisser	3.927	**0.019**	**0.329**

Table 6-12: Tests of within subject effects: f_c and B_w

Source	Trend (f_c)	Trend (B_w)	*F-Statistics*	*Sig. value*	*Partial Eta Squared*
f_c	**Linear**		**89.633**	**.000**	**.918**
	Quadratic		.550	.480	.064
	Cubic		2.576	.147	.244
B_w		**Linear**	**5.960**	**.040**	**.427**
		Quadratic	.256	.626	.031
		Cubic	.398	.546	.047
(f_c) (B_w)	**Linear**	**Linear**	**6.751**	**.032**	**.458**
		Quadratic	1.619	.239	.168
		Cubic	5.737	.043	.418
	Quadratic	Linear	2.797	.133	.259
		Quadratic	.401	.544	.048
		Cubic	.720	.421	.083
	Cubic	Linear	.626	.452	.073
		Quadratic	**7.136**	**.028**	**.471**
		Cubic	2.077	.188	.206

Table 6-13: Tests of within-subjects contrasts: f_c and B_w

The ANOVA results shown in *Table 6-12* indicate that f_c, B_w and the interaction between f_c and B_w have a significant effect on the perception of directionality. This is contrary to the effects observed in section 5.2.4 where B_w and the interaction term of f_c and B_w did not show any significant effect on perceived directionality. This may be due to the different range of bandwidths used in this experiment. Bandwidths up to 3.28 *cpd* were used in this experiment, while in section 6.2.4, the maximum value of bandwidth used was 4.69 *cpd*. In section 6.2.3, it was observed that there are significant differences in perceived directionality due to change in bandwidth up to 3.28 *cpd* and above that

differences in perceived directionality are not significant. Thus, when the value of bandwidth 4.69 *cpd* was excluded in this chapter, different effects were observed than those reported in *chapter 5*. However, the values of η show that f_c has a very large effect on perceived directionality compared to the effect of B_w and the interaction between f_c and B_w. *Contrast* results (*Table 6-13*) show that both f_c and B_w have linear trend with perceived directionality. For the interaction between f_c and B_w, perceived directionality varies with different combinations of f_c and B_w. These combinations are linear with both f_c and B_w, linear with f_c and cubic with B_w, cubic with f_c and quadratic with B_w.

6.3 A Measurement Model of Perceived Directionality

In this section a measurement model of perceived directionality will be developed based on the results described in section 6.2. A summary of the effects of parameters and combinations of two parameters on the perception of directionality is given in *Table 6-14.*

Parameter 1	Parameter 2	Is the effect of parameter 1 significant when observed with parameter 2?	Is the interaction between parameter 1 and parameter 2 is significant?
σ^2	δ	Yes	No
	f_c	Yes	No
	B_w	Yes	No
δ	σ^2	Yes	No
	f_c	Yes	No
	B_w	Yes	No
f_c	σ^2	Yes	No
	δ	Yes	No
	B_w	Yes	No
B_w	σ^2	No	No
	δ	No	No
	f_c	Yes	Yes

Table 6-14: Summary of interaction effects

It can be seen that changes in σ^2, δ and f_c always have a significant effect on the perception of directionality when observed with another parameter and therefore, these three parameters were considered for a measurement model of directionality. B_w has not been included in a measurement model of directionality for the following reasons.

1. Bandwidth (B_w) did not show any significant effect when its effect was observed along with σ^2 and δ.
2. When observed together with central radial frequency, bandwidth and its interaction with central radial frequency showed significant effects. However the effect sizes of B_w (η = 0.296) and the interaction between f_c and B_w (η = 0.329) are low compared to other parameters.
3. From *Figure 6-6*, it can be observed that effect of B_w is only apparent at low central radial frequency. Furthermore, the ANOVA test with only 3 levels of f_c (excluding f_c = 1.88 *cpd*) shows that bandwidth has no significant effect on perceived directionality ($p > 0.05$).

Therefore, perceived directionalities of surfaces used for the two-way interaction terms $\{\sigma^2, B_w\}$, $\{\delta, B_w\}$ and $\{f_c, B_w\}$) were not considered for the development of a model.

As the two-way interactions between parameters σ^2, δ and f_c do not show significant effects on perceived directionality and perceived directionality has shown linear trends with log (σ^2), δ and f_c, a multi-linear regression model shown in *Equation (6-1)* was used to define a measurement model of perceived directionality (ρ_{fit}).

$$\rho_{fit} = C + m_{\sigma^2}\,(\log(\sigma^2)) + \, m_{\delta}\,(\delta) + \, m_{f_c}\,(f_c) \tag{6-1}$$

Multi-linear regression was applied to mean perceived directionality (ρ) for the two-way interaction terms $\{\sigma^2, \delta\}$, $\{\sigma^2, f_c\}$ and $\{\delta, f_c\}$ to obtain a constant (C) and the slopes (m_{σ^2}, m_{δ} and m_{f_c}). A measurement model is given in *Equation (6-2)* with values obtained from multi-linear regression (the R^2*-value* was 0.97). *Figure 6-7* shows plots of ρ_{fit} and ρ for the interaction terms $\{\sigma^2, \delta\}$, $\{\sigma^2, f_c\}$ and $\{\delta, f_c\}$.

$$\rho_{fit} = 7.3 - 2.89\,(\log(\sigma^2)) + \, 110.62\,(\delta) + \, 0.49\,(f_c) \tag{6-2}$$

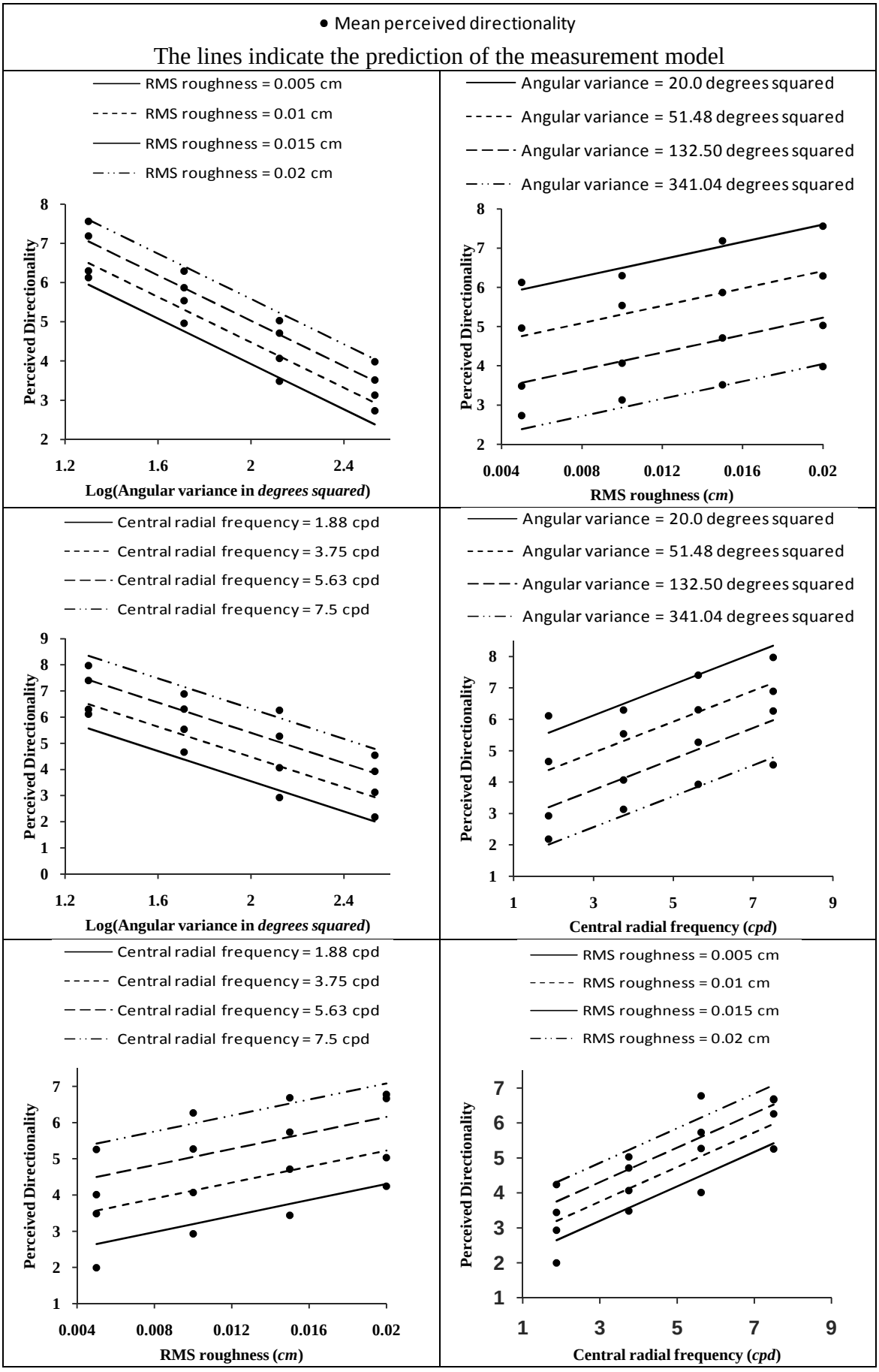

Figure 6-7: Multi-linear regression on mean perceived directionality

6.4 Summary

At the beginning of this chapter, difficulties in observing the effects of combinations of parameters on perceived directionality were discussed. Finally, it was decided to observe the one-way and two-way effects of parameters on perceived directionality. To observe these effects and to obtain perceived directionalities of surfaces, the *method of constant stimuli* and *direct ratio estimation* were used. All surfaces generated for each two-way interaction term were included in one experiment to ensure that each observer used a single scaling to judge the effects of all four parameters.

It was found that σ^2, f_c and δ have a significant effect on perceived directionality when observed with any other parameter, while B_w showed a significant effect only when observed with f_c. The interaction between B_w and f_c also showed a significant effect on perceived directionality. No significant effects were observed for the other two-way interaction terms. However, the effect sizes of B_w and the interaction term of B_w and f_c were small and so B_w was not included in deriving a measurement model.

Multi-linear regression was applied on mean perceived directionalities of surfaces to estimate parameters of a measurement model.

Chapter 7

Summary, Future Work and Conclusions

This thesis is summarized as a whole in section 7.1. The measurement model of perceived directionality and future work are discussed in section 7.2 and the final conclusion is given in section 7.3.

7.1 Summary of the Thesis

This thesis is concerned with the measurement of human perception of directionality, one of the most important perceived characteristics of surfaces, and the final goal of this thesis was to obtain a measurement model of perceived directionality of random-phase surfaces.

To achieve the goal of this thesis, different methods for investigating human perception of visual properties of textures were reviewed as described in *chapter 2*. The review concentrated on methods for mapping computational measures of visual characteristics on to data obtained from psychophysical experiments. In the past, such studies of perception of directionality of textures were not carried out under controlled and consistent illumination conditions. This introduces unknown biases both in human perception and in computational measures of visual characteristics as surface appearance changes with an illumination direction and computational features vary in sinusoidal manner with an illumination azimuth angle.

It was decided to investigate human perception of directionality using Padilla's novel method of a surface presentation, which eliminates biases in human perception due to illumination and viewpoint conditions, and to obtain computational measure of directionality from a surface height map, which is independent of illuminations. *Chapter 2* also discussed *photometric stereo*, a tool to obtain surface height maps, and different mathematical measures of directionality.

In *chapter 3*, the relationships between the two mathematical measures, *Tamura's variance* and *Davis' variance*, and human perception of directionality were tested independently of illumination conditions. It was found that variation in both measures has a significant effect on the perception of directionality, but that the relationships between each measure and human perception of directionality were not consistent across different sets of surfaces. This implied that other variables are also playing a role in human perception of directionality. The following four variables were proposed for experimental test:

- Parameters describing an angular distribution of frequency components
- Parameters describing a radial distribution of frequency components
- Phase spectrum
- RMS roughness

Because of the difficulty of characterising phase spectrum, the effects of the other three variables were tested in later chapters by using synthetic random-phase surfaces.

In *chapter 4*, the following criteria were set for a surface model and therefore a specific class of synthetic surfaces defined in the frequency domain (see *Equation (7-1)* and *(7-2)*) were used to investigate human perception of directionality.

- A surface model must be defined in such a way that each parameter can be varied independently of the other parameters.
- It must be possible to estimate surface parameters, if an unknown surface height map is given.
- The appearance of surface must be *naturalistic*.

$$M(f,\theta) = D(f)\,D(\theta)\left(\frac{\delta}{\delta_n}\right) \tag{7-1}$$

$$P_R(f,\theta) = \text{Random Numbers} \tag{7-2}$$

Two experiments in chapter 4 and chapter 5 revealed that there is no effect of variation in random phase spectra on perceived directionality of random-phase surfaces. The separate and combined effects of angular variance (σ^2) and RMS roughness (δ) were also observed in *chapter 4* and the following were found.

- Perceived directionality (ρ) is significantly affected by angular variance (σ^2), when the effect of σ^2 was observed separately. Perceived directionality increases as σ^2 decreases.
- Perceived directionality is significantly affected by RMS roughness (δ), when the effect of δ was observed separately. Perceived directionality increases as δ increases.
- When the combined effects of angular variance (σ^2) and RMS roughness (δ) were observed it was found that both parameters and their interaction have significant effects on perceived directionality.

In *chapter 5*, the effect of the radial distribution patterns was observed. For that, two parameters, central radial frequency (f_c) and bandwidth (B_w), were varied separately and together. The results are given below.

- Perceived directionality is significantly affected by central radial frequency (f_c), when the effect of f_c was observed separately. Perceived directionality increases as f_c increases. Furthermore, it was found that after f_c equal to 10.31 *cpd*, perceived directionality does not change significantly.
- Perceived directionality is significantly affected by bandwidth (B_w), when the effect of B_w was observed separately. Perceived directionality increases as B_w increases. However no significant difference in perceived directionality was observed for values of B_w equal to and greater than 3.28 cpd.
- When the combined effects of central radial frequency (f_c) and bandwidth (B_w) were observed, it was found that only f_c has a significant effect on perceived directionality and that there is no significant effect of B_w and no significant interaction between f_c and B_w.

In *chapter 6*, all parameters were varied together in a single experiment to determine how parameters interact with each other when perceiving directionality and to develop a measurement model of perceived directionality. However, only one-way (separate) and two-way interaction effects of parameters were tested as there were several difficulties in testing three-way and four-way interaction effects. In total, six two-way interaction of parameter pairs ($\{\sigma^2, \delta\}$, $\{\sigma^2, f_c\}$, $\{\sigma^2, B_w\}$, $\{\delta, f_c\}$, $\{\delta, B_w\}$ and $\{f_c, B_w\}$) were observed and the following were found.

- Angular variance (σ^2) has a significant effect on perceived directionality and there is no significant effect of an interaction of angular variance with any other parameter.
- RMS roughness (δ) has a significant effect on perceived directionality and there is no significant effect of an interaction of RMS roughness with any other parameter.
- Central radial frequency (f_c) has a significant effect on perceived directionality and f_c does not significantly interact with angular variance and RMS roughness when perceiving directionality. However f_c interacts with B_w.
- Bandwidth does not have significant effect on perceived directionality when it was observed with angular variance and RMS roughness. However, bandwidth has a significant effect on perceived directionality when it was observed along with central radial frequency. However the effect sizes of bandwidth and an interaction between f_c and B_w were small and therefore bandwidth was not considered for a measurement model of perceived directionality.

Finally, based on the above results, a measurement model of perceived directionality was developed by applying multi-linear regression on mean perceived directionality. In the next section, a measurement model of perceived directionality and future work in the perception of directionality are discussed.

7.2 Discussion and Future Work

This section discusses future work by pointing out open questions about a measurement model of perceived directionality developed in chapter 6.

1. A measurement model of perceived directionality is only applicable to surfaces having random phase spectra. Hence it is not known how phase spectra of structured directional surfaces affect perception of directionality. Earlier, it is mentioned that phase spectrum cannot be characterised directly. Also, to the author's knowledge no method utilizing phase-only statistics relevant to directionality of surfaces has been suggested. A possible approach to investigate the effect of phase spectrum on perceived directionality is mentioned below.

   Phase spectrum preserves information about the edges of elements of structured surfaces. Sine-waves, which are superimposed to make those edges, have the same phase. As phase spectrum is related to edges in surfaces, the statistics of orientations of edges in surfaces can be related to perception of directionality. There are various methods (Morrone *et al.*, 1986; Morrone and Burr, 1988; Kovesi, 1999) which obtain the phase congruency map (map of points at which phase congruency is maximum). The phase congruency map can then be used to measure the statistics of orientation of edges in order to relate phase spectrum to human perception of directionality.

   The gradual randomization of phase spectrum may distort edges in surface and consequently may affect appearance of surface and hence the perception of directionality. Thus, the effect of gradual phase-randomization of structured surfaces and hence the statistics of orientation of edges on perceived directionality can be tested. As magnitude spectrum and phase spectrum are independent of each other, a suitable psychophysical scaling method can be utilized to extend a proposed measurement model of perceived directionality of random-phase surfaces to phase-rich surfaces.
2. A measurement model is limited to uni-directional surfaces only. It is not known how directionality of surfaces having more than one dominant direction is perceived or whether these kinds of surfaces are considered as directional surfaces. Different psychophysical experiments can be carried out to determine how observers perceive directionality of these surfaces. In the case of two dominant directions, the effect of change in angular variance in one dominant direction can be tested when angular variance in the second is fixed or the effects of the simultaneous change in angular variances in both dominant directions can be tested. It can also be tested how the gradual introduction of

second dominant direction affect perceived directionality of uni-directional surfaces.

3. The measurement model was developed under fixed illumination conditions with a predefined wobble of a surface and so it is not sure how the model will react to such external factors. It would be interesting to determine how directionality is perceived as an illumination direction is gradually changed and aligned with dominant direction of a surface from a direction perpendicular to dominant direction. This will determine the amount of bias introduced by illumination direction when perceiving directionality of surface.

7.3 Final Conclusion

In this thesis, a measurement model of perceived directionality of random-phase surfaces has been developed through series of psychophysical experiments. The model is not biased by the unknown illumination and viewpoint conditions as psychophysical experiments were carried out with controlled and consistent illumination and viewpoint conditions. The experimental results suggest that human perception of directionality is affected by distribution of frequency components spatially and angularly i.e. spatial frequencies and orientations respectively as described *chapter 1*.

As mentioned in *chapter 1*, researchers carry out perceptual investigation of visual characteristics to improve the efficiency of applications such as automated surface classification and retrieval systems. The parameters of a measurement model of directionality can be mathematically estimated as described in *chapter 4*. Therefore, this model can be incorporated into surface classification or retrieval systems to classify or retrieve directional surfaces accurately as human would describe them. This model is limited to random-phase uni-directional surfaces, but provides the first step towards perception based classification/retrieval of directional surfaces.

The Bibliography

Abbadeni, N. 2000. Autocovariance-based Perceptual Textural Features Corresponding to Human Visual Perception. *Proceedings of the International Conference on Pattern Recognition - Volume 3.* IEEE Computer Society.

Abbadeni, N., Zhou, D. & Wang, S. 2000. Computational measures corresponding to perceptual textural features. *International Conference on Image Processing.*

Amadasun, M. & King, R. 1989. Textural features corresponding to textural properties. *IEEE Transactions on Systems, Man and Cybernetics,* 19**,** 1264-1274.

Bajcsy, R. K. 1972. *Computer Identification of Textured Visual Scene*.

Barnard, S., T. & Fischler, M., A. 1982. Computational Stereo. *ACM Comput. Surv.*, 14**,** 553-572.

Battiato, S., Gallo, G. & Nicotra, S. 2002. Glyph Representation of Directional Texture Properties. *Glyph Representation of Directional Texture Properties,* 10**,** 48-54.

Battiato, S., Gallo, G. & Nicotra, S. 2003. Perceptive visual texture classification and retrieval. *12th International Conference on Image Analysis and Processing, 2003,* 524-529.

Belhumeur, P., N., Kriegman, D., J. Kriegman & Yuille, A., L. Yuille 1999. The Bas-Relief Ambiguity. *Int. J. Comput. Vision,* 35**,** 33-44.

Blinn, J., F. 1977. Models of light reflection for computer synthesized pictures. *SIGGRAPH Comput. Graph.,* 11**,** 192-198.

Bovik, A. C., Clark, M. & Geisler, W. S. (1990) Multichannel Texture Analysis Using Localized Spatial Filters. *IEEE Transactions on Pattern Analysis and Machine Intelligence,* 12**,** 55-73.

Bovik, A., C., Clark, M. & Geisler, W., S. (1987) Texture segmentation using Gabor modulation/demodulation. *Pattern Recogn. Lett.,* 6**,** 261-267.

Brodatz, P. 1966. *Textures: A Photographic Album for Artists and Designers,* Dover, New York.

Campbell, F. W. & Robson, J. G. 1968. Application of Fourier analysis to the visibility of gratings. *Journal of Physiology,* 197**,** 551-566.

Chantler, M. J. 1994b. The effect of illumination direction on texture classification. *Department of Computing and Electrical Engineering.* Edinburgh, Heriot-Watt University.

Chantler, M. J. 1995. Why illuminant direction is fundamental to texture analysis. *IEE Proceedings on Vision, Image and Signal Processing,* 142**,** 199-206.

Chantler, M. J., Russell, G. T. & Linnett, L. M. 1994a. Illumination: a directional filter of texture? *Proceedings of BMVC94.* York.

Clarke, S. J. 1992. The analysis and synthesis of texture in side scan sonar data. *Department of Electrical and Electronics Engineering.* Edinburgh, Heriot-Watt University.

Cook, R. L. & Torrance, K. E. 1982. A Reflectance Model for Computer Graphics. *ACM Trans. Graph.,* 1**,** 7-24.

Dakin, S. C., Williams, C. B. & Hess, R. F. (1999) The interaction of first- and second-order cues to orientation. *Vision Research,* 39**,** 2867-2884.

Dana, K., J., Ginneken, B. V., Nayar, S., K. & Koenderink, J., J. 1999. Reflectance and texture of real-world surfaces. *ACM Trans. Graph.,* 18**,** 1-34.

Davis, L. S. 1981. Polarograms: A new tool for image texture analysis. *Pattern Recognition,* 13**,** 219-223.

Dhond, U. R. & Aggarwal, J. K. 1989. Structure from stereo-a review. *IEEE Transactions on Systems, Man and Cybernetics,* 19**,** 1489-1510.

Dong, J. & Chantler, M. J. 2005. Capture and Synthesis of 3D Surface Texture. *Int. J. Comput. Vision,* 62**,** 177-194.

Duda, R., O. & Hart, P., E. 1972. Use of the Hough transformation to detect lines and curves in pictures. *Commun. ACM,* 15**,** 11-15.

Ehrenstein, W., Ehrenstein, E., Windhorst, V. & Johansson, H. 1999. *Modern Techniques in Neuroscience Research,* Berlin, Springer.

Emrith, K. 2008. Perceptual Dimensions for Surface Texture Retrieval. *School of Mathematical and Computer Sciences.* Edinburgh, Heriot-Watt Univesity.

Field, A. 2005. *Discovering Statistics Using SPSS,* SAGE publication.

Flickner, M., Sawhney, H., Niblack, W., Ashley, J., Huang, Q., Dom, B., Gorkani, M., Hafner, J., Lee, D., Petkovic, D., Steele, D. & Yanker, P. 1995. Query by Image and Video Content: The QBIC System. *Computer,* 28**,** 23-32.

Fujii, K., Sugi, S. & Ando, Y. 2003. Textural properties corresponding to visual perception based on the correlation mechanism in the visual system. *Psychological Research,* 67**,** 197-208.

Gescheider, G. A. 1997. *Psychophysics: The Fundamentals,* Pscyhology Press.

Goodman, T., M. R., Bialek, A., Forbes, A., Rides, M., Whitaker, T. A., Overvliet & Krista, M. F., Van Der Heijden Gerie (2008) The Measurement of Naturalness (MONAT). *12th IMEKO TC1 & TC7 Joint Symposium on Man Scinece and Measurement.* Annecy, France.

Gurnsey, R. & Fleet, D. J. 2001. Texture space. *Vision Research,* 41**,** 745-757.

Haralick, R. M., Shanmugam, K. & Dinstein, I. H. 1973. Textural Features for Image Classification. *IEEE Transactions on Systems, Man and Cybernetics,* 3**,** 610-621.

Harvey, L. O. & Gervais, M. J. 1981. Internal representation of visual texture as the basis for the judgement of similarity. *Journal of Experimental Psychology: Human Perception and Performance,* 7**,** 741-753.

Heaps, C. & Handle, S. 1999. Similarity and features of natural textures. *Journal of Experimental Psychology: Human Perception and Performance***,** 229-320.

Ho, Y. X., Landy, M. S. & Maloney, L. T. 2006. How direction of illumination affects visually perceived surface roughness. *Journal of Vision,* 6**,** 634-648.

Ho, Y. X., Maloney, L. T. & Landy, M. S. 2007. The effect of viewpoint on perceived visual roughness. *Journal of Vision,* 7**,** 1-16.

Horn, B., K. P. & Brooks, M. J. 1989. *Shape from shading,* Cambridge, MA, The MIT press.

Horn, B., K. P. 1975. Obtaining shape from shading information. *The Psychology of Computer Vision.* New York, P.H. Winston ed.

Horn, B., K. P. 1986. *Robot vision,* McGraw-Hill Book Company, The MIT Press.

Irtel, H. 2005. Psychophysical Scaling. IN Everitt, B. S. & Howell, D. C. (Eds.) *Encyclopedia of Statistics in Behavioral Science.* John Wiley & Sons, Ltd, Chichester.

Kilgard, M. J. 2000. A practical and robust bump-mapping techique for today's GPUs. *Game Developers Conference.*

Koenderink, J. J., Van Doorn, A., Kappers, A. M., Te Pas, S. F. & Pont, S. C. 2003. Illumination direction from texture shading. *Journal of the Optical Society of America,* 20**,** 987-995.

Kourosh, J. K. & Hamid, S. Z. 2005. Radon Transform Orientation Estimation for Rotation Invariant Texture Analysis. *IEEE Trans. Pattern Anal. Mach. Intell.,* 27**,** 1004-1008.

Kovesi, P. 1999. Image features from phase congruency. *Videre: A Journal of Computer Vision Research,* 1.

Kube, P. & Pentland, A. 1988. On the Imaging of Fractal Surfaces. *IEEE Trans. Pattern Anal. Mach. Intell.,* 10**,** 704-707.

Landy, M. S. & Bergen, J. R. (1991) Texture segregation and orientation gradient. *Vision Research,* 31**,** 679-691.

Landy, M. S. & Oruç, I. (2002) Properties of second-order spatial frequency channels. *Vision Research,* 42**,** 2311-2329.

Lee, K.-L. & Chen, L.-H. 2005. An efficient computation method for the texture browsing descriptor of MPEG-7. *Image and Vision Computing,* 23**,** 479-489.

Lepistö, L., Kunttu, I. & Visa, A. 2003. Retrieval of non-homogenous textures based on directionality. *Proceedings of 4th European Workshop on Image Analysis for Multimedia Interactive Services.* London, UK.

Lepistö, L., Kunttu, I., Autio, J. & Visa, A. 2002. Comparison of some content-based image retrieval systems with rock texture images. *Proceedings of 10th Finnish Artificial Intelligence Conference.* Oulu, Finland.

Linnett, L. M. 1991. Multi-Texture Image Segmentation. *Department of Electrical and Electronic Engineering.* Edinburgh, Heriot-Watt University.

Liu, F. & Picard, R. W. (1999) A spectral 2-D Wold decomposition algorithm for homogeneous random fields. *Proceedings of the Acoustics, Speech, and Signal Processing, 1999. on 1999 IEEE International Conference - Volume 06.* IEEE Computer Society.

Liu, F. & Picard, R. W. 1996. Periodicity, directionality, and randomness: Wold features for image modelling and retrieval. *Pattern Analysis and Machine Intelligence, IEEE Transactions on,* 18**,** 722-733.

Long, H. & Leow, W. K. 2001. Perceptual texture space improves perceptual consistency of computational features. *In Proc. IJCAI.*

Maloney, L. T. & Yang, J. N. 2003. Maximum likelihood difference scaling. *Journal of Vision,* 3**,** 573-585.

Mandelbrot, B. B. 1982. *The Fractal Geometry of Nature,* New York, Freeman.

Mcgunnigle, G. 1998. The classification of textured surfaces under varying illuminant direction. *Department of Computing and Electrical Engineering.* Edinburgh, Heriot-Watt University.

Mulvaney, D. J., Newland, D. E. & Gill, K. F. 1989. A complete description of surface texture profiles. *Wear,* 132**,** 173-182.

Niblack, C. W., Barber, R., Equitz, W., Flickner, M. D., Glasman, E. H., Petkovic, D., Yanker, P., Faloutsos, C. & Taubin, G. 1993. QBIC project: querying images by content, using color, texture, and shape. *Storage and Retrieval for Image and Video Databases.* 1 ed. San Jose, CA, USA, SPIE.

Nicotra, S. 2002. Organizing Texture in a perceptual space *Eurographics Italial Chapter*.

Ogilvy, J. A. 1991. *Theory of wave scattering from random rough surfaces,* Adam Hilger.

Padilla, S. 2008. Mathematical models for perceived roughness of three-dimensional surface textures. *School of Mathematical and Computer Sciences.* Edinburgh, Heriot-Watt University.

Padilla, S., Drbohlav, O., Green, P. R., Spence, A. & Chantler, M. J. 2008. Perceived roughness of 1/f[beta] noise surfaces. *Vision Research,* 48**,** 1791-1797.

Palm, C. & Lehman, T., M. (2002) Classification of color textures by Gabor filtering. *MG\&V,* 11**,** 195-219.

Payne, J. S. & Stonham, T. J. 2001. Can texture and image content retrieval methods match human perception? *Intelligent Multimedia, Video and Speech Processing, 2001. Proceedings of 2001 International Symposium on.*

Payne, J. S., Hepplewhite, L., Stonham, T.J. 2000. Texture, human perception, and information retrieval measures. *SIGIR2000, TR-706.*

Payne, S. J., Hepplewhite, L. & Stonham, T. J. 1999. Perceptually Based Metrics for the Evaluation of Textural Image Retrieval Methods. *Proceedings of the IEEE International Conference on Multimedia Computing and Systems Volume II-Volume 2 - Volume 2.* IEEE Computer Society.

Pelli, D. G. & Farell, B. 1995. Psychophysical methods. *Handbook of Optics.* 2nd ed. New York, McGraw-Hill.

Pentland, A., Picard, R. W. & Sclaroff, S. 1996. Photobook: Content-based manipulation of image databases. *International Journal of Computer Vision,* 18**,** 233-254.

Phong, B. T. 1975. Illumination for computer generated pictures. *Commun. ACM,* 18**,** 311-317.

Randen, T. & Husoy, J., H. (1999) Filtering for Texture Classification: A Comparative Study. *IEEE Transactions on Pattern Analysis and Machine Intelligence,* 21**,** 291-310.

Rao, A. R. & Lohse, G. L. 1993a. Identifying high level features of texture perception. *CVGIP: Graph. Models Image Process.,* 55**,** 218-233.

Rao, A. R. & Lohse, G. L. 1993b. Towards a texture naming system: Identifying relevant dimensions of texture. *Visualization, 1993. Visualization '93, Proceedings., IEEE Conference on.*

Reed, T. R. & Wechsler, H. (1990) Segmentation of Textured Images and Gestalt Organization Using Spatial/Spatial-Frequency Representations. *IEEE Transactions on Pattern Analysis and Machine Intelligence,* 12**,** 1-12.

Russ, J. C. 1994. *Fractal Surfaces,* New York, Plenum.

Saupe, D. 1988. Algorithms for random fractals. IN Peitgen, H. O. & Saupe, D. (Eds.) *The science of fractal images.* Springer Verlag.

Tamura, H., Mori, S. & Yamawaki, T. 1978. Textural Features Corresponding to Visual Perception. *IEEE Transactions on Systems, Man and Cybernetics,* 8**,** 460-473.

Torgerson, W. S. 1958. *Theory and methods of scaling,* New York, Wiley.

Watson, A. B. 1988. Ideal shrinking and expansion of discrete sequence. *NASA Memorandum 88202.*

Weszka, J. S., Dyer, C. R. & Rosenfeld, A. 1976. A Comparative Study of Texture Measures for Terrain Classification. *IEEE Transactions on Systems, Man, and Cybernetics,* 6**,** 269-285.

Wold, H. (1938) A Study in the Analysis of Stationary Time Series. Stockholm, University of Stockholm.

Wold, H. (1954) *A study in the analysis of stationary time series,* second revised addition, with an appendix by Peter Whittle, Stockholm, Almqvist & Wiksell.

Woodham, R. J. 1980. Photometric method for determining surface orientation from multiple images. *Optical Engineering,* 19**,** 139-144.

Wu, J. 2003. Rotation Invariant Classification of 3D Surface Texture Using Photometric Stereo. *School of Mathematical and Computer Sciences.* Edinburgh, Heriot-Watt University.

Wu, J. J. 2002. Analyses and simulation of anisotropic fractal surfaces. *Chaos, Solitons & Fractals,* 13**,** 1791-1806.

Wu, P., Manjunanth, B. S., Newsam, S. D. & Shin, H. D. 1999. A Texture descriptor for image retrieval and browsing. *Content-Based Access of Image and Video Libraries, 1999. (CBAIVL '99) Proceedings. IEEE Workshop on.*

The Appendices

Appendix 3-A: MATLAB code to shrink and expand the surface height map

function ShrunkHgt = shrink_subideal(InHgt, ShrunkHgt_sz)

```
% Shrink the input surface height map to the specified size
% Input
% InHgt = Input surface height map
% ShrunkHgt_sz = Size of shrunk surface height map
% Output
% ShrunkHgt = Shrunk surface height map

[inr inc] = size(InHgt);  % Obtaining size of the input height map
% Obtaining size to which input height map is shrunk
outr = ShrunkHgt_sz(1);
outc = ShrunkHgt_sz(2);
infft = fftshift(fft2(InHgt)); % FFT
shrink_factor = (outr*outc)./(inr*inc); % Shrinking Factor

infft = infft./shrink_factor;
outfft = zeros(outr, outc);

inr_cen  = (inr/2)  + 1;  % location of zero Horizontal frequency (u = 0);
inc_cen  = (inc/2)  + 1; % location of zero Vertical frequency (v = 0);

y1 = inc_cen - (outc/2) + 1; % location of u = (-Ns/2) + 1
y2 = inc_cen + (outc/2) - 1; % location of u = (Ns/2) - 1
x1 = inr_cen - (outr/2) + 1;  % location of v = (-Ns/2) + 1
x2 = inr_cen + (outr/2) - 1;  % location of v = (Ns/2) – 1

% Discarding the frequencies above Nyquist Frequency (Ns/2)
outfft(2:end,2:end)=infft(x1:x2,y1:y2);
% Setting the magnitude of Nyquist Frequency zero
outfft(1,:) = 0;
outfft(:,1) = 0;
% Shrunk height map
ShrunkHgt=ifft2(fftshift(outfft));
ShrunkHgt = real(ShrunkHgt);
```

```
function  ExpdHgt = expand_subideal(InHgt, ExpdHgt_sz)

% Expand the input surface height map to the specified size
% Input
% InHgt = Input surface height map
% ExpdHgt_sz = Size of expanded surface height map
%Output
%ExpdHgt = Expanded surface height map

[inr inc] = size(InHgt);  % Obtaining size of the input height map

% Obtaining size to which input height map is shrunk
outr = ExpdHgt_sz(1);
outc = ExpdHgt_sz(2);

infft = fftshift(fft2(in_im)); % FFT
scale_factor = (outr*outc)./(inr*inc); % Expansion Factor
infft = infft./scale_factor;

% Setting the magnitude of Nyquist frequency zero
infft(1,:) = 0; infft(:,1) = 0;

% Padding Zeros above Nyquist frequencies
outfft = zeros(outr, outc);
outr_cen = (outr/2) + 1; % location of zero Horizontal frequency (u = 0);
outc_cen = (outc/2) + 1;% location of zero Vertical frequency (v = 0);

y1 = outc_cen - (inc/2) + 1; % location of u = (-N/2) + 1
y2 = outc_cen + (inc/2) - 1; % location of u = (N/2) - 1
x1 = outr_cen - (inr/2) + 1; % location of v = (-N/2) + 1
x2 = outr_cen + (inr/2) - 1; % location of v = (N/2) – 1
outfft(x1:x2,y1:y2)=infft(2:end,2:end);
% Expanded height map
ExpdHgt=ifft2(fftshift(outfft));
ExpdHgt = real(ExpdHgt)
```

Appendix 3-B: Sets of surfaces obtained using *shrinking* method

<table>
<tr><th colspan="2">Surfaces from Set 2</th></tr>
<tr><td>Original height map used to generate five surfaces
 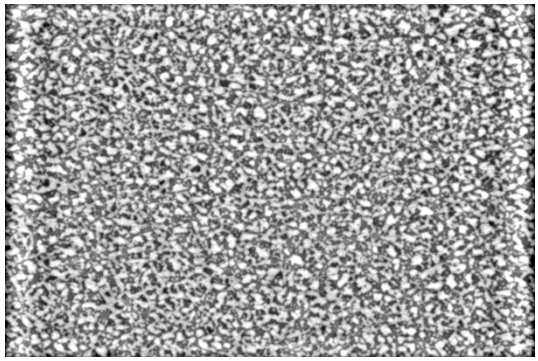 </td><td> 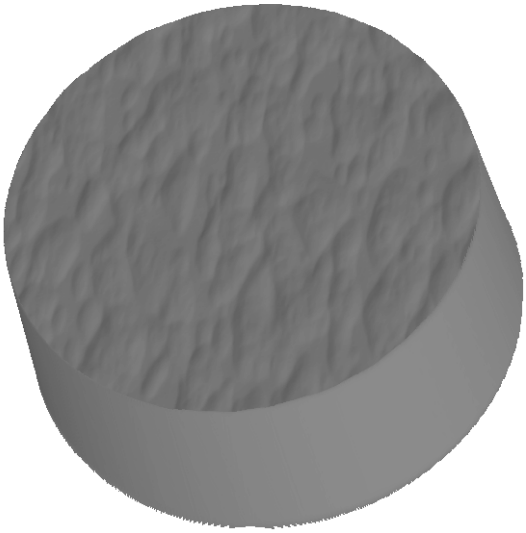 </td></tr>
<tr><td> 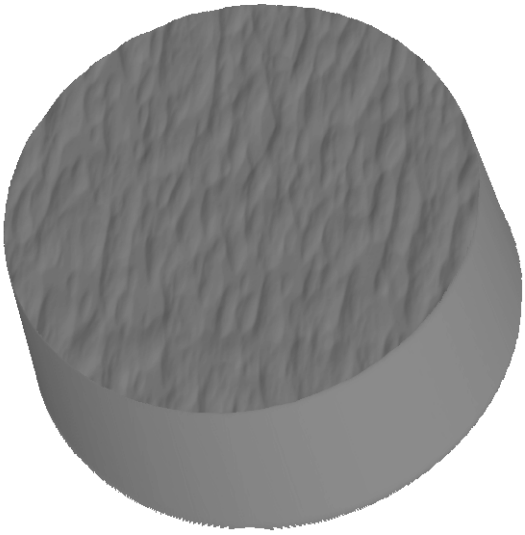 </td><td> 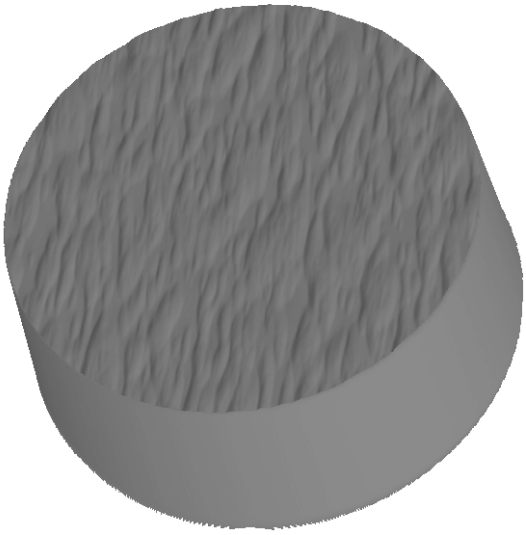 </td></tr>
<tr><td> 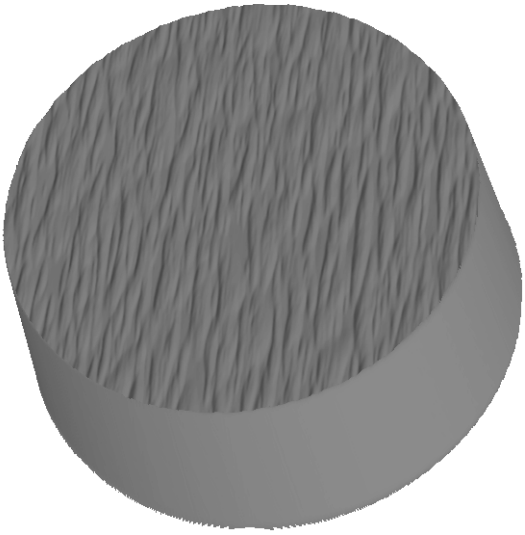 </td><td> 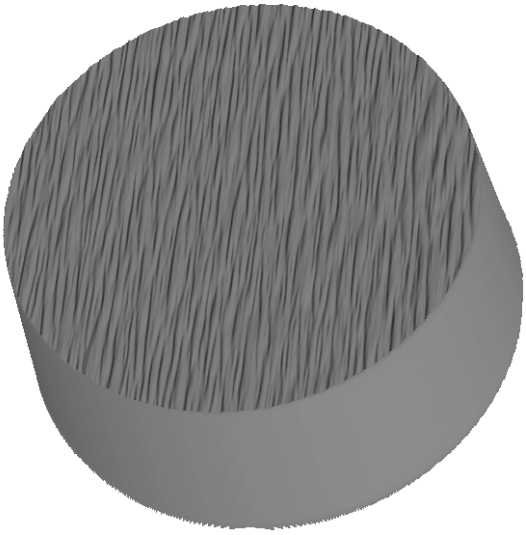 </td></tr>
</table>

Surfaces from Set 3	
Original height map used to generate five surfaces 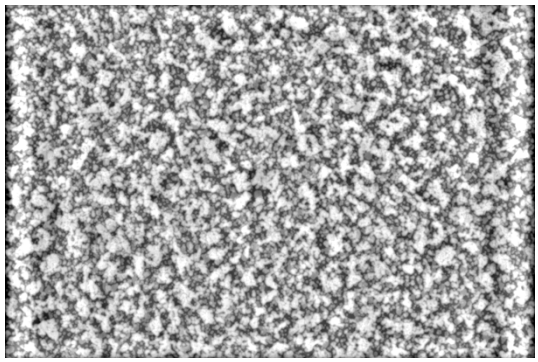	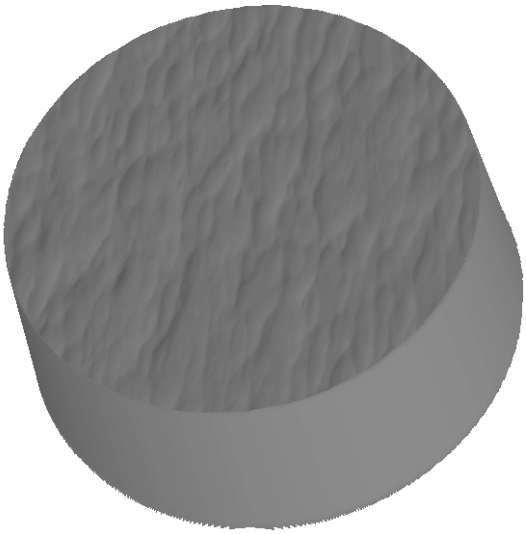
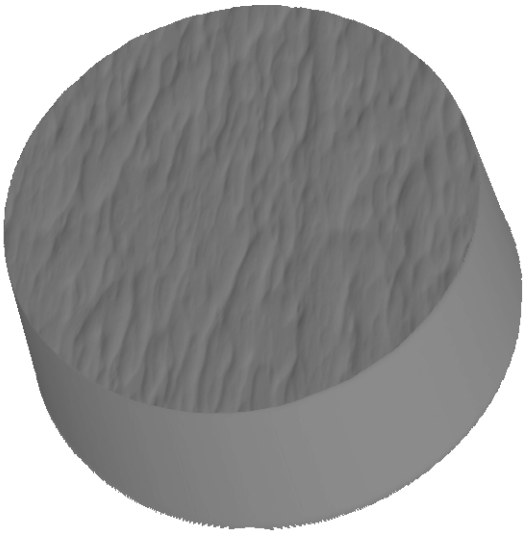	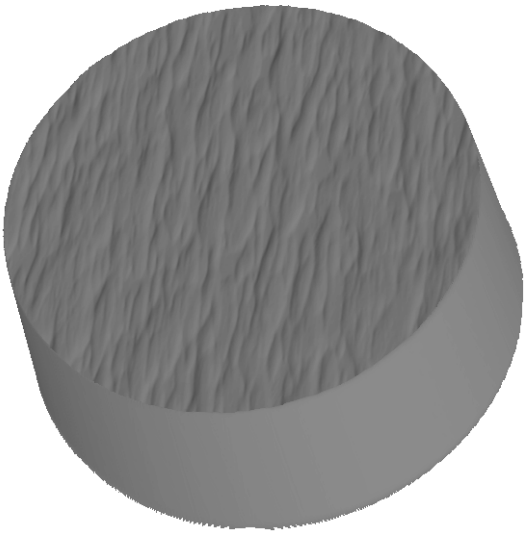
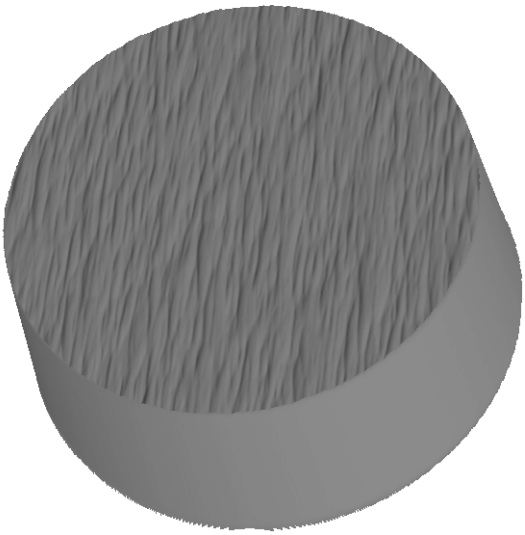	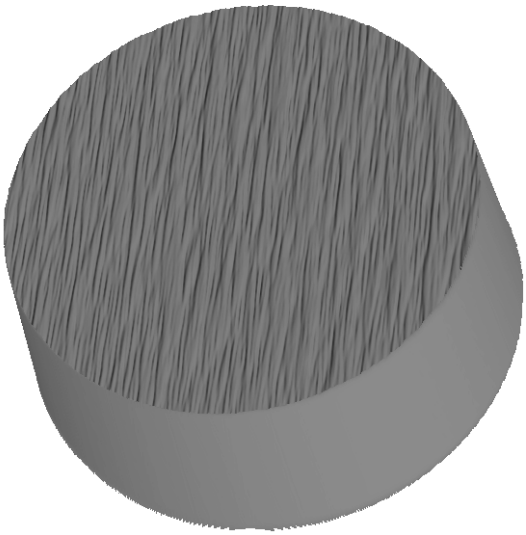

Surfaces from Set 4	
Original height map used to generate five surfaces 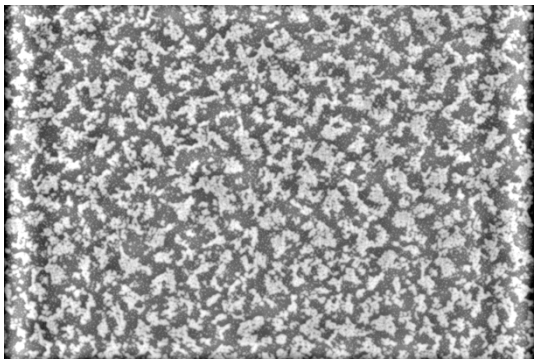	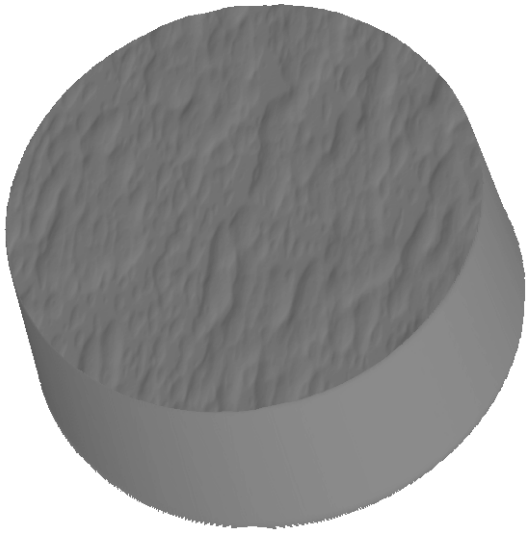
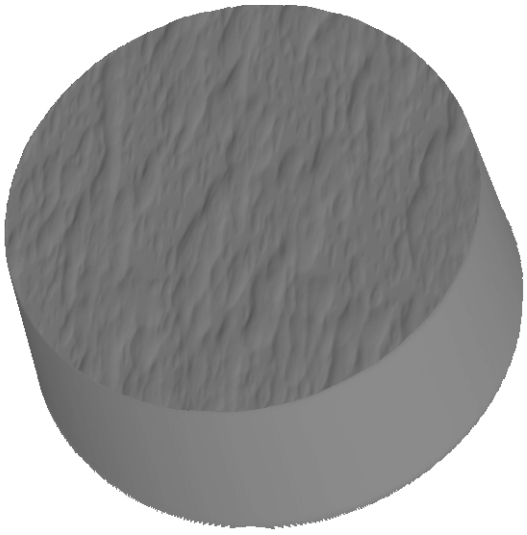	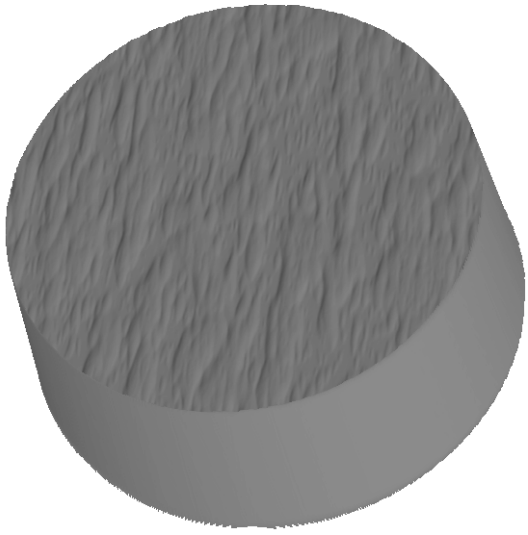
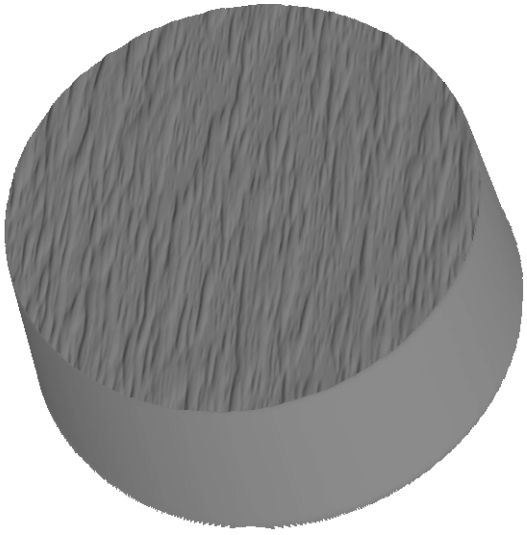	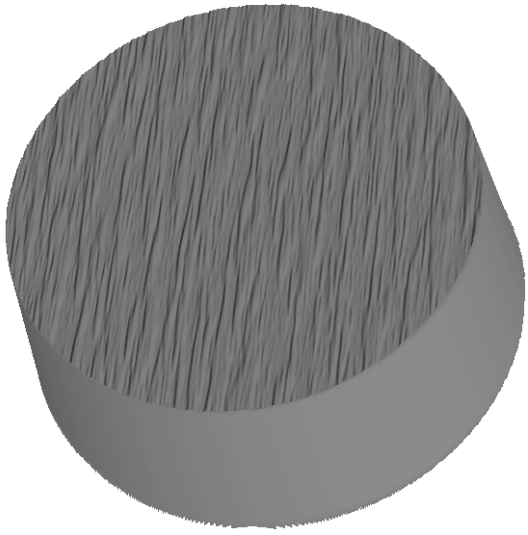

Surfaces from Set 5	
Original height map used to generate five surfaces 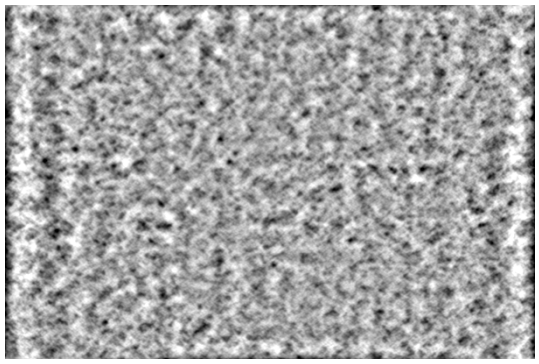	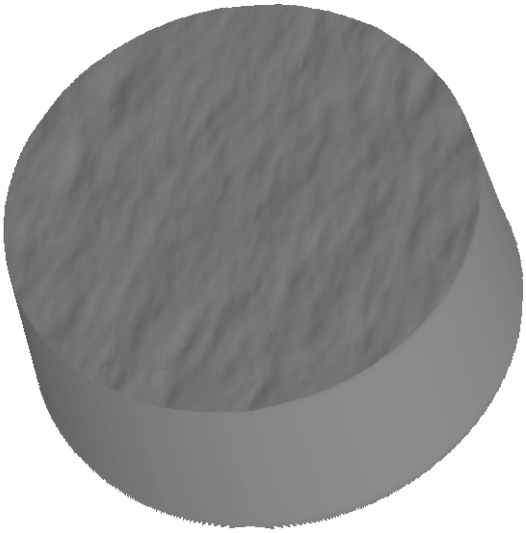
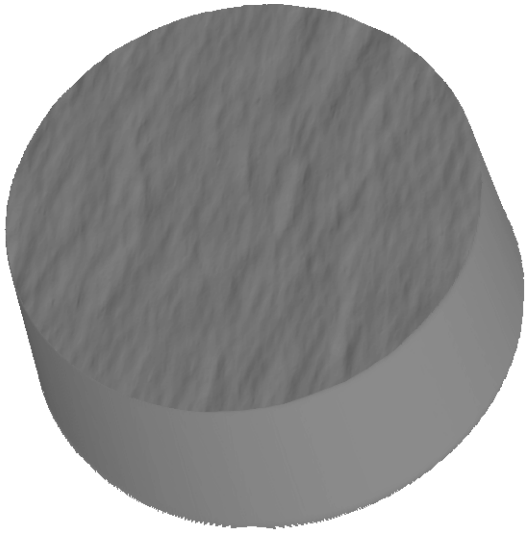	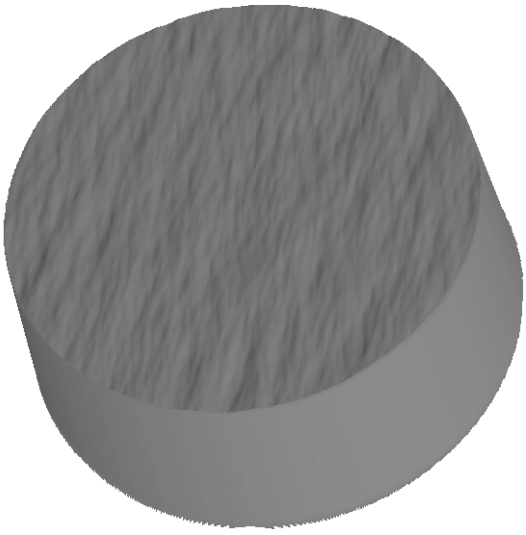
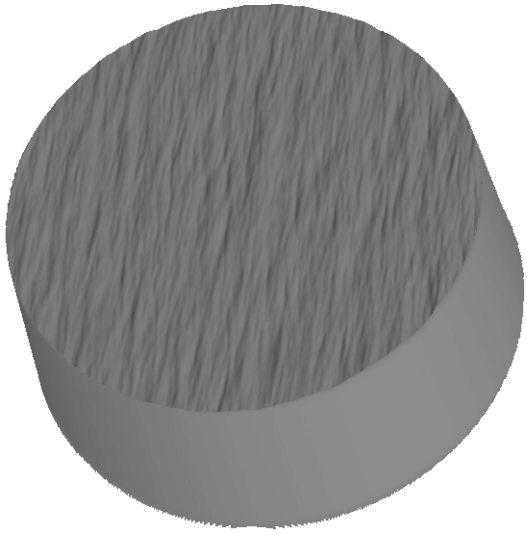	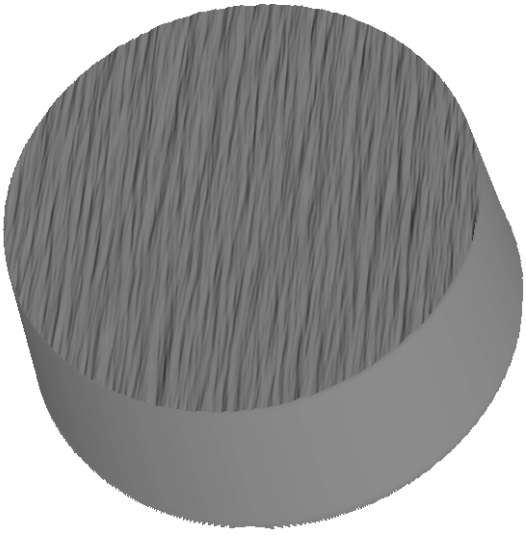

Surfaces from Set 6	
Original height map used to generate five surfaces 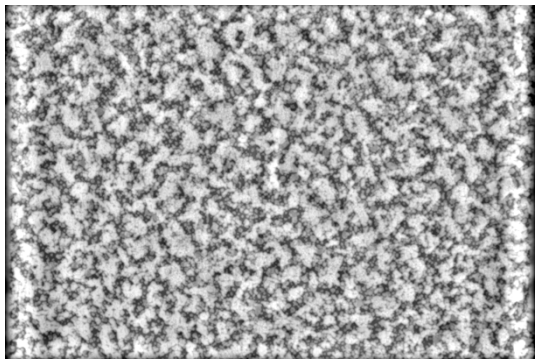	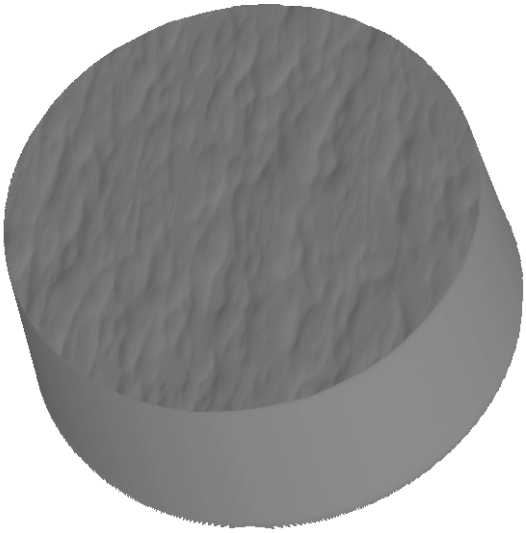
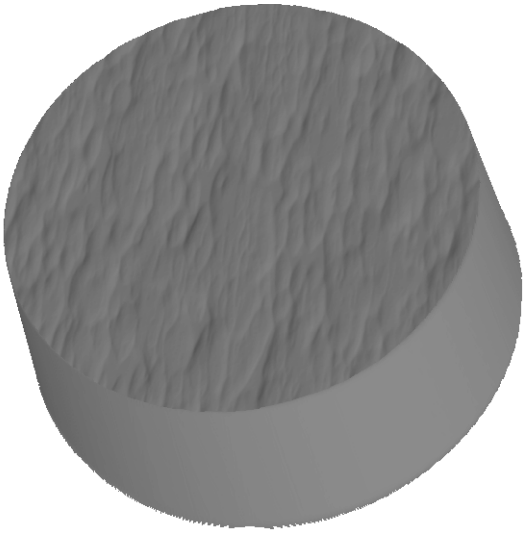	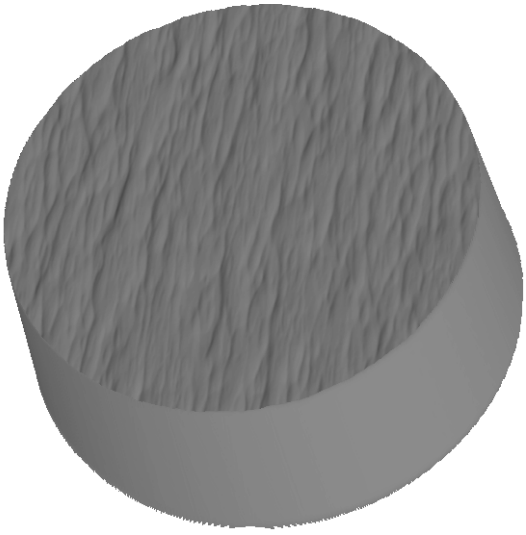
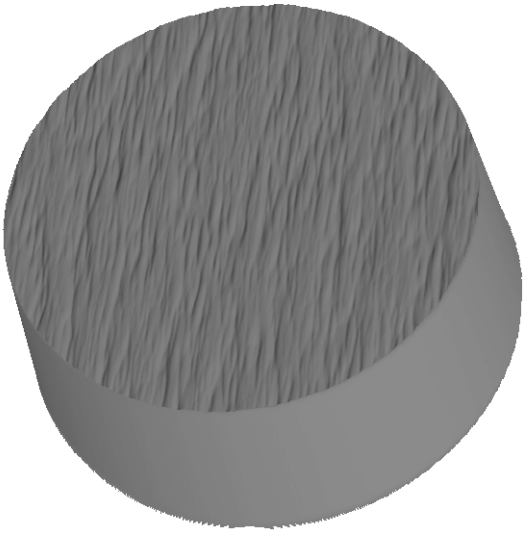	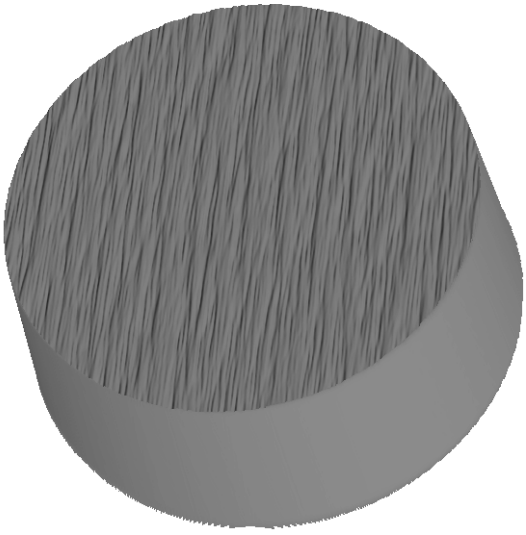

Appendix 3-C: MATLAB code to obtain surface gradients

```
function [p_grad q_grad] = SurfaceGradient (In_FFT)

%Input
% In_FFT = input Fourier transform (zero frequency at top left corner)
%Output
%p_grad = horizontal gradient
%q_grad = vertical gradient
%%%%%%%%%%%%%%%%%%%%%%%%%%%%%%%%%%%%%%%%
% Obtaining the size of input Fourier transform and generating horizontal and vertical frequency index
n = size(In_FFT,1); nq = n/2;
V = repmat((-nq:nq-1)', 1,2*nq);
U = repmat((-nq:nq-1), 2*nq,1);
% Arranging zero frequency in centre
In_FFT = fftshift(In_FFT);
% Obtaining horizontal and vertical gradient
P_FFT = i.*U.*2.*pi.*In_FFT;
p_grad = ifft2(ifftshift(P_FFT),'symmetric');   p_grad = real(p_grad);
Q_FFT = i.*V.*2.*pi.*In_FFT;
q_grad = ifft2(ifftshift(Q_FFT),'symmetric');   q_grad = real(q_grad);
```

Appendix 3-D: Ordering information of surface pairs and observers' responses for the experiment in section 3.3.4

- Screen 1 is on the left side of the observer and Screen 2 is on the right side of the observer
- If Swap Info = 0 then Surface 1 and 2 is presented on Screen 1 and 2 respectively
- If Swap Info = 1 then Surface 1 and 2 is presented on Screen 2 and 1 respectively
- Order Number shows when the pair is presented during the experiment
- If Selected Surface = 0 then surface on screen 1 is selected as more directional and ratio is equal to perceived directionality of surface on screen 1 to perceived directionality of surface on screen 2
- If Selected Surface = 1 then surface on screen 2 is selected as more directional and ratio is equal to perceived directionality of surface on screen 2 to perceived directionality of surface on screen 1

			Observer 1				**Observer 2**				**Observer 3**				**Observer 4**			
	Surface Pair		**Surface Order**		**Responses**		**Surface Order**		**Responses**		**Surface order**		**Responses**		**Surface Order**		**Responses**	
Set No	**Shrinking Factor of Surface 1**	**Shrinking Factor of Surface 2**	**Pair Order Number**	**Swap Info**	**Selected Surface**	**Ratio**	**Pair Order Number**	**Swap Info**	**Selected Surface**	**Ratio**	**Pair Order Number**	**Swap Info**	**Selected Surface**	**Ratio**	**Pair Order Number**	**Swap Info**	**Selected Surface**	**Ratio**
1	8/5	8/4	2	1	1	1.3	13	0	0	1.8	101	1	1	2	86	0	0	1.4
1	8/5	8/3	44	0	0	1.3	28	1	1	1.4	100	1	1	3	75	1	1	1.2
1	8/5	8/2	31	1	1	2	102	0	0	3	9	1	1	6	50	1	1	1.3
1	8/5	8/1	115	1	1	2.5	72	1	1	3	55	1	1	6	5	1	1	1.6
1	8/4	8/3	17	1	1	1.3	11	0	0	1.8	1	1	1	2	62	1	1	1.1
1	8/4	8/2	10	0	0	1.3	38	1	1	2.8	82	1	1	4	48	1	1	1.3
1	8/4	8/1	105	1	1	2.5	48	1	1	4	91	1	1	5	49	0	0	1.4
1	8/3	8/2	48	1	1	1.5	97	0	0	2	29	0	0	3	36	0	0	1.3
1	8/3	8/1	113	1	1	2	62	1	1	3.5	75	1	1	6	18	1	1	1.2
1	8/2	8/1	100	0	0	1.3	47	0	0	2	97	1	1	3	60	0	0	1.3
1	8/5	8/4	68	1	1	1.2	31	0	0	1.4	33	1	1	1.5	72	0	0	1.1
1	8/5	8/3	94	0	0	1.3	120	1	1	2.1	5	1	1	3	114	1	1	1.2
1	8/5	8/2	32	1	1	2	81	1	1	3	95	0	0	4	108	1	1	1.3
1	8/5	8/1	83	1	1	2.5	117	1	1	5	28	1	1	7	3	1	1	1.5
1	8/4	8/3	36	0	0	1.3	109	0	0	1.5	25	1	1	2.5	59	0	1	1.1
1	8/4	8/2	39	1	1	1.6	103	0	0	2.5	39	0	0	7	90	0	0	1.4
1	8/4	8/1	46	0	0	2.5	24	0	0	5.2	18	0	0	8	115	0	0	1.7
1	8/3	8/2	108	1	1	1.5	116	0	0	1.4	115	1	1	3	15	1	1	1.3
1	8/3	8/1	89	0	0	2	53	1	1	4	94	1	1	5	100	0	0	1.4
1	8/2	8/1	25	1	1	2.3	17	1	1	3	52	1	1	4	47	1	1	1.4
2	8/5	8/4	112	1	1	1.1	74	0	0	1.3	120	0	0	4	17	1	1	1.1
2	8/5	8/3	75	1	1	1.2	115	1	1	1.5	63	0	0	4	77	0	0	1.3
2	8/5	8/2	63	0	0	1.8	86	1	1	3.5	35	1	1	5	29	0	0	1.3
2	8/5	8/1	85	0	0	3	80	1	1	4.5	105	1	1	7	74	0	0	1.8

2	8/4	8/3	111	1	1	1.3	82	1	1	1.2	12	1	1	1.5	34	0	0	1.1
2	8/4	8/2	21	1	1	2.5	9	1	1	3	107	0	0	4	1	0	0	1.3
2	8/4	8/1	93	0	0	3	63	0	0	4	8	0	0	8	89	1	1	1.8
2	8/3	8/2	101	0	0	1.3	65	0	0	2.6	57	0	0	2.5	4	0	0	1.3
2	8/3	8/1	6	1	1	3	20	1	1	5.5	3	0	0	8	35	0	0	1.6
2	8/2	8/1	3	1	1	2	91	0	0	2	65	1	1	4	120	1	1	1.5
2	8/5	8/4	22	0	0	1.2	89	1	1	1.3	93	1	1	2	103	0	0	1.1
2	8/5	8/3	119	1	1	1.3	101	1	1	2	42	1	1	3	87	0	0	1.1
2	8/5	8/2	92	1	1	2	71	0	0	2	30	0	0	4	71	1	1	1.5
2	8/5	8/1	18	1	1	3.5	12	1	1	6.2	77	1	1	8	24	0	0	1.7
2	8/4	8/3	4	0	0	1.2	58	0	0	1.5	81	1	1	2	80	1	1	1.2
2	8/4	8/2	80	0	0	1.5	2	0	0	2	2	1	1	4	53	1	1	1.3
2	8/4	8/1	116	0	0	2.5	1	1	1	5	47	1	1	8	99	1	1	1.6
2	8/3	8/2	14	1	1	2	46	0	0	2.4	64	1	1	3	94	0	0	1.4
2	8/3	8/1	51	0	0	2.3	41	0	0	4.2	6	0	0	7	67	1	1	1.7
2	8/2	8/1	79	1	1	1.5	66	0	0	3	119	1	1	4	82	0	0	1.4
3	8/5	8/4	56	0	0	1.2	36	0	0	1.2	36	1	1	1.5	96	1	0	1.1
3	8/5	8/3	55	0	0	1.3	114	1	1	1.6	23	0	0	3	51	1	1	1.2
3	8/5	8/2	45	1	1	1.6	69	1	1	2.5	73	1	1	4	116	1	1	1.5
3	8/5	8/1	91	1	1	3.2	21	0	0	5.6	37	0	0	10	26	0	0	1.9
3	8/4	8/3	70	1	1	1.2	108	1	1	1.3	85	1	1	3	88	1	1	1.2
3	8/4	8/2	88	0	0	1.5	77	1	1	2.5	13	0	0	7	9	0	0	1.5
3	8/4	8/1	57	0	0	2.3	68	1	1	3	16	0	0	10	92	0	0	1.8
3	8/3	8/2	7	0	0	1.8	40	1	1	2	31	0	0	5	105	0	0	1.2
3	8/3	8/1	73	1	1	2.8	61	0	0	3	45	1	1	5	85	0	0	1.4
3	8/2	8/1	37	1	1	2	25	1	1	3	103	1	1	3.5	78	0	0	1.4
3	8/5	8/4	99	1	1	1.2	110	1	1	1.1	92	1	0	1.5	52	0	0	1.1
3	8/5	8/3	11	1	1	1.3	39	1	1	1.8	74	1	1	3	20	0	0	1.4
3	8/5	8/2	30	1	1	2	106	1	1	3	80	0	0	6	21	1	1	1.3
3	8/5	8/1	27	1	1	3.5	57	1	1	4.2	21	1	1	7	39	0	0	1.6
3	8/4	8/3	96	0	0	1.3	26	1	1	1.5	59	1	1	3	66	1	1	1.1
3	8/4	8/2	103	0	0	1.5	76	0	0	3	26	1	1	5	111	1	1	1.2
3	8/4	8/1	9	1	1	3	52	0	0	3	89	0	0	10	70	1	1	1.7
3	8/3	8/2	1	1	1	1.8	50	0	0	2	117	0	0	7	45	0	0	1.3
3	8/3	8/1	106	0	0	2.8	43	0	0	3.5	61	0	0	6	63	0	0	1.4
3	8/2	8/1	34	0	0	1.6	37	0	0	2.5	44	1	1	3	64	0	0	1.5
4	8/5	8/4	28	0	0	1.2	70	1	1	1.2	41	1	1	1.5	32	1	1	1.1
4	8/5	8/3	12	0	0	1.2	67	1	1	1.3	110	0	0	3.5	43	1	1	1.2
4	8/5	8/2	50	0	0	1.5	119	1	1	2.5	49	0	0	5	41	0	0	1.3
4	8/5	8/1	20	1	1	3.5	95	1	1	5	15	0	0	10	8	1	1	1.3
4	8/4	8/3	98	0	0	1.2	18	0	0	1.5	114	1	1	2	6	1	1	1.3
4	8/4	8/2	5	0	0	1.5	98	0	0	3	62	1	1	3	31	1	1	1.3
4	8/4	8/1	52	1	1	2.8	85	0	0	4.5	17	1	1	8	73	1	1	1.7
4	8/3	8/2	76	0	0	1.3	94	0	0	2.8	11	0	0	4	113	0	0	1.4
4	8/3	8/1	107	0	0	2.5	54	0	0	3.8	56	1	1	5	19	0	0	1.4
4	8/2	8/1	109	0	0	1.6	4	0	0	3.5	68	1	1	3	30	1	1	1.4
4	8/5	8/4	102	0	0	1	113	0	0	1.5	4	0	0	2	55	1	1	1.1
4	8/5	8/3	38	0	0	1.3	3	0	0	1.3	112	0	0	3	13	0	0	1.2

4	8/5	8/2	95	1	1	1.5	23	0	0	3	71	0	0	4	40	0	0	1.4
4	8/5	8/1	16	0	0	3	111	0	0	4	88	1	1	8	10	0	0	1.5
4	8/4	8/3	19	1	1	1.3	19	1	1	1.6	27	0	0	3	38	0	0	1.1
4	8/4	8/2	33	1	1	1.8	16	0	0	3.5	51	1	1	5	42	0	0	1.4
4	8/4	8/1	82	1	1	2.3	64	1	1	4.2	99	1	1	6	11	0	0	1.5
4	8/3	8/2	24	1	1	2	27	0	0	1.8	84	1	1	3	22	1	1	1.2
4	8/3	8/1	77	1	1	1.8	29	0	0	3.2	87	1	1	5	25	0	0	1.8
4	8/2	8/1	84	1	1	2	34	1	1	3	24	1	1	3	104	1	1	1.5
5	8/5	8/4	47	0	0	1.2	99	1	1	1.1	14	1	1	1.5	68	1	1	1.1
5	8/5	8/3	43	1	1	1.2	83	1	1	1.3	58	1	1	3	12	1	1	1.2
5	8/5	8/2	41	0	0	1.5	112	1	1	2.8	22	0	0	5	7	1	1	1.3
5	8/5	8/1	71	0	0	1.6	49	1	1	3	32	1	1	4	83	1	1	1.3
5	8/4	8/3	69	0	0	1.2	73	1	1	1.2	50	1	1	2	79	0	0	1.1
5	8/4	8/2	114	0	0	1.5	56	1	1	2	113	1	1	3	61	1	1	1.2
5	8/4	8/1	58	0	0	2.5	14	0	0	3	60	0	0	4	84	0	0	1.3
5	8/3	8/2	49	1	1	1.3	118	0	0	2	72	0	0	3	16	1	1	1.2
5	8/3	8/1	120	0	0	1.3	87	1	1	3	76	0	0	3	44	1	1	1.3
5	8/2	8/1	53	1	1	1.3	22	0	0	2.8	106	1	1	2	81	0	1	1.1
5	8/5	8/4	29	1	1	1.2	35	1	1	1.1	46	1	1	1.5	69	0	1	1.1
5	8/5	8/3	78	1	1	1.1	32	0	0	1.5	19	1	1	2	117	0	0	1.1
5	8/5	8/2	26	0	0	1.5	100	0	0	2	20	0	0	4	76	1	1	1.4
5	8/5	8/1	8	0	0	2	78	0	0	3.5	53	0	0	6	98	1	1	1.2
5	8/4	8/3	97	0	0	1.3	79	1	1	1.1	104	0	0	2.5	54	0	0	1.1
5	8/4	8/2	60	1	1	1.3	104	1	1	2.6	78	0	0	4	2	1	1	1.3
5	8/4	8/1	118	0	0	1.5	7	1	1	2.5	66	1	1	4	107	1	1	1.2
5	8/3	8/2	90	0	0	1.3	5	1	1	1.6	102	1	1	2	95	0	0	1.1
5	8/3	8/1	74	0	0	1.2	45	1	1	2.5	7	1	1	2	23	1	1	1.3
5	8/2	8/1	66	1	1	1.5	75	1	1	1.2	54	0	0	3	56	0	1	1.1
6	8/5	8/4	86	1	1	1.3	44	1	1	1.3	90	0	0	2.5	119	1	1	1.1
6	8/5	8/3	23	1	1	1.5	42	0	0	1.6	40	1	1	3	101	0	0	1.3
6	8/5	8/2	54	0	0	1.8	92	0	0	3	69	1	1	4	97	0	0	1.3
6	8/5	8/1	15	1	1	3.5	84	0	0	5	43	1	1	10	91	0	0	1.7
6	8/4	8/3	13	0	0	1.3	59	1	1	1.3	96	0	0	3.5	118	0	0	1.1
6	8/4	8/2	64	0	0	1.6	93	1	1	2.5	34	0	0	6	28	1	1	1.3
6	8/4	8/1	110	1	1	2.8	6	0	0	5.2	116	0	0	10	106	0	0	1.8
6	8/3	8/2	59	0	0	1.3	90	1	1	1.6	111	0	0	4	27	1	1	1.2
6	8/3	8/1	87	1	1	2	96	0	0	4	83	0	0	5	65	0	0	1.4
6	8/2	8/1	62	1	1	1.8	15	0	0	3.2	109	1	1	3	109	0	1	1.4
6	8/5	8/4	67	0	0	1.1	51	1	1	1.2	98	0	0	2.5	33	0	0	1.2
6	8/5	8/3	61	0	0	1.3	88	1	1	2	86	1	1	3	112	1	1	1.2
6	8/5	8/2	72	0	0	1.5	10	1	1	2.5	48	1	1	6	93	0	0	1.2
6	8/5	8/1	104	0	0	2.5	30	1	1	3.5	38	1	1	10	57	0	0	1.4
6	8/4	8/3	40	1	1	1.5	55	1	1	1.8	67	1	1	2.5	37	0	0	1.1
6	8/4	8/2	42	0	0	1.6	60	1	1	1.8	70	1	1	4	14	1	1	1.3
6	8/4	8/1	81	1	1	2.5	8	0	0	6	79	0	0	7	102	0	0	1.5
6	8/3	8/2	35	0	0	1.3	105	0	0	2	108	1	1	3	58	1	1	1.1
6	8/3	8/1	65	1	1	2	33	1	1	3.6	118	1	1	5	110	0	0	1.5
6	8/2	8/1	117	0	0	1.8	107	0	0	2.8	10	1	1	3	46	1	0	1.1

Appendix 3-E: Observer's perceived directionality and mean perceived directionality obtained from the experiment in section 3.3.4.

		Perceived directionality of surfaces				
Shrinking Factor		**8/5**	**8/4**	**8/3**	**8/2**	**8/1**
Set 1	**Observer 1**	0.56	0.70	0.88	1.30	2.22
	Observer 2	0.57	0.67	0.88	1.31	2.28
	Observer 3	0.57	0.64	0.88	1.43	2.19
	Observer 4	0.57	0.76	0.83	1.32	2.08
	Mean perceived directionality	0.57	0.69	0.87	1.34	2.19
Set 2	**Observer 1**	0.55	0.64	0.81	1.39	2.53
	Observer 2	0.56	0.68	0.77	1.35	2.50
	Observer 3	0.52	0.70	0.84	1.31	2.51
	Observer 4	0.57	0.65	0.77	1.32	2.64
	Mean perceived directionality	0.55	0.67	0.80	1.34	2.54
Set 3	**Observer 1**	0.54	0.69	0.78	1.32	2.58
	Observer 2	0.58	0.70	0.86	1.31	2.19
	Observer 3	0.57	0.53	0.83	1.63	2.45
	Observer 4	0.56	0.62	0.91	1.28	2.48
	Mean perceived directionality	0.56	0.63	0.84	1.39	2.42
Set 4	**Observer 1**	0.58	0.67	0.84	1.27	2.39
	Observer 2	0.60	0.64	0.81	1.34	2.39
	Observer 3	0.54	0.65	0.90	1.40	2.27
	Observer 4	0.64	0.64	0.83	1.29	2.29
	Mean perceived directionality	0.59	0.65	0.85	1.33	2.34
Set 5	**Observer 1**	0.66	0.75	0.97	1.23	1.68
	Observer 2	0.66	0.74	0.85	1.30	1.85
	Observer 3	0.63	0.72	0.99	1.35	1.66
	Observer 4	0.72	0.77	0.90	1.44	1.40
	Mean perceived directionality	0.67	0.75	0.93	1.33	1.65
Set 6	**Observer 1**	0.56	0.66	0.94	1.23	2.34
	Observer 2	0.59	0.65	0.87	1.22	2.47
	Observer 3	0.50	0.62	0.91	1.47	2.39
	Observer 4	0.60	0.70	0.90	1.52	1.74
	Mean perceived directionality	0.56	0.66	0.90	1.36	2.24

Appendix 3-F: Perceived directionality versus Davis' variance and Tamura's variance

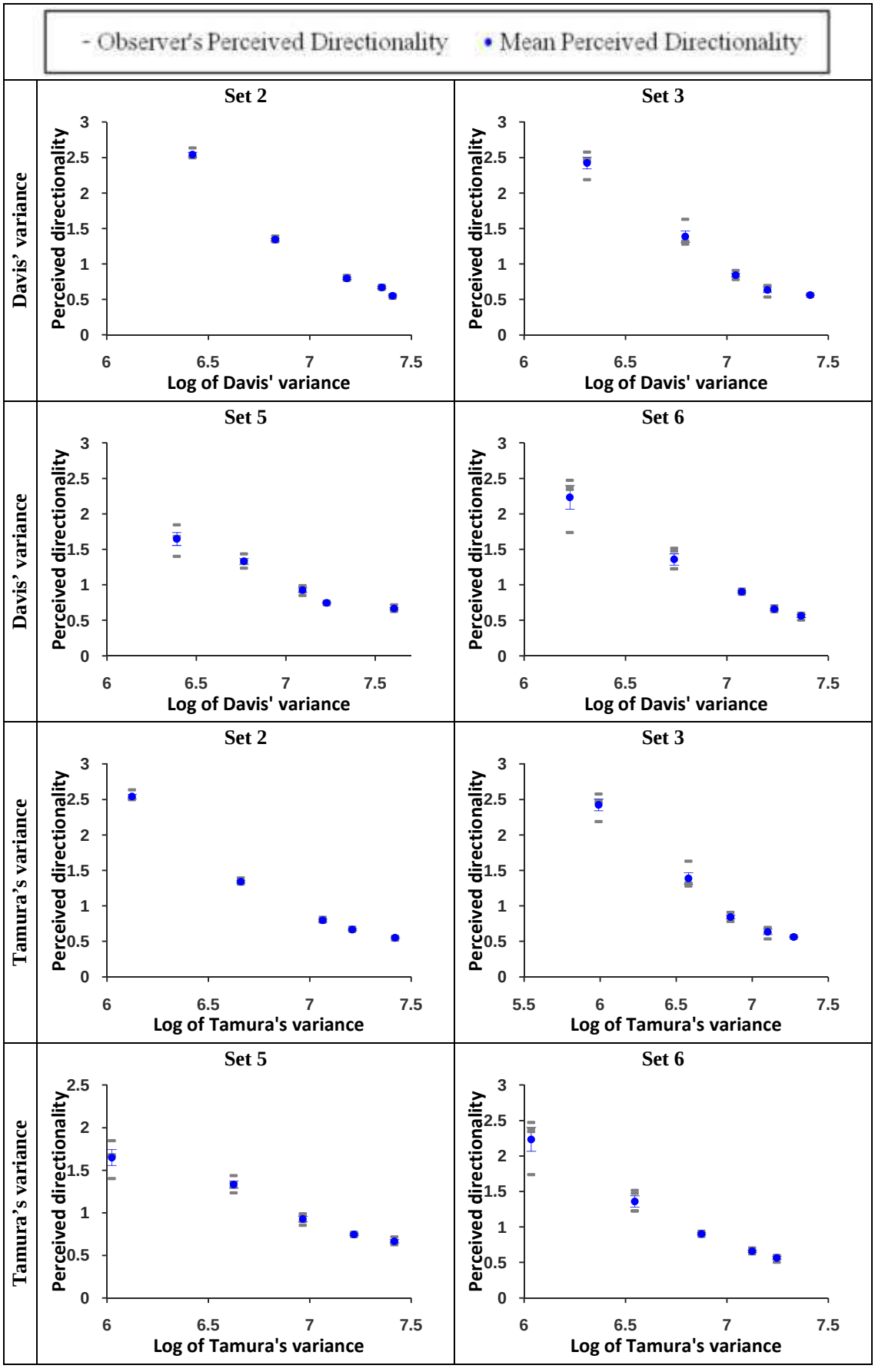

Appendix 3-G: Linear regression on log(ρ) when plotted against logarithm of mathematical measures of directionality

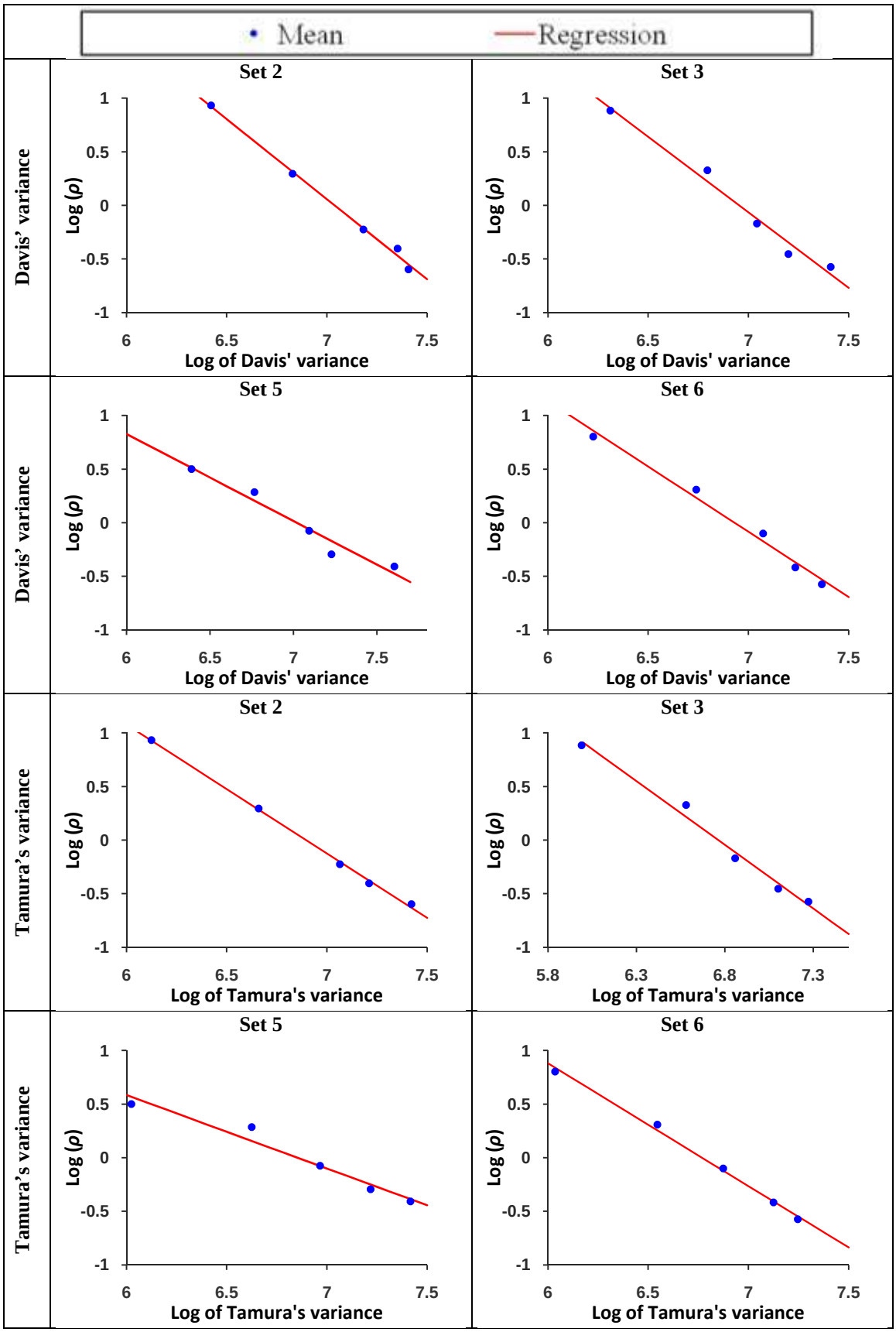

Appendix 3-H: Results of linear regression on log of observers' perceived directionality when plotted against logarithm of Davis' variance and Tamura's variance

		Results for Davis' variance			Results for Tamura's variance		
Linear regression parameter		**Constant**	**Slope**	**R2-Stat**	**Constant**	**Slope**	**R2-Stat**
Observer 1	**Set 1**	10.25	-1.48	1.00	8.47	-1.23	1.00
	Set 2	10.70	-1.52	1.00	8.40	-1.22	1.00
	Set 3	10.15	-1.46	0.99	8.29	-1.23	0.99
	Set 4	9.13	-1.31	1.00	8.43	-1.23	1.00
	Set 5	5.64	-0.80	0.97	4.67	-0.68	0.98
	Set 6	8.52	-1.23	0.99	7.82	-1.16	0.99
Observer 2	**Set 1**	10.49	-1.51	0.99	8.71	-1.27	0.99
	Set 2	10.35	-1.47	0.99	8.14	-1.18	1.00
	Set 3	8.71	-1.25	0.99	7.12	-1.05	0.99
	Set 4	9.23	-1.33	0.99	8.55	-1.24	0.99
	Set 5	6.35	-0.91	0.95	5.30	-0.77	0.98
	Set 6	8.79	-1.27	1.00	8.04	-1.19	1.00
Observer 3	**Set 1**	10.59	-1.53	0.98	8.77	-1.27	0.98
	Set 2	10.38	-1.48	0.98	8.24	-1.19	1.00
	Set 3	10.51	-1.51	0.92	8.67	-1.28	0.93
	Set 4	9.25	-1.33	0.97	8.61	-1.25	0.99
	Set 5	6.11	-0.87	0.95	5.00	-0.73	0.94
	Set 6	9.49	-1.37	0.97	8.74	-1.29	0.99
Observer 4	**Set 1**	9.54	-1.38	0.99	7.88	-1.15	0.99
	Set 2	10.71	-1.52	1.00	8.40	-1.22	0.99
	Set 3	9.83	-1.41	0.98	8.08	-1.20	0.99
	Set 4	8.66	-1.25	0.98	8.02	-1.17	0.99
	Set 5	4.63	-0.66	0.85	3.74	-0.55	0.82
	Set 6	6.74	-0.97	0.91	6.23	-0.92	0.92

Appendix 4-A: MATLAB code to generate random phase spectrum

function phase_spectrum = random_phase (n,seed)

```
% Input:  n = size of surface, seed = internal state of MATLAB to generate
% different random numbers
% Output: phase_spectrum = random phase spectrum
%%%%%%%%%%%%%%%%%%%%%%%%%%%%%%%%%%%%%%%%
rand (‘twister’, seed);
phase_spectrum = rand(n,n)*2*pi;
```

Appendix 4-B: MATLAB code to generate ???á noise spectrum (section 4.2)

function dfreq = fbeta_noise_spectrum (n,beta)

```
%Input
%  n = size of surface
% beta = roll of factor
% Output
% dfreq = ???á noise spectrum
%%%%%%%%%%%%%%%%%%%%%%%%%%%%%%%%%%%%%%%%
nq=n/2;
V = -repmat((-nq:nq-1)', 1,2*nq);
U = repmat((-nq:nq-1), 2*nq,1);
f = sqrt(U.*U+V.*V);

dfreq = power (f, -beta);
```

Appendix 4-C: MATLAB code to generate angular distribution of frequency components (section 4.2)

function dtheta = angular_distribution (n, DDir, AVariance) (section 4.2)

```
% Input
%  n = size of surface
%  DDir = Dominant Angular Frequency
%  AVariance = Angular Variance
%  Output
%  dtheta = angular frequency distribution
%%%%%%%%%%%%%%%%%%%%%%%%%%%%%%%%%%%%%%%

nq=n/2;
V=-repmat((-nq:nq-1)', 1,2*nq);
U=repmat((-nq:nq-1), 2*nq,1);
f=sqrt(U.*U+V.*V);
```

```
% ?[illegible]
theta = atan2(V,U)*180/pi;
dirn  = theta – DDir;
dirn(n/2+1,n/2+1) = 0;
expo = -(dirn.*dirn)/(2*AVariance);
dtheta = exp(expo);
```

Appendix 4-D: MATLAB code to generate surface height map (section 4.2)

function ht = generate_ht1 (n, DDir, AVariance, beta, delta)

```
% Input
%  n = size of surface
% beta = roll of factor
%  DDir = Dominant Angular Frequency
%  AVariance = Angular Variance
% delta = RMS_roughness
%  Output
%  ht = surface height map
%%%%%%%%%%%%%%%%%%%%%%%%%%%%%%%%%%%%%%%%%
%Generating Frequencies
nq=n/2;
V=-repmat((-nq:nq-1)', 1,2*nq); U=repmat((-nq:nq-1), 2*nq,1);
f=sqrt(U.*U+V.*V);

mag1 = fbeta_noise_spectrum (n, beta); % dfreq_noise spectrum
mag2 = angular_distribution (n, DDir, AVariance); %dtheta_angular distribution
magspec = mag1.*mag2;   magspec = ifftshift (magspec);
magspec(1,1) = 0;       % making the magnitude of zero frequency equal to zero
PhaseSpec = random_phase (n);
%Converting to Cartesian Co-ordinate
[x y] = pol2cart(Phase_Spec, magspec); FSpectrum = x + i*y;
FSpectrum = fftshift(FSpectrum);
% Forcing conjugate symmetry in magnitude spectrum
for col1=(n/2+1):n
      for row1=2:n
           u1=col1-(n/2+1); v1=(n/2+1)-row1;
           if (~((u1==0) && (v1==0)))
                  FSpectrum (n+2-row1,n+2-col1)=conj(FSpectrum (row1,col1));
           end
       end
End
% Removing lower frequencies to have realistic looking apperacne
FSpectrum(f<=8) = 0;
% Adjusting RMS roughness
FSpectrum = ifftshift(FSpectrum);
ht_temp = real (ifft2(FSpectrum));
deltan = std2(ht_temp); % calculating deltan to normalize the spectrum

FSpectrum = FSpectrum.* (delta./deltan);
ht = real(ifft2(FSpectrum));
```

Appendix 4-E: Order of surface pairs and observers' responses for the experiment in section 4.3.1

Separate effect of random phase (section 4.3.1)

- Screen 1 is on the left side of the observer and Screen 2 is on the right side of the observer
- Surface 1 = *comparison* surface and Surface 2 = *standard* surface
- rp1, rp2, rp3, rp4 and rp5 indicates different random phase spectra
- If Swap Info = 0 then Surface 1 and 2 is presented on Screen 1 and 2 respectively
- If Swap Info = 1 then Surface 1 and 2 is presented on Screen 2 and 1 respectively
- Order Number shows when the pair is presented during the experiment
- If Selected Surface = 0 then surface on screen 1 is selected as more directional and ratio is equal to perceived directionality of surface on screen 1 to perceived directionality of surface on screen 2
- If Selected Surface = 1 then surface on screen 2 is selected as more directional and ratio is equal to perceived directionality of surface on screen 2 to perceived directionality of surface on screen 1

Surface Pair			**Observer 1**				**Observer 2**				**Observer 3**			
***comparison* surface**		***standard* surface**												
Random Phase	**Angular Variance**	**Angular Variance**	**Order Number**	**Swap Info**	**Selected Surface**	**Ratio**	**Order Number**	**Swap Info**	**Selected Surface**	**Ratio**	**Order Number**	**Swap Info**	**Selected Surface**	**Ratio**
rp1	51.48	20	69	1	0	1.5	52	1	0	2	23	0	1	3
rp1	51.48	20	16	0	1	1.5	26	1	0	2	27	1	0	2
rp1	51.48	20	5	0	1	1.2	38	1	0	2.8	48	1	0	2
rp2	51.48	20	60	0	1	1.3	53	1	0	1.5	60	1	0	3
rp2	51.48	20	85	0	1	1.2	76	0	1	2.6	8	1	0	3
rp2	51.48	20	52	1	0	1.5	24	0	1	2.3	47	1	0	2
rp3	51.48	20	53	0	1	1.5	3	1	0	2	43	1	0	2
rp3	51.48	20	54	1	0	1.3	64	0	1	2.8	58	0	1	3
rp3	51.48	20	59	0	1	1.3	36	1	0	2.5	41	0	1	2
rp4	51.48	20	2	0	1	1.3	22	0	1	2.4	75	1	0	3
rp4	51.48	20	44	0	1	1.2	77	1	0	2	18	1	0	3
rp4	51.48	20	38	1	0	1.3	43	1	0	2.6	67	0	1	3
rp5	51.48	20	57	0	1	1.2	78	0	1	2.2	37	1	0	2
rp5	51.48	20	20	0	1	1.3	42	1	0	2	52	0	1	2
rp5	51.48	20	45	0	1	1.2	29	0	1	3	42	1	0	2
rp1	51.48	132.5	11	1	1	1.6	86	0	0	3	71	1	1	2
rp1	51.48	132.5	81	1	1	1.2	88	0	0	2.8	9	0	0	2
rp1	51.48	132.5	47	1	1	1.3	54	1	1	2.2	20	1	1	3
rp2	51.48	132.5	6	1	1	1.8	9	0	0	1.6	30	0	0	5
rp2	51.48	132.5	28	1	1	1.8	81	0	0	3	76	1	1	3
rp2	51.48	132.5	37	1	1	1.5	61	0	0	2.5	80	1	1	3
rp3	51.48	132.5	25	0	0	1.5	58	0	0	2.8	3	1	1	2
rp3	51.48	132.5	49	0	0	1.5	83	1	1	3	89	1	1	3
rp3	51.48	132.5	31	0	0	1.3	57	0	0	3.1	39	1	1	2
rp4	51.48	132.5	75	0	0	1.3	75	1	1	2.6	26	1	1	2
rp4	51.48	132.5	27	0	0	1.6	14	1	1	2.5	50	0	0	3
rp4	51.48	132.5	66	0	0	1.6	68	1	1	3.2	21	0	0	4
rp5	51.48	132.5	21	0	0	1.2	13	0	0	2	64	0	0	3
rp5	51.48	132.5	48	1	1	1.5	51	0	0	2.4	38	0	0	3
rp5	51.48	132.5	36	1	1	1.5	89	0	0	3.5	78	0	0	3
rp1	51.48	341.03	65	0	1	2.2	31	1	0	3.5	85	1	0	4
rp1	51.48	341.03	82	1	0	1.5	10	1	0	2.2	5	0	1	4
rp1	51.48	341.03	3	1	0	1.8	72	0	1	4.3	83	1	0	5

rp2	51.48	341.03	43	0	1	2	39	1	0	3.7	49	1	0	5
rp2	51.48	341.03	71	1	0	3	4	1	0	2.8	4	1	0	4
rp2	51.48	341.03	86	1	0	1.6	56	1	0	4	6	0	1	4
rp3	51.48	341.03	87	1	0	1.5	46	0	1	3.2	2	0	1	4
rp3	51.48	341.03	84	1	0	2.5	71	1	0	3.8	72	0	1	5
rp3	51.48	341.03	34	0	1	1.5	62	1	0	3.8	87	0	1	5
rp4	51.48	341.03	55	0	1	1.6	15	1	0	3	35	1	0	5
rp4	51.48	341.03	13	0	1	1.8	90	1	0	4.8	57	1	0	5
rp4	51.48	341.03	9	1	0	2	17	1	0	3.4	77	0	1	5
rp5	51.48	341.03	64	1	0	2	55	1	0	3.2	33	1	0	4
rp5	51.48	341.03	14	0	1	2	67	0	1	3.6	22	0	1	5
rp5	51.48	341.03	88	1	0	2.5	41	0	1	3	29	1	0	4
rp1	132.5	20	30	1	0	3	32	0	1	4	45	1	0	4
rp1	132.5	20	76	0	1	2.5	12	0	1	3	54	0	1	3
rp1	132.5	20	7	1	0	2.5	69	0	1	4	17	0	1	5
rp2	132.5	20	83	0	1	1.3	47	0	1	4	31	0	1	3
rp2	132.5	20	4	1	0	1.5	84	0	1	4.1	36	0	1	4
rp2	132.5	20	19	0	1	2	85	0	1	4.5	32	0	1	3
rp3	132.5	20	50	1	0	2.5	70	0	1	4.2	19	1	0	3
rp3	132.5	20	33	0	1	1.8	82	0	1	4.5	51	0	1	3
rp3	132.5	20	17	0	1	2	19	1	0	4	82	1	0	6
rp4	132.5	20	1	0	1	1.8	6	0	1	2.5	86	1	0	4
rp4	132.5	20	10	1	0	2	1	1	0	2.8	53	1	0	3
rp4	132.5	20	29	1	0	2.5	16	1	0	3.5	73	0	1	4
rp5	132.5	20	24	1	0	1.6	28	0	1	3.5	13	1	0	4
rp5	132.5	20	12	0	1	1.8	7	1	0	3	11	0	1	5
rp5	132.5	20	26	1	0	2	20	0	1	4.5	88	1	0	4
rp1	132.5	51.48	46	1	0	1.2	23	0	1	2.6	28	0	1	3
rp1	132.5	51.48	18	1	0	1.3	60	0	1	2.6	68	0	1	3
rp1	132.5	51.48	22	1	0	1.2	50	1	0	2.6	59	0	1	3
rp2	132.5	51.48	35	1	0	1.5	35	1	0	2	79	1	0	2
rp2	132.5	51.48	15	0	1	1.5	37	0	1	2.1	1	0	1	2
rp2	132.5	51.48	8	1	0	1.3	18	0	1	3	16	0	1	3
rp3	132.5	51.48	74	0	1	1.3	30	1	0	2.5	90	1	0	3
rp3	132.5	51.48	58	0	1	1.3	87	1	0	3.2	62	0	1	2
rp3	132.5	51.48	56	1	0	1.5	34	0	1	1.6	15	1	0	3
rp4	132.5	51.48	77	0	1	1.3	5	0	1	1.3	34	0	1	3
rp4	132.5	51.48	41	0	1	1.5	66	1	0	3	65	1	0	3
rp4	132.5	51.48	73	1	0	1.3	49	0	1	3	44	0	1	2
rp5	132.5	51.48	51	1	0	1.6	2	0	1	1.5	61	1	0	3
rp5	132.5	51.48	62	0	1	1.3	63	0	1	2.6	55	1	0	2
rp5	132.5	51.48	79	1	0	1.2	25	0	1	2	7	1	0	3
rp1	132.5	341.03	80	1	0	1.2	40	0	1	2	81	1	0	3
rp1	132.5	341.03	61	1	0	1.2	44	1	0	2.3	24	1	0	2
rp1	132.5	341.03	39	1	0	1.2	65	0	1	2	14	0	1	4
rp2	132.5	341.03	70	0	1	1.5	59	1	0	2.9	66	0	1	4
rp2	132.5	341.03	67	0	1	1.5	79	0	1	2.8	46	1	0	3
rp2	132.5	341.03	42	1	0	1.3	74	1	0	2	56	1	0	3
rp3	132.5	341.03	23	0	1	1.2	48	1	0	3	70	1	0	3
rp3	132.5	341.03	89	1	0	1.3	73	1	0	2.5	25	1	0	3
rp3	132.5	341.03	78	1	0	1.3	21	1	0	2	69	1	0	3
rp4	132.5	341.03	63	1	0	1.3	27	0	1	1.8	40	0	1	3
rp4	132.5	341.03	32	0	1	1.3	45	0	1	1.8	74	1	0	5
rp4	132.5	341.03	90	0	1	1.2	8	0	1	1.2	12	0	1	5
rp5	132.5	341.03	68	1	0	1.3	11	1	0	1.6	84	0	1	3
rp5	132.5	341.03	40	1	0	1.2	80	1	0	3	10	1	0	3
rp5	132.5	341.03	72	1	0	1.3	33	0	1	2	63	1	0	2

Separate effect of random phase (section 4.3.1)										
Surface Pair			**Observer 4**				**Observer 5**			
***comparison* surface**		***standard* surface**								
Random Phase	**Angular Variance**	**Angular Variance**	**Order Number**	**Swap Info**	**Selected Surface**	**Ratio**	**Order Number**	**Swap Info**	**Selected Surface**	**Ratio**
rp1	51.48	20	71	1	0	1.2	41	1	0	3
rp1	51.48	20	32	0	1	1.2	55	0	1	4
rp1	51.48	20	60	1	0	1.2	12	1	0	5
rp2	51.48	20	83	1	0	1.2	3	1	0	3
rp2	51.48	20	5	1	0	1.2	10	0	1	3
rp2	51.48	20	48	0	1	1.2	18	1	0	3
rp3	51.48	20	44	0	1	1.2	70	0	1	2
rp3	51.48	20	63	0	1	1.2	40	0	1	3.8
rp3	51.48	20	31	1	0	1.1	34	1	0	7
rp4	51.48	20	56	1	0	1.2	89	1	0	3.5
rp4	51.48	20	11	1	0	1.2	13	1	0	3
rp4	51.48	20	13	0	1	1.1	68	1	0	2
rp5	51.48	20	75	0	1	1.2	83	0	1	4
rp5	51.48	20	51	0	1	1.2	29	1	0	4
rp5	51.48	20	2	1	0	1.2	21	0	1	2.4
rp1	51.48	132.5	59	0	0	1.3	38	1	1	3
rp1	51.48	132.5	45	0	0	1.3	84	0	0	4
rp1	51.48	132.5	6	0	0	1.3	37	1	1	3
rp2	51.48	132.5	17	1	1	1.4	6	0	0	4
rp2	51.48	132.5	55	1	1	1.4	20	0	0	4
rp2	51.48	132.5	86	1	1	1.3	47	1	1	5
rp3	51.48	132.5	42	0	0	1.3	74	0	0	2.5
rp3	51.48	132.5	28	1	1	1.5	61	1	1	3
rp3	51.48	132.5	43	0	0	1.3	25	0	0	5
rp4	51.48	132.5	62	0	0	1.3	62	1	1	4
rp4	51.48	132.5	81	0	0	1.3	80	1	1	3.5
rp4	51.48	132.5	14	0	0	1.5	65	1	1	3
rp5	51.48	132.5	41	0	0	1.4	16	0	0	4
rp5	51.48	132.5	40	0	0	1.3	85	1	1	5
rp5	51.48	132.5	84	0	0	1.4	50	1	1	4
rp1	51.48	341.03	46	0	1	1.6	88	1	0	5
rp1	51.48	341.03	54	1	0	1.7	57	0	1	4
rp1	51.48	341.03	64	0	1	1.6	32	0	1	7
rp2	51.48	341.03	19	0	1	1.7	69	0	1	4
rp2	51.48	341.03	58	0	1	1.8	72	0	1	5
rp2	51.48	341.03	66	1	0	1.7	67	1	0	8
rp3	51.48	341.03	27	0	1	1.6	39	1	0	8
rp3	51.48	341.03	78	0	1	1.5	8	0	1	9
rp3	51.48	341.03	21	1	0	1.8	24	1	0	4
rp4	51.48	341.03	10	0	1	1.6	14	0	1	8
rp4	51.48	341.03	87	0	1	1.6	15	1	0	7
rp4	51.48	341.03	35	1	0	1.9	53	0	1	9
rp5	51.48	341.03	73	1	0	1.9	5	1	0	9
rp5	51.48	341.03	52	0	1	1.6	30	0	1	8
rp5	51.48	341.03	85	0	1	1.5	76	1	0	6
rp1	132.5	20	50	0	1	1.5	46	1	0	6
rp1	132.5	20	69	0	1	1.3	43	1	0	4
rp1	132.5	20	47	1	0	1.4	11	1	0	5
rp2	132.5	20	82	0	1	1.3	33	0	1	6
rp2	132.5	20	39	1	0	1.4	4	1	0	8
rp2	132.5	20	70	0	1	1.4	36	1	0	6

rp3	132.5	20	80	0	1	1.4	59	0	1	6
rp3	132.5	20	3	1	0	1.8	63	1	0	7
rp3	132.5	20	33	0	1	1.3	81	1	0	7
rp4	132.5	20	18	0	1	1.5	2	1	0	6
rp4	132.5	20	23	0	1	1.3	71	0	1	4
rp4	132.5	20	34	1	0	1.3	77	1	0	9
rp5	132.5	20	65	0	1	1.3	26	0	1	6
rp5	132.5	20	22	0	1	1.3	56	1	0	4
rp5	132.5	20	16	0	1	1.4	82	0	1	8
rp1	132.5	51.48	26	0	1	1.2	27	0	1	5
rp1	132.5	51.48	12	1	0	1.4	35	1	0	5
rp1	132.5	51.48	89	0	1	1.1	75	1	0	2.5
rp2	132.5	51.48	4	1	0	1.4	31	0	1	5
rp2	132.5	51.48	67	1	0	1.3	58	1	0	5
rp2	132.5	51.48	9	0	1	1.2	22	1	0	3
rp3	132.5	51.48	7	1	0	1.3	7	1	0	5
rp3	132.5	51.48	68	1	0	1.3	52	0	1	6
rp3	132.5	51.48	88	0	1	1.2	87	0	1	4
rp4	132.5	51.48	25	1	0	1.4	42	1	0	4
rp4	132.5	51.48	29	0	1	1.3	28	0	1	6
rp4	132.5	51.48	30	1	0	1.2	54	0	1	6
rp5	132.5	51.48	79	0	1	1.15	17	1	0	5
rp5	132.5	51.48	24	0	1	1.4	64	1	0	7
rp5	132.5	51.48	38	1	0	1.5	49	1	0	3.5
rp1	132.5	341.03	77	0	1	1.2	9	0	1	3
rp1	132.5	341.03	61	0	1	1.2	48	0	1	3
rp1	132.5	341.03	90	0	1	1.15	90	1	0	2
rp2	132.5	341.03	49	1	0	1.4	86	1	0	5
rp2	132.5	341.03	20	1	0	1.5	19	0	1	3
rp2	132.5	341.03	15	1	0	1.3	1	0	1	5
rp3	132.5	341.03	53	0	1	1.3	66	0	1	4
rp3	132.5	341.03	76	0	1	1.3	73	0	1	3
rp3	132.5	341.03	72	0	1	1.2	60	0	1	4
rp4	132.5	341.03	74	1	0	1.6	44	0	1	3
rp4	132.5	341.03	37	1	0	1.4	51	0	1	8
rp4	132.5	341.03	57	1	0	1.4	78	0	1	3
rp5	132.5	341.03	36	0	1	1.3	45	0	1	3.2
rp5	132.5	341.03	8	0	1	1.4	23	1	0	3
rp5	132.5	341.03	1	1	0	1.5	79	0	1	2

Appendix 4-F: Order of surface pairs and observers' responses for the experiment in section 4.3.2

Separate effect of angular variance (section 4.3.2)

- Screen 1 is on the left side of the observer and Screen 2 is on the right side of the observer
- If Swap Info = 0 then Surface 1 and 2 is presented on Screen 1 and 2 respectively
- If Swap Info = 1 then Surface 1 and 2 is presented on Screen 2 and 1 respectively
- Order Number shows when the pair is presented during the experiment
- If Selected Surface = 0 then surface on screen 1 is selected as more directional and ratio is equal to perceived directionality of surface on screen 1 to perceived directionality of surface on screen 2
- If Selected Surface = 1 then surface on screen 2 is selected as more directional and ratio is equal to perceived directionality of surface on screen 2 to perceived directionality of surface on screen 1

RMS roughness	Surface Pair		Observer 1				Observer 2				Observer 3			
	Surface 1	Surface 2												
	Angular variance	Angular Variance	Order Number	Swap Info	Selected Surface	Ratio	Order Number	Swap Info	Selected Surface	Ratio	Order Number	Swap Info	Selected Surface	Ratio
0.012	20	51.48	10	1	0	1.4	30	1	0	2	59	1	0	1.5
	20	51.48	31	1	0	1.3	78	1	0	2	34	1	0	1.8
	20	132.5	69	1	0	1.4	15	1	0	4	38	1	0	8
	20	132.5	8	1	0	1.5	52	1	0	5	8	1	0	2.5
	20	341	14	1	0	2.2	37	1	0	9	51	1	0	8
	20	341	75	0	1	2	3	1	0	10	48	1	0	5.5
	20	877.8	68	1	0	1.5	43	0	1	9.5	20	0	1	9
	20	877.8	12	0	1	3.4	62	0	1	10	12	1	0	8
	51.48	132.5	43	1	0	1.4	18	0	1	2.5	70	1	0	6
	51.48	132.5	22	1	0	1.5	32	1	0	2.8	33	1	0	3
	51.48	341	60	1	0	2	77	1	0	7	14	0	1	6
	51.48	341	78	1	0	1.9	66	1	0	4	77	1	0	4
	51.48	877.8	67	0	1	1.9	51	0	1	6	42	0	1	8
	51.48	877.8	26	1	0	2.8	13	0	1	7	55	0	1	6
	132.5	341	73	1	0	1.4	38	0	1	4.5	50	0	1	9
	132.5	341	44	1	0	1.8	50	1	0	3	56	0	1	3
	132.5	877.8	50	0	1	2	39	1	0	3.5	44	1	0	1.8
	132.5	877.8	5	1	0	3	35	1	0	5	24	1	0	3
	341	877.8	72	1	0	1.4	24	1	0	2	28	0	1	1.1
	341	877.8	74	1	0	1.9	17	0	1	2	22	0	1	1.5
0.016	20	51.48	13	1	0	1.9	16	1	0	2	53	0	1	2
	20	51.48	42	1	0	1.2	31	1	0	2.6	21	0	1	2
	20	132.5	15	1	0	2.5	80	0	1	4	68	0	1	4
	20	132.5	21	0	1	1.6	4	1	0	7	43	0	1	6
	20	341	1	1	0	4	53	0	1	9	65	0	1	10
	20	341	79	1	0	2.3	21	0	1	8	11	1	0	8
	20	877.8	40	0	1	2.3	55	0	1	10	26	0	1	8
	20	877.8	11	0	1	3.5	73	0	1	9	73	0	1	7
	51.48	132.5	64	0	1	1.7	70	1	0	2.5	37	1	0	7
	51.48	132.5	33	1	0	1.2	19	1	0	3	10	0	1	2
	51.48	341	49	1	0	2.7	76	0	1	6	63	0	1	7
	51.48	341	24	0	1	3.4	12	0	1	4.3	27	0	1	7
	51.48	877.8	54	0	1	3	1	0	1	8	66	0	1	8
	51.48	877.8	51	1	0	2.6	10	1	0	5	6	0	1	10
	132.5	341	35	1	0	1.5	74	1	0	3	5	1	0	5
	132.5	341	53	1	0	2	63	1	0	3	62	1	0	1.5
	132.5	877.8	18	0	1	2.9	7	1	0	4	17	0	1	2
	132.5	877.8	57	1	0	1.8	54	1	0	5	72	1	0	3
	341	877.8	46	0	1	2.3	22	0	1	3	75	1	0	1.5
	341	877.8	66	0	1	1.6	48	1	0	2.9	1	0	1	1.5
0.02	20	51.48	41	0	1	1.3	6	0	1	3	7	0	1	2.5
	20	51.48	25	1	0	1.4	41	0	1	2.6	78	0	1	2.1
	20	132.5	37	1	0	1.6	20	0	1	6	69	0	1	9
	20	132.5	55	0	1	1.8	65	1	0	3	39	1	0	6
	20	341	45	1	0	3.5	9	1	0	4	29	0	1	8
	20	341	7	1	0	2.8	2	1	0	9	80	1	0	3.5
	20	877.8	38	1	0	2.7	5	1	0	8	16	0	1	10
	20	877.8	23	0	1	3.8	60	1	0	9	45	0	1	9
	51.48	132.5	28	1	0	1.5	58	1	0	7	18	1	0	5
	51.48	132.5	56	1	0	1.6	14	0	1	3.5	31	0	1	1.5
	51.48	341	52	1	0	2.6	49	1	0	5	32	0	1	3
	51.48	341	71	0	1	2	46	0	1	9.5	60	0	1	8
	51.48	877.8	80	1	0	2.5	42	1	0	7.8	47	1	0	6
	51.48	877.8	61	1	0	2.2	34	0	1	8	74	1	0	8

	132.5	341	30	1	0	2	44	0	1	3.5	25	1	0	4
	132.5	341	16	0	1	2.8	23	0	1	3.5	76	0	1	2
	132.5	877.8	19	1	0	3.6	11	1	0	3	67	0	1	5
	132.5	877.8	65	0	1	1.8	27	1	0	5	9	1	0	2
0.024	341	877.8	6	1	0	1.7	59	0	1	3	46	1	0	1.5
	341	877.8	63	1	0	1.6	29	0	1	2.5	79	0	1	1.5
	20	51.48	3	0	1	1.5	69	0	1	3	57	1	0	2.5
	20	51.48	9	1	0	1.5	67	0	1	2.5	2	1	0	1.5
	20	132.5	47	0	1	1.7	40	0	1	6.8	35	1	0	5
	20	132.5	4	1	0	3	56	1	0	3	61	1	0	7
	20	341	39	1	0	2.8	28	0	1	9	13	1	0	10
	20	341	58	0	1	2.5	33	1	0	7.5	49	0	1	9
	20	877.8	59	1	0	2.7	64	0	1	11	3	1	0	10
	20	877.8	77	0	1	2.5	45	1	0	10	40	1	0	10
	51.48	132.5	2	0	1	2.5	72	0	1	3	30	0	1	2.5
	51.48	132.5	27	0	1	1.8	79	0	1	3.4	23	0	1	2
	51.48	341	34	0	1	2.3	36	1	0	9	58	0	1	5
	51.48	341	36	0	1	2	75	1	0	6	15	1	0	8
	51.48	877.8	17	0	1	3	68	1	0	8	36	1	0	8
	51.48	877.8	29	1	0	3.2	26	1	0	6	64	0	1	9
	132.5	341	70	0	1	2	61	0	1	3	4	0	1	5
	132.5	341	20	1	0	3.9	57	1	0	4	71	0	1	4
	132.5	877.8	32	0	1	3.5	47	1	0	6.8	54	1	0	4
	132.5	877.8	48	1	0	3.6	71	0	1	3	41	1	0	9
	341	877.8	62	1	0	1.7	25	0	1	2.5	52	1	0	1.5
	341	877.8	76	0	1	2	8	1	0	1.5	19	0	1	1.5

Separate effect of angular variance (section 4.3.2)										
RMS roughness	**Surface Pair**		**Observer 4**				**Observer 5**			
	Surface 1	**Surface 2**								
	Angular variance	**Angular variance**	**Order Number**	**Swap Info**	**Selected Surface**	**Ratio**	**Order Number**	**Swap Info**	**Selected Surface**	**Ratio**
0.012	20	51.48	26	1	0	4	68	1	0	1.4
	20	51.48	56	1	0	3	71	0	1	1.4
	20	132.5	30	0	1	5	80	0	1	1.8
	20	132.5	28	0	1	4	70	0	1	1.5
	20	341	20	1	0	4	28	0	1	2
	20	341	22	1	0	5	77	1	0	1.8
	20	877.8	54	1	0	5	32	1	0	2.5
	20	877.8	61	0	1	6	17	0	1	1.8
	51.48	132.5	71	0	1	3	50	1	0	1.3
	51.48	132.5	41	1	0	3	34	0	1	1.3
	51.48	341	10	0	1	5	7	0	1	2.5
	51.48	341	62	1	0	5	46	1	0	1.8
	51.48	877.8	51	0	1	8	22	0	1	2
	51.48	877.8	46	1	0	4	65	1	0	2.2
	132.5	341	78	0	1	3	25	0	1	1.4
	132.5	341	53	0	1	5	33	0	1	1.4
	132.5	877.8	57	1	0	4	31	0	1	1.5
	132.5	877.8	18	1	0	5	36	1	0	1.5
	341	877.8	32	0	1	3	10	1	0	1.3
	341	877.8	16	0	1	4	8	1	0	1.3

0.016	20	51.48	27	0	1	2	39	0	1	1.5
	20	51.48	34	0	1	3	9	0	1	1.4
	20	132.5	79	0	1	4	60	0	1	1.8
	20	132.5	48	0	1	5	1	1	0	2
	20	341	43	0	1	6	63	0	1	2
	20	341	1	0	1	8	6	1	0	2.5
	20	877.8	58	1	0	6	52	0	1	2.8
	20	877.8	3	1	0	6	73	0	1	2.8
	51.48	132.5	77	1	0	3	12	0	1	1.5
	51.48	132.5	8	1	0	3	16	0	1	1.4
	51.48	341	21	0	1	5	45	0	1	2
	51.48	341	45	1	0	5	13	0	1	1.8
	51.48	877.8	76	0	1	6	29	0	1	2.5
	51.48	877.8	66	1	0	5	67	1	0	2.2
	132.5	341	55	1	0	4	15	0	1	1.5
	132.5	341	72	0	1	6	23	0	1	1.5
	132.5	877.8	47	0	1	4	42	1	0	1.8
	132.5	877.8	4	0	1	4	20	1	0	1.4
	341	877.8	19	1	0	3	56	0	1	1.2
	341	877.8	24	0	1	4	62	0	1	1.4
0.02	20	51.48	40	0	1	4	78	1	0	1.5
	20	51.48	38	0	1	3	48	1	0	1.4
	20	132.5	75	1	0	4	64	1	0	1.8
	20	132.5	35	0	1	5	18	1	0	2
	20	341	25	0	1	5	55	1	0	3
	20	341	31	1	0	6	37	1	0	2.5
	20	877.8	59	0	1	6	41	1	0	3
	20	877.8	2	0	1	9	24	0	1	3
	51.48	132.5	12	0	1	4	5	1	0	1.8
	51.48	132.5	65	1	0	4	40	0	1	1.8
	51.48	341	11	0	1	4	2	1	0	2
	51.48	341	5	0	1	5	43	1	0	2.5
	51.48	877.8	13	1	0	6	51	1	0	3
	51.48	877.8	68	1	0	6	53	1	0	2.5
	132.5	341	60	1	0	4	26	0	1	1.3
	132.5	341	67	0	1	3	14	1	0	1.5
	132.5	877.8	70	1	0	4	74	1	0	1.8
	132.5	877.8	37	0	1	5	59	1	0	1.8
0.024	341	877.8	36	1	0	4	75	0	1	1.3
	341	877.8	44	1	0	4	57	1	0	1.2
	20	51.48	74	0	1	4	27	1	0	1.4
	20	51.48	42	0	1	4	11	1	0	1.2
	20	132.5	49	0	1	6	35	0	1	1.8
	20	132.5	14	0	1	5	38	1	0	2.5
	20	341	52	1	0	7	3	1	0	2
	20	341	63	1	0	6	58	0	1	2.5
	20	877.8	6	0	1	5	72	0	1	2.8
	20	877.8	9	0	1	6	30	1	0	3
	51.48	132.5	33	0	1	4	21	1	0	1.5
	51.48	132.5	80	1	0	4	47	1	0	1.5
	51.48	341	17	0	1	4	79	0	1	1.5
	51.48	341	50	0	1	7	61	1	0	2
	51.48	877.8	15	1	0	6	49	1	0	2.5
	51.48	877.8	69	1	0	5	54	0	1	2.5
	132.5	341	23	0	1	3	44	0	1	1.4
	132.5	341	7	1	0	4	19	0	1	1.4
	132.5	877.8	39	1	0	5	69	1	0	1.5
	132.5	877.8	73	0	1	7	66	0	1	1.6
	341	877.8	64	1	0	4	4	1	0	1.4
	341	877.8	29	1	1	3	76	0	1	1.4

Appendix 4-G: Order of surface pairs and observers' responses for the experiment in section 4.3.3

Separate effect of RMS roughness (section 4.3.3)

- Screen 1 is on the left side of the observer and Screen 2 is on the right side of the observer
- If Swap Info = 0 then Surface 1 and 2 is presented on Screen 1 and 2 respectively
- If Swap Info = 1 then Surface 1 and 2 is presented on Screen 2 and 1 respectively
- Order Number shows when the pair is presented during the experiment
- If Selected Surface = 0 then surface on screen 1 is selected as more directional and ratio is equal to perceived directionality of surface on screen 1 to perceived directionality of surface on screen 2
- If Selected Surface = 1 then surface on screen 2 is selected as more directional and ratio is equal to perceived directionality of surface on screen 2 to perceived directionality of surface on screen 1

Angular variance	Surface Pair		Observer 1				Observer 2				Observer 3			
	Surface 1	Surface 2												
	RMS roughness	RMS roughness	Order Number	Swap Info	Selected Surface	Ratio	Order Number	Swap Info	Selected Surface	Ratio	Order Number	Swap Info	Selected Surface	Ratio
20	0.012	0.016	30	1	1	1.8	59	1	1	1.2	48	0	0	1.4
	0.012	0.016	78	1	1	2	34	1	1	1.3	52	1	1	1.3
	0.012	0.02	15	1	1	3	38	1	1	1.3	56	1	1	1.6
	0.012	0.02	52	1	1	2.5	8	1	1	1.6	17	1	1	1.4
	0.012	0.024	37	1	1	3.5	51	1	1	1.3	58	0	0	1.9
	0.012	0.024	3	1	1	2	48	1	1	1.5	50	0	0	1.6
	0.012	0.028	43	0	0	4.6	20	0	0	1.4	7	1	1	1.4
	0.012	0.028	62	0	0	4	12	1	1	1.7	5	1	1	1.3
	0.016	0.02	18	0	0	2	70	1	0	1.1	33	0	0	1.8
	0.016	0.02	32	1	1	3	33	1	0	1.1	53	0	0	1.9
	0.016	0.024	77	1	1	3	14	0	0	1.6	74	1	1	1.3
	0.016	0.024	66	1	1	2.3	77	1	1	1.3	35	0	0	1.4
	0.016	0.028	51	0	0	2	42	0	0	1.6	29	0	0	1.9
	0.016	0.028	13	0	0	4	55	0	0	1.8	77	1	1	1.5
	0.02	0.024	38	0	0	3	50	0	0	1.2	20	1	1	1.8
	0.02	0.024	50	1	0	1.3	56	0	0	1.4	26	1	1	1.3
	0.02	0.028	39	1	1	3	44	1	1	1.1	61	1	0	1.5
	0.02	0.028	35	1	1	3	24	1	0	1.2	32	1	1	1.5
	0.024	0.028	24	1	1	2.5	28	0	0	1.4	44	0	0	1.4
	0.024	0.028	17	0	0	2	22	0	0	1.5	65	0	0	1.6
51.48	0.012	0.016	16	1	1	2	53	0	0	1.6	16	0	0	1.4
	0.012	0.016	31	1	1	1.5	21	0	0	1.4	42	1	1	1.3
	0.012	0.02	80	0	0	3	68	0	0	1.3	79	0	0	1.9
	0.012	0.02	4	1	1	3	43	0	0	1.3	51	0	0	1.8
	0.012	0.024	53	0	0	3	65	0	0	1.4	67	1	1	1.8
	0.012	0.024	21	0	0	3	11	1	1	1.8	45	1	1	1.5
	0.012	0.028	55	0	0	3.5	26	0	0	1.5	49	0	0	2
	0.012	0.028	73	0	0	3.5	73	0	0	1.2	40	1	1	1.5
	0.016	0.02	70	1	1	2.5	37	1	1	1.2	13	1	0	1.2
	0.016	0.02	19	1	0	2	10	0	0	1.5	63	0	0	1.9
	0.016	0.024	76	0	0	2.3	63	0	0	1.6	73	0	0	2
	0.016	0.024	12	0	0	3	27	0	0	1.6	34	0	0	1.9
	0.016	0.028	1	0	0	3	66	0	0	1.5	1	1	1	1.5
	0.016	0.028	10	1	1	2	6	0	0	1.6	25	0	0	1.6
	0.02	0.024	74	1	1	1.6	5	1	1	1.5	75	0	0	2
	0.02	0.024	63	1	1	2.3	62	1	1	1.3	15	0	0	1.9
	0.02	0.028	7	1	1	2	17	0	0	1.5	22	0	0	2.3
	0.02	0.028	54	1	1	3	72	1	1	1.3	41	1	1	1.8
	0.024	0.028	22	0	0	2	75	1	0	1.4	11	1	0	1.3

	0.024	0.028	48	1	0	1.3	1	0	0	2	64	1	0	1.3
132.5	0.012	0.016	6	0	0	2	7	0	0	1.4	72	0	0	1.9
	0.012	0.016	41	0	0	3	78	0	0	1.2	76	1	1	1.6
	0.012	0.02	20	0	0	1.5	69	0	0	1.4	18	1	1	1.6
	0.012	0.02	65	1	1	3	39	1	1	1.1	36	0	0	1.6
	0.012	0.024	9	1	1	2	29	0	0	1.5	12	1	1	2
	0.012	0.024	2	1	1	1.5	80	1	1	1.4	28	0	0	2.5
	0.012	0.028	5	1	1	2	16	0	0	1.5	2	0	0	1.9
	0.012	0.028	60	1	1	3	45	0	0	1.3	27	1	1	2
	0.016	0.02	58	1	1	2.1	18	1	1	1.4	43	1	1	1.6
	0.016	0.02	14	0	0	3	31	0	0	1.4	4	1	0	1.5
	0.016	0.024	49	1	1	2.3	32	0	0	1.6	54	0	0	1.6
	0.016	0.024	46	0	0	1.5	60	0	0	1.6	6	0	0	2
	0.016	0.028	42	1	1	2.5	47	1	1	1.3	23	1	1	2.1
	0.016	0.028	34	0	0	2.5	74	1	1	1.5	14	0	0	2.1
	0.02	0.024	44	0	0	3.5	25	1	1	1.1	57	1	1	2
	0.02	0.024	23	0	0	2	76	0	0	1.3	39	0	0	1.5
	0.02	0.028	11	1	1	2	67	0	0	1.2	37	1	1	1.2
	0.02	0.028	27	1	1	2	9	1	1	1.6	69	1	1	1.9
	0.024	0.028	59	0	0	2.6	46	1	1	1.2	59	0	0	2
	0.024	0.028	29	0	0	2	79	0	0	1.5	8	0	0	1.5
341	0.012	0.016	69	0	0	2	57	1	1	1.6	68	1	1	1.9
	0.012	0.016	67	0	0	1.6	2	1	1	1.5	30	0	0	2.3
	0.012	0.02	40	0	0	2.3	35	1	1	1.2	78	0	0	2
	0.012	0.02	56	1	1	2.3	61	1	1	1.4	62	1	1	1.8
	0.012	0.024	28	0	0	3	13	1	1	1.5	31	1	1	2.8
	0.012	0.024	33	1	1	2	49	0	0	1.6	47	1	1	1.6
	0.012	0.028	64	0	0	2.3	3	1	1	1.8	80	1	1	2.1
	0.012	0.028	45	1	1	2.5	40	1	1	1.5	10	0	0	2.2
	0.016	0.02	72	0	0	1.3	30	0	0	1.3	38	0	0	1.6
	0.016	0.02	79	0	0	1.6	23	0	0	1.2	9	0	0	2
	0.016	0.024	36	1	1	2.5	58	0	0	1.5	70	1	1	2
	0.016	0.024	75	1	1	2.2	15	1	1	1.4	24	0	0	2.5
	0.016	0.028	68	1	1	2.3	36	1	1	1.1	60	1	1	2
	0.016	0.028	26	1	1	1.5	64	0	0	1.5	66	0	0	2
	0.02	0.024	61	0	0	2	4	0	0	1.5	55	1	1	1.9
	0.02	0.024	57	1	1	2	71	0	0	1.2	71	0	1	2
	0.02	0.028	47	1	1	2.5	54	1	1	1.5	21	0	0	2.3
	0.02	0.028	71	0	0	2	41	1	1	1.3	19	0	0	2
	0.024	0.028	25	0	0	1.6	52	1	1	1.5	3	1	1	2
	0.024	0.028	8	1	1	2	19	0	0	1.3	46	1	0	1.3

Separate effect of RMS roughness (section 4.3.3)										
Angular variance	**Surface Pair**		**Observer 4**				**Observer 5**			
	Surface 1	**Surface 2**								
	RMS roughness	**RMS roughness**	**Order Number**	**Swap Info**	**Selected Surface**	**Ratio**	**Order Number**	**Swap Info**	**Selected Surface**	**Ratio**
20	0.012	0.016	26	1	1	1.1	66	1	1	3
	0.012	0.016	56	1	1	1.05	43	0	0	4
	0.012	0.02	30	0	0	1.2	80	0	0	6
	0.012	0.02	28	0	0	1.2	20	0	0	6
	0.012	0.024	20	1	1	1.1	34	0	0	8
	0.012	0.024	22	1	1	1.2	15	1	1	5
	0.012	0.028	54	1	1	1.1	47	0	0	8
	0.012	0.028	61	0	0	1.1	35	1	1	9
	0.016	0.02	71	0	0	1.05	10	1	1	6

	0.016	0.02	41	1	1	1.05	16	1	1	3
	0.016	0.024	10	0	0	1.3	37	0	0	5
	0.016	0.024	62	1	1	1.05	31	1	1	7
	0.016	0.028	51	0	0	1.2	11	1	1	5
	0.016	0.028	46	1	1	1.1	46	0	0	8
	0.02	0.024	78	0	0	1.05	29	0	0	4
	0.02	0.024	53	0	0	1.1	54	0	0	6
	0.02	0.028	57	1	1	1.05	64	1	1	7
	0.02	0.028	18	1	1	1.1	79	0	0	6
	0.024	0.028	32	0	0	1.1	22	0	0	5
	0.024	0.028	16	0	0	1.2	28	0	0	4
51.48	0.012	0.016	27	0	0	1.2	52	0	0	6
	0.012	0.016	34	0	0	1.1	65	0	0	6
	0.012	0.02	79	0	0	1.3	7	1	1	5
	0.012	0.02	48	0	0	1.3	3	1	1	4
	0.012	0.024	43	0	0	1.3	9	1	1	8
	0.012	0.024	1	0	0	1.4	21	1	1	8
	0.012	0.028	58	1	1	1.1	51	0	0	9
	0.012	0.028	3	1	1	1.2	25	1	1	8
	0.016	0.02	77	1	0	1.05	60	0	0	8
	0.016	0.02	8	1	1	1.1	2	0	0	4
	0.016	0.024	21	0	0	1.2	73	1	1	4
	0.016	0.024	45	1	1	1.1	48	1	1	7
	0.016	0.028	76	0	0	1.2	18	0	0	7
	0.016	0.028	66	1	1	1.05	39	0	0	7
	0.02	0.024	55	1	1	1.05	38	1	1	4
	0.02	0.024	72	0	0	1.05	8	0	0	6
	0.02	0.028	47	0	0	1.2	27	0	0	7
	0.02	0.028	4	0	0	1.2	14	1	1	6
	0.024	0.028	19	1	1	1.1	33	1	1	6
	0.024	0.028	24	0	0	1.2	53	0	0	7
132.5	0.012	0.016	40	0	0	1.1	72	1	1	3
	0.012	0.016	38	0	0	1.2	12	1	1	7
	0.012	0.02	75	1	1	1.1	56	0	0	8
	0.012	0.02	35	0	0	1.2	40	0	0	8
	0.012	0.024	25	0	0	1.3	23	0	0	8
	0.012	0.024	31	1	1	1.2	49	0	0	9
	0.012	0.028	59	0	0	1.3	63	0	0	8
	0.012	0.028	2	0	0	1.3	68	1	1	7
	0.016	0.02	12	0	0	1.2	74	0	0	4
	0.016	0.02	65	1	1	1.05	62	0	0	7
	0.016	0.024	11	0	0	1.2	61	1	1	6
	0.016	0.024	5	0	0	1.2	57	0	0	6
	0.016	0.028	13	1	1	1.2	70	1	1	6
	0.016	0.028	68	1	1	1.1	55	1	1	7
	0.02	0.024	60	1	1	1.05	4	1	1	4
	0.02	0.024	67	0	0	1.1	30	0	0	7
	0.02	0.028	70	1	1	1.05	69	0	0	6
	0.02	0.028	37	0	0	1.1	44	0	0	5
	0.024	0.028	36	1	1	1.05	36	0	0	5
	0.024	0.028	44	1	1	1.05	67	0	0	4
341	0.012	0.016	74	0	0	1.1	77	1	1	4
	0.012	0.016	42	0	0	1.05	5	0	0	4
	0.012	0.02	49	0	0	1.1	13	1	1	7
	0.012	0.02	14	0	0	1.2	71	0	0	5
	0.012	0.024	52	1	1	1.1	17	0	0	4
	0.012	0.024	63	1	1	1.1	78	0	0	8
	0.012	0.028	6	0	0	1.3	75	0	0	6
	0.012	0.028	9	0	0	1.3	42	0	0	8
	0.016	0.02	33	0	0	1.2	6	0	0	5

	0.016	0.02	80	1	0	1.05	41	1	1	6
	0.016	0.024	17	0	0	1.2	26	0	0	6
	0.016	0.024	50	0	0	1.1	50	0	0	9
	0.016	0.028	15	1	1	1.2	58	1	1	7
	0.016	0.028	69	1	1	1.05	19	0	0	8
	0.02	0.024	23	0	0	1.1	45	1	1	4
	0.02	0.024	7	1	1	1.1	32	0	0	6
	0.02	0.028	39	1	1	1.1	24	0	0	7
	0.02	0.028	73	0	0	1.1	59	0	1	7
	0.024	0.028	64	1	1	1.05	1	0	0	3
	0.024	0.028	29	1	1	1.05	76	0	0	5

Appendix 4-H: Order of surface pairs and observers' responses for the experiment in section 4.3.4

Combined effects of angular variance and RMS roughness (section 4.3.4)

- Screen 1 is on the left side of the observer and Screen 2 is on the right side of the observer
- Values of angular variance: v1 = 20.0, v2 = 51.48, v3 = 132.5, v4 = 341.0 and v5 = 877.8
- Values of RMS roughness: r1 = 0.012, r2 = 0.016, r3 = 0.02 and r4 = 0.024
- If Swap Info = 0 then Surface 1 and 2 is presented on Screen 1 and 2 respectively
- If Swap Info = 1 then Surface 1 and 2 is presented on Screen 2 and 1 respectively
- Order Number shows when the pair is presented during the experiment
- If Selected Surface = 0 then surface on screen 1 is selected as more directional and ratio is equal to perceived directionality of surface on screen 1 to perceived directionality of surface on screen 2
- If Selected Surface = 1 then surface on screen 2 is selected as more directional and ratio is equal to perceived directionality of surface on screen 2 to perceived directionality of surface on screen 1

Surface pair				**Observer 1**				**Observer 2**				**Observer 3**				**Observer 4**			
Surface 1		**Surface 2**																	
?á	?á	?á	?á	**Order Number**	**Swap Info**	**Selected Surface**	**Ratio**	**Order Number**	**Swap Info**	**Selected Surface**	**Ratio**	**Order Number**	**Swap Info**	**Selected Surface**	**Ratio**	**Order Number**	**Swap Info**	**Selected Surface**	**Ratio**
v1	r1	v2	r1	95	0	1	2	97	0	1	1.3	126	0	1	3.5	177	1	0	1.1
v1	r1	v3	r1	183	1	0	3	36	1	0	1.7	13	1	0	6	26	0	1	3.2
v1	r1	v4	r1	18	1	0	3	145	0	1	1.5	181	1	0	8	178	0	1	1.8
v1	r1	v5	r1	34	0	1	2.5	86	1	0	1.8	169	1	0	10.5	106	1	0	3
v1	r1	v1	r2	175	0	0	1.5	176	0	0	1.2	51	0	0	3	137	1	1	1.1
v1	r1	v2	r2	125	0	1	2	154	1	0	1.3	103	0	1	4	54	1	0	1.5
v1	r1	v3	r2	33	0	1	2	44	1	0	1.7	154	1	0	7.7	58	1	0	2.2
v1	r1	v4	r2	5	1	0	3.5	4	0	1	1.8	132	0	1	7	22	0	1	3
v1	r1	v5	r2	185	1	0	2.5	43	1	0	1.5	168	0	1	12	10	0	1	3.2
v1	r1	v1	r3	81	0	0	1.5	17	1	1	1.5	100	1	1	3	122	0	0	2
v1	r1	v2	r3	117	0	0	1.5	174	1	0	1.3	188	1	0	4	38	1	1	1.5
v1	r1	v3	r3	7	0	1	2.5	23	1	0	1.8	v1	1	0	7	33	0	1	3
v1	r1	v4	r3	45	1	0	2.5	70	0	1	1.7	68	0	1	9	169	0	1	3
v1	r1	v5	r3	22	1	0	2.5	118	0	1	1.7	62	0	1	10	24	0	1	3.5
v1	r1	v1	r4	43	0	0	2	85	1	1	1.3	29	0	0	4	101	0	0	1.5
v1	r1	v2	r4	151	0	0	1.5	100	1	0	1.6	61	1	1	2.5	155	1	0	1.2
v1	r1	v3	r4	69	0	1	2.5	3	0	1	1.7	109	1	0	5.6	98	1	0	3.5
v1	r1	v4	r4	12	1	0	2.5	72	1	0	1.6	114	0	1	10	17	1	0	5
v1	r1	v5	r4	155	0	1	3	150	0	1	1.6	1	1	0	12	161	0	1	3
v2	r1	v3	r1	17	1	0	2	105	1	0	1.3	32	1	0	4	31	1	0	2.5
v2	r1	v4	r1	94	1	0	2	147	1	0	1.6	152	1	0	9	108	0	1	2.2
v2	r1	v5	r1	110	1	0	2.5	24	1	0	1.7	25	1	0	8	180	0	1	2

v2	r1	v1	r2	122	0	0	2	76	0	0	1.5	60	0	0	5.5	23	0	0	1.5
v2	r1	v2	r2	53	1	1	1.5	58	1	1	1.2	21	1	1	2.5	179	0	0	1.5
v2	r1	v3	r2	184	1	0	2	52	1	0	1.3	190	0	1	3	34	1	0	2.3
v2	r1	v4	r2	47	0	1	2	16	1	0	1.8	135	1	0	9.9	113	1	0	2.5
v2	r1	v5	r2	177	1	0	2.5	117	0	1	1.7	58	0	1	9	124	1	0	2.1
v2	r1	v1	r3	160	0	0	2	32	0	0	1.7	30	0	0	4.5	47	0	0	1.8
v2	r1	v2	r3	6	1	1	2	146	0	0	1.2	41	1	1	3	171	0	0	1.2
v2	r1	v3	r3	133	1	0	1.5	167	1	0	1.2	117	1	0	2	115	0	1	2
v2	r1	v4	r3	100	1	0	2	9	1	0	1.7	3	1	0	9	1	0	1	4
v2	r1	v5	r3	115	0	1	2.5	83	1	0	1.5	110	0	1	11.5	15	1	0	4.5
v2	r1	v1	r4	112	0	0	2	48	1	1	1.6	31	1	1	3.5	44	0	0	2
v2	r1	v2	r4	107	1	1	1.5	171	1	1	1.5	99	0	0	5.5	145	1	1	1.3
v2	r1	v3	r4	21	1	0	1.5	53	0	1	1.2	93	1	0	3.5	153	1	0	1.5
v2	r1	v4	r4	8	1	0	2	188	1	0	1.3	89	0	1	8	63	1	0	1.8
v2	r1	v5	r4	148	1	0	2.5	98	0	1	1.8	15	1	0	11	136	0	1	3
v3	r1	v4	r1	157	1	0	2	40	1	0	1.3	113	1	0	3	181	0	1	1.3
v3	r1	v5	r1	180	0	1	2	133	0	1	1.2	127	0	1	5	72	1	0	2.2
v3	r1	v1	r2	52	1	1	2.5	177	0	0	1.3	59	1	1	6.8	141	1	1	1.9
v3	r1	v2	r2	163	0	0	2	157	0	0	1.6	162	1	1	3.5	93	1	1	1.5
v3	r1	v3	r2	59	1	1	2	131	1	1	1.1	64	0	0	3.5	46	1	1	1.2
v3	r1	v4	r2	23	0	1	1.5	166	0	1	1.3	150	0	1	3.5	118	0	1	2.1
v3	r1	v5	r2	29	1	0	1.5	187	0	1	1.3	53	1	0	3.5	183	0	1	1.9
v3	r1	v1	r3	27	1	1	2.5	186	1	1	1.5	173	0	0	7	56	1	1	1.9
v3	r1	v2	r3	154	1	1	2.5	152	1	1	1.7	179	0	0	3.5	140	0	0	1.5
v3	r1	v3	r3	174	1	1	1.5	88	1	1	1.2	129	0	0	3.2	2	0	1	2
v3	r1	v4	r3	172	0	1	2	46	0	1	1.3	18	0	0	2.3	68	0	1	1.5
v3	r1	v5	r3	1v1	1	0	1.5	178	0	1	1.7	63	1	0	6	107	0	1	2
v3	r1	v1	r4	167	1	1	3	12	0	0	2	90	1	1	4.5	90	0	0	2.5
v3	r1	v2	r4	146	1	1	2.5	19	1	1	1.5	189	1	1	4	32	1	1	2.4
v3	r1	v3	r4	101	1	1	1.5	82	0	0	1.1	34	1	1	3.5	176	0	0	1.5
v3	r1	v4	r4	118	1	0	2	50	1	0	1.3	35	1	1	3.2	163	0	1	1.5
v3	r1	v5	r4	93	0	1	2	103	1	0	1.4	182	0	1	8	28	1	0	2
v4	r1	v5	r1	71	0	1	1.5	38	1	0	1.3	178	0	1	2.5	142	0	1	1.1
v4	r1	v1	r2	73	0	0	2.5	125	1	1	1.7	94	1	1	9.9	99	1	1	3
v4	r1	v2	r2	65	1	1	2.5	138	0	0	1.7	166	1	1	5.5	138	1	1	2
v4	r1	v3	r2	13	1	1	1.5	84	0	0	1.6	85	1	1	3.5	16	0	0	2.5
v4	r1	v4	r2	72	1	1	1.5	27	0	0	1.2	184	1	1	2	189	0	0	1.5
v4	r1	v5	r2	156	1	0	1.5	165	1	0	1.2	86	1	1	2.2	64	0	1	1.3
v4	r1	v1	r3	58	1	1	3	144	0	0	1.9	56	0	0	8.5	83	1	1	2.5
v4	r1	v2	r3	171	0	0	2.5	95	0	0	1.5	133	1	1	9	144	0	0	2
v4	r1	v3	r3	150	1	1	2	77	1	1	1.5	49	0	0	5	164	1	1	1.6
v4	r1	v4	r3	46	1	1	1.5	30	0	0	1.5	155	0	0	2.2	6	1	0	2
v4	r1	v5	r3	91	0	0	1.5	184	1	0	1.2	153	0	1	3.2	45	1	0	1.5
v4	r1	v1	r4	147	0	0	4	108	0	0	1.8	138	1	1	12	186	0	0	3.5
v4	r1	v2	r4	111	1	1	2.5	162	0	0	1.2	52	0	0	5.5	36	0	0	2.8
v4	r1	v3	r4	28	0	0	2	33	1	1	1.4	83	0	0	3.4	146	0	0	1.8
v4	r1	v4	r4	60	1	1	2	37	1	1	1.4	67	0	0	2	8	0	1	1.2
v4	r1	v5	r4	70	0	0	1.5	54	1	1	1.3	37	0	0	2.2	61	0	1	1.3
v5	r1	v1	r2	159	1	1	4	31	1	1	1.8	137	1	1	12	114	1	1	3
v5	r1	v2	r2	90	0	0	1.5	15	1	1	1.7	87	0	0	8	185	0	0	2.2
v5	r1	v3	r2	1	0	0	2.5	91	1	1	1.3	95	1	1	5	75	0	0	1.6
v5	r1	v4	r2	64	0	0	1.5	169	0	1	1.1	163	1	1	2.5	66	0	0	1.5
v5	r1	v5	r2	153	0	0	1.5	73	1	0	1.1	176	1	1	2	70	0	0	1.2
v5	r1	v1	r3	142	0	0	4	81	1	1	1.4	134	1	1	11	188	0	0	3
v5	r1	v2	r3	57	0	0	2.5	99	1	1	1.6	115	0	0	10	135	1	1	2.2
v5	r1	v3	r3	48	1	1	1.5	18	1	1	1.7	46	0	0	4	57	1	1	2
v5	r1	v4	r3	76	1	1	1.5	5	1	1	1.4	77	0	0	4.5	73	0	0	1.5
v5	r1	v5	r3	102	0	0	1.5	136	0	0	1.3	24	0	0	2	131	1	1	1.2
v5	r1	v1	r4	126	0	0	4	137	0	0	1.9	72	1	1	10	49	0	0	3
v5	r1	v2	r4	99	0	0	2.5	181	0	0	1.8	39	0	0	9	48	0	0	2.5

v5	r1	v3	r4	165	1	1	2.5	26	1	1	1.5	143	0	0	8	154	1	1	1.6
v5	r1	v4	r4	181	1	1	1.5	126	0	0	1.3	38	1	1	2	110	0	0	1.8
v5	r1	v5	r4	63	0	0	1.5	128	1	1	1.3	47	0	0	2.5	27	1	1	1.2
v1	r2	v2	r2	39	0	1	2	13	0	1	1.7	183	1	0	2	41	1	1	1.2
v1	r2	v3	r2	42	0	1	3	29	0	1	1.6	33	0	1	5	42	0	1	2
v1	r2	v4	r2	15	0	1	2.5	79	0	1	1.9	8	0	1	9	116	1	0	2.2
v1	r2	v5	r2	86	0	1	2.5	123	1	0	1.6	106	1	0	12	52	0	1	2.2
v1	r2	v1	r3	3	0	0	2	28	1	1	1.1	11	1	1	3.5	85	0	0	1.5
v1	r2	v2	r3	105	0	1	2	102	1	0	1.8	157	0	0	2.5	166	0	1	1.5
v1	r2	v3	r3	24	0	1	2	143	0	1	1.4	141	0	1	6	4	0	1	4
v1	r2	v4	r3	113	1	0	2.5	189	1	0	1.7	142	0	1	11	170	1	0	3.2
v1	r2	v5	r3	132	1	0	3	115	1	0	1.6	175	1	0	12	126	1	0	2.9
v1	r2	v1	r4	19	1	1	2	109	1	1	1.6	156	1	1	2.5	123	1	1	1.5
v1	r2	v2	r4	179	1	1	2	80	0	0	1.2	160	1	1	2.6	77	0	1	1.3
v1	r2	v3	r4	141	1	0	2.5	89	1	0	1.6	161	1	0	5.5	78	1	0	1.8
v1	r2	v4	r4	143	0	1	3.5	71	1	0	1.6	44	1	0	11	173	1	0	2.5
v1	r2	v5	r4	186	0	1	3.5	180	0	1	1.6	171	1	0	11.6	165	0	1	2.2
v2	r2	v3	r2	161	1	0	2	139	1	0	1.2	50	0	1	3.5	86	1	0	1.8
v2	r2	v4	r2	108	0	1	2	119	0	1	1.7	48	1	0	7	37	0	1	3
v2	r2	v5	r2	168	1	0	2.5	51	0	1	1.4	9	0	1	10	102	1	0	2.5
v2	r2	v1	r3	131	1	1	2.5	68	0	0	1.8	165	0	0	4.5	162	1	1	1.2
v2	r2	v2	r3	87	1	1	2	22	1	1	1.4	6	1	1	3	80	1	1	1.2
v2	r2	v3	r3	170	0	1	1.5	61	0	1	1.5	55	1	0	3.5	139	0	1	1.8
v2	r2	v4	r3	178	1	0	2.5	55	1	0	1.4	5	1	0	7	121	1	0	2
v2	r2	v5	r3	182	0	1	3	87	1	0	1.7	92	0	1	11.5	95	0	1	1.5
v2	r2	v1	r4	66	0	0	2	175	0	0	1.3	7	1	1	3.5	87	1	1	1.8
v2	r2	v2	r4	173	1	1	2	155	0	0	1.6	144	1	1	3.5	55	1	1	1.4
v2	r2	v3	r4	88	0	1	2	92	1	0	1.5	124	1	0	5	88	1	0	2
v2	r2	v4	r4	106	1	0	2.5	112	0	1	1.8	185	1	0	9	190	1	0	1.9
v2	r2	v5	r4	41	0	1	3	160	1	0	1.8	57	1	0	8	103	1	0	2.6
v3	r2	v4	r2	103	0	1	2	45	1	0	1.7	149	1	0	4	150	0	1	1.5
v3	r2	v5	r2	116	0	1	2	21	0	1	1.6	88	1	0	5.6	159	1	0	2
v3	r2	v1	r3	10	1	1	2.5	47	1	1	1.5	159	1	1	4	168	0	0	2.5
v3	r2	v2	r3	119	0	0	2	59	0	0	1.3	97	0	0	4	18	0	0	3.8
v3	r2	v3	r3	144	1	1	1.5	60	0	0	1.3	82	1	1	3	35	0	0	1.2
v3	r2	v4	r3	176	1	0	2	183	0	1	1.4	43	1	0	3.5	51	0	1	1.5
v3	r2	v5	r3	51	0	1	1.5	56	0	1	1.4	111	0	1	8	1v1	1	0	1.5
v3	r2	v1	r4	62	0	0	3.5	127	0	0	1.9	84	1	1	6.7	149	0	0	2
v3	r2	v2	r4	4	1	1	2.5	111	1	1	1.4	78	1	1	6	130	1	1	1.6
v3	r2	v3	r4	138	1	1	1.5	78	1	1	1.5	140	0	0	4	104	1	1	1.3
v3	r2	v4	r4	137	1	0	2	140	1	0	1.3	80	0	1	2.3	71	1	0	2
v3	r2	v5	r4	85	0	1	2	153	0	1	1.8	104	0	1	8	30	0	1	3
v4	r2	v5	r2	123	1	0	1.5	124	0	0	1.1	98	1	0	3.3	157	1	0	1.2
v4	r2	v1	r3	40	0	0	3.5	172	1	1	1.6	10	0	0	12	187	1	1	2.6
v4	r2	v2	r3	145	0	0	3	164	0	0	1.6	71	1	1	6	127	1	1	2
v4	r2	v3	r3	158	1	1	2.5	74	0	0	1.3	118	1	1	3.5	11	1	1	2.8
v4	r2	v4	r3	92	0	0	1.5	141	0	0	1.2	16	1	1	2.6	40	0	0	1.5
v4	r2	v5	r3	188	1	0	2	130	0	1	1.1	174	0	1	2	152	1	0	1.3
v4	r2	v1	r4	77	0	0	3	185	0	0	1.6	186	0	0	12	97	0	0	3.5
v4	r2	v2	r4	25	0	0	2	114	0	0	1.6	96	1	1	8	5	1	1	3
v4	r2	v3	r4	v1	0	0	1.5	7	1	1	1.6	65	0	0	3.3	94	1	1	1.6
v4	r2	v4	r4	109	1	1	1.5	179	0	0	1.1	66	1	1	2.6	74	1	1	1.1
v4	r2	v5	r4	121	0	0	1.5	104	1	1	1.1	121	1	1	2	50	1	0	1.3
v5	r2	v1	r3	74	1	1	3	75	1	1	1.6	42	0	0	12	53	1	1	3
v5	r2	v2	r3	135	1	1	3	35	0	0	1.8	26	1	1	9	182	1	1	2
v5	r2	v3	r3	139	1	1	2	2	0	0	1.8	128	1	1	4.5	134	0	0	2.2
v5	r2	v4	r3	189	1	1	1.5	39	0	0	1.2	81	1	1	2.3	67	1	1	1.2
v5	r2	v5	r3	134	1	1	1.5	41	0	0	1.2	45	1	1	2	100	0	0	1.2
v5	r2	v1	r4	130	1	1	4	168	0	0	1.9	14	1	1	10.8	59	0	0	2.8
v5	r2	v2	r4	49	1	1	2	129	0	0	1.7	54	0	0	8	3	0	0	4.5

v5	r2	v3	r4	38	0	0	1.5	113	1	1	1.9	75	1	1	6	96	0	0	1.8
v5	r2	v4	r4	96	0	0	1.5	v1	1	1	1.3	101	1	1	2.3	81	1	1	1.5
v5	r2	v5	r4	55	0	0	1.5	107	1	1	1.1	102	0	0	2	132	1	1	1.1
v1	r3	v2	r3	140	0	1	2	182	0	1	1.5	119	1	0	3.3	125	1	0	1.2
v1	r3	v3	r3	50	1	0	3	93	0	1	1.5	180	1	0	7.2	129	1	0	1.5
v1	r3	v4	r3	9	1	0	3.5	63	0	1	1.8	22	1	0	7	111	1	0	2.2
v1	r3	v5	r3	83	1	0	2.5	11	1	0	2	146	1	0	12	133	1	0	3
v1	r3	v1	r4	190	1	1	2	149	0	0	1.2	147	0	0	3	21	1	1	1.2
v1	r3	v2	r4	67	0	0	1.5	1v1	0	1	1.2	69	1	0	3	76	1	0	1.2
v1	r3	v3	r4	98	1	0	2	158	0	1	1.8	79	0	1	5.6	117	1	0	2
v1	r3	v4	r4	2	0	1	3	42	1	0	1.6	107	1	0	12	148	1	0	2.5
v1	r3	v5	r4	127	1	0	4	173	1	0	1.9	105	1	0	12	158	1	0	2
v2	r3	v3	r3	124	0	1	2	116	1	0	1.2	91	0	1	5	79	0	1	1.6
v2	r3	v4	r3	32	0	1	2.5	6	1	0	1.8	108	1	0	9	12	1	0	4
v2	r3	v5	r3	89	1	0	2	142	1	0	1.7	122	0	1	6	174	0	1	2.3
v2	r3	v1	r4	169	1	1	2	94	0	0	1.6	27	1	1	4	62	0	0	1.3
v2	r3	v2	r4	31	1	1	2	106	0	0	1.3	73	0	0	3	156	1	1	1.1
v2	r3	v3	r4	187	1	0	2	25	0	1	1.7	23	1	0	5	105	1	0	1.5
v2	r3	v4	r4	56	0	1	2.5	170	0	1	1.6	116	1	0	11.5	172	0	1	2
v2	r3	v5	r4	37	0	1	2.5	101	1	0	1.3	177	1	0	9	19	1	0	4
v3	r3	v4	r3	44	1	0	1.5	96	1	0	1.6	136	0	1	5.6	13	1	0	2
v3	r3	v5	r3	166	0	1	2.5	65	1	0	1.6	125	0	1	6	128	0	1	1.9
v3	r3	v1	r4	129	1	1	2.5	122	0	0	1.6	76	1	1	8	69	1	1	2.2
v3	r3	v2	r4	97	1	1	2.5	57	0	0	1.3	40	0	0	3.5	43	0	0	1.8
v3	r3	v3	r4	78	1	0	1.5	148	0	0	1.1	164	0	0	2.3	60	1	1	1.2
v3	r3	v4	r4	80	1	0	2	14	1	0	1.6	187	1	0	3.5	25	0	1	3
v3	r3	v5	r4	82	1	0	1.5	190	0	1	1.7	36	1	0	3.3	84	1	0	2
v4	r3	v5	r3	152	1	0	1.5	69	0	1	1.2	158	0	0	2	184	0	1	1.2
v4	r3	v1	r4	61	0	0	4	121	0	0	1.7	151	0	0	10.5	119	1	1	2.3
v4	r3	v2	r4	54	0	0	2	156	1	1	1.5	139	0	0	10	151	0	0	2.5
v4	r3	v3	r4	16	1	1	2	163	0	0	1.3	28	1	1	5	147	0	0	1.9
v4	r3	v4	r4	104	0	0	1.5	49	1	0	1.1	130	1	1	2.2	v1	0	1	1.1
v4	r3	v5	r4	114	1	0	1.5	1	1	0	1.3	1v1	0	1	3.5	89	0	1	1.1
v5	r3	v1	r4	164	0	0	4	135	0	0	1.9	19	1	1	10.8	29	0	0	5
v5	r3	v2	r4	26	1	1	3	34	1	1	1.5	123	1	1	10	39	1	1	3
v5	r3	v3	r4	36	1	1	2	90	1	1	1.4	112	1	1	7	160	1	1	2.2
v5	r3	v4	r4	149	1	1	2	64	1	1	1.3	131	0	0	3	82	0	0	1.5
v5	r3	v5	r4	11	0	0	1.5	134	1	1	1.1	17	0	0	2	92	1	1	1.1
v1	r4	v2	r4	84	0	1	1.5	151	1	0	1.8	4	1	0	3	7	1	0	1.2
v1	r4	v3	r4	79	1	0	2	10	1	0	1.9	148	1	0	5	65	1	0	2
v1	r4	v4	r4	75	0	1	3	161	0	1	1.8	74	0	1	11	91	0	1	3
v1	r4	v5	r4	68	0	1	3	62	0	1	1.7	167	0	1	11.5	109	0	1	3.8
v2	r4	v3	r4	128	1	0	2.5	67	1	0	1.3	2	1	0	7	175	1	0	1.9
v2	r4	v4	r4	14	1	0	3	132	1	0	1.6	172	1	0	8	14	1	0	3.8
v2	r4	v5	r4	30	0	1	2.5	8	0	1	1.9	170	1	0	9	143	0	1	1.6
v3	r4	v4	r4	35	0	1	1.5	110	1	0	1.2	145	1	0	4	112	1	0	1.9
v3	r4	v5	r4	162	0	1	2.5	159	1	0	1.7	70	1	0	6	167	0	1	2
v4	r4	v5	r4	136	0	1	1.5	66	0	1	1.1	12	0	1	4	9	1	0	1.5
				Observer 5				**Observer 6**				**Observer 7**				**Observer 8**			
v1	r1	v2	r1	122	1	0	1.2	77	0	1	1.2	17	0	1	3	130	1	0	2
v1	r1	v3	r1	161	0	1	1.4	163	0	1	1.8	v1	1	0	4	186	1	0	6
v1	r1	v4	r1	66	0	1	2	186	0	1	2	117	0	1	3	49	0	1	9.9
v1	r1	v5	r1	15	0	1	2	148	1	0	4	157	1	0	6	72	1	0	10
v1	r1	v1	r2	13	1	0	1.2	31	1	1	1.1	127	0	1	1.5	135	0	1	2
v1	r1	v2	r2	8	0	1	1.3	166	0	0	1.1	25	1	0	2	117	0	1	1.8
v1	r1	v3	r2	142	1	0	2	18	0	1	1.3	62	1	0	2	95	1	0	7
v1	r1	v4	r2	73	1	0	2.5	131	1	0	1.8	68	1	0	4	101	1	0	10
v1	r1	v5	r2	71	1	0	3	1	1	0	4	41	1	0	8	99	1	0	10
v1	r1	v1	r3	148	1	1	1.1	164	1	1	1.1	1v1	1	0	2	87	1	0	1.1

v1	r1	v2	r3	135	1	0	1.2	113	1	0	1.1	9	0	1	3	10	1	0	4
v1	r1	v3	r3	150	0	1	1.4	56	0	1	1.5	67	1	0	3	69	1	0	7
v1	r1	v4	r3	127	1	0	2	49	1	0	3	81	0	1	4.5	6	0	1	9
v1	r1	v5	r3	134	1	0	2.5	158	1	0	4	55	1	0	5	18	1	0	10
v1	r1	v1	r4	123	0	0	1.4	47	0	0	1.5	88	0	1	2	28	0	0	1.1
v1	r1	v2	r4	1	0	1	1.3	17	1	1	1.5	173	1	0	3	40	1	0	6
v1	r1	v3	r4	159	0	1	1.3	22	0	1	1.3	83	0	1	4	105	1	0	6
v1	r1	v4	r4	87	1	0	2	78	1	0	1.8	95	0	1	5	165	0	1	7
v1	r1	v5	r4	19	0	1	2	84	1	0	3.5	53	0	1	6	90	1	0	9.8
v2	r1	v3	r1	62	0	1	1.2	41	1	0	1.4	56	1	0	1.5	93	1	0	4
v2	r1	v4	r1	155	0	1	1.5	38	0	1	3	92	1	0	3	187	1	0	7.8
v2	r1	v5	r1	149	1	0	1.6	124	0	1	3	79	0	1	4	170	0	1	10
v2	r1	v1	r2	176	1	1	1.2	177	1	1	1.2	190	0	0	1.5	144	1	1	3
v2	r1	v2	r2	25	1	1	1.1	42	0	0	1.1	71	0	1	2	26	1	1	1.2
v2	r1	v3	r2	137	1	0	1.2	187	0	1	1.1	145	0	1	2.5	149	1	0	3
v2	r1	v4	r2	188	1	0	2	179	0	1	1.4	166	1	0	3	131	0	1	7
v2	r1	v5	r2	141	1	0	2.4	146	1	0	3.5	69	0	1	5	100	0	1	10
v2	r1	v1	r3	42	0	0	1.4	37	0	0	1.5	107	1	1	2	172	0	0	1.1
v2	r1	v2	r3	55	0	0	1.2	142	0	0	1.3	133	0	1	3	74	0	1	3
v2	r1	v3	r3	138	0	1	1.2	127	0	1	1.1	22	0	1	4	142	0	1	4
v2	r1	v4	r3	186	0	1	2.5	89	1	0	2	130	1	0	4	48	1	0	8
v2	r1	v5	r3	164	0	1	1.6	171	1	0	2.5	54	0	1	5	3	0	1	8
v2	r1	v1	r4	101	0	0	1.6	97	0	0	1.5	126	1	0	2	155	0	0	3
v2	r1	v2	r4	178	0	0	1.2	46	1	1	1.7	154	0	1	3	34	1	1	1.1
v2	r1	v3	r4	182	0	1	1.2	85	1	0	1.2	75	1	0	3	67	0	1	5
v2	r1	v4	r4	79	0	1	1.8	105	0	1	3	78	1	0	3	160	1	0	9
v2	r1	v5	r4	167	0	1	1.6	125	0	1	3.5	33	1	0	7	54	1	0	7
v3	r1	v4	r1	190	1	0	1.4	107	0	1	1.5	163	1	0	2.5	132	0	1	4
v3	r1	v5	r1	91	1	0	1.5	43	0	1	2.5	131	0	1	3	141	0	1	4
v3	r1	v1	r2	83	1	1	1.4	133	1	1	1.5	167	0	0	2.5	1	1	1	6
v3	r1	v2	r2	177	1	1	1.3	24	0	0	1.7	38	0	0	2	7	0	0	7
v3	r1	v3	r2	184	0	0	1.2	172	1	1	1.1	46	1	0	1.5	71	0	0	3
v3	r1	v4	r2	48	0	1	1.2	58	0	1	2	8	1	0	2	136	0	1	4
v3	r1	v5	r2	170	0	1	1.3	76	0	1	3	16	0	1	4	161	1	0	9.9
v3	r1	v1	r3	60	1	1	1.8	106	1	1	2	150	0	0	4	29	1	1	5
v3	r1	v2	r3	145	1	1	1.4	132	0	0	1.5	153	0	0	2	70	0	0	6
v3	r1	v3	r3	143	1	1	1.4	40	0	0	1.3	49	1	0	1.5	151	1	0	1.3
v3	r1	v4	r3	2	1	0	1.5	178	1	0	1.5	73	1	0	2	53	0	1	4
v3	r1	v5	r3	92	0	1	1.5	80	0	1	2.5	139	0	1	5	133	1	0	5
v3	r1	v1	r4	77	1	1	2	39	1	1	2	51	0	0	3	150	0	0	7
v3	r1	v2	r4	1v1	1	1	1.4	170	0	0	2	149	1	0	2	106	1	1	2
v3	r1	v3	r4	171	0	0	1.1	168	0	0	1.3	177	1	0	3	43	0	0	1.1
v3	r1	v4	r4	69	1	0	1.1	112	0	1	1.3	35	1	0	4	86	0	1	1.8
v3	r1	v5	r4	41	0	1	1.5	3	0	1	3	105	1	0	4	126	1	0	4
v4	r1	v5	r1	14	1	0	1.1	114	1	0	1.05	47	1	0	1.8	25	1	0	1.5
v4	r1	v1	r2	121	1	1	2	169	0	0	2	114	0	0	4	97	1	1	9.9
v4	r1	v2	r2	152	0	0	1.8	60	1	1	1.3	165	0	0	4	171	1	1	10
v4	r1	v3	r2	160	0	0	1.3	150	1	1	1.4	3	1	1	2.5	1v1	0	0	3
v4	r1	v4	r2	52	0	0	1.1	109	1	1	1.2	7	1	1	1.2	39	0	0	1.1
v4	r1	v5	r2	165	1	0	1.1	26	0	1	2	89	0	1	2.5	76	0	1	2
v4	r1	v1	r3	128	0	0	3.5	6	0	0	3.5	60	1	1	4	80	0	0	9.5
v4	r1	v2	r3	116	1	1	2	7	1	1	4	48	1	1	2	123	0	0	9.5
v4	r1	v3	r3	118	1	1	1.6	95	1	1	1.4	187	1	1	3	5	0	0	4
v4	r1	v4	r3	27	0	0	1.1	55	1	1	1.5	94	0	1	2	139	0	0	1.9
v4	r1	v5	r3	30	0	1	1.2	11	1	0	1.5	91	1	0	2	168	1	0	2
v4	r1	v1	r4	102	1	1	3	93	1	1	3	141	1	1	4	166	0	0	10
v4	r1	v2	r4	180	1	1	1.5	4	0	0	3	18	0	0	5	173	1	1	9
v4	r1	v3	r4	32	0	0	1.5	73	1	1	2	116	1	1	2	47	0	0	4
v4	r1	v4	r4	51	0	0	1.2	59	1	1	1.3	5	1	1	1.2	35	1	1	2
v4	r1	v5	r4	44	1	0	1.1	183	0	1	1.1	124	0	1	2	128	0	1	1.01

v5	r1	v1	r2	31	0	0	2.5	2	1	1	4	186	1	1	4	181	0	0	10
v5	r1	v2	r2	100	0	0	2	27	1	1	4	152	1	1	4	175	0	0	10
v5	r1	v3	r2	109	1	1	1.5	101	1	1	3	2	1	1	5	22	0	0	4
v5	r1	v4	r2	189	0	0	1.2	33	0	0	1.5	106	1	1	2	89	1	1	1.6
v5	r1	v5	r2	26	0	1	1.1	61	0	0	1.1	99	1	1	1.2	46	1	0	1.3
v5	r1	v1	r3	58	1	1	3.5	147	1	1	4	121	0	0	5	188	0	0	9.6
v5	r1	v2	r3	114	0	0	1.8	116	0	0	4	162	1	1	5	167	0	0	10
v5	r1	v3	r3	74	1	1	2	162	1	1	2.5	97	0	0	3	37	1	1	3
v5	r1	v4	r3	174	1	1	1.1	83	0	0	2	15	0	0	3	108	1	1	4
v5	r1	v5	r3	153	0	1	1.1	87	0	0	1.01	77	0	1	1.5	79	0	0	1.5
v5	r1	v1	r4	88	1	1	3	66	1	1	4	36	1	1	10	112	1	1	10
v5	r1	v2	r4	24	0	0	3	13	0	0	4	159	0	0	5	56	0	0	10
v5	r1	v3	r4	65	1	1	1.6	138	0	0	2.6	58	1	1	4	103	0	0	8
v5	r1	v4	r4	113	1	1	1.2	190	1	1	1.6	142	0	0	3	125	0	0	2
v5	r1	v5	r4	139	1	0	1.1	9	0	0	1.2	82	0	1	2	184	1	1	1.1
v1	r2	v2	r2	75	1	0	1.5	79	0	1	1.3	66	0	1	2.5	162	1	0	2
v1	r2	v3	r2	37	1	0	2	51	1	0	1.8	168	1	0	2.5	16	1	0	8
v1	r2	v4	r2	89	0	1	3	45	0	1	2.5	178	0	1	5	15	0	1	9.8
v1	r2	v5	r2	146	0	1	2.5	176	1	0	3	76	1	0	4	27	0	1	9.9
v1	r2	v1	r3	21	0	0	1.1	86	1	0	1.1	125	0	1	2	55	1	1	1.5
v1	r2	v2	r3	76	0	1	1.2	110	0	1	1.1	111	0	1	3	118	1	0	1.7
v1	r2	v3	r3	151	0	1	1.4	23	0	1	1.2	1	0	1	3	96	1	0	8
v1	r2	v4	r3	16	0	1	2.5	64	1	0	2	37	1	0	8	98	0	1	9.9
v1	r2	v5	r3	34	0	1	2.8	111	0	1	3	136	1	0	6	102	0	1	9.6
v1	r2	v1	r4	144	0	0	1.2	74	1	1	1.5	175	1	0	2.5	84	1	1	1.2
v1	r2	v2	r4	49	1	0	1.4	82	0	0	1.4	61	1	0	2	9	1	0	3
v1	r2	v3	r4	156	1	0	1.5	100	1	0	1.3	102	0	1	3	8	1	0	8
v1	r2	v4	r4	68	1	0	1.8	48	1	0	3	158	1	0	4	114	0	1	9
v1	r2	v5	r4	185	0	1	3	174	0	1	3.5	90	0	1	4	64	1	0	9.5
v2	r2	v3	r2	104	1	0	1.4	5	0	1	1.5	180	1	0	3	73	0	1	4
v2	r2	v4	r2	107	0	1	1.8	188	1	0	1.8	34	1	0	6	24	1	0	3
v2	r2	v5	r2	22	0	1	1.8	139	0	1	3.5	10	0	1	8	122	1	0	7
v2	r2	v1	r3	163	1	1	1.1	25	1	1	1.2	98	1	1	1.5	110	0	0	1.1
v2	r2	v2	r3	7	1	0	1.1	63	1	0	1.1	104	1	1	1.2	2	0	1	1.3
v2	r2	v3	r3	119	0	1	1.4	118	0	1	1.2	128	1	0	3	121	1	0	5
v2	r2	v4	r3	84	0	1	1.4	81	0	1	2.5	137	0	1	5	32	0	1	9.8
v2	r2	v5	r3	40	0	1	2.8	182	0	1	3	181	1	0	7	185	1	0	7.9
v2	r2	v1	r4	124	1	1	1.2	121	0	0	1.1	64	1	1	2	23	1	1	1.1
v2	r2	v2	r4	9	1	1	1.1	137	1	1	1.1	170	1	0	2	169	1	1	2
v2	r2	v3	r4	103	1	0	1.2	181	0	1	1.1	27	0	1	3	81	1	0	5
v2	r2	v4	r4	93	1	0	1.5	72	1	0	2	84	0	1	4	45	0	1	8
v2	r2	v5	r4	110	0	1	1.5	134	0	1	2.5	174	0	1	5	58	0	1	9.8
v3	r2	v4	r2	23	0	1	1.5	140	1	0	2	113	0	1	2	124	0	1	4
v3	r2	v5	r2	98	1	0	1.5	108	0	1	3	143	0	1	4	17	1	0	1.6
v3	r2	v1	r3	136	0	0	1.5	160	0	0	1.4	172	1	1	3	41	0	0	8
v3	r2	v2	r3	86	0	0	1.5	180	0	0	1.2	50	1	1	1.5	145	1	1	6
v3	r2	v3	r3	130	0	0	1.2	135	1	1	1.1	4	1	0	1.2	138	0	0	1.1
v3	r2	v4	r3	59	1	0	1.3	165	1	0	1.7	171	0	1	2	75	0	1	6
v3	r2	v5	r3	64	0	1	1.5	14	1	0	4	169	1	0	4	65	1	0	8.7
v3	r2	v1	r4	126	1	1	1.4	167	1	1	1.4	14	0	0	5	127	0	0	8
v3	r2	v2	r4	172	0	0	1.3	94	0	0	1.8	44	0	0	2.5	164	1	1	1.8
v3	r2	v3	r4	96	0	0	1.1	155	0	0	1.1	74	0	1	1.5	146	1	1	2
v3	r2	v4	r4	179	0	1	1.1	144	0	1	1.2	39	0	1	3	134	1	0	4
v3	r2	v5	r4	46	0	1	1.5	153	0	1	2.5	11	0	1	6	60	0	1	7
v4	r2	v5	r2	29	1	0	1.2	29	1	0	1.4	129	1	0	2	63	1	0	1.7
v4	r2	v1	r3	56	0	0	3	90	0	0	2.5	185	0	0	5	177	0	0	8.6
v4	r2	v2	r3	99	1	1	1.6	65	0	0	3	32	0	0	5	158	0	0	6
v4	r2	v3	r3	11	0	0	1.5	12	0	0	2.5	155	0	0	2.5	12	0	0	3
v4	r2	v4	r3	12	1	0	1.1	175	0	0	1.1	87	0	1	1.5	190	0	0	1.1
v4	r2	v5	r3	169	0	1	1.2	52	0	1	1.4	100	0	1	2	156	1	0	1.5

v4	r2	v1	r4	39	0	0	3.5	v1	1	1	2.5	110	0	0	5	147	1	1	7
v4	r2	v2	r4	10	0	0	2	189	1	1	2.6	176	0	0	4	154	1	1	6
v4	r2	v3	r4	3	0	0	1.6	123	0	0	2	86	1	1	2.5	50	0	0	3
v4	r2	v4	r4	115	0	0	1.1	152	0	0	1.1	184	1	1	1.5	116	0	0	1.1
v4	r2	v5	r4	95	0	1	1.1	28	0	1	2	93	0	1	3	59	0	1	3
v5	r2	v1	r3	175	1	1	2.8	143	1	1	3	189	1	1	6	148	1	1	9.8
v5	r2	v2	r3	38	1	1	2.5	157	1	1	3.5	65	1	1	5	179	0	0	9.6
v5	r2	v3	r3	5	0	0	1.5	30	1	1	3	118	0	0	3	189	1	1	6.8
v5	r2	v4	r3	90	0	0	1.1	68	1	1	1.4	115	1	1	2	143	1	1	2
v5	r2	v5	r3	154	1	1	1.05	44	1	1	1.5	183	1	1	1.5	44	1	1	1.05
v5	r2	v1	r4	168	0	0	2.5	103	1	1	4	132	1	1	6	77	0	0	8
v5	r2	v2	r4	158	0	0	3	129	1	1	2.5	156	1	1	5	14	1	1	10
v5	r2	v3	r4	117	1	1	1.8	16	1	1	2.5	26	0	0	4	33	1	1	6
v5	r2	v4	r4	67	0	0	1.2	54	1	1	1.7	146	1	1	2.5	31	1	1	1.3
v5	r2	v5	r4	162	0	1	1.1	128	1	1	1.1	112	1	1	1.5	163	1	0	1.1
v1	r3	v2	r3	4	0	1	1.3	185	0	1	1.2	29	1	0	2.5	11	0	1	2
v1	r3	v3	r3	57	1	0	2	184	0	1	1.2	63	0	1	3	4	1	0	10
v1	r3	v4	r3	111	0	1	2	34	0	1	2.5	28	0	1	5	140	0	1	6
v1	r3	v5	r3	157	0	1	2.5	102	0	1	4	13	0	1	10	178	0	1	7.8
v1	r3	v1	r4	50	0	0	1.1	173	0	0	1	101	1	1	1.5	109	0	0	2
v1	r3	v2	r4	166	0	1	1.2	67	1	0	1.6	96	0	1	2.5	119	0	0	1.2
v1	r3	v3	r4	105	0	1	1.5	145	1	0	1.4	40	1	0	5	83	1	0	6
v1	r3	v4	r4	133	0	1	2.8	96	1	0	1.8	12	1	0	6	92	0	1	9
v1	r3	v5	r4	33	1	0	2.8	104	1	0	3.5	80	1	0	5	182	1	0	9.9
v2	r3	v3	r3	108	1	0	1.5	8	1	0	1.5	85	0	1	3	115	1	0	4
v2	r3	v4	r3	72	0	1	2.5	71	1	0	2.5	179	0	1	5	113	0	1	9
v2	r3	v5	r3	63	1	0	1.8	122	0	1	2.5	108	0	1	4	21	1	0	8
v2	r3	v1	r4	85	1	1	1.2	115	0	0	1.1	24	1	1	3	19	1	1	2
v2	r3	v2	r4	140	0	0	1.2	99	1	0	1.1	57	0	1	1.2	68	0	0	1.1
v2	r3	v3	r4	47	0	1	1.2	154	1	0	1.2	59	1	0	2	36	1	0	1.7
v2	r3	v4	r4	131	0	1	1.5	10	0	1	2	6	1	0	5	51	1	0	7
v2	r3	v5	r4	43	0	1	2.8	88	0	1	2.5	70	0	1	6	82	0	1	9.9
v3	r3	v4	r3	53	0	1	1.2	21	0	1	1.6	30	1	0	2	111	1	0	2
v3	r3	v5	r3	35	0	1	2	130	1	0	3	42	0	1	4	129	1	0	6
v3	r3	v1	r4	78	1	1	1.8	35	1	1	1.6	138	1	1	4	174	0	0	8.5
v3	r3	v2	r4	125	0	0	1.3	159	1	1	1.2	151	1	1	3	157	1	1	2
v3	r3	v3	r4	147	1	1	1.05	149	0	1	1.1	122	1	0	1.5	180	1	1	1.4
v3	r3	v4	r4	106	1	0	1.2	53	1	0	2	188	0	1	3	62	1	0	6
v3	r3	v5	r4	v1	1	0	1.6	36	0	1	3	144	1	0	3	153	0	1	4
v4	r3	v5	r3	97	1	0	1.2	136	0	1	1.2	19	1	0	3	57	1	0	1.3
v4	r3	v1	r4	54	0	0	2.8	50	1	1	3.5	103	1	1	5	176	1	1	9.5
v4	r3	v2	r4	80	0	0	2.5	15	0	0	3.5	109	0	0	3	104	1	1	8.2
v4	r3	v3	r4	61	1	1	1.3	32	1	1	1.5	161	1	1	4	30	0	0	3
v4	r3	v4	r4	173	0	0	1.1	126	1	1	1.01	135	1	1	1.5	107	0	0	1.8
v4	r3	v5	r4	6	1	0	1.3	91	0	1	2	43	0	1	3	61	1	0	1.1
v5	r3	v1	r4	112	1	1	2.8	117	1	1	4	45	0	0	6	88	1	1	6
v5	r3	v2	r4	81	0	0	3	141	1	1	2.5	160	1	1	6	152	1	1	7
v5	r3	v3	r4	187	0	0	1.8	98	0	0	2.5	21	1	1	7	52	1	1	5
v5	r3	v4	r4	70	1	1	1.1	156	0	0	1.8	147	1	1	2	13	1	1	1.4
v5	r3	v5	r4	183	1	1	1.05	151	0	0	1.01	164	0	1	1.5	137	1	1	1.01
v1	r4	v2	r4	18	0	1	1.4	57	0	1	1.4	140	0	1	3	38	1	0	2
v1	r4	v3	r4	132	0	1	1.5	1v1	1	0	1.2	23	0	1	5	94	0	1	6
v1	r4	v4	r4	181	1	0	2.5	75	0	1	2.5	119	0	1	5	85	0	1	8.9
v1	r4	v5	r4	94	0	1	3.2	161	0	1	3	72	1	0	6	91	1	0	9.9
v2	r4	v3	r4	82	0	1	1.2	19	1	0	1.2	182	1	0	4	v1	1	0	4
v2	r4	v4	r4	36	0	1	2.4	62	0	1	1.3	148	1	0	3	42	0	1	8
v2	r4	v5	r4	129	1	0	3.8	119	0	1	2	134	0	1	6	78	1	0	9
v3	r4	v4	r4	28	1	0	1.3	69	1	0	1.6	123	1	0	2	66	1	0	6
v3	r4	v5	r4	45	0	1	1.6	70	1	0	2.5	31	1	0	3	159	1	0	8
v4	r4	v5	r4	17	1	0	1.4	92	1	0	1.8	52	0	1	3	183	1	0	1.3

Appendix 5-A: MATLAB code to generate surface height map (section 5.1)

function ht = generate_ht2 (n, DDir, AVariance, beta, delta, nOrder, Flower, Fupper)

```
% Input
%  n = size of surface,  beta = roll of factor
% DDir = Dominant Angular Frequency
% AVariance = Angular Variance
% delta = RMS_roughness
% nOrder = Butterworth band-pass filter order
% Flower = lower cut-off frequency of band-pass filter
% Fupper = upper cut-off frequency of band-pass filter
%  Output, ht = surface height map
%%%%%%%%%%%%%%%%%%%%%%%%%%%%%%%%%%%%%%%%%
nq=n/2;  V=-repmat((-nq:nq-1)', 1,2*nq);  U=repmat((-nq:nq-1), 2*nq,1);
f=sqrt(U.*U+V.*V);  %Generating Frequencies

mag1 = fbeta_noise_spectrum (n, beta); % dfreq_noise spectrum
mag2 = angular_distribution (n, DDir, AVariance); %dtheta_angular distribution
magspec = mag1.*mag2;  magspec = ifftshift (magspec);
magspec(1,1) = 0;       % making the magnitude of zero frequency equal to zero
PhaseSpec = random_phase (n);
%Converting to Cartesian Co-ordinate
[x y] = pol2cart(Phase_Spec, magspec); FSpectrum = x + i*y;
FSpectrum = fftshift(FSpectrum);
% Forcing conjugate symmetry in magnitude spectrum
for col1=(n/2+1):n
    for row1=2:n
        u1=col1-(n/2+1); v1=(n/2+1)-row1;
        if (~((u1==0) && (v1==0)))
            FSpectrum (n+2-row1,n+2-col1)=conj(FSpectrum (row1,col1));
        end
    end
End
%Butter-worth Band-pass filter
Bw = Fupper - Flower;   Fo = sqrt(Fupper*Flower);
t = (1/Bw).*((f.^2-Fo.^2)./f);
bpf = 1./(1+t.^(2*nOrder)); bpf = sqrt(bpf);
FSpectrum = FSpectrum.*bpf;
%Removing lower frequencies to have naturalistic appearance
FSpectrum(f<=8) = 0;
% Adjusting RMS roughness
FSpectrum = ifftshift(FSpectrum); ht_temp = real (ifft2(FSpectrum));
deltan = std2(ht_temp); % calculating deltan to normalize the spectrum
FSpectrum = FSpectrum.* (delta./deltan);
ht = real(ifft2(FSpectrum));
```

Appendix 5-B: Order of surface pairs and observer' responses for the experiment in section 5.2.1

Separate effect of random phase spectrum (section 5.2.1)

- Screen 1 is on the left side of the observer and Screen 2 is on the right side of the observer
- Surface 1 = *comparison* surface and Surface 2 = *standard* surface
- rp1, rp2, rp3, rp4 and rp5 indicates different random phase spectra
- If Swap Info = 0 then Surface 1 and 2 is presented on Screen 1 and 2 respectively
- If Swap Info = 1 then Surface 1 and 2 is presented on Screen 2 and 1 respectively
- Order Number shows when the pair is presented during the experiment
- If Selected Surface = 0 then surface on screen 1 is selected as more directional and ratio is equal to perceived directionality of surface on screen 1 to perceived directionality of surface on screen 2
- If Selected Surface = 1 then surface on screen 2 is selected as more directional and ratio is equal to perceived directionality of surface on screen 2 to perceived directionality of surface on screen 1

Surface Pair			**Observer 1**				**Observer 2**				**Observer 3**			
***comparison* surface**		***standard* surface**												
Random Phase	**Central radial frequency**	**Central radial frequency**	**Order Number**	**Swap Info**	**Selected Surface**	**Ratio**	**Order Number**	**Swap Info**	**Selected Surface**	**Ratio**	**Order Number**	**Swap Info**	**Selected Surface**	**Ratio**
rp1	1.88	3.28	88	0	0	1.3	62	0	0	4	63	1	1	4
rp1	1.88	3.28	36	1	1	1.3	50	0	0	3	24	0	0	3
rp1	1.88	3.28	1	0	0	1.3	55	0	0	4	11	1	1	3
rp2	1.88	3.28	48	1	1	1.2	84	1	1	3	33	0	0	4
rp2	1.88	3.28	80	1	1	1.2	6	0	0	3	73	1	1	3
rp2	1.88	3.28	49	1	1	1.2	14	0	0	2.8	31	0	0	3
rp3	1.88	3.28	63	1	1	1.2	28	0	0	2.6	55	0	0	4
rp3	1.88	3.28	42	0	0	1.2	61	1	1	4.6	34	1	1	3
rp3	1.88	3.28	59	1	1	1.2	71	1	1	3	49	1	1	3
rp4	1.88	3.28	30	0	0	1.2	24	0	0	4	36	0	0	4
rp4	1.88	3.28	16	0	0	1.2	30	1	1	2	66	1	1	2
rp4	1.88	3.28	65	1	1	1.2	67	0	0	2.5	1	1	1	3
rp5	1.88	3.28	9	1	1	1.2	41	1	1	2.9	88	0	0	4
rp5	1.88	3.28	39	0	0	1.2	31	1	1	2.2	50	0	0	3
rp5	1.88	3.28	40	1	1	1.2	59	1	1	4	40	0	0	3
rp1	1.88	4.69	73	0	1	1.5	34	1	0	4	32	0	1	5
rp1	1.88	4.69	47	0	1	1.5	54	1	0	5	85	0	1	5
rp1	1.88	4.69	11	0	1	1.5	90	0	1	5.5	9	1	0	5
rp2	1.88	4.69	52	1	0	1.2	68	0	1	3.6	82	0	1	4
rp2	1.88	4.69	83	0	1	1.5	20	1	0	4	28	1	0	5
rp2	1.88	4.69	4	0	1	1.5	40	0	1	3.5	5	1	0	3
rp3	1.88	4.69	78	0	1	1.6	64	1	0	4	39	0	1	4
rp3	1.88	4.69	87	0	1	1.3	51	1	0	4	74	1	0	5
rp3	1.88	4.69	76	0	1	1.3	9	0	1	4.5	12	0	1	4
rp4	1.88	4.69	79	0	1	1.8	37	0	1	4	4	0	1	4
rp4	1.88	4.69	45	1	0	1.3	58	1	0	3.5	45	1	0	5
rp4	1.88	4.69	46	1	0	1.3	80	0	1	5	54	1	0	5
rp5	1.88	4.69	55	0	1	1.3	86	1	0	4.5	19	1	0	5
rp5	1.88	4.69	27	1	0	1.3	65	1	0	4	38	0	1	5
rp5	1.88	4.69	61	0	1	1.8	3	1	0	4.5	37	0	1	4
rp1	1.88	6.09	58	0	0	1.5	2	0	0	4	52	0	0	7
rp1	1.88	6.09	28	1	1	2.5	26	0	0	7.2	56	0	0	8

rp1	1.88	6.09	85	0	0	1.8	78	1	1	8.2	58	0	0	8
rp2	1.88	6.09	6	0	0	1.6	44	0	0	5	79	0	0	7
rp2	1.88	6.09	12	1	1	2	49	0	0	5	76	1	1	7
rp2	1.88	6.09	19	0	0	2	33	0	0	3.5	62	0	0	8
rp3	1.88	6.09	90	1	1	1.8	25	0	0	7	47	0	0	6
rp3	1.88	6.09	53	1	1	1.3	88	0	0	5	46	0	0	6
rp3	1.88	6.09	41	1	1	2.5	56	1	1	6	30	0	0	6
rp4	1.88	6.09	62	0	0	1.8	76	1	1	8	14	0	0	6
rp4	1.88	6.09	37	1	1	2.8	75	1	1	7	69	0	0	8
rp4	1.88	6.09	14	1	1	2.5	7	0	0	5	25	1	1	6
rp5	1.88	6.09	67	1	1	1.8	12	0	0	4	3	0	0	5
rp5	1.88	6.09	69	1	1	2	8	1	1	6	13	0	0	5
rp5	1.88	6.09	7	1	1	2.2	17	1	1	6	29	1	1	6
rp1	4.69	1.88	5	1	1	1.8	69	0	0	4	65	0	0	5
rp1	4.69	1.88	13	1	1	1.8	60	1	1	4.5	26	1	1	5
rp1	4.69	1.88	82	1	1	1.6	70	0	0	5	90	1	1	5
rp2	4.69	1.88	18	1	1	1.5	72	0	0	6	51	1	1	5
rp2	4.69	1.88	75	1	1	1.5	22	0	0	4	87	1	1	6
rp2	4.69	1.88	21	0	0	1.5	89	1	1	5	21	1	1	6
rp3	4.69	1.88	81	0	0	1.5	73	0	0	6	10	0	0	4
rp3	4.69	1.88	34	1	1	1.6	82	0	0	4.5	68	1	1	6
rp3	4.69	1.88	24	0	0	1.8	43	0	0	4.5	22	1	1	5
rp4	4.69	1.88	64	0	0	1.3	74	0	0	6.2	75	0	0	6
rp4	4.69	1.88	66	0	0	1.3	16	0	0	4	61	1	1	5
rp4	4.69	1.88	77	1	1	1.8	13	1	1	4.5	81	1	1	5
rp5	4.69	1.88	22	1	1	1.8	83	0	0	4.2	8	1	1	5
rp5	4.69	1.88	38	1	1	2	77	0	0	6	70	1	1	6
rp5	4.69	1.88	50	0	0	1.3	19	0	0	4.2	67	1	1	5
rp1	4.69	3.28	44	0	0	1.2	48	1	1	2	42	1	1	3
rp1	4.69	3.28	15	0	0	1.2	29	0	0	2.5	35	0	0	3
rp1	4.69	3.28	71	1	1	1.2	63	1	1	3	57	0	0	4
rp2	4.69	3.28	68	0	0	1.3	52	0	0	2.5	84	0	0	3
rp2	4.69	3.28	51	0	0	1.3	36	0	0	3.8	77	0	0	3
rp2	4.69	3.28	57	0	0	1.2	39	1	1	3	20	1	1	3
rp3	4.69	3.28	2	0	0	1.2	53	0	0	3	16	0	0	3
rp3	4.69	3.28	20	1	1	1.2	21	0	0	2.5	17	1	1	3
rp3	4.69	3.28	29	1	1	1.2	46	1	1	3	60	1	1	3
rp4	4.69	3.28	17	0	0	1.2	27	1	1	4	44	0	0	2
rp4	4.69	3.28	35	0	0	1.3	66	1	1	4	2	0	0	3
rp4	4.69	3.28	43	1	1	1.2	18	1	1	4	59	0	0	3
rp5	4.69	3.28	89	0	0	1.2	81	1	1	4.2	41	0	0	3
rp5	4.69	3.28	60	1	1	1.3	87	1	1	3	83	0	0	3
rp5	4.69	3.28	23	1	1	1.3	10	0	0	3	86	1	1	4
rp1	4.69	6.09	86	0	0	1.2	1	0	0	2	48	1	1	3
rp1	4.69	6.09	33	1	1	1.2	38	0	0	2	53	1	1	3
rp1	4.69	6.09	54	1	1	1.3	47	0	0	1.8	18	0	0	3
rp2	4.69	6.09	25	0	0	1.2	15	1	1	3.5	23	0	0	2
rp2	4.69	6.09	84	1	1	1.2	57	1	1	3.5	7	1	1	2
rp2	4.69	6.09	10	0	0	1.2	23	1	1	3.5	6	0	0	2
rp3	4.69	6.09	70	1	1	1.2	32	0	0	2.5	15	1	1	2
rp3	4.69	6.09	32	1	1	1.2	11	1	1	3	72	1	1	3
rp3	4.69	6.09	3	1	1	1.2	45	0	0	1.8	78	1	1	2
rp4	4.69	6.09	31	1	1	1.3	5	0	0	2.5	71	0	0	4
rp4	4.69	6.09	72	1	1	1.3	79	1	1	4	43	0	0	3
rp4	4.69	6.09	74	0	0	1.2	85	0	0	4	27	0	0	3
rp5	4.69	6.09	56	0	0	1.2	42	1	1	4	80	1	1	2
rp5	4.69	6.09	8	1	1	1.2	35	1	1	3	64	0	0	2
rp5	4.69	6.09	26	0	0	1.2	4	1	1	2.8	89	1	1	3

Separate effect of random phase (section 5.2.1)										
Surface Pair			Observer 4				Observer 5			
comparison surface		standard surface								
Random Phase	Central radial frequency	Central radial frequency	Order Number	Swap Info	Selected Surface	Ratio	Order Number	Swap Info	Selected Surface	Ratio
rp1	1.88	3.28	63	1	1	1.4	53	1	1	4
rp1	1.88	3.28	24	0	0	1.5	4	1	1	6
rp1	1.88	3.28	11	1	1	1.4	14	0	0	3.5
rp2	1.88	3.28	33	0	0	1.2	57	1	1	4
rp2	1.88	3.28	73	1	1	1.3	78	0	0	5
rp2	1.88	3.28	31	0	0	1.3	90	1	1	4
rp3	1.88	3.28	55	0	0	1.2	2	0	0	4
rp3	1.88	3.28	34	1	1	1.3	38	0	0	3
rp3	1.88	3.28	49	1	1	1.4	77	0	0	4
rp4	1.88	3.28	36	0	0	1.4	73	0	0	2.5
rp4	1.88	3.28	66	1	1	1.3	88	0	0	3.5
rp4	1.88	3.28	1	1	1	1.5	15	1	1	6
rp5	1.88	3.28	88	0	0	1.3	71	1	1	2
rp5	1.88	3.28	50	0	0	1.4	48	1	1	5
rp5	1.88	3.28	40	0	0	1.3	11	0	0	3
rp1	1.88	4.69	32	0	1	1.4	5	0	1	7
rp1	1.88	4.69	85	0	1	1.5	52	0	1	8.5
rp1	1.88	4.69	9	1	0	1.4	59	0	1	7
rp2	1.88	4.69	82	0	1	1.4	39	1	0	6
rp2	1.88	4.69	28	1	0	1.4	50	0	1	8
rp2	1.88	4.69	5	1	0	1.7	60	0	1	7
rp3	1.88	4.69	39	0	1	1.7	33	1	0	8.5
rp3	1.88	4.69	74	1	0	1.3	24	0	1	8.9
rp3	1.88	4.69	12	0	1	1.7	69	1	0	8
rp4	1.88	4.69	4	0	1	1.5	56	0	1	7
rp4	1.88	4.69	45	1	0	1.8	80	1	0	5
rp4	1.88	4.69	54	1	0	1.4	51	0	1	8
rp5	1.88	4.69	19	1	0	1.6	6	1	0	8
rp5	1.88	4.69	38	0	1	1.6	68	1	0	6
rp5	1.88	4.69	37	0	1	1.6	54	1	0	6
rp1	1.88	6.09	52	0	0	1.7	25	0	0	10
rp1	1.88	6.09	56	0	0	1.6	83	1	1	10
rp1	1.88	6.09	58	0	0	1.6	43	1	1	10
rp2	1.88	6.09	79	0	0	1.5	18	1	1	10
rp2	1.88	6.09	76	1	1	1.6	41	1	1	10
rp2	1.88	6.09	62	0	0	1.5	58	1	1	10
rp3	1.88	6.09	47	0	0	1.9	89	1	1	10
rp3	1.88	6.09	46	0	0	1.7	19	0	0	10
rp3	1.88	6.09	30	0	0	1.6	31	0	0	10
rp4	1.88	6.09	14	0	0	1.7	46	1	1	10
rp4	1.88	6.09	69	0	0	1.7	45	1	1	10
rp4	1.88	6.09	25	1	1	1.7	64	0	0	9.5
rp5	1.88	6.09	3	0	0	2	74	1	1	8.9
rp5	1.88	6.09	13	0	0	1.8	85	0	0	10
rp5	1.88	6.09	29	1	1	1.6	37	1	1	9
rp1	4.69	1.88	65	0	0	1.5	67	1	1	8
rp1	4.69	1.88	26	1	1	1.6	82	1	1	8
rp1	4.69	1.88	90	1	1	1.5	13	1	1	8
rp2	4.69	1.88	51	1	1	1.5	72	0	0	3
rp2	4.69	1.88	87	1	1	1.4	75	0	0	9
rp2	4.69	1.88	21	1	1	1.7	84	1	1	9

rp3	4.69	1.88	10	0	0	1.6	47	0	0	9
rp3	4.69	1.88	68	1	1	1.5	12	0	0	7
rp3	4.69	1.88	22	1	1	1.8	61	1	1	8
rp4	4.69	1.88	75	0	0	1.3	66	1	1	6.8
rp4	4.69	1.88	61	1	1	1.4	27	1	1	8
rp4	4.69	1.88	81	1	1	1.5	62	1	1	8
rp5	4.69	1.88	8	1	1	1.7	28	0	0	7.5
rp5	4.69	1.88	70	1	1	1.5	49	0	0	7.8
rp5	4.69	1.88	67	1	1	1.5	81	1	1	7
rp1	4.69	3.28	42	1	1	1.3	30	1	1	4
rp1	4.69	3.28	35	0	0	1.3	7	0	0	4
rp1	4.69	3.28	57	0	0	1.3	35	0	0	5
rp2	4.69	3.28	84	0	0	1.2	79	0	0	3
rp2	4.69	3.28	77	0	0	1.25	34	0	0	6
rp2	4.69	3.28	20	1	1	1.4	36	0	0	4
rp3	4.69	3.28	16	0	0	1.3	32	1	1	4
rp3	4.69	3.28	17	1	1	1.3	16	0	0	5
rp3	4.69	3.28	60	1	1	1.2	65	1	1	3.5
rp4	4.69	3.28	44	0	0	1.3	10	1	1	2.4
rp4	4.69	3.28	2	0	0	1.5	87	1	1	2.2
rp4	4.69	3.28	59	0	0	1.2	26	0	0	3.4
rp5	4.69	3.28	41	0	0	1.2	63	1	1	4
rp5	4.69	3.28	83	0	0	1.15	22	0	0	3
rp5	4.69	3.28	86	1	1	1.2	29	1	1	6
rp1	4.69	6.09	48	1	1	1.2	8	1	1	3
rp1	4.69	6.09	53	1	1	1.2	44	0	0	3
rp1	4.69	6.09	18	0	0	1.4	76	1	1	4.3
rp2	4.69	6.09	23	0	0	1.3	9	1	1	3
rp2	4.69	6.09	7	1	1	1.4	86	1	1	4
rp2	4.69	6.09	6	0	0	1.4	55	0	1	1.5
rp3	4.69	6.09	15	1	1	1.3	70	0	0	2.5
rp3	4.69	6.09	72	1	1	1.2	3	0	0	3
rp3	4.69	6.09	78	1	1	1.2	17	0	0	3
rp4	4.69	6.09	71	0	0	1.15	21	1	1	1.6
rp4	4.69	6.09	43	0	0	1.25	42	1	1	5
rp4	4.69	6.09	27	0	0	1.3	20	0	0	1.5
rp5	4.69	6.09	80	1	1	1.2	23	1	1	3
rp5	4.69	6.09	64	0	0	1.2	1	0	0	1.2
rp5	4.69	6.09	89	1	1	1.3	40	1	1	3.5

Appendix 5-C: Order of surface pair and observers' responses for the experiment in section 5.2.2.1

Separate effect of central radial frequency at low bandwidth (section 5.2.2.1)
• Screen 1 is on the left side of the observer and Screen 2 is on the right side of the observer • If Swap Info = 0 then Surface 1 and 2 is presented on Screen 1 and 2 respectively • If Swap Info = 1 then Surface 1 and 2 is presented on Screen 2 and 1 respectively • Order Number shows when the pair is presented during the experiment • If Selected Surface = 0 then surface on screen 1 is selected as more directional and ratio is equal to perceived directionality of surface on screen 1 to perceived directionality of surface on screen 2 • If Selected Surface = 1 then surface on screen 2 is selected as more directional and ratio is equal to

perceived directionality of surface on screen 2 to perceived directionality of surface on screen 1													
Surface Pair		**Observer 1**				**Observer 2**				**Observer 3**			
Surface 1	**Surface 2**												
Central radial frequency	**Central radial frequency**	**Order Number**	**Swap Info**	**Selected Surface**	**Ratio**	**Order Number**	**Swap Info**	**Selected Surface**	**Ratio**	**Order Number**	**Swap Info**	**Selected Surface**	**Ratio**
1.88	2.58	74	0	0	1.2	29	1	1	1.4	32	0	0	2.5
1.88	3.28	85	0	0	1.3	2	1	1	1.4	92	0	0	2
1.88	3.98	113	0	0	1.3	62	0	0	2	120	0	0	3
1.88	4.69	49	0	0	1.5	55	0	0	2.3	20	1	1	4
1.88	5.39	31	0	0	1.3	48	0	0	2.8	25	0	0	4
1.88	6.09	15	1	1	1.2	19	1	1	3	65	0	0	3
1.88	6.80	34	1	1	1.5	107	1	1	3.5	54	0	0	4
1.88	7.50	75	0	0	2	112	0	0	3	31	1	1	5
1.88	8.20	92	1	1	2	82	1	1	4	108	1	1	4
1.88	8.91	19	1	1	2	106	1	1	4	41	0	0	6
1.88	9.61	53	0	0	2	3	0	0	3.5	104	1	1	4
1.88	10.31	84	0	0	3	119	0	0	4.5	37	0	0	8
1.88	11.02	4	1	1	2	30	1	1	4	11	1	1	7
1.88	11.72	23	0	0	1.1	35	0	0	4	1	1	1	6
1.88	12.42	79	1	1	3	17	1	1	4.5	91	1	1	5
2.58	3.28	40	1	1	1.2	23	0	0	1.2	29	0	0	2
2.58	3.98	58	0	0	1.1	28	0	0	1.5	39	1	1	3
2.58	4.69	71	1	1	1.2	108	0	0	2	30	0	0	3
2.58	5.39	119	0	0	1.3	26	1	1	2	40	0	0	4
2.58	6.09	60	0	0	1.3	24	1	1	2	42	0	0	4
2.58	6.80	83	0	0	2	31	1	1	3.8	116	1	1	3
2.58	7.50	50	1	1	1.5	87	1	1	3.5	71	0	0	3
2.58	8.20	66	1	1	1.8	40	1	1	2.6	73	0	0	5
2.58	8.91	63	1	1	2	51	0	0	2.8	111	0	0	5
2.58	9.61	80	1	1	2.5	43	0	0	3.5	59	0	0	6
2.58	10.31	112	1	1	1.8	25	0	0	3.5	43	0	0	5
2.58	11.02	78	1	1	2	57	1	1	4	62	1	1	5
2.58	11.72	7	1	1	2	71	1	1	4	110	0	0	6
2.58	12.42	61	0	0	2	64	0	0	4.2	52	0	0	8
3.28	3.98	54	0	0	1.2	20	1	1	1.6	13	0	0	3
3.28	4.69	73	1	1	1.2	27	0	0	1.8	44	0	0	3
3.28	5.39	11	0	0	1.2	89	0	0	2.4	53	0	0	3
3.28	6.09	106	1	1	1.2	95	0	0	2.5	107	1	1	2
3.28	6.80	111	0	0	1.6	33	0	0	2	47	0	0	3
3.28	7.50	87	1	1	1.5	9	1	1	2.8	99	0	0	2.5
3.28	8.20	62	0	0	2.5	77	1	1	2.5	48	0	0	5
3.28	8.91	18	0	0	2	101	1	1	3	63	0	0	4
3.28	9.61	21	1	1	1.3	11	1	1	3	14	0	0	5
3.28	10.31	56	1	1	2	12	0	0	3.5	19	1	1	5
3.28	11.02	69	1	1	2.5	86	0	0	4	93	1	1	4
3.28	11.72	46	1	1	1.5	97	0	0	3.5	3	1	1	5
3.28	12.42	110	1	1	1.6	90	0	0	3.8	78	0	0	6
3.98	4.69	82	0	0	1.2	76	1	1	1.3	83	0	0	1.5
3.98	5.39	43	1	1	1.1	14	1	1	1.5	58	1	1	1.5
3.98	6.09	68	1	1	1.2	36	0	0	1.8	26	1	1	2
3.98	6.80	91	0	0	1.3	75	1	1	1.8	46	1	1	2
3.98	7.50	107	0	0	1.3	54	1	1	2	45	0	0	3
3.98	8.20	6	1	1	1.2	8	1	1	2	94	1	1	3
3.98	8.91	51	0	0	1.3	81	1	1	3	82	0	0	3
3.98	9.61	35	1	1	1.5	50	1	1	2.2	76	0	0	3

3.98	10.31	76	0	0	1.2	18	0	0	4.2	86	1	1	3.5
3.98	11.02	29	1	1	1.3	115	1	1	2.9	72	0	0	4
3.98	11.72	59	0	0	2	66	0	0	3.5	18	0	0	4
3.98	12.42	101	0	0	1.1	117	0	0	3	64	1	1	3
4.69	5.39	13	1	1	1.1	53	1	1	1.5	69	1	0	1.5
4.69	6.09	65	1	1	1.2	79	0	0	1.5	67	1	1	2
4.69	6.80	9	0	0	1.3	52	1	1	1.5	85	1	1	2
4.69	7.50	95	0	0	1.3	37	0	0	2.2	33	1	1	3
4.69	8.20	12	1	1	1.2	39	0	0	2.3	89	1	1	2
4.69	8.91	32	1	1	1.2	38	1	1	2.5	90	0	0	2.5
4.69	9.61	52	0	0	1.2	1	1	1	2.8	22	1	1	3
4.69	10.31	117	1	1	1.2	72	1	1	3.5	6	1	1	4
4.69	11.02	118	1	1	1.3	42	0	0	2.9	9	0	0	5
4.69	11.72	103	1	1	1.2	103	0	0	3.7	23	0	0	5
4.69	12.42	57	1	1	2	105	1	1	3.2	84	1	1	4
5.39	6.09	39	0	1	1.1	41	0	0	1.1	98	0	0	1.5
5.39	6.80	2	0	0	1.2	111	0	0	1.5	106	1	1	1.5
5.39	7.50	38	1	1	1.2	73	1	1	2	16	1	1	2
5.39	8.20	28	1	1	1.2	109	1	1	2	114	0	0	3
5.39	8.91	97	1	1	1.2	4	1	1	2	79	0	0	4
5.39	9.61	70	1	1	1.3	88	0	0	3	36	1	1	2.5
5.39	10.31	108	0	0	1.6	120	0	0	3.2	118	0	0	4
5.39	11.02	86	0	0	1.3	16	1	1	2.1	51	1	1	3
5.39	11.72	33	0	0	1.2	102	0	0	3.5	57	1	1	4
5.39	12.42	5	1	1	1.2	100	1	1	2.5	87	1	1	4
6.09	6.80	45	0	0	1.1	34	0	0	1.1	81	0	0	1.5
6.09	7.50	64	0	0	1.2	116	0	0	1.5	4	0	0	2
6.09	8.20	41	1	1	1.1	49	0	0	2	24	0	0	3
6.09	8.91	114	0	0	1.2	67	0	0	2.5	70	1	1	2
6.09	9.61	25	0	0	1.1	45	0	0	2.6	60	1	1	2
6.09	10.31	1	0	0	1.3	84	1	1	2.3	38	1	1	3
6.09	11.02	26	1	1	1.1	118	0	0	2.5	95	0	0	3
6.09	11.72	109	1	1	1.2	63	1	1	2.2	10	1	1	3
6.09	12.42	16	0	1	1.1	94	0	0	2.5	34	0	0	3
6.80	7.50	67	0	0	1.2	78	1	1	1.3	112	0	0	3
6.80	8.20	24	0	0	1.1	70	1	1	1.5	21	1	1	2
6.80	8.91	37	1	1	1.1	65	1	1	2.8	119	0	0	2.5
6.80	9.61	100	0	0	1.1	5	1	1	2.5	105	1	1	2.5
6.80	10.31	30	0	0	1.2	114	0	0	2	66	1	1	2
6.80	11.02	44	1	1	1.2	58	0	0	2.8	77	1	1	3
6.80	11.72	36	0	0	1.1	15	0	0	2	7	1	1	4
6.80	12.42	104	1	1	1.1	13	0	0	3	28	0	0	4
7.50	8.20	8	1	1	1.1	59	0	0	1.8	115	1	0	2
7.50	8.91	105	1	1	1.1	83	0	0	1.3	50	1	0	1.5
7.50	9.61	14	0	1	1.1	60	1	1	1.5	56	1	1	2
7.50	10.31	77	1	1	1.1	104	1	1	2.1	35	0	0	3
7.50	11.02	72	1	1	1.2	22	0	0	1.5	102	0	0	2.5
7.50	11.72	3	1	1	1.1	68	0	0	2	88	0	0	3
7.50	12.42	55	0	0	1.1	96	1	1	2.8	103	1	1	2
8.20	8.91	27	0	1	1.1	113	1	1	1.3	8	1	1	2
8.20	9.61	88	1	1	1.1	69	0	0	1.3	74	1	1	1.5
8.20	10.31	98	0	0	1.2	44	1	1	1.3	101	0	0	2
8.20	11.02	94	1	1	1.1	7	0	0	1.5	100	0	0	2
8.20	11.72	89	1	1	1.1	85	1	1	2	17	0	0	3
8.20	12.42	102	0	1	1.1	56	0	0	1.5	27	1	1	3
8.91	9.61	20	0	0	1.1	61	0	0	1.05	2	0	0	2
8.91	10.31	115	1	1	1.1	46	0	0	1.4	15	0	0	1.4
8.91	11.02	120	1	1	1.1	80	1	1	1.2	109	1	1	2
8.91	11.72	81	0	0	1.1	110	0	0	1.2	80	0	0	3
8.91	12.42	42	1	1	1.1	93	1	1	1.4	75	1	1	2

9.61	10.31	10	1	1	1.1	91	1	1	1.5	49	0	0	2
9.61	11.02	93	1	1	1.1	47	1	1	1.3	113	0	0	2
9.61	11.72	90	0	0	1.1	74	0	0	1.1	55	1	1	2
9.61	12.42	48	0	0	1.2	92	0	1	1.1	12	0	0	3
10.31	11.02	96	0	0	1.1	98	0	0	1.2	97	0	0	2
10.31	11.72	47	1	1	1.1	6	0	1	1.2	117	0	0	2
10.31	12.42	22	0	1	1.1	99	1	1	1.2	96	1	1	2
11.02	11.72	116	1	1	1.1	10	1	1	1.5	5	0	0	2
11.02	12.42	99	0	1	1.1	21	1	1	1.2	68	0	0	2
11.72	12.42	17	1	1	1.1	32	0	1	1.2	61	0	0	1.5
		Observer 4				**Observer 5**				**Observer 6**			
1.88	2.58	92	0	0	1.2	32	0	0	2	92	0	0	1.3
1.88	3.28	88	0	0	1.4	92	0	0	4	88	0	0	1.2
1.88	3.98	36	1	1	1.5	120	0	0	3	36	1	1	2
1.88	4.69	1	0	0	1.7	20	1	1	6	1	0	0	3
1.88	5.39	48	1	1	1.8	25	0	0	9	48	1	1	3
1.88	6.09	100	1	1	1.5	65	0	0	7.8	100	1	1	3
1.88	6.80	80	0	0	1.6	54	0	0	8	80	0	0	4
1.88	7.50	49	1	1	2	31	1	1	8	49	1	1	4
1.88	8.20	63	0	0	1.6	108	1	1	9.5	63	0	0	4
1.88	8.91	115	0	0	1.5	41	0	0	9	115	0	0	5
1.88	9.61	42	1	1	1.6	104	1	1	10	42	1	1	6
1.88	10.31	59	1	1	1.5	37	0	0	10	59	1	1	5
1.88	11.02	30	1	1	2	11	1	1	10	30	1	1	4
1.88	11.72	16	0	0	2.1	1	1	1	10	16	0	0	7
1.88	12.42	104	0	0	2	91	1	1	10	104	0	0	5
2.58	3.28	65	1	1	1.1	29	0	0	1.3	65	1	1	2
2.58	3.98	9	1	1	1.3	39	1	1	3	9	1	1	2
2.58	4.69	39	0	0	1.3	30	0	0	2.5	39	0	0	2
2.58	5.39	101	0	0	1.3	40	0	0	2.5	101	0	0	2
2.58	6.09	40	1	1	1.4	42	0	0	7	40	1	1	3
2.58	6.80	113	0	0	1.6	116	1	1	4	113	0	0	3
2.58	7.50	5	1	1	1.6	71	0	0	7	5	1	1	3
2.58	8.20	13	1	1	1.6	73	0	0	6.6	13	1	1	4
2.58	8.91	107	1	1	1.4	111	0	0	9	107	1	1	5
2.58	9.61	82	0	0	1.4	59	0	0	9.9	82	0	0	3
2.58	10.31	18	0	0	1.7	43	0	0	8	18	0	0	8
2.58	11.02	75	0	0	1.8	62	1	1	10	75	0	0	10
2.58	11.72	109	1	1	1.8	110	0	0	9	109	1	1	5
2.58	12.42	21	0	0	1.8	52	0	0	9.5	21	0	0	8
3.28	3.98	81	1	1	1.1	13	0	0	2	81	1	1	1.5
3.28	4.69	34	0	0	1.3	44	0	0	2.5	34	0	0	1.5
3.28	5.39	24	1	1	1.3	53	0	0	2	24	1	1	4
3.28	6.09	64	0	0	1.3	107	1	1	3.5	64	0	0	3
3.28	6.80	111	1	1	1.2	47	0	0	6	111	1	1	3
3.28	7.50	66	1	1	1.2	99	0	0	5	66	1	1	3
3.28	8.20	114	1	1	1.4	48	0	0	6.5	114	1	1	3
3.28	8.91	77	1	1	1.4	63	0	0	5	77	1	1	3
3.28	9.61	22	0	0	1.7	14	0	0	8	22	0	0	5
3.28	10.31	38	1	1	1.6	19	1	1	7	38	1	1	4
3.28	11.02	50	0	0	1.4	93	1	1	8	50	0	0	4
3.28	11.72	97	0	0	1.4	3	1	1	9	97	0	0	4
3.28	12.42	58	1	1	1.4	78	0	0	8.9	58	1	1	4
3.98	4.69	105	1	1	1.1	83	0	1	1.2	105	1	0	1.2
3.98	5.39	28	0	0	1.3	58	1	1	2	28	0	0	1.5
3.98	6.09	85	1	1	1.2	26	1	1	4	85	1	1	1.5
3.98	6.80	6	1	1	1.3	46	1	1	3.5	6	1	1	2
3.98	7.50	12	1	1	1.3	45	0	0	4.3	12	1	1	3
3.98	8.20	19	1	1	1.5	94	1	1	7	19	1	1	4

3.98	8.91	90	1	1	1.2	82	0	0	4	90	1	1	1.5
3.98	9.61	53	1	1	1.3	76	0	0	4.5	53	1	1	3
3.98	10.31	41	0	0	1.3	86	1	1	6	41	0	0	4
3.98	11.02	62	0	0	1.4	72	0	0	5	62	0	0	3
3.98	11.72	94	1	1	1.3	18	0	0	6	94	1	1	4
3.98	12.42	37	0	0	1.6	64	1	1	8.5	37	0	0	4
4.69	5.39	119	0	1	1.1	69	1	1	2	119	0	0	3
4.69	6.09	14	0	0	1.2	67	1	1	2.8	14	0	0	1.5
4.69	6.80	67	1	1	1.2	85	1	1	3	67	1	1	1.1
4.69	7.50	69	1	1	1.1	33	1	1	3	69	1	1	1.5
4.69	8.20	7	1	1	1.2	89	1	1	2.8	7	1	1	3
4.69	8.91	95	0	0	1.2	90	0	0	4	95	0	0	3
4.69	9.61	93	0	0	1.3	22	1	1	5	93	0	0	3
4.69	10.31	44	1	1	1.3	6	1	1	7	44	1	1	3
4.69	11.02	99	0	0	1.3	9	0	0	6	99	0	0	2
4.69	11.72	103	0	0	1.3	23	0	0	8	103	0	0	3
4.69	12.42	15	1	1	1.6	84	1	1	3.5	15	1	1	4
5.39	6.09	71	0	1	1.2	98	0	0	2	71	0	1	1.1
5.39	6.80	68	1	1	1.15	106	1	1	2	68	1	1	1.5
5.39	7.50	51	1	1	1.2	16	1	1	3	51	1	1	2
5.39	8.20	57	1	1	1.2	114	0	0	2.3	57	1	1	1.5
5.39	8.91	118	0	0	1.3	79	0	0	3.5	118	0	0	4
5.39	9.61	2	1	1	1.3	36	1	1	3	2	1	1	4
5.39	10.31	116	1	1	1.4	118	0	0	3.5	116	1	1	3
5.39	11.02	20	1	1	1.3	51	1	1	5	20	1	1	4
5.39	11.72	29	1	1	1.6	57	1	1	3.5	29	1	1	1
5.39	12.42	17	1	1	1.3	87	1	1	4	17	1	1	4
6.09	6.80	35	0	1	1.1	81	0	0	1.2	35	0	1	1.1
6.09	7.50	43	0	0	1.1	4	0	0	2	43	0	0	2
6.09	8.20	89	1	1	1.2	24	0	0	4	89	1	1	1.5
6.09	8.91	106	0	0	1.1	70	1	1	3.6	106	0	0	1.5
6.09	9.61	60	0	0	1.3	60	1	1	3.5	60	0	0	2
6.09	10.31	23	0	0	1.5	38	1	1	4	23	0	0	4
6.09	11.02	73	0	0	1.3	95	0	0	2.6	73	0	0	2
6.09	11.72	47	1	1	1.3	10	1	1	6	47	1	1	2
6.09	12.42	120	1	1	1.3	34	0	0	2	120	1	1	4
6.80	7.50	11	0	0	1.1	112	0	0	1.2	11	0	1	1.5
6.80	8.20	52	0	0	1.1	21	1	1	2	52	0	0	1.5
6.80	8.91	83	1	1	1.3	119	0	0	2.8	83	1	1	1.5
6.80	9.61	4	0	0	1.2	105	1	1	1.5	4	0	0	3
6.80	10.31	78	1	1	1.4	66	1	1	3.5	78	1	1	3
6.80	11.02	87	1	1	1.1	77	1	1	3.8	87	1	1	1.5
6.80	11.72	76	0	0	1.5	7	1	1	3	76	0	0	2
6.80	12.42	117	0	0	1.3	28	0	0	1.3	117	0	0	3
7.50	8.20	79	0	0	1.2	115	1	0	1.2	79	0	0	1.2
7.50	8.91	45	1	1	1.2	50	1	1	1.2	45	1	1	1.5
7.50	9.61	46	0	0	1.2	56	1	1	1.5	46	0	0	1.5
7.50	10.31	55	0	0	1.2	35	0	0	1.5	55	0	0	1.5
7.50	11.02	102	0	0	1.2	102	0	0	2	102	0	0	2
7.50	11.72	27	0	0	1.5	88	0	0	3	27	0	0	2
7.50	12.42	108	0	0	1.3	103	1	1	1.5	108	0	0	2
8.20	8.91	112	0	1	1.1	8	1	1	2	112	0	1	1.5
8.20	9.61	96	1	1	1.1	74	1	1	1.2	96	1	1	2
8.20	10.31	61	1	1	1.2	101	0	0	1.2	61	1	1	1.1
8.20	11.02	86	0	0	1.1	100	0	0	2	86	0	0	1.5
8.20	11.72	98	1	1	1.2	17	0	0	2	98	1	1	1.5
8.20	12.42	33	0	0	1.3	27	1	1	1.5	33	0	0	3
8.91	9.61	54	0	0	1.1	2	0	0	1.2	54	0	1	1.5
8.91	10.31	25	1	1	1.1	15	0	0	1.5	25	1	1	1.5
8.91	11.02	84	1	1	1.2	109	1	1	1.2	84	1	1	1.1

8.91	11.72	10	0	0	1.2	80	0	0	1.2	10	0	0	2
8.91	12.42	70	1	1	1.2	75	1	1	2.5	70	1	1	1.5
9.61	10.31	32	0	0	1.1	49	0	0	1.2	32	0	1	1.1
9.61	11.02	3	1	1	1.1	113	0	0	1.2	3	1	1	1.1
9.61	11.72	31	1	1	1.2	55	1	1	1.2	31	1	1	1.1
9.61	12.42	91	1	1	1.2	12	0	0	2	91	1	1	1.1
10.31	11.02	110	1	1	1.1	97	0	1	1.2	110	1	1	1.5
10.31	11.72	72	1	1	1.1	117	0	0	1.2	72	1	1	1.1
10.31	12.42	74	0	0	1.1	96	1	0	1.2	74	0	0	1.5
11.02	11.72	56	0	0	1.1	5	0	1	1.2	56	0	1	1.1
11.02	12.42	8	1	1	1.1	68	0	1	1.2	8	1	1	1.1
11.72	12.42	26	0	0	1.1	61	0	1	1.2	26	0	1	1.1

Appendix 5-D: Order of surface pairs and observers' responses for the experiment in section 5.2.2.2

Separate effect of central radial frequency at higher bandwidth (section 5.2.2.2)

- Screen 1 is on the left side of the observer and Screen 2 is on the right side of the observer
- If Swap Info = 0 then Surface 1 and 2 is presented on Screen 1 and 2 respectively
- If Swap Info = 1 then Surface 1 and 2 is presented on Screen 2 and 1 respectively
- Order Number shows when the pair is presented during the experiment
- If Selected Surface = 0 then surface on screen 1 is selected as more directional and ratio is equal to perceived directionality of surface on screen 1 to perceived directionality of surface on screen 2
- If Selected Surface = 1 then surface on screen 2 is selected as more directional and ratio is equal to perceived directionality of surface on screen 2 to perceived directionality of surface on screen 1

Bandwidth	Surface Pair		Observer 1				Observer 2				Observer 3			
	Surface 1	Surface 2												
	Central radial frequency	Central radial frequency	Order Number	Swap Info	Selected Surface	Ratio	Order Number	Swap Info	Selected Surface	Ratio	Order Number	Swap Info	Selected Surface	Ratio
0.94	2.81	4.22	34	0	0	5.2	11	1	1	4	12	1	1	1.4
	2.81	4.22	52	1	1	3.4	30	1	1	3	27	0	0	2
	2.81	4.22	41	0	0	3	28	1	1	3	8	1	1	1.6
	2.81	5.63	38	0	0	8	26	1	1	5	51	0	0	1.5
	2.81	5.63	24	1	1	10	46	1	1	4	1	0	0	2
	2.81	5.63	47	0	0	7	50	0	0	6	31	0	0	2.5
	2.81	7.03	15	0	0	10	35	1	1	8	17	1	1	1.1
	2.81	7.03	53	1	1	11	54	0	0	8	4	1	1	2
	2.81	7.03	30	0	0	11	6	0	0	7	10	0	0	2.5
	4.22	5.63	44	1	1	4	13	1	1	2.5	7	1	1	1.5
	4.22	5.63	14	1	1	5	10	0	0	3	23	1	1	1.2
	4.22	5.63	2	0	0	5	38	0	0	3	37	0	0	1.3
	4.22	7.03	17	0	0	9.5	42	1	1	4	47	0	0	1.3
	4.22	7.03	22	1	1	7	49	1	1	5	3	1	1	1.7
	4.22	7.03	42	1	1	8	52	1	1	3	15	0	1	1.1
	5.63	7.03	6	1	1	5.5	17	1	1	3	14	0	0	1.1
	5.63	7.03	31	0	0	4.2	20	0	0	2	42	0	0	1.3
	5.63	7.03	48	0	0	5	37	1	1	3	19	1	1	1.1
1.8	2.81	4.22	9	0	0	6	16	1	1	2	22	0	0	2

	2.81	4.22	43	0	0	2.2	2	0	0	2.5	44	0	0	2
	2.81	4.22	7	1	1	5	24	1	1	4	36	1	1	1.6
	2.81	5.63	10	1	1	7	25	1	1	5	5	1	1	1.6
	2.81	5.63	45	0	0	8	44	0	0	5	11	0	0	2.4
	2.81	5.63	29	1	1	6	40	1	1	5	45	1	1	2.5
	2.81	7.03	25	1	1	10	43	1	1	6	32	0	0	2.5
	2.81	7.03	39	1	1	8	31	0	0	7	52	0	0	1.8
	2.81	7.03	3	0	0	9	15	0	0	7	13	0	0	2.2
	4.22	5.63	26	0	0	7	4	0	0	3	54	1	1	1.5
	4.22	5.63	13	1	1	6	33	0	0	3	20	0	0	1.4
	4.22	5.63	28	0	0	4	8	0	0	3	33	1	1	1.8
	4.22	7.03	18	0	0	8.9	3	0	0	4	18	1	1	1.7
	4.22	7.03	37	0	0	7	36	1	1	4	41	1	1	1.5
	4.22	7.03	16	1	1	8	29	0	0	6	50	0	0	1.5
	5.63	7.03	40	0	0	4	32	1	1	3	16	1	1	1.1
	5.63	7.03	1	0	0	3	47	0	0	3	35	1	1	1.1
	5.63	7.03	8	0	0	3.5	18	0	0	3	29	1	1	1.3
2.81	2.81	4.22	20	1	1	4.2	39	0	0	4	48	1	1	1.6
	2.81	4.22	33	0	0	8.2	45	0	0	4	24	0	0	1.8
	2.81	4.22	5	0	0	4	34	0	0	4	39	1	1	1.7
	2.81	5.63	32	0	0	10	9	0	0	6	34	1	1	2
	2.81	5.63	4	1	1	8	5	1	1	5	30	0	0	2.3
	2.81	5.63	51	0	0	8.5	51	0	0	6	2	0	0	1.8
	2.81	7.03	49	0	0	9.9	19	0	0	7	53	0	0	1.8
	2.81	7.03	11	1	1	9	14	1	1	8	9	0	0	2.3
	2.81	7.03	19	1	1	10.5	41	0	0	8	46	1	1	2.5
	4.22	5.63	35	0	0	5	12	0	0	4	26	0	0	1.1
	4.22	5.63	23	1	1	6	23	1	1	2	28	0	0	1.5
	4.22	5.63	50	0	0	3.2	53	0	0	3	43	1	1	1.8
	4.22	7.03	21	1	1	5	1	1	1	3	49	1	1	2
	4.22	7.03	36	0	0	4	21	0	0	4	21	1	1	1.8
	4.22	7.03	46	0	0	6.5	7	0	0	4	25	0	0	1.2
	5.63	7.03	54	0	0	3	48	0	0	3	38	1	1	1.1
	5.63	7.03	27	1	1	5.8	27	0	0	3	6	0	0	1.2
	5.63	7.03	12	0	0	2.5	22	1	1	3	40	1	1	1.1
			Observer 4				**Observer 5**				**Observer 6**			
0.94	2.81	4.22	40	0	0	2	2	1	1	1.3	20	1	1	2
	2.81	4.22	26	0	0	2.6	9	1	1	1.4	8	0	0	3
	2.81	4.22	17	0	0	2	50	0	0	1.5	45	1	1	2
	2.81	5.63	36	0	0	3	14	1	1	2	38	1	1	3
	2.81	5.63	2	0	0	5	22	0	0	2.3	1	0	0	3
	2.81	5.63	54	0	0	4	26	1	1	2.5	40	1	1	6
	2.81	7.03	42	1	1	3.5	17	0	0	3	48	0	0	6
	2.81	7.03	16	1	1	3	27	1	1	3	13	1	1	8
	2.81	7.03	27	0	0	5.5	29	0	0	3.5	17	0	0	8
	4.22	5.63	30	1	1	3	21	1	1	1.5	30	0	0	2
	4.22	5.63	18	1	1	1.5	7	0	0	1.3	34	1	1	2
	4.22	5.63	23	0	0	3.5	53	0	0	1.3	44	1	1	2
	4.22	7.03	3	1	1	2.8	43	1	1	1.8	14	1	1	8
	4.22	7.03	5	1	1	3	6	0	0	2.4	53	0	0	6
	4.22	7.03	9	0	0	5.5	18	0	0	2.8	25	1	1	3
	5.63	7.03	20	1	1	2.8	10	1	1	1.3	50	0	0	2
	5.63	7.03	6	0	0	3.5	15	0	0	1.4	23	1	1	2
	5.63	7.03	29	0	0	2.6	39	1	1	1.3	27	0	1	2
1.88	2.81	4.22	19	1	1	2.5	23	1	1	1.5	29	0	0	3
	2.81	4.22	15	0	0	1.6	16	1	1	1.4	9	0	0	3
	2.81	4.22	47	0	0	2	49	0	0	1.6	2	0	0	5
	2.81	5.63	8	1	1	5	4	1	1	2.5	22	1	1	4
	2.81	5.63	31	0	0	3.6	31	0	0	2.5	41	1	1	4

	2.81	5.63	34	0	0	4	36	1	1	2.8	24	1	1	3
	2.81	7.03	48	0	0	4	48	1	1	3	15	1	1	8
	2.81	7.03	14	0	0	5	40	1	1	2.3	26	1	1	2
	2.81	7.03	25	1	1	5	8	1	1	2.8	52	0	0	5
	4.22	5.63	53	0	0	3	45	1	1	1.3	46	1	1	3
	4.22	5.63	7	0	0	4	28	1	1	2.2	37	1	1	2
	4.22	5.63	50	0	0	2	47	0	0	1.2	19	1	1	4
	4.22	7.03	39	0	0	4	3	0	0	2.5	18	0	0	8
	4.22	7.03	22	0	0	4	13	1	1	1.3	36	1	1	5
	4.22	7.03	45	1	1	3	42	1	1	2.3	43	0	0	2
	5.63	7.03	4	0	0	3	11	1	1	1.2	39	0	0	3
	5.63	7.03	38	0	0	2.4	32	0	0	1.3	42	0	0	2
	5.63	7.03	46	0	0	1.5	34	0	0	1.2	3	0	0	3
2.81	2.81	4.22	52	0	0	1.8	33	1	1	1.4	31	1	1	2
	2.81	4.22	44	0	0	2.8	41	1	1	1.5	10	1	1	2
	2.81	4.22	13	1	1	2	20	0	0	1.8	12	1	1	3
	2.81	5.63	10	1	1	3.2	30	0	0	3	32	0	0	2
	2.81	5.63	12	1	1	4.5	5	1	1	2	28	1	1	3
	2.81	5.63	43	0	0	3	52	1	1	2.8	54	1	1	4
	2.81	7.03	33	0	0	5	25	1	1	3	33	0	0	6
	2.81	7.03	24	0	0	6	37	0	0	3	51	0	0	6
	2.81	7.03	11	1	1	3.5	44	0	0	3.5	21	1	1	6
	4.22	5.63	51	0	0	1.5	46	1	0	1.2	16	0	0	5
	4.22	5.63	37	0	0	3.2	12	1	1	1.3	5	1	1	6
	4.22	5.63	41	1	0	1.5	54	1	1	1.2	47	1	1	3
	4.22	7.03	21	0	0	5	24	1	1	1.8	11	0	0	6
	4.22	7.03	49	0	0	3	35	1	1	2	6	1	1	6
	4.22	7.03	35	0	0	6	51	1	1	1.3	4	1	1	6
	5.63	7.03	28	1	1	3	38	0	0	1.3	35	0	0	6
	5.63	7.03	1	0	0	4	1	1	1	1.3	7	1	1	3
	5.63	7.03	32	0	0	3.5	19	1	1	1.3	49	1	1	3

Appendix 6-A: Order of surfaces and observers' responses for the experiment in section 6.2

Effects of (one-way and two-way) four parameters together in a single experiment (section – 6.2)																					
All *comparison* surfaces were paired with the *standard* surface and observers provided the ratio between *comparison* and *standard* surfaces																					
Values of parameters of *comparison* surfaces				**Observer 1**		**Observer 2**		**Observer 3**		**Observer 4**		**Observer 5**		**Observer 6**		**Observer 7**		**Observer 8**		**Observer 9**	
?â²â	?áâ	?âᵦâ	?á	**Order No.**	**Ratio**	**Order No.**	**Ratio**	**Order No.**	**Ratio**	**Order No.**	**Ratio**	**Order No.**	**Ratio**	**Order No.**	**Ratio**	**Order No.**	**Ratio**	**Order No.**	**Ratio**	**Order No.**	**Ratio**
20.00	3.75	2.34	0.01	81	7.6	143	7.6	16	14	12	7	88	1.9	86	9	53	2.4	90	8.75	28	4
20.00	3.75	2.34	0.01	92	7.6	9	9.5	6	21.5	84	6.5	7	2.1	30	6	26	3.5	72	8.5	4	3
20.00	3.75	2.34	0.02	120	8.2	56	6.2	105	20	44	7.5	72	3.5	70	7	86	3.6	16	10	79	7
20.00	3.75	2.34	0.02	128	9.4	37	8	122	20	99	8	19	3.5	37	7	13	3.5	44	12	80	7
51.48	3.75	2.34	0.01	56	4.8	47	5.1	127	18	80	5.5	58	1.7	78	5	5	2	123	10.25	57	3
51.48	3.75	2.34	0.01	6	4.5	28	7	66	17	62	7	31	1.3	106	6	79	3.4	18	9	75	3.5
51.48	3.75	2.34	0.02	4	7.8	26	7.5	42	17	27	6.5	110	2.9	145	6	18	3	116	8.5	51	4
51.48	3.75	2.34	0.02	2	9.6	52	4.5	81	15	45	6	49	3.6	26	5	72	3.5	34	11	24	6
132.50	3.75	2.34	0.01	38	1.4	87	3.1	128	9	35	5	118	1.6	94	3	146	2.4	140	11	95	1.8
132.50	3.75	2.34	0.01	22	1.4	35	3.5	61	16	135	5.5	136	1.6	108	6	43	2.2	61	8.75	17	2
132.50	3.75	2.34	0.02	41	7.1	103	3	4	12	9	4	68	2.6	52	4	131	2.5	121	11.25	32	3
132.50	3.75	2.34	0.02	82	5.2	55	2.2	75	8	18	3.5	20	3.4	129	5	136	3	132	11.25	146	3
341.04	3.75	2.34	0.01	99	1.1	7	3	107	5	1	2	98	1.9	76	2	24	1.4	126	11	70	1.2
341.04	3.75	2.34	0.01	26	1.1	17	2.6	55	5.5	123	4.5	103	1.6	21	2.5	106	1.7	95	11	26	1.5
341.04	3.75	2.34	0.02	60	1.2	14	2.8	49	14	10	3	104	1.8	14	3	130	1.9	91	11.5	133	1.4
341.04	3.75	2.34	0.02	91	1.8	111	2.2	2	8	73	4	107	2	144	5	27	1.9	102	12	65	1.8
132.50	1.88	2.34	0.01	11	1.2	101	1.1	17	3.5	16	3	34	1	97	2	143	1.1	52	6	141	1.2
132.50	1.88	2.34	0.01	30	1.1	77	1.3	114	4	70	4	3	1.5	16	3	54	2.2	115	8	53	1.5
132.50	1.88	2.34	0.02	86	1.4	136	1.7	47	11	103	5	86	1.6	83	3	19	2	139	10.5	1	2
132.50	1.88	2.34	0.02	47	2.8	16	3.2	126	12	61	6	74	1.9	91	4	11	2.5	96	9.75	71	2.2
132.50	5.63	2.34	0.01	65	2	60	4.5	82	7	89	5	48	1.7	146	6	59	2	58	8.5	41	2
132.50	5.63	2.34	0.01	78	5	49	5	29	17	76	6	142	2	47	5	10	3	10	9	45	3
132.50	5.63	2.34	0.02	126	7.4	68	3.3	148	21.5	51	6	123	3.5	110	5	41	1.9	29	10.5	40	4
132.50	5.63	2.34	0.02	67	7.5	39	4.8	39	21	82	6	59	5	136	9	47	3.3	68	11	20	6
132.50	7.50	2.34	0.01	90	7.2	119	6.2	63	22	63	6	132	1.7	36	6	52	2.2	92	10.5	6	1.5
132.50	7.50	2.34	0.01	57	7.5	142	4.9	132	21	79	6	121	4	60	7	132	3.2	24	9.5	10	3
132.50	7.50	2.34	0.02	73	7.6	127	4.4	111	22	40	6	62	6	81	9	50	2.4	147	10	81	3.5
132.50	7.50	2.34	0.02	70	7.6	75	5.1	133	22	95	6.5	111	4.5	93	10	48	2.5	8	9.5	123	5
51.48	3.75	0.94	0.01	87	1.6	4	2.5	86	10	37	6.5	124	1.9	5	4	55	2.5	120	10.75	38	1.8
51.48	3.75	0.94	0.01	119	6.4	129	3	96	7	139	6.5	122	2.6	143	5	111	2.8	39	10.5	91	4
51.48	3.75	0.94	0.02	85	7.2	45	4.9	85	16	52	6.5	21	3.2	29	4	64	3.5	1	8	54	4
51.48	3.75	0.94	0.02	14	7.8	82	4.4	37	17	109	7	91	3.5	128	7	75	3.4	25	9	129	7
51.48	3.75	3.75	0.01	68	7.2	139	4.5	116	14	71	6	115	1.8	132	8	67	2.3	129	10.25	89	3
51.48	3.75	3.75	0.01	61	7.6	109	3.7	101	18.5	119	6	25	2	8	6	49	2.5	7	7.5	121	3
51.48	3.75	3.75	0.02	80	7.5	116	5.3	67	18	38	7.5	50	2.8	77	6	81	3	87	9	116	4
51.48	3.75	3.75	0.02	139	7.4	137	4.4	12	19	57	6	128	2.8	84	5	95	3.2	85	9.5	140	5
51.48	3.75	5.16	0.01	134	7.2	130	4.1	84	20	145	6	116	1.5	123	8	88	2	11	8.5	122	2.2
51.48	3.75	5.16	0.01	133	7.6	43	6.8	7	19	28	7	129	1.8	57	8	20	2.3	110	9.5	124	3.5
51.48	3.75	5.16	0.02	18	7.6	145	5.1	5	22	146	7	55	2.8	69	5	44	2.6	15	9.5	18	4

51.48	3.75	5.16	0.02	113	8.2	108	4	11	17	143	7	117	2.2	31	8	7	3	131	9.75	119	4
20.00	1.88	2.34	0.01	118	7.6	6	9	146	20.5	46	4	92	2.1	18	9	51	2.3	99	9.25	76	6
20.00	5.63	2.34	0.01	94	9.6	125	7.5	62	22	128	9	35	3	141	9	113	3	83	9.5	52	5
20.00	7.50	2.34	0.01	69	9.6	40	9.6	138	22	75	9	145	3	116	10	119	3.5	133	10.75	55	7
51.48	1.88	2.34	0.01	25	7.2	86	3	35	15	87	5	37	1.3	49	7	57	2.5	43	10.5	68	2.5
51.48	5.63	2.34	0.01	146	7.7	140	4.7	60	20	58	6.5	29	3.4	134	7	33	3.5	26	9.5	134	2.5
51.48	7.50	2.34	0.01	28	7.8	59	7	104	21	43	6.5	1	6.5	22	6	101	3	31	10	34	3.5
341.04	1.88	2.34	0.01	63	1.2	12	1.8	53	2.5	86	4	41	1.2	142	2	9	1.4	74	9	137	1.2
341.04	5.63	2.34	0.01	76	1.6	13	4	9	9	54	3	137	1.8	50	3	125	1.5	118	11.5	147	3.5
341.04	7.50	2.34	0.01	53	1.6	126	4.5	95	10	60	3.5	52	4	111	6	35	1.7	66	10.5	12	2.3
20.00	3.75	0.94	0.01	117	7.5	102	4.6	64	10	138	7	38	1.8	126	8	36	3	81	8.5	39	5
20.00	3.75	3.75	0.01	145	7.8	133	8	143	21.5	114	8	24	2.2	28	7	110	2	146	10.25	87	4
20.00	3.75	5.16	0.01	89	7.6	44	7.2	100	20	14	7.5	147	1.8	20	10	121	2.5	148	10.5	142	4
132.50	3.75	0.94	0.01	50	3.2	96	3.7	22	7	13	4	61	2	105	5	114	2.8	69	9	117	2.5
132.50	3.75	3.75	0.01	75	4.8	15	4.5	45	8	17	4	106	1.5	64	5	148	2.9	104	8.75	101	1.9
132.50	3.75	5.16	0.01	98	6	113	2.1	14	8	141	4.5	51	1.6	68	4	100	1.9	12	9	126	2.2
341.04	3.75	0.94	0.01	131	1.3	94	3.4	124	11	91	4.5	5	2.5	56	3	38	1.7	45	10.5	8	1.3
341.04	3.75	3.75	0.01	114	1.1	115	1.8	103	2.5	132	4	47	1.5	4	3	2	1.5	122	11	143	1.3
341.04	3.75	5.16	0.01	13	1.4	74	1.2	131	4	94	5	4	1.8	34	2	60	1.4	114	10.5	5	1.2
82.58	1.88	0.47	0.01	58	1.5	85	1.6	102	4	72	5	120	1.2	92	3	99	1.8	48	8.5	62	1.5
82.58	1.88	1.41	0.01	42	2	24	4.2	23	5.8	68	5.5	79	1.2	119	4	78	2.8	86	8	110	1.8
82.58	1.88	2.34	0.01	83	6.5	70	1.9	99	12	116	6.5	135	1.4	130	4	32	2.8	17	8.5	48	1.3
82.58	1.88	3.28	0.01	36	5	58	2.6	58	20	142	5.5	114	1.9	115	8	105	2.3	97	9	77	3.5
82.58	3.75	0.47	0.01	1	1.5	48	4.8	41	16	130	6.5	40	2.3	55	5	74	3.1	38	10.5	92	3.5
82.58	3.75	1.41	0.01	66	5	50	4	44	14	108	6.5	63	1.5	124	6	42	2.4	47	10	64	2
82.58	3.75	2.34	0.01	108	6.8	11	4	144	17.5	65	6.5	139	2.2	63	6	139	2.8	13	9	107	3.2
82.58	3.75	3.28	0.01	20	6.2	23	4.5	77	17	4	6	101	1.9	66	6	90	2.6	33	10.5	67	2.2
82.58	5.63	0.47	0.01	72	7	120	4.8	38	19	59	7.5	66	3.2	85	4	141	3.1	65	8.75	33	4
82.58	5.63	1.41	0.01	16	7.5	64	4.3	71	7	23	6	87	3.1	131	6	77	3	84	9.5	50	2
82.58	5.63	2.34	0.01	102	7.2	123	4.4	20	19	77	6	80	3.2	27	4	1	2.5	21	9.5	69	3
82.58	5.63	3.28	0.01	19	6.2	38	5	68	19	34	7.5	46	3.1	118	6	17	3	124	10.5	135	3
82.58	7.50	0.47	0.01	39	7.6	57	5	83	22	8	7	89	4	103	9	103	3.3	23	9.5	56	3
82.58	7.50	1.41	0.01	130	7.6	110	4.6	110	21	131	8	95	4	104	9	76	3.5	60	9.5	144	3
82.58	7.50	2.34	0.01	59	7.6	63	5.5	25	20	83	7	16	6	65	7	61	3	103	10.75	128	4
82.58	7.50	3.28	0.01	124	7.6	104	6.2	57	22	117	6	130	3	40	8	63	3.3	111	10.25	36	2.5
20.00	3.75	2.34	0.01	140	7.4	121	7.6	142	22	104	7.5	140	1.5	9	8	62	2.5	32	10	125	4
20.00	3.75	2.34	0.01	144	8.5	29	8.5	89	12	124	7	90	3	140	8	147	3	19	9.5	99	4
20.00	3.75	2.34	0.02	7	9.6	32	7.8	69	21	134	7.5	112	2.9	54	8	25	3.5	78	8.75	132	6
20.00	3.75	2.34	0.02	125	9.5	88	7.5	98	20	140	7	22	3	147	8	96	3.2	113	10.5	25	7
51.48	3.75	2.34	0.01	110	7	144	6.5	78	15	50	5.5	133	1.3	38	5	66	2.5	94	8.5	100	3
51.48	3.75	2.34	0.01	64	7.2	107	3.8	123	15	85	7	57	2.1	82	5	127	3	125	10	16	3.5
51.48	3.75	2.34	0.02	46	7	92	4.6	139	18	126	6	85	2	58	6	129	3.2	141	10.5	85	3.2
51.48	3.75	2.34	0.02	9	7.6	81	3.9	109	16	92	6	109	3	72	6	65	3.5	93	10.5	3	4
132.50	3.75	2.34	0.01	45	1.2	79	2.4	125	9	144	5	11	1.2	44	3	6	1.5	143	9.75	118	1.1
132.50	3.75	2.34	0.01	35	1.8	106	2.6	94	5.5	105	6	39	2.1	148	6	145	2.7	63	8.5	98	2.5
132.50	3.75	2.34	0.02	104	6.8	80	3.1	134	15	90	5.5	82	2.1	79	4	135	2.9	2	8.5	61	1.5
132.50	3.75	2.34	0.02	77	5.6	18	3.5	43	20	42	6	32	2.9	39	4	97	3.1	27	10.5	60	2.5
341.04	3.75	2.34	0.01	115	1.1	5	2	108	3	29	2.5	71	1.3	139	2	133	1.4	145	11	145	1.1
341.04	3.75	2.34	0.01	93	1.1	20	3.5	93	3.5	19	2.5	17	1.8	137	3	28	1.6	112	11.02	102	1.2
341.04	3.75	2.34	0.02	40	1.6	8	3.5	54	6	30	2	96	2.6	89	3	112	1.9	98	11.5	103	1.3
341.04	3.75	2.34	0.02	12	1.6	84	2.7	113	20	11	3.5	23	3.6	112	4	144	1.7	49	11	49	1.2
132.50	1.88	2.34	0.01	52	1.2	112	1.1	115	3.2	66	4	54	1.01	35	2	40	1.2	76	8	9	1.2
132.50	1.88	2.34	0.01	71	1.3	148	1.2	79	6	69	6	77	1.4	7	4	126	2	55	7	109	2
132.50	1.88	2.34	0.02	5	1.3	42	2	51	13	21	3.5	105	1.4	122	4	124	2.6	6	6.5	22	3
132.50	1.88	2.34	0.02	48	3	76	1.8	92	8	133	5	36	2	43	4	58	3	119	11	86	1.8
132.50	5.63	2.34	0.01	121	1.8	78	2.9	3	11	31	4.5	93	2.3	10	6	140	2.7	100	10.25	44	1.5
132.50	5.63	2.34	0.01	32	5.6	72	4.1	59	21	47	5	126	1.8	42	5	8	2.8	105	10.5	113	3.5
132.50	5.63	2.34	0.02	8	7.2	105	2.1	147	21.5	137	6.5	70	4.6	80	5	73	3.3	71	9.5	2	3
132.50	5.63	2.34	0.02	33	7.6	114	3.5	33	19	64	6.5	78	4	138	7	91	2.8	35	11.5	74	4.5
132.50	7.50	2.34	0.01	116	7.2	66	4.9	65	22	113	7	97	2.7	59	6	69	2.7	5	6	43	2.1

132.50	7.50	2.34	0.01	142	7.5	25	6.5	40	22	122	6	102	3	107	8	108	3.2	75	10	115	2.5
132.50	7.50	2.34	0.02	23	7.6	89	6.8	46	22	53	7	127	3.4	88	9	142	3.3	22	10	136	4
132.50	7.50	2.34	0.02	74	7.7	132	4.9	36	20	88	5	143	4	90	8	15	3.5	51	11.5	11	4
51.48	3.75	0.94	0.01	31	2.5	51	3	130	15	127	7	84	1.3	99	3	87	2.7	67	8.5	138	1.5
51.48	3.75	0.94	0.01	44	5.5	95	4.7	56	14	107	7.5	15	2	33	3	118	3	36	9.5	47	3
51.48	3.75	0.94	0.02	107	6.5	61	3	72	6.5	101	7.5	27	2.5	19	4	23	3.5	3	9	114	4
51.48	3.75	0.94	0.02	143	7.4	54	2.8	91	13	148	7.5	10	4	87	6	102	3.4	54	8.5	93	5
51.48	3.75	3.75	0.01	37	4.8	138	3.8	137	20	6	6	30	1.1	135	8	16	2	137	9.5	106	3
51.48	3.75	3.75	0.01	51	6.2	117	4.5	28	14	20	7.5	76	1.8	6	6	94	2.8	101	9.75	84	3.5
51.48	3.75	3.75	0.02	43	7.6	33	6.8	24	14	32	6	8	2.3	74	8	89	3.2	138	10.25	82	5
51.48	3.75	3.75	0.02	147	7.6	21	5	52	19.5	120	7	131	2.2	11	7	29	3.5	14	9.5	13	6
51.48	3.75	5.16	0.01	111	6.8	46	6.2	48	22	3	6	12	1.1	2	7	138	2	37	9.5	90	2.5
51.48	3.75	5.16	0.01	15	7.6	93	4.3	30	22	56	5.5	100	1.9	73	8	82	2.3	136	9.75	14	5
51.48	3.75	5.16	0.02	112	7	141	2.6	15	12	67	6.5	94	2.6	62	8	3	2.5	73	8.5	139	3
51.48	3.75	5.16	0.02	135	7.6	22	4.8	50	18	15	6	45	2.1	120	6	39	3.5	50	10	83	5
20.00	1.88	2.34	0.01	148	7.5	27	8	90	19.5	96	7	9	1.5	12	10	37	2.5	64	7.5	88	3.5
20.00	5.63	2.34	0.01	132	9.8	97	7.6	1	20	111	8.5	148	2.5	51	8	83	3.5	142	10.25	15	7
20.00	7.50	2.34	0.01	21	9.8	36	9.5	119	22	5	9	99	3	61	9	107	3.5	80	9.25	29	6
51.48	1.88	2.34	0.01	138	6.5	124	3.1	21	8	106	7	18	1.2	1	6	84	2.7	59	7.5	97	1.8
51.48	5.63	2.34	0.01	84	7.5	134	7.8	32	17	2	7	42	3.4	101	6	128	3.2	127	11	94	3.5
51.48	7.50	2.34	0.01	79	7.6	1	10	10	16	55	6.5	44	5.5	71	7	46	3.5	117	9.5	66	4
341.04	1.88	2.34	0.01	10	1.1	3	1.5	136	3	26	3.5	6	1.1	98	1.5	92	1.2	9	6.5	7	1.1
341.04	5.63	2.34	0.01	62	1.4	69	3.6	112	18	36	3	75	2.6	53	4	120	1.9	79	10.5	105	2.5
341.04	7.50	2.34	0.01	34	2.6	34	4.6	76	22	102	3	14	2.2	117	8	137	1.9	41	11.5	35	2
20.00	3.75	0.94	0.01	95	9	131	6	88	15	74	7	2	3	23	5	93	3	28	9.5	148	4
20.00	3.75	3.75	0.01	105	8.2	41	7.8	74	20	125	7.5	65	2.2	113	10	68	3	134	10.25	108	4
20.00	3.75	5.16	0.01	101	8	99	7.9	87	21	41	8	125	1.8	102	10	31	3	56	7.5	30	5
132.50	3.75	0.94	0.01	96	1.3	100	3.8	19	9	48	5	56	2.4	95	2.5	109	2.8	130	11	104	2
132.50	3.75	3.75	0.01	109	5	147	2.6	129	11	81	5.5	43	1.6	32	4	80	2.4	109	9.5	78	1.8
132.50	3.75	5.16	0.01	129	2	31	4	34	9	118	6.5	113	2.2	25	6	85	1.9	88	8	21	3
341.04	3.75	0.94	0.01	27	1.3	53	2.6	70	4	98	6	141	1.7	100	2	70	1.9	30	9	120	1.5
341.04	3.75	3.75	0.01	122	1.2	90	2.1	8	7	129	2.5	144	1.2	96	2	104	1.7	42	10.5	46	1.2
341.04	3.75	5.16	0.01	127	1.2	19	1.8	13	4	100	5	146	1.1	109	4	134	1.6	40	11	31	1.6
82.58	1.88	0.47	0.01	88	1.2	71	1.5	121	4	115	6	83	1.1	121	3	21	1.8	107	7.5	42	1.9
82.58	1.88	1.41	0.01	49	2	10	2.8	117	8	24	4	69	1.2	46	2.5	117	2.5	128	9.75	112	2
82.58	1.88	2.34	0.01	141	2.2	83	1.5	118	7	22	3	73	1.5	17	3	115	2.4	77	8.25	63	1.8
82.58	1.88	3.28	0.01	17	7.2	67	2.5	106	19	39	5	13	1.4	13	9	71	2.6	70	7.5	58	2.5
82.58	3.75	0.47	0.01	137	4.5	91	3	120	9	25	6.5	53	2.6	48	3	4	2.5	4	7.5	130	2.9
82.58	3.75	1.41	0.01	136	4.5	62	2.8	18	14	121	6.5	81	2	125	6	98	3	46	10	37	2
82.58	3.75	2.34	0.01	100	6.5	146	4.8	27	9	93	6.5	67	2.4	127	6	116	2.7	20	8.5	19	4
82.58	3.75	3.28	0.01	97	6.8	128	3.6	31	15	147	6.5	108	2	15	5	122	2.7	57	9	127	3
82.58	5.63	0.47	0.01	55	5.8	122	5.3	97	13	97	7.5	60	3	41	6	30	3.6	108	9	96	3
82.58	5.63	1.41	0.01	103	7.4	73	4.7	140	21	33	7	33	2.8	24	5	12	3	82	9.25	111	4
82.58	5.63	2.34	0.01	54	5.5	30	6.5	80	8	110	7.5	28	3.3	45	4	123	2.8	106	11	72	3
82.58	5.63	3.28	0.01	29	7.6	2	7	135	21	49	6	26	3	67	6	22	3	53	9	59	4
82.58	7.50	0.47	0.01	123	7.2	135	6.7	73	22	7	7	138	2.9	75	7	34	2.8	144	10.5	73	4
82.58	7.50	1.41	0.01	106	7.8	98	7.3	26	22	78	6.5	134	4	133	9	45	3.5	89	9.75	27	2
82.58	7.50	2.34	0.01	24	7.6	65	5	141	22	112	8	119	3.5	114	10	14	3.6	135	10	131	3.5
82.58	7.50	3.28	0.01	3	7.6	118	6	145	22	136	6.5	64	4	3	5	56	3	62	9	23	5